FORMULATING TRANSETHOSOMES FOR TRANSDERMAL DELIVERY OF COSMECEUTICALS IN TREATMENT OF ATOPIC DERMATITIS

by

Derya Karagöz Girişgen

B.S., Chemistry, Boğaziçi University, 2013

M.S., Chemistry, Boğaziçi University, 2017

Submitted to the Institute for Graduate Studies in
Science and Engineering in partial fulfillment of
the requirements for the degree of
Doctor of Philosophy

Graduate Program in Institute for Graduate Studies in Science and Engineering

Boğaziçi University

2024

ACKNOWLEDGEMENTS

I would like to thank my supervisor, Prof. Naz Zeynep Atay Gök for her patience, guidance and encouragement in every stage of my doctoral research. She has been a great advisor who taught me how to explore, learn and keep at finishing my studies. I am incredibly appreciative that I got to collaborate with her and benefit from her experience.

I am grateful to Prof. Şaron Çatak, Prof. Arzu Çelik Fuss, Prof. Tarık Eren and Prof. Fethiye Aylin Sungur for being in my thesis jury, reviewing my manuscript and making guiding comments.

I would like to express my gratitude to Boğaziçi University Advanced Technologies Research & Development Center and Center for Life Sciences & Technologies for their help in electron microscopy and dynamic light scattering analyses during my research.

My deepest thanks go to my beloved husband and son for their invaluable support, endless love and patience. Without the motivation and help that came from my husband, it was impossible to finish this study and dissertation. My son showed great patience for the days he couldn't be with me, without complaining. This dissertation is dedicated to you my boy!

My sincere thanks go to my family for always standing behind me and supporting my academic adventure. My father has the biggest contribution in my eternal curiosity and my mother gave lots of unconditional support during my years of studying.

I would also like to thank all my friends and former research students for their precious supports. I would give my special thanks to Başak Koca, İpek Munar, Emre Çelebi, Ece Çiftçi, Duygu Baykal, Canan Güler, Sevgi Yasemin Baysal, Burcu İsaoğlu, Elif Mey Öztürk, Özge Ceren Yalçın, Belgin Okumuş, Helen Taş, Büşra Ertem, Bilgesu

Başaran, Muzaffer Eren, Yaren Demirel, Gülfem Yurttaş, Senay Sözüanık and Zeynep Gözkara. I also would like to thank all the members of the faculty in the Chemistry Department.

Lastly, thanks to Novodist Türkiye for donating cosmeceuticals for this dissertation.

This study is supported by Boğaziçi University Research Fund with the project numbers of 19241 and 24BP3.

ABSTRACT

FORMULATING TRANSETHOSOMES FOR TRANSDERMAL DELIVERY OF COSMECEUTICALS IN TREATMENT OF ATOPIC DERMATITIS

In this dissertation three different types of transethosomes have been formulated and produced for the treatment of atopic dermatitis. Transethosomes, vesicles containing ethanol and a surfactant in their formulations, are superior to regular liposomes when it comes to flexibility, permeability and loading efficiency. The aim of this study was to facilitate forming nano-systems with better skin delivery properties. All transethosomes contained Soy PC, cholesterol, either Tween 80 or oleic acid as surfactant and ethanol within their formulations. Into these systems ceramides, vitamins and proteins were incorporated, respectively.

Initial formulations were carried out with Cer3, due to its critical function in regulating transdermal water loss. Cer3-containing transethosomes were successfully loaded with both hydrophilic and hydrophobic cargo, with high loading efficiencies. The impact of surfactant type on loading efficiency was investigated in the second set, which involved with VitC and VitE. Both single and dual loading of the two vitamins into transethosomes were successfully carried out with Tween 80 or oleic acid as surfactants. These formulations looked promising candidates for usage in transdermal administration tests. The chitosan coating, which was intended to broaden the range of applications of these transethosomes was also implemented with increased stability and loading efficiency. Since proteins have the potential to enhance atopic dermatitis therapy, they were used in the third set of formulations. Filaggrin, PAD-1 and caspase-14 proteins were successfully loaded into vesicles. All transethosomes were analyzed in terms of size, homogeneity, morphology and loading efficiencies.

ÖZET

ATOPİK DERMATİT TEDAVİSİNDE KOZMESÖTİK MADDELERİN DERİ ALTINA İLETİMİ İÇİN TRANSETOZOMLARIN FORMÜLE EDİLMESİ

Bu tezde, atopik dermatit tedavisi için üç farklı transetozom türü formüle edilmiş ve üretilmiştir. Transetozomlar, formülasyonlarında etanol ve bir yüzey aktif madde içeren veziküller, esneklik, geçirgenlik ve yükleme etkinliği söz konusu olduğunda normal lipozomlardan daha üstündür. Bu çalışmada amaç, daha iyi cilt iletim özelliklerine sahip nano-sistemler oluşturmayı kolaylaştırmaktır. Tüm transetozom formülasyonları Soya PC, kolesterol, yüzey aktif madde olarak Tween 80 veya oleik asit ve etanol içermektedir. Bu sistemlere sırasıyla seramidler, vitaminler ve proteinler dahil edilmiştir.

İlk formülasyonlar, transdermal su kaybını düzenlemedeki kritik işlevi nedeniyle Cer3 ile gerçekleştirilmiştir. Cer3 içeren transetozomlara hem hidrofilik hem de hidrofobik kargo ile yüksek yükleme verimlilikleriyle, başarılı bir şekilde yüklenmiştir. Yüzey aktif madde türünün yükleme verimliliği üzerindeki etkisi VitC ve VitE ile ilgili olan ikinci sette araştırılmıştır. İki vitaminin transetozomlara hem tekli hem de ikili yüklenmesi, yüzey aktif madde olarak Tween 80 veya oleik asit ile başarıyla gerçekleştirilmiştir. Bu formülasyonlar transdermal uygulama testlerinde kullanım için umut verici adaylar olarak görülmektedir. Bu transetozomların uygulama yelpazesini genişletmeyi amaçlayan kitosan kaplama da artan stabilite ve yükleme verimliliği ile uygulanmıştır. Proteinler atopik dermatit tedavisini geliştirme potansiyeline sahip olduklarından, üçüncü formülasyon setinde kullanılmışlardır. Filaggrin, PAD-1 ve caspase-14 proteinleri veziküllere başarıyla yüklenmiştir. Tüm transetozomlar boyut, homojenlik, morfoloji ve yükleme verimlilikleri açısından analiz edilmiştir.

TABLE OF CONTENTS

ACKNOWLEDGEMENTS iii
ABSTRACT v
ÖZET vi
LIST OF FIGURES x
LIST OF TABLES xxi
LIST OF SYMBOLS xxiii
LIST OF ACRONYMS/ABBREVIATIONS xxiv
1. INTRODUCTION 1
1.1. The Human Skin 1
1.1.1. Skin Structure and Functions 1
1.1.2. Common Skin Diseases 3
1.1.3. Cosmeceuticals Used for Common Skin Diseases 5
1.1.4. Transdermal Delivery of Cosmeceuticals 7
1.1.5. Factors Affecting the Skin Absorption of Cosmeceuticals 10
1.2. Liposomes and New Age Deformable Liposomes 13
1.2.1. Liposomes 13
1.2.2. Preparation of Liposomes 14
1.2.3. Characterization of Liposomes 16
1.2.3.1. Size, Size Distribution and Morphology Determination 16
1.2.3.2. Surface Charge Determination 17
1.2.3.3. LE% Calculation 17
1.2.3.4. In Vitro and in Vivo Drug Release Studies 17
1.2.3.5. Melting Point Determination 18
1.2.4. Difficulties in using Liposomes in Topical Formulations 19
1.2.5. Enhancing The Liposome Efficacy : New age liposomes 20
1.2.5.1. Transfersomes 20
1.2.5.2. Ethosomes 20
1.2.5.3. Transethosomes 21

1.2.6. Current Applications of Liposomes in Cosmeceuticals Industry . 23
2. RESEARCH OVERVIEW 26
3. CERAMIDE 3 EFFECT ON PHYSICAL PROPERTIES OF AMBORA EXTRACT AND CHROMABRIGHT LOADED TRANSETHOSOMES . . . 28
3.1. Introduction 28
3.2. Experimental 31
3.2.1. Materials 31
3.2.2. Methods 32
3.2.2.1. Preparation of TEs 32
3.2.2.2. Characterization of TEs 34
3.2.2.3. Calculation of LE% 35
3.2.2.4. Statistical Analysis 36
3.3. Results and Discussion 36
3.3.1. Preparation and Characterization of Cer3 Containing TEs . . . 36
3.3.1.1. Addition of Tween 80 to the Formulation 36
3.3.1.2. Addition of Cholesterol to the Formulation 38
3.3.1.3. Addition of Cholesteryl Sulphate to the Formulation . 39
3.3.1.4. Addition of Cer3 to the Formulation 43
3.3.1.5. Stability and Breakdown of the Final TE Formulation 47
3.3.2. Cer3 Effect on Physical Properties of Ambora Extract and Chromabright Loaded TEs 48
3.4. Conclusions 58
4. EFFECT OF SURFACTANT TYPE ON VITAMIN C AND VITAMIN E LOADED TRANSETHOSOMES AND A STUDY OF DUAL LOADING . . 60
4.1. Introduction 60
4.2. Experimental 64
4.2.1. Materials 64
4.2.2. Methods 65
4.2.2.1. Preparation of TEs 65
4.2.2.2. Characterization of TEs 66
4.2.2.3. Loading Efficiency Studies 66

4.3. Results and Discussion . . . 68
4.3.1. Effect of Surfactant Type on Physical Properties of TEs . . . 68
4.3.2. Chitosan Coating Studies . . . 77
4.4. Conclusions . . . 89
5. PROTEIN LOADING STUDIES WITHIN TRANSETHOSOMES . . . 92
5.1. Introduction . . . 92
5.2. Experimental . . . 97
5.2.1. Materials . . . 97
5.2.2. Methods . . . 98
5.2.2.1. Preparation and Characterization of TEs . . . 98
5.2.2.2. Loading Efficiency Studies . . . 99
5.2.2.3. Following the Stability of the Protein Structures . . . 99
5.3. Results and Discussion . . . 101
5.3.1. Preparation and Characterization of Protein Loaded TEs . . . 101
5.3.2. The Stability of the Protein Structures During Vesicle Preparation . . . 104
5.3.3. Protein Loading Efficiency Studies . . . 107
5.4. Conclusions . . . 110
6. CONCLUSIONS . . . 113
REFERENCES . . . 115
APPENDIX A: DLS RESULTS OF THE TEs IN CHAPTER 3 . . . 136
APPENDIX B: DLS RESULTS OF THE TEs IN CHAPTER 4 . . . 157
APPENDIX C: DLS RESULTS OF THE TEs IN CHAPTER 5 . . . 193
APPENDIX D: COPYRIGHT NOTICES . . . 210

LIST OF FIGURES

Figure 1.1. A schematic diagram of the structure of the skin 2

Figure 1.2. Illustrated examples of common skin diseases 4

Figure 1.3. A schematic diagram of transdermal delivery pathways 9

Figure 1.4. A schematic diagram of liposome structure 13

Figure 1.5. A schematic diagram of thin film hydration method 15

Figure 1.6. A schematic diagram of skin penetration mechanisms of liposomes, transferomes, ethosomes and TEs 22

Figure 3.1. General structure of ceramides 29

Figure 3.2. Structure of Cer3 30

Figure 3.3. Schematic representation of cold method TE preparation 34

Figure 3.4. Schematic representation of ultra-centrifugation method 35

Figure 3.5. STEM images showing TE3 samples 37

Figure 3.6. Optical microscopy image of TE8 under 50x magnification 40

Figure 3.7. STEM images showing TE5 samples 41

Figure 3.8. Optical microscopy and STEM image of TE9 42

Figure 3.9. Statistical regression analysis between Cer3 increase and TE mean diameter 44

Figure 3.10. Statistical regression analysis between Cer3 increase and PDI . . . 44

Figure 3.11. Optical microscopy image of TE11 under 50x magnification 45

Figure 3.12. STEM images of TE11 sample 46

Figure 3.13. Effect of lipid additions and increase in lipid concentrations on size for various TE formulations 47

Figure 3.14. Effect of lipid additions and increase in lipid concentrations on homogeneity values for various TE formulations 47

Figure 3.15. Effect of Cer3 addition on average sizes for empty, chromabright or ambora extract loaded TEs 50

Figure 3.16. Effect of Cer3 addition on PDI values for empty, chromabright or ambora extract loaded TEs 50

Figure 3.17. Effect of Cer3 addition on percent change in size after one month . 51

Figure 3.18. Effect of Cer3 addition on percent change in size after one month . 52

Figure 3.19. Maximum absorbance wavelengths of the lipids used in TE formation, TE11 and the payloads 53

Figure 3.20. Absorbance versus concentration data of ambora extract 54

Figure 3.21. Absorbance versus concentration data of chromabright 54

Figure 3.22. Statistical analysis on the effect of Cer3 existence on hydrophilic and hydrophobic payload containing TEs in terms of mean size . . 55

Figure 3.23. Statistical analysis on the effect of Cer3 existence on hydrophilic and hydrophobic payload containing TEs in terms of homogeneity 56

Figure 3.24. Images of ambora extract containing dispersions 57

Figure 3.25. Images of chromabright containing dispersions 57

Figure 4.1. Structure of Tween 80 61

Figure 4.2. Structure of Oleic acid 61

Figure 4.3. Structure of VitE 62

Figure 4.4. Structure of VitC 62

Figure 4.5. Structure of chitosan 65

Figure 4.6. End point color of the iodometric titration 67

Figure 4.7. Calibration curve of VitC at 258 nm 67

Figure 4.8. Calibration curve of VitE at 258 nm 68

Figure 4.9. Effect of surfactant type on mean sizes of various TE formulations 70

Figure 4.10. Effect of surfactant type on LE% of various TE formulations . . . 70

Figure 4.11. Effect of surfactant type on percent change in sizes upon one month of storage 71

Figure 4.12. Effect of surfactant type on percent change in LE% upon one month of storage for various TE formulations 71

Figure 4.13. Effect of surfactant type on percent change in size upon six month of storage for various TE formulations 72

Figure 4.14. Effect of surfactant type on percent change in LE% upon six month of storage for various TE formulations 72

Figure 4.15. STEM image of a sample from Dual 4 formulation set 75

Figure 4.16. STEM image of a sample from Dual 8 formulation set 76

Figure 4.17. STEM of CHIT0, only chitosan nano-particles 79

Figure 4.18. STEM of DMPG1, non-coated TE nano-particles 79

Figure 4.19. STEM of CHIT5, chitosan coated TEs 80

Figure 4.20. Effect of chitosan coating on mean size with respect to non coated vesicles 81

Figure 4.21. Effect of chitosan coating on LE% 83

Figure 4.22. Effect of chitosan coating on mean size upon one month storage with respect to non coated vesicles 84

Figure 4.23. Effect of chitosan coating on LE% upon one month storage with respect to non coated vesicles 84

Figure 4.24. STEM of CHIT8, chitosan coated dual loaded TEs 85

Figure 5.1. Four levels of protein structure 93

Figure 5.2. Illustrated scheme of filaggrin working pathway 95

Figure 5.3. Typical CD spectra of proteins 100

Figure 5.4. STEM images of the vesicles belonging to the data set of FLG . . 102

Figure 5.5. STEM images of caspase-14 proteins 103

Figure 5.6. STEM images of the vesicles belonging to the data set of CAS . . 103

Figure 5.7. STEM images of PAD-1 proteins 104

Figure 5.8. STEM images of the vesicles belonging to the data set of PAD . . 104

Figure 5.9. CD results of Filaggrin before and after ethanolic process 106

Figure 5.10. CD results of Caspase-14 before and after ethanolic process 106

Figure 5.11. CD results of PAD-1 before and after ethanolic process 107

Figure 5.12. Maximum absorbance wavelength of Filaggrin protein 108

Figure 5.13. Calibration curve of Filaggrin protein 108

Figure 5.14. Calibration curve of PAD-1 protein 109

Figure 5.15. Calibration curve of caspase-14 protein 109

Figure A.1. DLS results belonging to the three trials of TE1 samples 137

Figure A.2. DLS results belonging to the three trials of TE2 samples 138

Figure A.3. DLS results belonging to the three trials of TE3 samples 139

Figure A.4. DLS results belonging to the samples of TE4, TE5 and TE6 . . . 140

Figure A.5. DLS results belonging to the samples of TE7, TE8 and TE9 . . . 141

Figure A.6. DLS results belonging to the three trials of TE10 samples 142

Figure A.7. DLS results belonging to the three trials of TE11 samples 143

Figure A.8. DLS results belonging to the three trials of TE12 samples 144

Figure A.9. DLS results belonging to the three trials of TE13 samples 145

Figure A.10. DLS results belonging to the three trials of TE14 samples 146

Figure A.11. DLS results belonging to the three trials of TE15 samples 147

Figure A.12. DLS results belonging to the three trials of TE16 samples 148

Figure A.13. DLS results belonging to the three trials of TE17 samples 149

Figure A.14. DLS results showing one month stabilities of the TE5 samples . . 150

Figure A.15. DLS results showing one month stabilities of the TE11 samples . . 151

Figure A.16. DLS results showing one month stabilities of the TE 10, 12 and 13 samples 152

Figure A.17. DLS results showing one month stabilities of the TE14 samples . . 153

Figure A.18. DLS results showing one month stabilities of the TE15 samples . . 154

Figure A.19. DLS results showing one month stabilities of the TE16 samples . . 155

Figure A.20. DLS results showing one month stabilities of the TE17 samples . . 156

Figure B.1. DLS results of sample 5-1, belongs to the data set of Dual 1 158

Figure B.2. 1-month DLS results of sample 5-1 159

Figure B.3. 3-month DLS results of sample 5-1 160

Figure B.4. DLS results of sample 17-1, belongs to the data set of Dual 2 . . . 161

Figure B.5. 1-month DLS results of sample 17-1 162

Figure B.6. 6-month DLS results of sample 17-1 163

Figure B.7. DLS results of sample 18-1, belongs to the data set of Dual 3 . . . 164

Figure B.8. 1-month DLS results of sample 18-1 165

Figure B.9. 6-month DLS results of sample 18-1 166

Figure B.10. DLS results of sample 19-1, belongs to the data set of Dual 4 . . . 167

Figure B.11. 1-month DLS results of sample 19-1 168

Figure B.12. 6-month DLS results of sample 19-1 169

Figure B.13. DLS results of sample 4-1, belongs to the data set of Dual 5 170

Figure B.14. 1-month DLS results of sample 4-1 171

Figure B.15. 3-month DLS results of sample 4-1 172

Figure B.16. DLS results of sample 17-2, belongs to the data set of Dual 6 . . . 173

Figure B.17. 1-month DLS results of sample 17- 174

Figure B.18. 6-month DLS results of sample 17-2 175

Figure B.19. DLS results of sample 18-2, belongs to the data set of Dual 7 . . . 176

Figure B.20. 1-month DLS results of sample 18-2 177

Figure B.21. 6-month DLS results of sample 18-2 178

Figure B.22. DLS results of sample 19-2, belongs to the data set of Dual 8 . . . 179

Figure B.23. 1-month DLS results of sample 19-2 180

Figure B.24. 6-month DLS results of sample 19-2 181

Figure B.25. DLS results of sample CHIT9, belongs to the data set of CHIT1 . 182

Figure B.26. 1-month DLS results of sample CHIT24 183

Figure B.27. 1-month DLS results of sample CHIT25 184

Figure B.28. DLS results of sample CHIT31, belongs to the data set of CHIT4 . 185

Figure B.29. 1-month DLS results of sample CHIT31 186

Figure B.30. DLS results of sample CHIT14, belongs to the data set of CHIT5 . 187

Figure B.31. 1-month DLS results of sample CHIT28 188

Figure B.32. DLS results of sample CHIT29, belongs to the data set of CHIT7 . 189

Figure B.33. 1-month DLS results of sample CHIT29 190

Figure B.34. DLS results of sample CHIT34, belongs to the data set of CHIT8 . 191

Figure B.35. 1-month DLS results of sample CHIT34 192

Figure C.1. DLS results belonging to the three trials of FLG samples 194

Figure C.2. 4-month DLS result of FLG1 belonging to the data set of FLG samples 195

Figure C.3. 4-month DLS result of FLG2 belonging to the data set of FLG samples 196

Figure C.4. 4-month DLS result of FLG3 belonging to the data set of FLG samples 197

Figure C.5. DLS result of CAS1 belonging to the data set of CAS samples . . 198

Figure C.6. 4-month DLS result of CAS1 belonging to the data set of CAS samples 199

Figure C.7. DLS result of CAS2 belonging to the data set of CAS samples . . 200

Figure C.8. 4-month DLS result of CAS2 belonging to the data set of CAS samples 201

Figure C.9. DLS result of CAS3 belonging to the data set of CAS samples . . 202

Figure C.10. 4-month DLS result of CAS3 belonging to the data set of CAS samples 203

Figure C.11. DLS result of PAD1 belonging to the data set of PAD samples . . 204

Figure C.12. 4-month DLS result of PAD1 belonging to the data set of PAD samples 205

Figure C.13. DLS result of PAD2 belonging to the data set of PAD samples . . 206

Figure C.14. 4-month DLS result of PAD2 belonging to the data set of PAD samples 207

Figure C.15. DLS result of PAD3 belonging to the data set of PAD samples . . 208

Figure C.16. 4-month DLS result of PAD3 belonging to the data set of PAD samples 209

Figure D.1. Copyright licence of [40] 210

Figure D.2. Copyright licence of [145] 211

LIST OF TABLES

Table 3.1. The mass ratios of Soy PC:Tween 80:cholesterol:cholesteryl sulphate (Chol. sulphate): Cer3 in different TE formulations 33

Table 3.2. Effect of Tween 80 Content on Size and Homogeneity of TEs . . . 37

Table 3.3. Formulations with varying mass ratios of Soy PC, Tween 80 and cholesterol and comparison of mean size and PDI values 38

Table 3.4. Varying mass ratios of Soy PC, Tween 80, cholesterol and cholesteryl sulphate and comparison of mean size and PDI values 40

Table 3.5. Formulations with various mass ratios of Soy PC:Cer3, together with their mean size, PDI, and one-month stability data 43

Table 3.6. One- month stability of TE5 (no Cer3) and TE11 (Cer3 containing) formulations with respect to mean size and PDI values 48

Table 3.7. Effect of Cer3 addition on physical properties or ambora extract or chromabright loaded TEs 49

Table 4.1. The mass ratios of Soy PC:cholesterol:Tween 80 or oleic acid and cargo types in different TE formulations coded under the abbreviation of "Dual" 66

Table 4.2. Effect of surfactant type on physical properties of VitC or VitE loaded TEs in terms of mean size, PDI and %LE and their one month stabilities 69

Table 4.3. Size, size distribution and 6 month stability comparisions of DMPG containing non-coated (DMPG 1 and 5) and chitosan coated (CHIT1 and 5) vesicles 78

Table 4.4. Mass ratios of Soy PC:cholesterol (Chol.):Tween 80 or oleic acid (O. acid) and chitosan in different TE formulations coded under the abbreviation of CHIT 80

Table 4.5. The solubility, charge and molar weight comparison of the used materials 82

Table 4.6. Effect of surfactant type on physical properties of VitC or VitE loaded, chitosan coated TEs in terms of mean size, PDI and %LE and their one month stabilities 86

Table 4.7. Comparison of coated and non-coated vesicles in terms of mean size, PDI and %LE and their one month stabilities 87

Table 4.8. Comparison of coated and non-coated vesicles in terms of mean size, PDI and %LE and their 6-month stabilities 88

Table 5.1. The mass ratios of Soy PC, cholesterol, Tween 80 and Cer3 with the indicated cargo types in different TE formulations coded as FLG, PAD and CAS 99

Table 5.2. Mean size and homogeneity values of TEs (number of trials, n=3) 101

LIST OF SYMBOLS

α	Alpha
β	Beta
µ	Mikro

LIST OF ACRONYMS/ABBREVIATIONS

3D	Three Dimensional
AD	Atopic Dermatitis
ANOVA	Analysis of variance
CPEs	Chemical Penetration Enhancers
CD	Circular dichroism
Cer3	Ceramide 3
DSC	Differential scanning calorimetry
DLS	Dynamic light scattering
DMPG	1,2-dimyristoyl-sn-glycero-3-phosphorac-1-glycerolsodium salt
FDA	Food and Drug Administration
LE	Loading Efficiency
nm	nanometer
PAD-1	Protein-arginine-deiminase-type-1
PDI	Poly dispersity index
SC	Stratum Corneum
SEC	Size Exclusion Chromatography
SEM	Scanning electron microscopy
Soy PC	Soybean phosphatidylcholin
STEM	Scanning transmission electron microscopy
TE	Transethosome
TEM	Transmission electron microscopy
UV	Ultra-violet
UV/Vis	Ultraviolet-visible
VitC	Vitamin C
VitE	Vitamin E

1. INTRODUCTION

1.1. The Human Skin

1.1.1. Skin Structure and Functions

Outermost barrier of human body which protects itself from external influences is the skin and it has an area of roughly 1.2 – 2.2 m2 total with a weight of 4 – 5 kg with intertwined areas such as sweat glands, nerve fibres, hair follicles and sebaceous glands. Some substances such as medications delivered via transdermal patches or topical skincare products, can be absorbed through the skin. So, the skin could be one of the main entry points into the body targeting specific skin conditions and understanding the skin structure deeply is an important issue to create alternative medications through transdermal delivery.

The skin is a multi-functional organ that performs several crucial functions essential for overall health and well-being. The primary functions of the skin are protection, sensation, regulation, synthesis and storage, immune defense, excretion and absorption. The skin consists of three distinct regions: epidermis, dermis and hypodermis as illustrated in Figure 1.1. Comprising about 5 % of full thickness of the skin, the epidermis is the upmost layer of the skin and serves as a protective barrier against external elements such as pathogens, chemicals, and ultra-violet (UV) radiation. It consists mainly of epithelial cells and is further divided into sub-layers from the outermost to the innermost as stratum corneum (SC), stratum granulosum, stratum spinosum, and stratum basale.

The topmost layer of the epidermis is called the SC and it is composed of flattened, keratin-filled cells called corneocytes. These cells are continuously shed and replaced by cells from the lower layers. The lipids between corneocytes help prevent excessive water loss and maintain skin hydration. The corneocytes are the primary structural compo-

nents filled with keratin. The main lipid classes in SC are ceramides, free fatty acids and cholesterol. Under the SC, there is stratum granulosum. Cells in this layer start to flatten and produce keratin filaments and proteins, contributing to the structural integrity and water resistance of the skin. The stratum spinosum is located between the granular layer and the basal layer and cells in this layer are metabolically active, producing keratin and synthesizing lipids crucial for skin barrier function. It provides structural integrity and allow cells to withstand mechanical stress. The stratum basale is the deepest layer of the epidermis, in close contact with the dermis. It consists of a single layer of cells sitting on the basement membrane. Basal keratinocytes found in this layer are stem-like cells that give rise to keratinocytes for higher layers and melanin pigments absorb and dissipate UV radiation, helping to protect against sunburn, skin aging, and skin cancer.

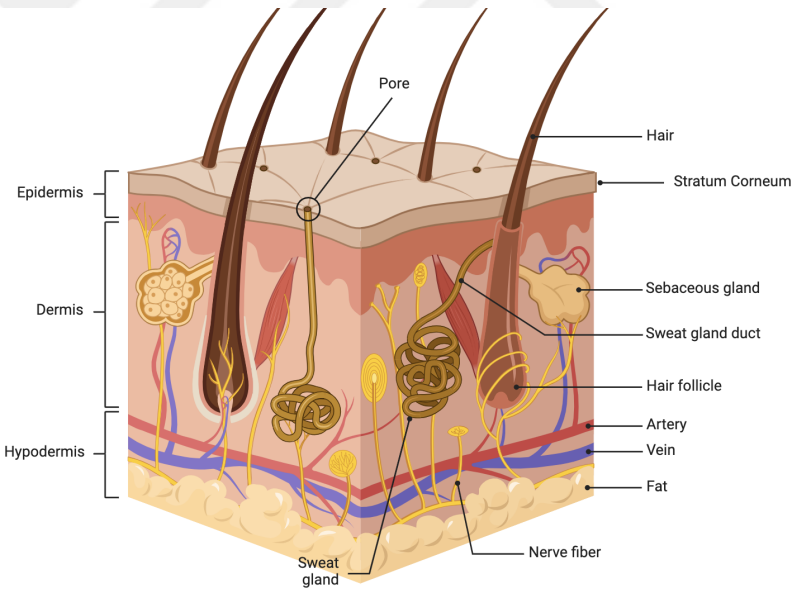

Figure 1.1. A schematic diagram of the structure of the skin (Created with BioRender.com, accessed on June 2024)

Beneath the epidermis comes the dermis, a thicker layer of connective tissue composed of elastic and collagen fibers. It contains blood vessels, nerve endings, hair follicles, sweat glands, and sebaceous glands. The dermis provides structural support, elasticity, and nourishment to the skin. The dermis is highly vascularized, with arterioles, venules, and capillaries supplying nutrients, oxygen, and immune cells to skin

cells. These vessels also help regulate skin temperature. Various nerve endings in the dermis detect sensations such as touch, pain, temperature, and pressure. Embedded in the dermis, hair follicles produce hair shafts and are associated with sebaceous glands which secrete sebum. Sweat glands, distributed throughout the dermis, produce sweat for thermoregulation and excretion of metabolic waste products such as urea and salts. Sebaceous glands secrete oily sebum into hair follicles, lubricating the skin and hair, and providing antibacterial protection. Sunlight exposure to the skin triggers the production of vitamin D, essential for calcium absorption and bone health. The subcutaneous fat in the hypodermis also serves as an energy reserve and provides insulation to regulate body temperature. Specialized immune cells help to detect and neutralize pathogens that breach the skin barrier, contributing to local immune defense. In response to injury or infection, the skin initiates an inflammatory response to contain and eliminate pathogens, promote tissue repair, and stimulate immune defenses [1].

1.1.2. Common Skin Diseases

Certain lifestyle factors can lead to the development of certain skin diseases. Skin diseases encompass a wide range of conditions that affect the skin, hair, and nails and vary greatly in their symptoms, severity, and causes. Some of the most common skin diseases are illustrated in Figure 1.2. Acne is the most prevalent skin disease that affects millions of people from a very wide range of age. It is a common condition where hair follicles become clogged with oil and dead skin cells that lead to pimples, blackheads, and sometimes cysts. It primarily affects the face, back, and shoulders [2]. Infections also have a negative impact on skin and they can be bacterial, fungal or viral. Bacterial infections include conditions like impetigo and cellulitis whereas athlete's foot, ringworm, and yeast can be examples for fungal infections. Viral infections includes herpes simplex and varicella-zoster virus. There can be also pigmentation disorders throughout the skin. Vitiligo is one of the most known skin diseases that causes loss of skin color in patches due to the destruction of melanocytes. There is also melasma that can be characterized by brown or gray-brown patches, typically on the face, often triggered by sun exposure or hormonal changes [3].



Figure 1.2. Illustrated examples of common skin diseases (Created with BioRender.com, accessed on June 2024)

Rosacea is a chronic disorder characterized by facial redness, visible blood vessels, and sometimes pimples. It often affects the central part of the face. Lupus is an autoimmune disease that can cause a variety of skin issues, including a characteristic butterfly-shaped rash on the face. Basal cell carcinoma is the most common and least aggressive type of skin cancer whereas squamous cell carcinoma is a more aggressive type that can metastasize if not treated. Melanoma is the most dangerous form of skin cancer, originating in the melanocytes and known for its ability to spread rapidly [4–6].

Dermatitis is a common condition that causes swelling and irritation of the skin. It has many causes and forms and often involves itchy, dry skin or a rash. Four common types of this condition are atopic dermatitis (AD), contact dermatitis, psoriasis and seborrheic dermatitis. Contact dermatitis is a rash on your skin that develops by exposure to allergens or irritants and leads a to red, itchy, and sometimes blistered skin. Generally, avoiding from the source of the rash helps prevent it from returning. Seborrheic dermatitis affects areas with high sebaceous gland activity, like the scalp and face. It appears as red, dry, flaky, itchy skin on the scalp and other parts of the body and is common but not contagious. Medications should be used to manage the symptoms. Psoriasis and seborrheic dermatitis can mimic each other, both are patches of red skin with flakes and can be found on scalp and back. Psoriasis is a

chronic autoimmune condition where skin cells multiply rapidly by forming red and scaly plaques. It commonly affects the scalp, elbows, and knees [7].

AD is a chronic, non-contiguous condition characterized by dry, itchy and inflamed skin and the main topic of interest of this doctoral dissertation. It is often hereditary and associated with other allergic conditions like asthma and allergic rhinitis. Typically, it starts in childhood, and flare-ups can persist until maturity. A 2007 population-based survey in the United States estimated that 17.8 million people are living with AD, with the majority of cases remaining un-diagnosed [8]. Dermatitis and eczema both refer to inflammation of the skin but eczema is a broad, umbrella term describing a group of conditions. AD is the most common type of eczema. AD has no known treatment, although it can be controlled with the right attention. The most suggested symptomatic remedy is the use of emollients, with recommended use for every day. When emollient use alone is not sufficient, first and second-line treatments like corticosteroid creams, calcineurin inhibitors and antihistamines are available which come with serious side effects. When there are clear signs of secondary inflammation, antibiotic use is recommended [9,10]. Also, there is a brand new injectable medication that have potential to treat people with severe AD, Dupilumab. Dupilumab is the first Food and Drug Administration (FDA) approved (2017) treatment of AD that blocks the signaling of the immune response mediators that drive atopic and many other inflammatory skin diseases. Although this medicine shows promise, there are not adequate studies highlighting the effectiveness and the possible adverse effects yet [11]. This study will concentrate on three alternative approaches of treatment that can be utilized to manage AD.

1.1.3. Cosmeceuticals Used for Common Skin Diseases

European legislation defines a cosmetic product as any substance or preparation intended to be applied to the various external parts of the human body with the sole or primary intention of cleaning, perfuming, altering appearance, correcting body odors, protecting or maintaining good condition is considered a cosmetic product.

As cosmetic products increasingly incorporate various delivery methods that alter skin physiology, the need for a new category has emerged. Consequently, Reed and Kligman coined the term "cosmeceuticals" to describe these innovative products that bridge the gap between cosmetics and pharmaceuticals [12]. When a cosmetic product has pharmacological therapeutic benefits but not always biologic benefits, it is referred to by this term. A drug is defined as having a biological effect on living tissue; in contrast, a cosmeceutical does not. Other distinctive difference of cosmeceutical products is that, they undergo in vitro and small clinical trials, often supported by cosmetic companies, with rigorous testing is not mandatory compared to pharmaceuticals.

With longer lifespans, people are getting more concerned with minimizing the visible signs of photo-aging and chronological aging. There are hundreds of products on the market that promise to reduce wrinkles and fine lines, reduce redness, smooth texture, remove discolouration, and make skin look younger. These goods are all listed in the diverse category of cosmeceuticals which include antioxidants, growth factors, peptides, anti-inflammatories, botanicals, polysaccharides, and pigment-lightening agents. For example, when the free radicals form due to environmental oxidative stress that can lead to cell damage and subsequently to aging of the skin, antioxidants such as vitamins A, B, C, E, alpha lipoic acid and Coenzyme Q-10 are used. Or, to treat hyper-pigmentation and the appearance of fine lines, niacinamide which is a complex in the vitamin B group is used [13]. Another example is hyaluronic acid that has many qualities for skin regeneration, with moisturizing and anti-ageing effects [14]. Oils with high levels of linoleic acid are also crucial cosmeceuticals for skin care because they prevent development of eczema and AD. These vital fatty acids integrate into the cell membranes, repair the damaged lipid barrier, and limit the loss of water [15]. Topical retinoids are primarily indicated for the treatment of psoriasis, acne vulgaris, photoaging where natural and synthetic bio-active peptides are also used as cosmeceutical ingredients to treat various skin conditions. Zinc is another cosmeceutical ingredient that is incorporated in various skincare products for its antioxidant, anti-inflammatory, antimicrobial and wound healing properties [16]. Lastly, green tea helps to increase collagen formation, and protect against UV damage. Sunscreens containing green tea

extract may provide better protection against destructive effects of the sun.

1.1.4. Transdermal Delivery of Cosmeceuticals

Delivery routes for cosmeceuticals involve various methods to ensure effective treatment and targeted therapy. These various routes and methods are chosen based on the type of skin disease, the desired rate of drug release, the need for localized and systemic effects, and patient-specific factors. Topical delivery of creams, ointments and gels that are applied directly to the skin are the most common methods for treating local skin conditions like eczema, psoriasis, and fungal infections. Topical applications often have difficulty penetrating deeper layers of the skin, limiting their effectiveness for conditions that affect deeper tissues. Also, many topical formulations require frequent reapplication, which can be inconvenient and affect patient adherence to the treatment regimen. Also, topical applications show limited systemic effects. While this is often an advantage, it can be a limitation for conditions that might benefit from systemic treatment, as topical creams primarily provide localized effects. To overcome this, transdermal patches provide a controlled release of medication over time, useful for localized pain relief and systemic delivery of certain drugs. However, only certain drugs are suitable for delivery via patches, primarily those with low molecular weight and sufficient lipid solubility to pass through the skin. Also, patches may not adhere well to all skin types or in areas with a lot of movement or sweating, leading to incomplete or inconsistent drug delivery [17, 18].

In oral medication, pills and capsules are used for systemic conditions that affect the skin, such as acne, severe psoriasis, and infections. Even though oral route is preferred widely, there are many limitations. Oral medications can cause systemic side effects affecting various organs and systems. Drugs taken orally are metabolized by the liver before reaching systemic circulation, which can reduce the bioavailability and effectiveness of the medication. The absorption of oral drugs can be inconsistent due to factors such as food intake, gastrointestinal pH, and individual patient differences, leading to variability in drug effectiveness. High doses required to achieve therapeutic

levels in the skin may increase the risk of systemic toxicity, limiting the dosage that can be safely administered orally. Most importantly, oral delivery may not be effective for localized skin conditions where high local concentrations of the drug are needed, as the drug may not adequately reach the affected skin areas [19]. In addition to being more comfortable and easy, transdermal drug delivery has the advantage of less localized side effects over oral or intravenous drug delivery.

Transdermal absorption refers to the process by which substances pass through the skin and enter the bloodstream or deeper tissues. This method of delivery can be used for medications and certain compounds that can be absorbed through the skin. Transdermal drug delivery enhances the bioavailability of medications that undergo bio-transformation while avoiding the issues associated with oral administration, such as pH shift, food interaction in the gastrointestinal tract, and first-pass hepatic metabolism. This topical route is the preferred route for the administration of drugs having a short biological half-life and provides patient compliance with reduced dosing frequency. Innovative drug delivery systems have been developed to address issues associated with conventional topical formulations, potentially leading to improved treatment efficacy and decreased side effects and adverse consequences.

There are three major pathways of transdermal absorption which are transcellular, intercellular and follicular absorptions as illustrated in Figure 1.3. The transcellular route involves crossing the skin directly by passing through the lipid structures and moving across corneocytes. The drugs can also be transferred around the corneocytes in the lipid-rich extracellular regions, which is called intercellular absorption. While non-polar molecules with molecular weights less than 500 Da may easily diffuse, it is widely acknowledged that polar molecules can not easily pass through the intercellular pathway. Hair follicles are also a possible route for drug penetration because they make up around 0.1% of the skin's surface. Follicular absorption includes hair follicles and sweat glands serving as pathways for absorption, especially for smaller molecules that can penetrate openings [20].

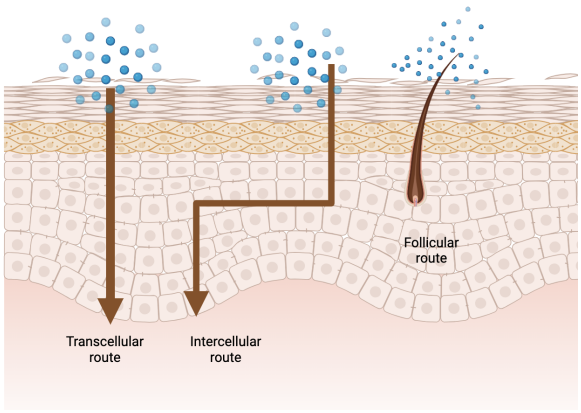

Figure 1.3. A schematic diagram of transdermal delivery pathways (Created with BioRender.com, accessed on June 2024)

The skin consists of densely packed corneocytes which are mostly lipophilic within the extracellular SC lipid matrix. Therefore, lipophilic molecules can penetrate more readily through the skin, but this is also limited due to the hydrophilic regions. Overcoming the skin barrier for transdermal delivery involves a combination of chemical, physical, mechanical, and nanotechnology-based approaches. Some of these include creams, hypodermic needles, microneedles, patches, chemical/lipid enhancers, iontophoresis and electroporation. Each method has its advantages and limitations, and often a combination of methods is used to achieve optimal results. The main goal of transdermal delivery studies is to enhance drug delivery while minimizing side effects and maintaining patient comfort. Most of these methods involve disrupting the SC barrier and delivering the drug molecule underneath it [21].

Iontophoresis uses a small electric charge to drive charged particles through the skin. While iontophoresis enhances drug penetration compared to topical application, it still primarily affects superficial skin layers and may not deliver sufficient medication to deeper tissues. The procedure requires specialized equipment and trained personnel to administer, which may limit its availability and convenience compared to other delivery methods [22].

Dermatologists have been highlighting the many benefits of micro-needling, a relatively new treatment option for skin rejuvenation, acne scarring, rhytides, surgical scars, dyschromia, melasma, enlarged pores, and transdermal drug administration. In micro-needling, tiny needles create micro-channels in the skin, allowing drugs to penetrate more deeply. The procedure can also cause pain and bleeding during application and requires specialized equipment and trained personnel to administer which restricts the availability and reliability [23].

Injectable medications include subcutaneous, intramuscular, or intravenous injections delivering drugs directly into the bloodstream or muscles for systemic effects. Biologics for severe psoriasis and eczema are often administered this way. However, injections can cause pain, discomfort, and anxiety for many patients, making this route less preferable compared to non-invasive methods. Injectable medications often require administration by healthcare professionals, necessitating clinic visits and increasing healthcare costs [16].

Chemical penetration enhancers (CPEs) include substances that increase skin permeability to allow better drug absorption. Many CPEs can cause skin irritation, redness, itching, and burning sensations, particularly with prolonged use or higher concentrations. CPEs can disrupt the natural skin barrier, increasing the risk of infections, dehydration, and further irritation. The effectiveness of CPEs can vary based on individual skin characteristics, the type of drug being delivered, and the specific enhancer used, leading to inconsistent results. Also, not all drugs are compatible with CPEs, limiting their applicability [24].

1.1.5. Factors Affecting the Skin Absorption of Cosmeceuticals

To determine the best application site and route for a cosmeceutical, it is necessary to understand the factors affecting skin absorption characteristics of that substance. Penetration ability and absorption through the skin can be optimized if the variables influencing the absorption through the skin is studied well. Major factors that

determines the efficacy of transdermal delivery of the cosmeceuticals can be grouped under three main headings; skin physiological conditions and administration sites, physico-chemical characteristics of penetrating molecules and physico-chemical properties of the formulation.

Physiological factors involve concerns like skin pH, application site, skin hydration, age, race, sex and the pathology of the skin. The skin tends to have a broad pH range, with the acidity ranging between 4 and 7 but the ideal pH level should be around 5.5. So, more acidic-based skin care ingredients may help to maintain healthy skin conditions by keeping the pH levels below 6. Also pH is also important to regulate permeability of the applied substances because only unionized substances can penetrate through skin. So, the proportion of unionized drug within a formulation determines the drug concentration in skin. The most crucial element boosting skin penetration is hydration. A healthy barrier is brought about by the SC being properly hydrated. A water concentration of between 20 and 50 percent encourages corneocyte swelling, which lowers cell compaction and ability of water vapor to pass through diffusion. Humectants are therefore used in transdermal delivery. Application site of the cosmeceuticals affects the penetration efficiency directly. Site-specific differences include skin thickness, SC type, and appendage density. Age, skin type, and sex hormones all affect the permeability of the skin because of the changes in the chemical composition of SC structure. Therefore, these elements also have a big impact on skin penetration.

Physico-chemical characteristics of penetrating molecules involve concerns like partition coefficient, molecular size and shape, concentration, half life and stability. The pKa of the penetrating molecule need to be carefully selected since only the non-ionized portion of the molecule will be transferred to the viable epidermis. Since highly lipophilic molecules would diffuse more readily in the SC but would find it difficult to leave it and migrate to the deeper layers of the skin, the oil/water partition coefficient should favor diffusion in both water and lipids. However, a hydrophilic material will also have trouble at melting with the lipids that make up sebum, which will hinder

the absorption of the latter. So a partition coefficient between 1 and 4 is ideal for effective skin penetration. The molar mass of the permeating agents must be less than 400 Da in order to effectively penetrate through the skin. This characteristic still leaves the possibility that bigger molecules may be able to enter SC by facilitating the introduction of other molecules and/or nanoparticles. Substances should stay stable when they get contact to the skin but should leave the body at an appropriate time. So, they should have low melting points with a half life of less than 10 hours. Also, the gradient in concentration across the barrier determines the rate of delivery, and a higher gradient indicates a higher concentration of drug across the barrier.

Physico-chemical properties of the formulation include release characteristics, usage of physical or CPEs and pH of the vehicle system. Viscous formulations have the potential to decrease the molecule's diffusion coefficient by postponing or preventing skin partitioning and subsequent absorption. It will be challenging to partition highly for lipophilic formulations because they will compete with the lipophilic SC. Conversely, occlusive formulations have the potential to somewhat improve absorption. Furthermore, the SC can be altered or damaged by the presence of solvent molecules, surfactants, absorption enhancers, and other compounds in the formulation through a variety of mechanisms, leading to a marked increase in the absorption of all formulation components applied topically. Very acidic and alkaline cosmeceutical formulations can damage the skin barrier and affect the release and penetration dynamics of the actives used. So, keeping the pH at around 5.5 is an important parameter to prepare effective cosmeceutical formulations [25, 26].

As research progresses, new transdermal delivery systems for unconventional administration routes have been designed. The form and composition of the entire delivery system formulation, in addition to the active ingredient, have received attention in an effort to overcome these challenges. Novel approaches to skin delivery of bioactive substances may be based on the gathering of therapeutically active compounds in nanocarriers, which are gradually exploited in skin targeting and topical delivery. Due to their enhanced SC penetration and targeting capabilities, nanocarriers like liposomes,

solid lipid nanoparticles, and polymeric nanoparticles especially have drawn interest to load drugs by improving stability and providing controlled-release. Liposomes are tiny spherical vesicles composed of phospholipid bilayers and can load various substances by making them useful for a range of applications, particularly in medicine, dermatology and biotechnology. Liposomes and their derivatives like ethosomes, transfersomes and transethosomes (TEs) are the main subject of this study and will be described in more detail in the next section.

1.2. Liposomes and New Age Deformable Liposomes

1.2.1. Liposomes

Liposomes are spherical structures with a hollow interior that are covered in two lipid layers. They contain a combination of phospholipids and cholesterol that form small artificial vesicles. Liposomes are formed artificially by the self-assembly of phospholipids in aqueous environments, resulting in structures that can range in size from nanometers to micrometers. The discovery of liposomes dates back to the mid-1960s by Dr. Alec D. Bangham and his colleague R. W. Horne, who observed these structures using an electron microscope as illustrated in Figure 1.4 [27].

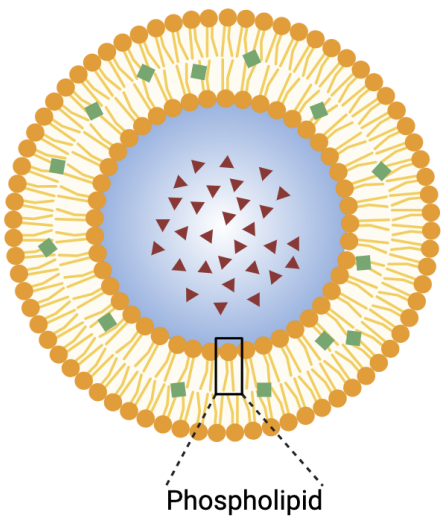

Figure 1.4. A schematic diagram of liposome structure (Created with BioRender.com, accessed on June 2024)

The structure of liposomes allows them to carry both hydrophilic and hydrophobic substances. The hydrophilic heads face the aqueous environment inside and outside the vesicle, while the hydrophobic tails face inward, away from the water. This dual nature makes liposomes particularly versatile in loading various drugs and biological molecules. The choice of bilayer components determines the rigidity, fluidity and the charge of the bilayer. For instance, unsaturated phosphatidylcholine species from natural sources give much more permeable and less stable bilayers, whereas the saturated phospholipids with long acyl chains form a rigid and impermeable bilayer structure. So they can have broad range of application areas by changing the lipid composition and the loaded cargo type.

Liposomes have several key advantages in drug delivery systems. They protect loaded drugs from degradation, enhance drug stability, improve therapeutic efficacy by targeting specific tissues, and reduce side effects by controlling drug release. These features make them valuable in a wide range of biomedical applications, including cancer therapy, vaccine delivery, and treatment of infections and inflammatory diseases. Various methods exist for liposome preparation, including mechanical dispersion techniques like thin film hydration, as well as solvent dispersion methods such as ethanol injection and reverse-phase evaporation. Each method has its own advantages and limitations in terms of liposome size, loading efficiency (LE), and stability [28].

1.2.2. Preparation of Liposomes

There are several methods for the preparation of liposomes. The traditional thin-film hydration method involves dissolving lipids in an organic solvent to form a thin film, which is then hydrated with an aqueous solution as illustrated in Figure 1.5. This results in the formation of multi-lamellar vesicles. The liposomes can then be sized down using techniques such as extrusion or sonication to obtain uni-lamellar vesicles [29]. Sonication involves the use of ultrasonic waves to break down multi-lamellar vesicles into smaller vesicles. There are two types of sonications; probe sonication and bath sonication. Probe sonication involves direct application of ultrasonic energy to

the liposome dispersion, while bath sonication involves placing the liposome dispersion in an ultrasonic bath. This method is effective but can cause degradation of sensitive compounds. Extrusion involves forcing the liposome suspension through polycarbonate membranes with defined pore sizes, resulting in liposomes of uniform size. This method is gentle and preserves the integrity of loaded materials better than sonication.

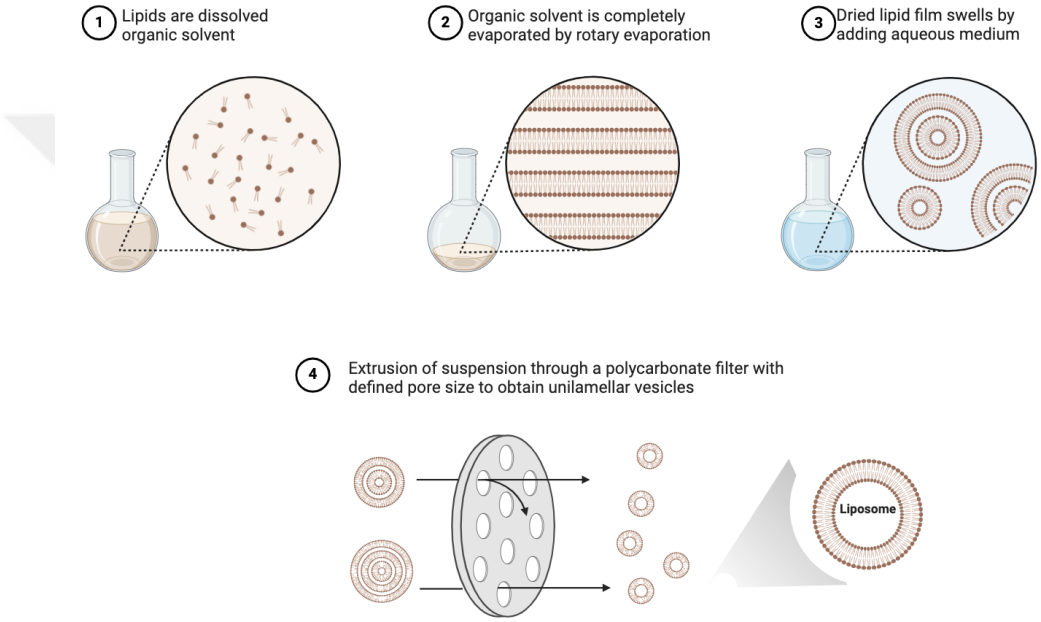

Figure 1.5. A schematic diagram of thin film hydration method (Created with BioRender.com, accessed on June 2024)

In 1985, Ohsana et al devised a novel liposome preparation method, the freeze-thaw method, to overcome issues such as complete solvent removal, sterilization, scale up and stability, while enabling better LE% and a simpler preparation [30]. The freeze-thaw method involves freezing the liposome suspension in liquid nitrogen and then thawing it, which helps in fusing small vesicles into larger uni-lamellar vesicles. It is particularly useful for increasing LE%. The reverse-phase evaporation technique involves creating water-in-oil emulsions using sonication, followed by the removal of the organic solvent under reduced pressure to form liposomes. This method allows for high LE and large internal aqueous volume [28].

An intriguing strategy for increasing the generation of liposomes at a larger scale is the ethanol injection method. In order to avoid the sonication process, which might be destructive to the phospholipid layers, and to achieve a more efficient process, Batzri and Korn have developed the ethanol injection method [31]. It has a number of benefits, such as ease of use, rapid implementation, repeatability, and the absence of oxidative changes or lipid degradation. In the ethanol injection method, lipids dissolved in ethanol are rapidly injected into water, forming liposomes within ethanol dilution. This method is simple but can result in heterogeneous liposome sizes [32]. After the liposomal suspensions are obtained, they become ready for characterization.

1.2.3. Characterization of Liposomes

1.2.3.1. Size, Size Distribution and Morphology Determination. Determining the size and size distribution of liposomes is crucial for their application in drug delivery, as these parameters influence the pharmaco-kinetics, bio-distribution, and overall therapeutic efficacy of liposomal formulations. Size distribution is denoted with the polydispersity index (PDI) from the Dynamic Light Scattering (DLS) data. DLS is a widely used technique for measuring the size of small particles, including liposomes, in suspension. It determines the hydrodynamic diameter by analyzing the scattering pattern of laser light passing through the sample. This method provides information about the average size and the PDI.

Transmission electron microscopy (TEM) and scanning electron microscopy (SEM) are powerful tools for directly visualizing the size and morphology of liposomes. These techniques offer high-resolution images, allowing for detailed size analysis and confirmation of the vesicle structures.

Size Exclusion Chromatography (SEC) separates liposomes based on their size by passing the sample through a column packed with porous beads. Smaller liposomes enter the pores and are retained longer than larger ones, resulting in size-based separation. This method can be coupled with other analytical techniques to determine the

size distribution [33].

1.2.3.2. Surface Charge Determination . Zeta potential measurement is commonly used to assess the surface charge of liposomes. This parameter helps in understanding the stability and behavior of liposomes in different environments. Studies have shown that the zeta potential can significantly influence the interaction of the liposomes with biological membranes and their overall stability. For example, even though they are both neutral lipids, di-palmitoyl-phosphatidylcholine and di-oleoyl-phosphatidylcholine liposomes exhibit different zeta potentials within vesicles depending on the solution conditions, which can impact their stability and hydrolysis by the enzymes [34].

1.2.3.3. LE% Calculation. There are several methods to measure LE%. Ultra-centrifugation is one of them and involves separating the loaded drug from the free drug by spinning the liposome solution at high speeds. The concentration of the drug in the supernatant (free drug) is measured, and the LE% is then calculated based on the initial drug concentration [35].

In dialysis method, the liposome suspension is placed in a dialysis bag, allowing free drugs to diffuse out while retaining loaded drugs. The concentration of the drug outside the dialysis bag is then measured [36].

In the gel filtration chromatography technique, free and loaded drugs are separated based on their size. The loaded drug is quantified after eluting the liposomes from the gel [37].

Fluorescence spectroscopy uses fluorescent markers to quantify the loaded drug. The fluorescence intensity correlates with the concentration of the loaded drug [38]

1.2.3.4. In Vitro and in Vivo Drug Release Studies . As much as it is important to load active materials in liposomal systems, it is also imperative that we know the

release mechanics. In vitro release studies are typically carried out for one or more of the following reasons: batch quality control, method evaluation, identification of crucial elements that may affect bioavailability, and assessment of drug availability during preliminary research. Developing in vitro release tests for liposomes presents several challenges, primarily due to the unique properties of liposomal formulations and their complex release mechanisms. Liposomes can release their payload through various mechanisms, including diffusion, degradation of the liposomal membrane, and triggered release by environmental factors (e.g., pH, temperature). This complexity makes it difficult to develop standardized in vitro release tests that accurately mimic in vivo conditions. There is no universally accepted method for liposomal in vitro release testing. Different studies use various techniques, including dialysis, centrifugation, and size-exclusion chromatography, leading to variability in results and making it challenging to compare data across different studies [39].

Animals like rats and mice are used in skin disposition studies to determine the drug distribution mechanism across the various layers of skin after the application of the vesicular formulation. By using fluorescence spectrophotometer, the amount of drug deposited in the SC is determined after administration. Skin deposition studies are performed by Confocal Laser Scanning Microscopy technique to observe the drug distribution through the different skin layers [40].

1.2.3.5. Melting Point Determination. Determining the melting point of liposomes involves understanding the phase transition temperatures of the lipids within the liposomal bilayer. Differential scanning calorimetry (DSC) is the primary technique used for this purpose due to its ability to measure the heat flow associated with phase transitions in lipid membranes. DSC is widely used to study the thermal behavior of lipids and liposomal stability. It measures the heat required to increase the temperature of a sample and reference, allowing the identification of phase transition temperatures, such as the melting point of lipid components. This method provides insights into the stability and fluidity of liposomal membranes, crucial for their function and storage. One of the main challenges in determining the melting point of liposomes is their

complex composition. Liposomes often consist of a mixture of different lipids and loaded agents, which can alter the thermal behavior. Moreover, factors like hydration level, pH, and the presence of salts can significantly impact the phase transition temperatures. Therefore, accurate melting point determination requires careful control of experimental conditions and consideration of all components in the liposomal formulation [41].

1.2.4. Difficulties in using Liposomes in Topical Formulations

Liposomal drug delivery systems offer several advantages over traditional drug delivery methods, making them a prominent area of research and application in the pharmaceutical and cosmeceutical fields. Liposomes can be engineered to target specific tissues or cells, improving the therapeutic index of drugs. This targeted approach is particularly beneficial in cancer treatment, where liposomes can deliver chemotherapeutic agents directly to tumor cells, minimizing damage to healthy cells. Some liposomal systems can protect loaded drugs from degradation and clearance, enhancing their stability and bioavailability. They can also provide sustained or controlled release of drugs, reducing the frequency of dosing and improving patient compliance [42].

By loading drugs, liposomes can significantly reduce the systemic toxicity of many therapeutic agents. This loading minimizes exposure of the drug to non-target tissues, thereby reducing side effects. Liposomes can load a wide variety of drugs, including hydrophilic, hydrophobic, and amphiphilic molecules. This versatility makes them suitable for delivering a broad range of therapeutic agents, from small molecules to proteins and nucleic acids [43].

There are of course come drawbacks to liposomal systems, especially when in topical formulations. The SC poses a significant barrier, restricting liposome penetration. This makes it challenging for liposomes to deliver drugs effectively to deeper skin layers or systemic circulation. Liposomes are prone to physical and chemical instability, such as aggregation, fusion, and oxidation. After being placed to the skin's surface,

liposomes only live in the top layer of the SC, acting as a reservoir for drugs. Because of their fragility and low skin penetration, they are therefore only suitable for topical medication delivery.These issues can compromise the delivery efficiency and shelf life of the formulation. When considering the scale up of liposomal formulations, the production requires sophisticated technology and precise conditions, leading to higher manufacturing costs and complexity, which can hinder large-scale production and commercialization. Also, regarding the LE, achieving high drug loading and consistent LE can be difficult, limiting the amount of drug delivered transdermally [42].

1.2.5. Enhancing The Liposome Efficacy : New age liposomes

In order to overcome the drawbacks of liposomes, new types of liposomal systems are being developed. Some of these systems include transferomes, ethosomes and TEs.

1.2.5.1. Transfersomes. First defined by Cevc et al., the transfersome was the first elastic liposomal system, where surfactants (such as sodium cholate, spans and tweens) are added as edge activators. Edge activators make the system adaptable to stress and allow the vesicle to pass through smaller openings than themselves. It is possible to payload both hydrophilic and hydrophobic molecules in transfersomes. The choice and amount of the edge activator plays and important role in the nature of the vesicles, such as size, LE and surface charge. The various skin layers exhibit different hydration levels. While the upper layers have around 15% of water, the epidermis has around75%. This causes a hydration gradient. Since the transfersomes are hydrophobic, main mechanism of action is thought to be through this hydration gradient [44].

1.2.5.2. Ethosomes. First introduced by Touitou et al., ethosomes are made of high concentrations of ethanol and water, in addition to the phospholipids. The ratio is usually 2 - 5% phosphatidylcholine, 20 - 45% ethanol and water to 100% (w/w). This composition provides them with unique properties that improve drug penetration and efficacy. Due to the ethanol included in the lipid bilayer, these vesicles show smaller

particle sizes, negative zeta potential, high LE and better stability, which allows them to be more efficient in drug delivery and provide a negative surface charge which prevents electrostatic attraction, also preventing aggregation. Another effect of ethanol is that is disrupts the SC layer, allowing a better passage of the vesicle [45, 46].

1.2.5.3. Transethosomes. In a novel study, Song et al. described a new type of vesicle, combining the properties of transfersomes and ethosomes, and named these new generation of liposomes, TEs. TEs contain ethanol and a permeation enhancer or edge activator (tween 80, tween 60, tween 20, sodium deoxycholate, and propylene glycol). When compared, the elasticity and permeation of TEs were superior to their precursors; conventional liposomes, transfersomes and ethosomes [47].

TEs contain about $10 - 20$ % ethanol that acts on the skin to increase permeability and lends softness to the vesicles. The LE is directly related to the ethanol content as it increases the solubility of of both hydrophilic and lipophilic active ingredients that are loaded into the vesicles. It is important that the ethanol content is kept at the optimum level, since too much ethanol would lead to vesicles that are too soft and give way to leakages [48].

Permeation enhancers increase the fluidity of the vesicles. Edge activators lend deformability to the vesicle membrane. Anionic, cationic and non-ionic surfactants are suitable as edge activators. Drugs with molecular weights from 130 to 325 kDa are suitable for loading in TEs. Similar to transfersomes, it is thought that the TES also permeate the skin layer due to the hydration gradient, since the SC has about 15% less water than the other skin layers. The elasticity of the vesicles is key to their penetration [46]. Skin penetration mechanisms of new age vesicular structures are illustrated in Figure 1.6.

The most common method used to create TEs is the cold approach. This technique works well for medications that are heat-sensitive. This process involves mixing lipids with room-temperature ethanol while stirring constantly. Next, edge activator is

added, and the liquid is heated to ambient temperature while being vigorously stirred. After that, the created mixture is stirred for five minutes in a covered container. Before adding the water to the alcoholic mixture, it is also heated in a separate container. Subsequently, sonication is applied in order to reduce TE size. The resulting formulation is then stored in a refrigerated environment.

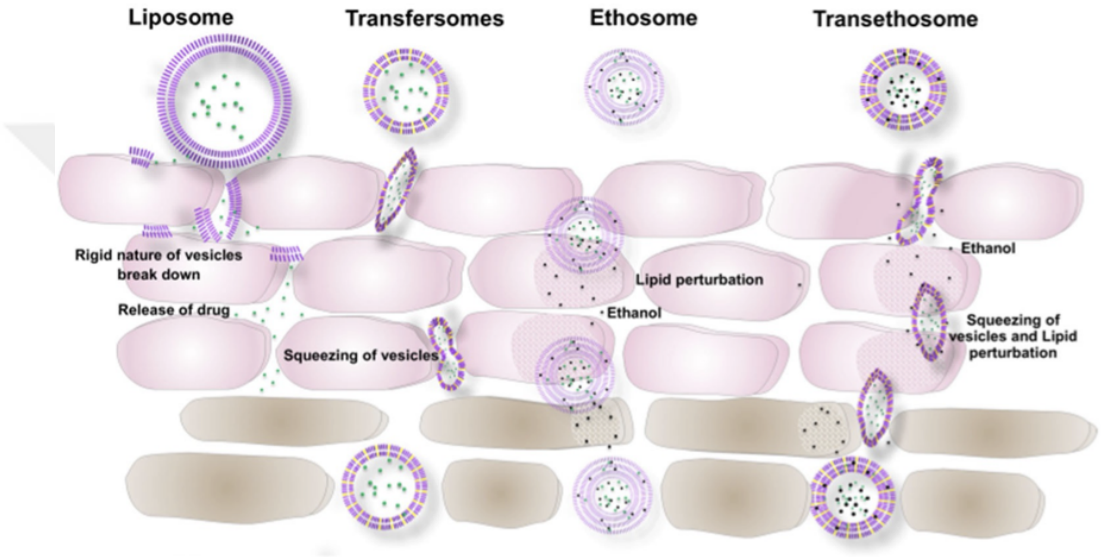

Figure 1.6. A schematic diagram of skin penetration mechanisms of liposomes, transferomes, ethosomes and TEs [40]

The usage of TEs in transdermal delivery is a highlighting study topic for cosmeceutical and pharma industry. The majority of the research is still in the experimental or clinical trial phases. Studies have shown promising results for the use of TEs in delivering various drugs, including anti-inflammatory agents, antifungal medications, and even vaccines. Ascenso et al. has formulated TEs with a dual loading of vitamin E and caffeine and found that TEs were more stable and had better drug flux than ethosomes and transfersomes [49]. Anwar et al. has loaded green tea and found that the TE systems had better skin penetration than ethosomes [50]. Kim et al. has loaded palmitoyl pentapeptide (anti-aging) and found that TEs were promising carriers [51].

1.2.6. Current Applications of Liposomes in Cosmeceuticals Industry

The global liposome cosmetics market was estimated to be worth 2861.58 million USD in 2020 and was projected to increase at a compound annual growth rate of 7.67% from 2020 to 2027, according to the liposome cosmetic market size and share report 2021. Among the leading companies in the liposomal cosmetic market; there are Lipoid Cosmetic Firm, Lucas Meyer Cosmetic Firm, Nippon Fine Chemical Company, Enoc Pharma Enterprise, Nanovec producers, and Lipotec Company [52]. Acne is a problem, affecting 85% of the population, typically teenagers. Tetracycline and tretinoin are widely used antibiotics for acne treatment. However, prolonged use of such broad-spectrum antibiotics leads to acne-building pathogen resistance. It was found that when these antibiotics are loaded within liposomes, they were more effective in smaller doses [53]. Similarly, when the anti-comedogenic clindamycin was loaded in a liposomal system, it was found to be more effective not just for open comedones, but also for closed comedones, pustules and papules [54]. While using anti-acne actives, side effects and stability issues must also be considered. Many actives such as clindamycin, tretinoin, azelaic acid and niacinamide are susceptible to degradation by UV, oxygen or heat. These actives may benefit greatly from liposomal encapsulation [52].

Liposomal systems are also of great importance for moisturizing. The phospholipids in the liposomes fuse with the skin and support the barrier, minimizing trans-epidermal water loss. Adding to the positive effect of the liposome bilayer itself, loaded actives also help to moisturize the skin. It was discovered that liposomal gels containing loaded active compounds like L-arginine, curcuma extract, hyaluronic acid, lactic acid, and tocopherol—decreased trans-epidermal water loss and increased the skin moisture. Some commercial examples of moisturizers with liposomal systems include Lancome noisome cream by L'oreal, Lysofix, Lecigel and Heliofeel, with actives such as glycerine, soja seed extract and lecithin [55].

The negative effects of the solar radiation are well-known and prolonged exposure to UV rays can even lead to carcinoma lesions on the skin. Sunscreens are not

meant to penetrate into systemic circulation but some actives tend to be absorbed. Encapsulation can help to prevent this absorption and maximize the sun protection effects by retaining actives for longer on the skin. Similar to the anti-acne actives, sunscreen actives are also susceptible to degradation and encapsulation may lead to more effective formulations [56].

When treating skin conditions, topical administration offers a number of benefits. Topical astaxanthin treatment significantly reduced AD skin inflammations, but due to its hydrophobic properties astaxanthin is not recommended for topical administration. Numerous strategies have been explored to address this issue and it was found that liposome composition may improve astaxanthin transdermal delivery [57].

Since in many topical uses it is desired that the actives penetrate the SC layer, research into ultra-deformable vesicles such as TEs is increasing. When Montanari et al. used sunlight-activated ultra-deformable liposomes, they saw encouraging results. These photodynamic liposomes were created to include zinc phthalocyanine for the purpose of curing infections caused by Leishmania braziliensis. Nevertheless, the percentage of inhibition increased dramatically when the compound was loaded in ultra-deformable liposomes and rather than ordinary liposomes, zinc phthalocyanine had a homogenous distribution across the SC and had a transcutaneous penetration that was roughly ten times higher with that new age liposomes [58]. The complexing of anesthetics and their subsequent encapsulation in new-generation liposomes was discussed by Maestrelli et al. After being complexed with cyclodextrins, benzocaine and butadiene were loaded in ultra deformable liposomes. The acquired results showed an increase in the anesthetic in vivo effect's duration and intensity, in addition to an increase in the skin penetration of the actives [59]. Melatonin was selected by Dubey et al. to create a novel transdermal application due to its short half-life, low molecular weight, and variable oral absorption. Melatonin's cutaneous penetration was boosted by roughly 5 and 12.3 times, respectively, when it was loaded into elastic liposomes as opposed to conventional liposomes and the free melatonin solution [60]. These investigations demonstrate the adaptability of liposomal systems in encapsulating various

compounds, yielding encouraging outcomes for transdermal delivery.

2. RESEARCH OVERVIEW

This dissertation encompasses three research projects under one objective which is design and fabrication of TEs for AD patients. This aim has been accomplished by formulation of three different kinds of TEs that contain mainly ceramides, vitamins and proteins. In all of the systems, TE based nano-particles were used to provide enhanced skin delivery for AD. AD is a chronic, non-contiguous condition characterized by dry, itchy and inflamed skin that has no current cure but can be managed with the correct care.

Approaches involved utilization of ceramide, VitC, VitE and filaggrin, caspase-14 and PAD-1 proteins within TEs. TEs are kind of vesicles that contain ethanol and an edge activator like Tween 80 within their compositions and superior to conventional liposomes in terms of elasticity, permeation, loading capacity and efficiency. TEs have been widely utilized for transdermal delivery of the cosmeceuticals and pharmaceuticals, with promising results in anti-inflammatory agents, anti-fungal medications, and vaccines in recent studies. In this study TEs containing Soy PC, cholesterol, Tween 80 or oleic acid, Cer3 and ethanol were formulated.

Cer3 was included in the first approach for its crucial role in controlling trans epidermal water loss which is a function of water permeability of the skin barrier. It is the main ceramide subtype found in healthy skin that decreased levels of this molecule causes AD symptoms. Cer3 is used specifically in a broad variety of cosmeceutical products because of its known efficiency in improving skin barrier function and reducing the risk of trans-epidermal water loss as well as being a restoring lipid in AD treatment. Cer3 containing TEs were formulated successfully to be used in transdermal delivery studies and they were capable of loading both hydrophilic and hydrophobic cargo. TEs were analyzed in terms of size, homogeneity, morphology and LE% and Cer3 inclusion findings can be used in potential topical applications in AD curing studies.

VitC and VitE were used in the second approach for AD treatment and effect of surfactant type on loading efficiency was analyzed. VitC is a crucial antioxidant in dermatology, involved in tissue repair, collagen synthesis, and neurotransmitter production, but its stability is essential for its usefulness. ViE is known for its antioxidant properties against free radicals and anti-inflammatory properties. It has been reported that free radicals contribute to allergic inflammation and oxidative stress, leading to the development of AD. The antioxidant and anti-inflammatory properties of VitE and VitC, when delivered through transdermal agents, could be a promising supplementary treatment for AD skin disease. Dual loading of VitC and VitE within TEs either containing Tween 80 or oleic acid was successful for both formulations to be used in transdermal delivery studies. With chitosan coating, application areas of the obtained TEs was intended to be broaden like oral medications and face masks. All the TEs were characterized in terms of size, size distribution, morphology, stability and LE% and they were capable in using AD treatment studies. VitC and VitE were successfully loaded within TEs with reinforced stability and LE% with chitosan.

Proteins were used in the third approach for their enhancing effects on AD treatments. The study explored a passive delivery strategy for delivering filaggrin, PAD-1, and caspase-14 proteins through TEs to strengthen the skin barrier and treat or prevent AD. The proteins were loaded into vesicles containing Soy PC, Tween 80, Cer3, and cholesterol. The study found that all protein loaded vesicles were within acceptable size and PDI range for transdermal delivery studies.

Applicability of developed systems as transdermal delivery agents is the future work of this thesis. In particular, transdermal skin delivery capacity and cyto-toxicity studies may result in a promising treatment for AD patients. In just United States more than 17.8 million people are living with AD, with the majority of cases remaining undiagnosed. According to the liposome cosmetic market size and share study 2021, the worldwide liposome cosmetics market was 2861.58 million USD in 2020 and expected to rise at a rate of 7.67% from 2020 to 2027. So further studies to develop cosmetic products by implementing the obtained systems could be a wise move.

3. CERAMIDE 3 EFFECT ON PHYSICAL PROPERTIES OF AMBORA EXTRACT AND CHROMABRIGHT LOADED TRANSETHOSOMES

3.1. Introduction

Human skin is the vital organ that acts as the main barrier for protection against outer agents and the function of skin barrier is basically characterized by skin lipids such as ceramides, cholesterol, cholesteryl esters and fatty acids and the ratio between these lipids determines the skin integrity and health. Among these lipids, ceramides play a key role to keep the skin barrier healthy and it has been reported that disorganization in ceramides, fatty acids, cholesteryl esters and cholesterol ratio causes skin impairments such as psoriasis, ichthyosis, AD and acne [61, 62].

The primary lipid components of the lamellar sheets found within the intercellular gaps of the skin barrier are the ceramides. They represent about 50 % of the total lipid amount of the skin lipids. Ceramides are a complex and structurally varied class of sphingolipids that are formed from the linkage of fatty acids to sphingosine bases by amide bonds. There are at least eight major free ceramides and two major protein-bound ceramides found in the human skin lipid composition. More than 340 types of ceramides have been identified in the outermost layer of the human skin alone. Factors like variations in chain length, head groups, position and degree of hydroxylation and saturation are responsible for the diversification in the structures of ceramides as shown with an "R" in Figure 3.1. Fatty acid chain lengths can vary between 16 and 60 carbon atoms and ceramides are named based on their molecular structure, mainly determined by the chain length and the position of amide linkage between the head group and the fatty acid chain [63–65].

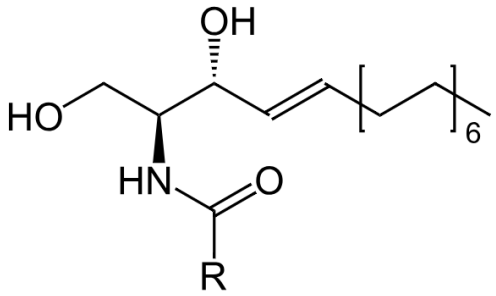

Figure 3.1. General structure of ceramides (Created with Chem Draw, accessed on June 2024)

Ceramides with higher number of carbons, such as ceramide 1 and 3, are the most crucial subgroups for maintaining the skin barrier function. One of the main roles of these ceramides is to control trans epidermal water loss which is a function of water permeability of the skin barrier, by determining water retention capacity. Ceramide 3 (Cer3), which is N-acylated phytosphingosine is the main ceramide subtype found in healthy skin that decreased levels of this molecule causes AD symptoms [61], [66,67]. Many brands like Triple Lipid Restore, SkinCeuticals, Avène, Dr. Jart develop formulations containing ceramides jointly with fatty acids and cholesterols in order to replace the skin barrier components and improve the skin barrier. Cer3 is used specifically in a broad variety of cosmeceutical products like Eucerin Smoothing Repair Dry Skin Lotion, Eucerin Eczema Relief Body Crème, CeraVe Moisturizing Lotion, CeraVe Suncare Sunscreen Face SPF 30, because of its known efficiency in improving skin barrier function and reducing the risk of trans-epidermal water loss as well as being a restoring lipid in AD treatment. Clinical studies performed within the patients with AD have showed the effectiveness of these products at improving skin hydration and skin barrier function [64], [68–70].

Patients with AD have hereditary abnormalities that result in changes in the contents of ceramides and a decrease in Cer3. According to latest studies, total ceramides:cholesterol ratios in AD patients were considerably lower than those of people with normal skin. Total ceramide levels in healthy skin were approximately 30% higher

than in skin with AD; the ratio of total ceramide to cholesterol was 2.24 in healthy skin and 1.53 in skin with AD. Additionally, trans epidermal water loss, an active indicator of AD, was found to be substantially correlated with the relevance of Cer3 across all ceramide subgroups [62], [65], [71, 72]. Therefore, transdermal delivery of this lipid may provide opportunities for reducing ceramide deficiency and enhancing the skin condition. However, the skin can only absorb a limited amount of conventional formulations, and the inclusion of these components into nano-carriers has been extensively researched [64], [70], [73, 74].

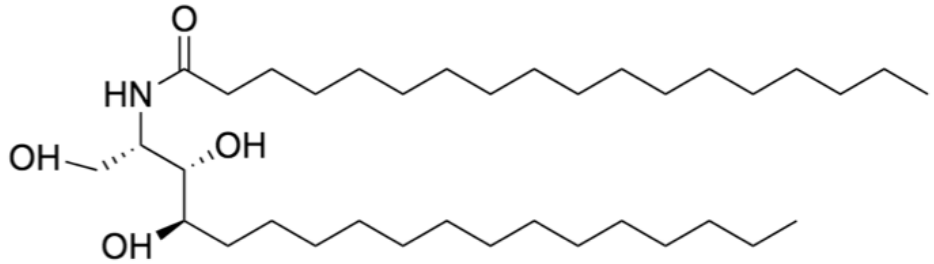

Figure 3.2. Structure of Cer3 (Created with Chem Draw, accessed on June 2024)

Direct application of cosmeceuticals to the skin promotes penetration through the skin's bilayers, and used for many years as an effective way to deliver the required compounds to the targeted locations [75]. Topical treatments that mimic the biological skin membrane can penetrate the skin more deeply if their structures are comparable to those of the epidermis [76]. Recently, topical delivery agents at the nanoscale, such as liposomes, have been used in skin applications to influence the various skin layer components through their unique physicochemical properties simulating the epidermis [77,78]. TEs are liposomes that are prepared with ethanol and an edge activator; while edge activator increases the flexibility of liposomes during penetration, ethanol acts as a penetration enhancer via skin layers. Therefore, because of their special qualities, TE usage has recently become quite essential in the cosmeceutical transdermal delivery [49], [79–81].

In this chapter, a TE formulation comprising cholesterol, cholesteryl sulphate, Tween 80, Cer3, and soybean phosphatidylcholine (Soy PC) was developed for the

skin conformity of AD patients and increasing the efficacy of AD treatment solutions was aimed. Physical properties of the TEs in terms of size, morphology, size distribution and stability was examined in relation to the impact of Cer3 addition. Strong hydrophobicity of Cer3 was mitigated by using ethanol and tween 80 in the formulation and Cer3 incorporation within the lipid bilayers was optimized. Two payloads, Ambora extract and Dimethylmethoxy Chromanyl Palmitate, with different solubilities, were chosen to investigate the loading yields of the obtained TEs. Ambora extract was chosen as a hydrophilic cargo because of its therapeutic outcomes on rosacea and eczema skin diseases. It is abundant in flavonoids, which may be used in cosmeceutical formulations as an anti-inflammatory, anti- irritant and anti-oxidant [82]. Dimethylmethoxy Chromanyl Palmitate (Chromabright™), which is a novel molecule for skin glowing was preferred as a hydrophobic cargo due to its preventive effect on photo-aging. Studies conducted in vitro have demonstrated that, it controls the process of skin pigmentation by preventing the formation of melanin, which causes skin coloration [83]. Obtained TEs were analyzed via DLS, optical microscopy and scanning transmission electron microscopy (STEM) and LE% were followed by ultraviolet-visible (UV/Vis) spectroscopy.

3.2. Experimental

3.2.1. Materials

Soy PC with 94 % PC content, in light orange colored grease form, was kindly provided by Lipoid GmBH (Ludwigshafen, Germany) under the brand name of Lipoid S 100. Soy PC was chosen as the main lipid in designing of TEs because it is the most abundant phospholipid found in eukaryotic cell membranes and it has a high amount of polyunsaturated fatty acids to preserve a good oxidative stability [84, 85].

Cholesterol in white powder form with more than %99 purity and cholesteryl sulphate in white powder form with more than %99 purity were purchased from Sigma Aldrich. The addition of cholesterol to the lipid composition provides fluidity, flexibility, and permeability to the bilayer structure by stabilizing the bilayers. It also helps

to reduce the leakage problems during the loading studies [86–88]. To obtain a bilayer system that mimics the skin composition, cholestryl sulphate should be added to the lipid composition. Role of cholestryl sulphate in epidermal cells is very important; it regulates epidermal differentiation, sustains barrier function and helps desquamation process [89].

Tween®80 and ethanol with 99 % purity were purchased from Merck. Tween®80 was in the form of yellow liquid and used as an edge activator. Ethanol was used to solubilize the hydrophobic materials used in the formulation.

Cer3, chromabright and ambora extract were kindly provided by Novodist Turkey in white solid forms. Ambora extract was used as a hydrophilic cargo material where as chromabright was used as a hydrophobic cargo material.

Water was used as the main solvent for the hydrophilic materials. It is used to produce vesicular dispersions. All the experiments were performed using ultrapure Milli-Q water (Type 1) from Millipore instrument.

3.2.2. Methods

3.2.2.1. Preparation of TEs. TEs were prepared using the cold method [29,90]. Briefly, after dissolving all the lipids and hydrophobic contents fully in ethanol within a 25 mL round bottom flask, the temperature of the medium was conserved as 35°C during magnetic stirring at 750 rpm. Ambora extract was dissolved in aqueous phase containing ultra pure water and heated separately and kept at 35°C. The aqueous phase was added to the ethanol solution drop by drop using a 1 mL syringe with a speed of 250 µL/min as illustrated in Figure 3.3. In all the formulations, total lipid concentration in the final TE dispersion was preserved constant as 10 mg lipid per ml of total dispersion and ethanol:water volume ratio was fixed as 3:7.

Table 3.1. The mass ratios of Soy PC:Tween 80:cholesterol:cholesteryl sulphate (Chol. sulphate): Cer3 in different TE formulations

Sample	**Soy PC**	**Tween 80**	**Cholesterol**	**Chol. Sulphate**	**Cer3**
TE1	15	0.5	-	-	-
TE2	15	1.0	-	-	-
TE3	15	1.5	-	-	-
TE4	15	1.5	1.0	-	-
TE5	15	1.5	1.5	-	-
TE6	15	1.5	2.0	-	-
TE7	15	1.5	1.5	0.37	-
TE8	15	1.5	1.5	0.74	-
TE9	15	1.5	1.5	1.1	-
TE10	15	1.5	1.5	-	0.9
TE11	15	1.5	1.5	-	1.5
TE12	15	1.5	1.5	-	1.9
TE13	15	1.5	1.5	-	2.8

TE sizes were reduced and homogenized by using Avanti Polar Lipids mini extruder equipped with 0.1 µm pore size polycarbonate membranes and 1000 µL syringes. Each dispersion was subjected to 11 consecutive filtrations through the polycarbonate filters to ensure uniformity. The final dispersions were wrapped in aluminum foil and placed in the refrigerator at 4°C for further usage and analysis. The lipid mass ratios used in different TE formulations can be found in Table 3.1, presented as Soy PC:Tween80:cholesterol:cholesteryl sulphate:Cer3 mass ratios. Each new experiment (i.e., TE4, TE5 and TE6) was conducted with the best candidate formulation of the previous experiment (i.e., TE3) in terms of size and homogeneity.

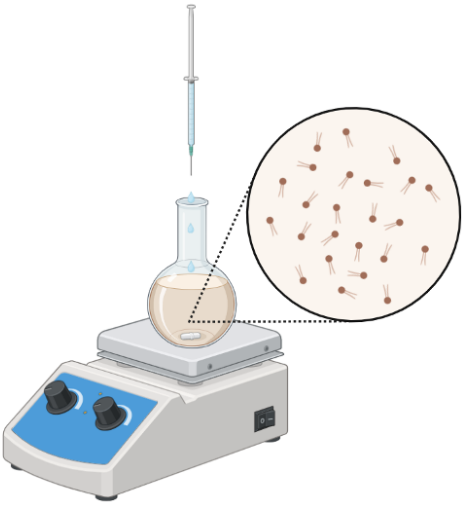

Figure 3.3. Schematic representation of cold method TE preparation (Created with BioRender.com, accessed on June 2024)

3.2.2.2. Characterization of TEs. The Brookhaven Instruments 90 Plus Particle Size Analyzer was used to operate DLS measurements to follow the size and size distribution of the samples. The measurements were carried out after diluting each final TE dispersion with Type 1 water (1:10). TEs were analyzed in terms of size and PDI which gives the overall quality of the TE solution with respect to homogeneity. For optimal skin penetration, the ideal vesicle size was predicted to be about 120 nm, while PDI values less than 0.2 suggested a mono-disperse, acceptable size distribution for homogeneous vesicle systems [91]. Leica DMI 6000 B optical microscopy was used as a primary and rapid visualization method to obtain images of the vesicles. Basic light microscopy itself is unable to provide comprehensive information about the lipid bilayer, so the samples that were certain of being in good condition were then subjected to electron microscopy [92]. Briefly, a drop of sample was put on the microscope glass and enclosed with cover glass. Vesicles were observed freshly under either 10 times or 20 times magnification. The shapes, sizes, and surface morphologies of the TEs were also examined STEM technique using Thermoscientific QUATTRO S SEM equipment centered at Boğaziçi University Center for Life Sciences and Technologies. Before being examined, wet samples were placed onto formvar copper grids and allowed to air dry

for three hours. Dried film specimens were imaged at 8-12 kV with a magnification range changing from 50.000 to 300.000.

3.2.2.3. Calculation of LE%. To separate the loaded vesicles from the bulk solution, the ultracentrifugation technique was used as a quick and effective option as represented in Figure 3.4. The Vivascience Vivaspin 2 mL concentrator and the Rotafix 32 Hettich centrifuge were used in conjunction to filter the loaded vesicle suspensions. Every sample was centrifuged at room temperature at 6000 rpm. Periodically, solutions at the bottom of the filtration tube were inspected using UV/Vis spectrophotometer, and by this way any excess payload was removed. Maximum absorbance wavelength for ambora extract was detected as 286 nm whereas it was 274 nm for chromabright. There was no observed interference between the maximum absorbance wavelenght of the loaded components and the other lipid compounds. After they had all been removed from their external media, the loaded TEs were broken down and their released payload was measured using a UV/Vis spectrophotometer.

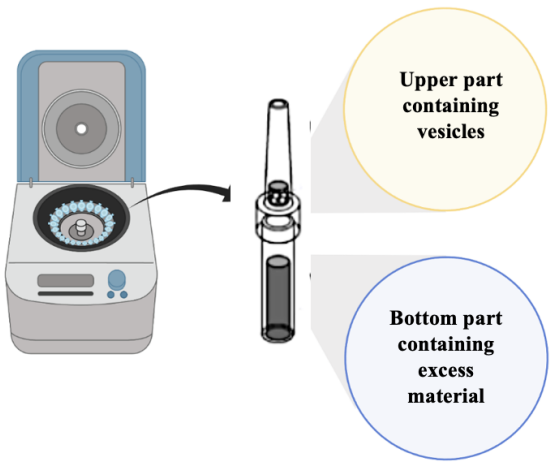

Figure 3.4. Schematic representation of ultra-centrifugation method (Created with BioRender.com, accessed on June 2024)

Breakdown of the TEs was carried out upon dilution of each samples with 1:10 (v/v) ethanol:water and 30 min vigorous shaking with a vortex to be able to ana-

lyze their LE%. DLS measurements of the broken TEs revealed no significant peaks, indicating that the lipid bilayer had been disrupted successfully. Additionally, the characteristic blue color of the vesicles vanished during the breakage process. By comparing the amount of loaded payload to the amount of payload that was initially added, the LE% were determined. Particle size, homogeneity, and percent LE% data were assessed for each sample after a month of storage, during which time they were all refrigerated at 4°C to monitor their physical stabilities.

3.2.2.4. Statistical Analysis. Every experiment was conducted in a minimum of three duplicates, and the data were then displayed as the mean ± standard deviation. The effect of increasing the Cer3 content on the size and uniformity of the TEs was examined using linear regression analysis. The statistical analysis to examine the impact of Cer3 addition on loading hydrophilic and lipophilic payloads was conducted using two-way analysis of variance (ANOVA). If a difference in p-value was less than 0.05, it was considered statistically significant.

3.3. Results and Discussion

3.3.1. Preparation and Characterization of Cer3 Containing TEs

3.3.1.1. Addition of Tween 80 to the Formulation. In order to create a TE, Tween 80 was initially added as an edge activator with Soy PC:Tween 80 mass ratios of 15:0.5, 15:1, and 15:1.5. The impact of these mass ratios on the size, homogeneity, and morphology of the vesicles were examined. DLS was used to measure size and size distributions, while STEM was used to visualize the resulting vesicular dispersions. TEs obtained using all mass ratios of Tween 80 exhibited excellent homogeneity with very low PDI values, and sizes within the permissible range for applications involving skin penetration. Table 3.2 shows that size was decreased without affecting the homogeneity as Tween 80 content was increased. The surface tension of the vesicle membranes could be balanced by increasing the mass ratio of Tween 80, which would promote stability and reduce payload leakage. But when Tween 80 was added in excess of a specific

threshold, it could disrupt the orderly arrangement of phospholipids and damage the liposome structure, which lowers LE%. Therefore, increasing the stability and the LE% of the TEs were facilitated by adding an appropriate amount of Tween 80 [93–95].

Table 3.2. Effect of Tween 80 Content on Size and Homogeneity of TEs

Sample	**Soy PC**	**Tween 80**	**Size (nm)**	**PDI**
TE1	15	0.5	71.40± 2.96	0.09±0.01
TE2	15	1.0	64.77± 4.97	0.09±0.01
TE3	15	1.5	62.60± 4.25	0.11±0.06

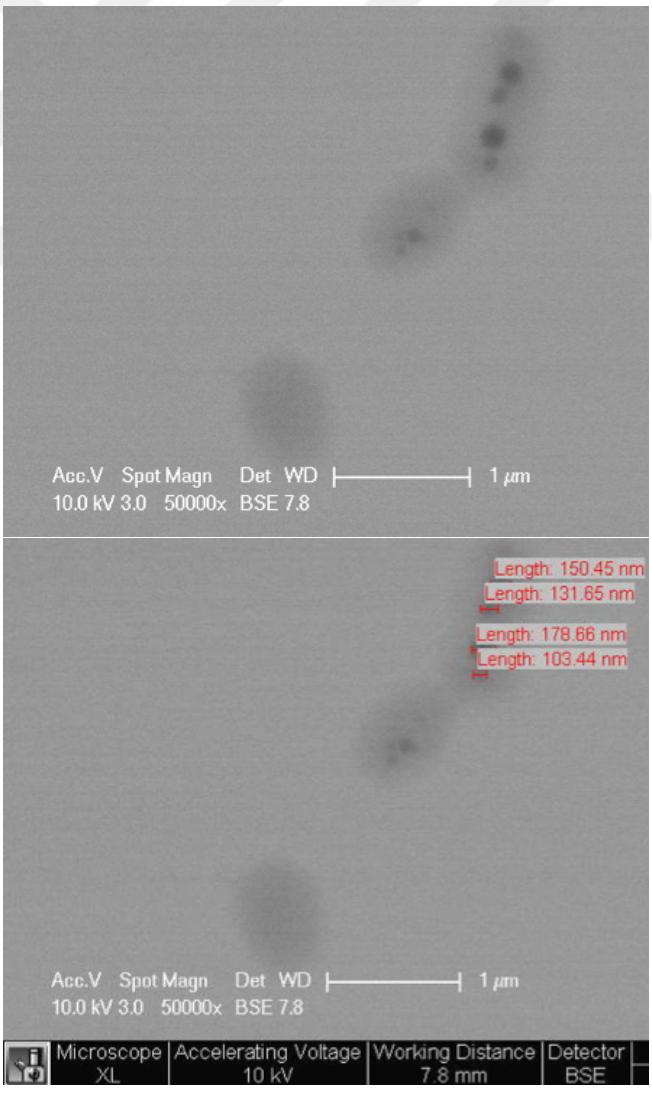

Figure 3.5. STEM images showing TE3 samples, containing 15:1.5 mass ratio of Soy PC:Tween 80 ; with and without size tags

So, 15:1.5 Soy PC:Tween 80 containing TE3 formulations were selected for the following experiments. In Figure 3.5, STEM image of uniformly distributed TE3, containing 15:1.5 Tween 80 with around 100 nm size range could be seen with and without size tags.

3.3.1.2. Addition of Cholesterol to the Formulation. In the lipid composition, cholesterols provide fluidity, flexibility, and permeability to the vesicle membranes. A rigid and more saturated membrane with a greater cholesterol content improves vesicle stability and helps to reduce the leakage problems [86–88]. Ceramides, cholesterol, and free fatty acids are the main lipids present in human skin and account for roughly 50, 25 percent, and 15 percent of the SC lipid matrix by mass, respectively [96]. Therefore, adding cholesterol to our vesicular system up to a maximum of 25 mass percent may be a smart idea to produce more stable vesicles with improved skin penetrating capabilities. In order to accomplish this, three different formulations including Soy PC:Tween 80:Cholesterol were made with mass ratios of 15:1.5:1, 15:1.5:1.5, and 15:1.5:2.0. Comparision of TEs with varying cholesterol amounts is shown in Table 3.3.

Table 3.3. Formulations with varying mass ratios of Soy PC, Tween 80 and cholesterol and comparison with respect to mean size and PDI values

Sample	**Soy PC**	**Tween 80**	**Cholesterol**	**Size (nm)**	**PDI**
TE3	15	1.5	-	62.60±4.25	0.11±0.06
TE4	15	1.5	1.0	53.70±4.12	0.09±0.01
TE5	15	1.5	1.5	75.28±15.17	0.07±0.03
TE6	15	1.5	2.0	76.90±3.76	0.16±0.08

Vesicle size was first reduced by immersion in 15:1.5:1 cholesterol, but it later began to rise as the cholesterol concentration increased. The intended size range was reached with every TE formulation; however, when more than 15:1.5:1.5 cholesterol was added, i.e., TE6, the mono-dispersity of the colloidal solutions began to break

down. The outcomes aligned with the literature data provided by S.C. Lee et al., who deduced that the average particle size increased in proportion to the increase in cholesterol concentration [97]. The vesicle sizes and PDIs were all within the desired range (less than 120 nm size and less than 0.2 PDI); however, LE% would be reduced if the cholesterol ratio was increased beyond 15:1.5:1.5, as cholesterol would enter the bilayer system and compete with the loaded materials [98]. Consequently, the TE5 formulation, which had a mass ratio of 15:1.5:1.5 for Soy PC:Tween 80:Cholesterol, was selected for additional investigations since it sustained a more homogenous system with a lower PDI value and wouldn't reduce the LE% in the following loading studies. The STEM data presented in Figure 3.7, which depicts a TE medium containing roughly 100 nm-sized, uniformly distributed, round-shaped particles, further confirmed the size and homogeneity results obtained by the particle size analyzer.

3.3.1.3. Addition of Cholesteryl Sulphate to the Formulation. Cholesteryl sulphate should be added to the lipid composition around 10% by total mass in order to create a vesicle system that most closely resembles the composition of the human skin. In epidermal cells, cholestryl sulphate plays a crucial role in controlling epidermal differentiation, maintaining barrier function, and bringing about desquamation. The process of skin cell creation, shedding, and replacement is called desquamation [89]. To achieve this, three different formulations with Soy PC:Tween 80:cholesterol:cholesteryl sulphate containing mass ratios of 15:1.5:1.5:0.37, 15:1.5:1.5:0.74 and 15:1.5:1.5:1.11 were prepared.

In Table 3.4, comparison of mean size and homogeneity values of the vesicles with different cholestryl sulphate mass ratios can be seen. Even though their size range were applicable to be used in transdermal delivery, none of the vesicles containing cholestryl sulphate were within the acceptable PDI range, which meant that they had to be smaller than 0.2. High PDI values indicated elevated heterogeneity levels of the vesicular dispersion.

Table 3.4. Varying mass ratios of Soy PC, Tween 80, cholesterol and cholesteryl sulphate (Chol. S.) and comparison with respect to mean size and PDI values

Sample	**Soy PC**	**Tween 80**	**Cholesterol**	**Chol. S.**	**Size (nm)**	**PDI**
TE5	15	1.5	1.5	-	75.28±15.17	0.07±0.03
TE7	15	1.5	1.5	0.37	41.3±16.72	0.34±0.13
TE8	15	1.5	1.5	0.74	89.4±18.17	0.23±0.16
TE9	15	1.5	1.5	1.11	98.0±13.46	0.36±0.18

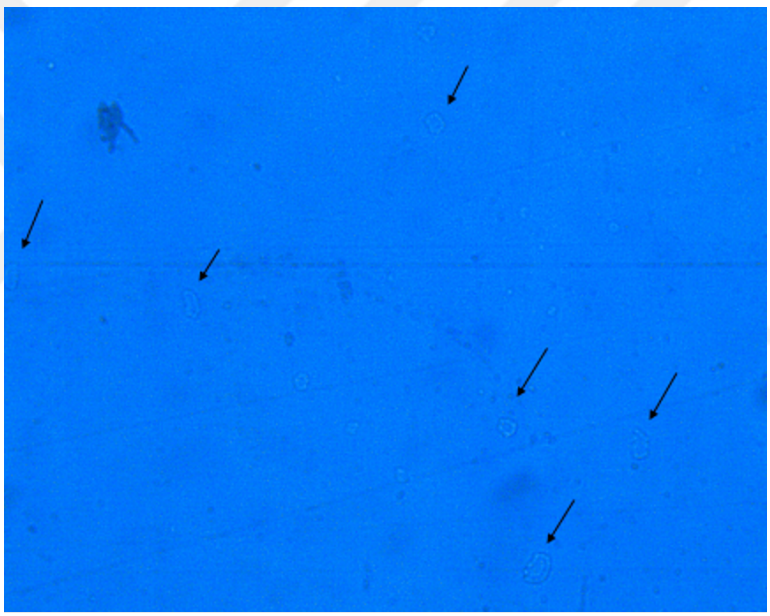

Figure 3.6. Optical microscopy image of TE8 under 50x magnification

From the optical microscopy image seen in Figure 3.6, necklace-like aggregation batches and big agglomerations within the formulation of TE8, containing 15:1.5:1.5:0.74 mass ratios of Soy PC:Tween80:Cholesterol:Cholesteryl Sulphate, could be clearly observed exhibiting the cause of heterogeneity. Also, Figure 3.8 indicated the small and big aggregations within the liposomal suspension of TE9, containing 15:1.5:1.5:1.11 mass ratios of Soy PC:Tween80:Cholesterol:Cholesteryl Sulphate. From this optical microscopy image, there could be seen both distinct and clustered TEs where from STEM image of the same formulation a big chunk of TEs that were stuck together could be observed. Also,each of the three formulations containing cholestryl sulphate

showed milky aggregations within the colloidal dispersions upon a few days of storage. As a result, it could be concluded that addition of cholesteryl sulphate to the vesicle medium was ineffective with cold method process and it was dismissed from the further formulations due to stability and heterogeneity problems.

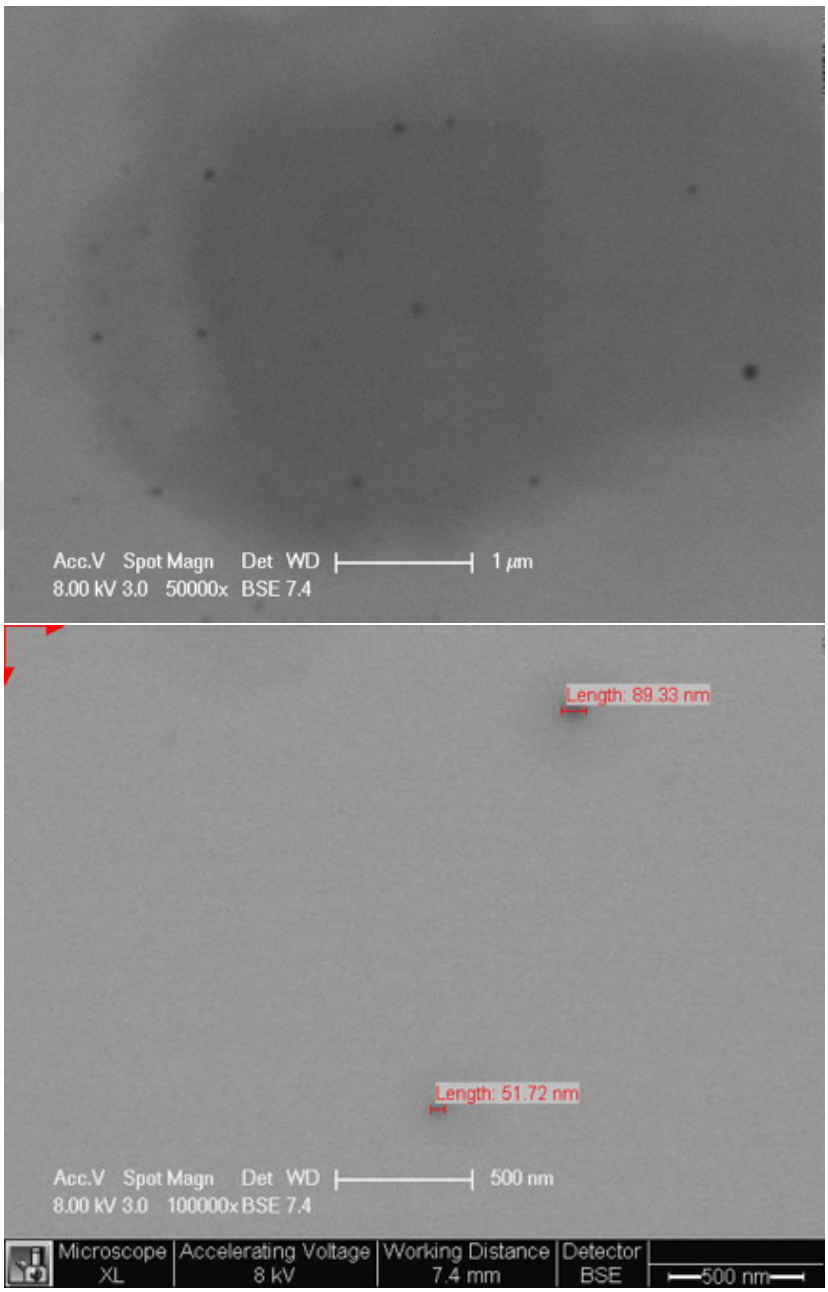

Figure 3.7. STEM images showing TE5 samples, containing 15:1.5:1.5 mass ratio of Soy PC:Tween 80:Cholesterol; with and without size tags

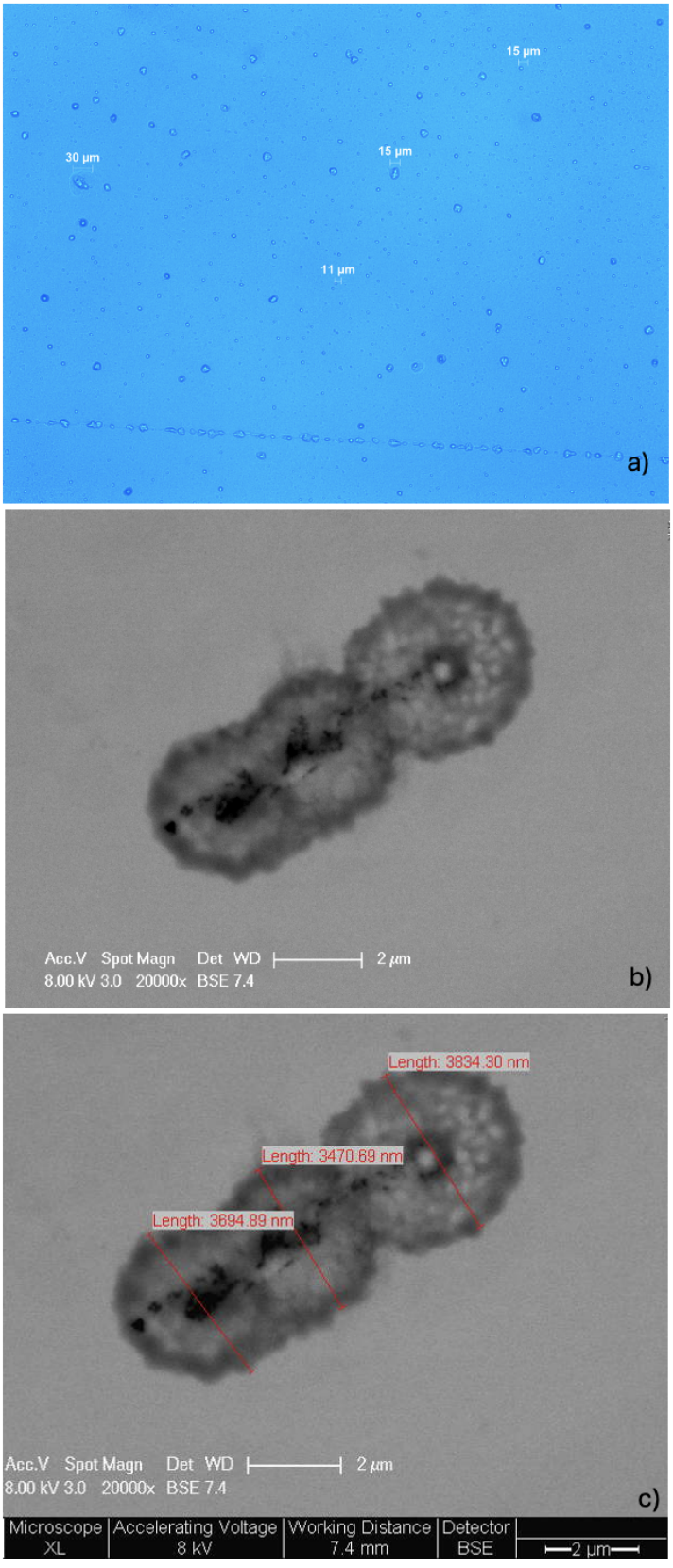

Figure 3.8. a) Optical microscopy image of TE9 under 50x magnification b)STEM image of TE9 c) STEM image of TE9 with size tags

3.3.1.4. Addition of Cer3 to the Formulation. Patients with AD have genetic abnormalities that result in changes to the contents of ceramides and a decrease in Cer3 levels and studies showed that, total ceramides:cholesterol ratios in AD patients were 30% lower than healthy skin. So, transdermal delivery of this lipid may present chances to improve ceramide insufficiency and enhance the skin health. In order to provide Cer3 to AD patients through transdermal distribution by utilizing TEs, an experiment was designed with four different mass ratios containing 15:1.5:1.5:0.9, 15:1.5:1.5:1.5, 15:1.5:1.5:1.9, and 15:1.5:1.5:2.8 of Soy PC:Tween80:cholesterol:Cer3, respectively as summarized in Table 3.5.

Table 3.5. Formulations with various mass ratios of Soy PC:Cer3, together with their mean size, PDI, and one-month stability data

Sample	**Cer3**	**Size (nm)**	**PDI**	**1-mo size (nm)**	**1-mo PDI**
TE5	15:0	75.28±15.17	0.07±0.03	80.46±18.66	0.06±0.04
TE10	15:0.9	83.30±8.09	0.07±0.01	377.60±14.50	0.24±0.04
TE11	15:1.5	80.17±8.60	0.06±0.03	85.12±6.51	0.09±0.03
TE12	15:1.9	88.04±5.32	0.07±0.04	250.50±34.20	0.15±0.02
TE13	15:2.8	110.90±51.71	0.14±0.10	1846.30±917.10	0.16±0.05

According to the results shown in Table 3.5, the addition of Cer3 produced a slight increase in size without significantly altering homogeneity, which was the intended outcome. These outcomes were also compatible with earlier studies performed by Mir-Palomo, which showed that introducing ceramides or another lipophilic chemical into TE systems, increased the mean diameters of the resulting vesicles [99]. Using a simple linear regression model with 21 observations, as shown in Figure 3.9 and 3.10, the effect of Cer3 concentration on size and PDI was also examined. With a p-value of 0.0102, the model demonstrated statistical significance for the size-Cer3 link, indicating a positive and significant relationship between Cer3 amount and size. Changes in the amount of Cer3 were not significantly correlated with changes in the homogeneity of the TEs within the confidence levels taken into consideration, according to the coefficient for

the Cer3 effect on PDI values, which was 0.0014 with a p-value of 0.309.

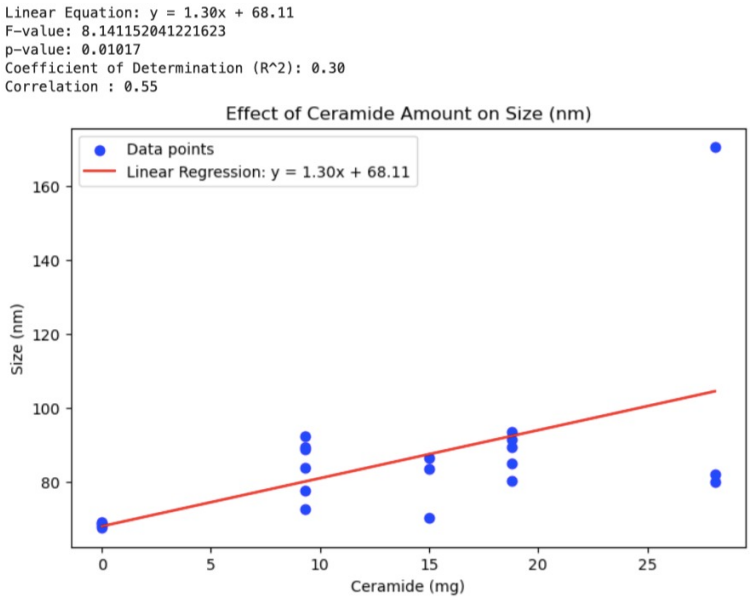

Figure 3.9. Statistical regression analysis showing a positive relationship between Cer3 increase and TE mean diameter results with a p-value of 0.0102

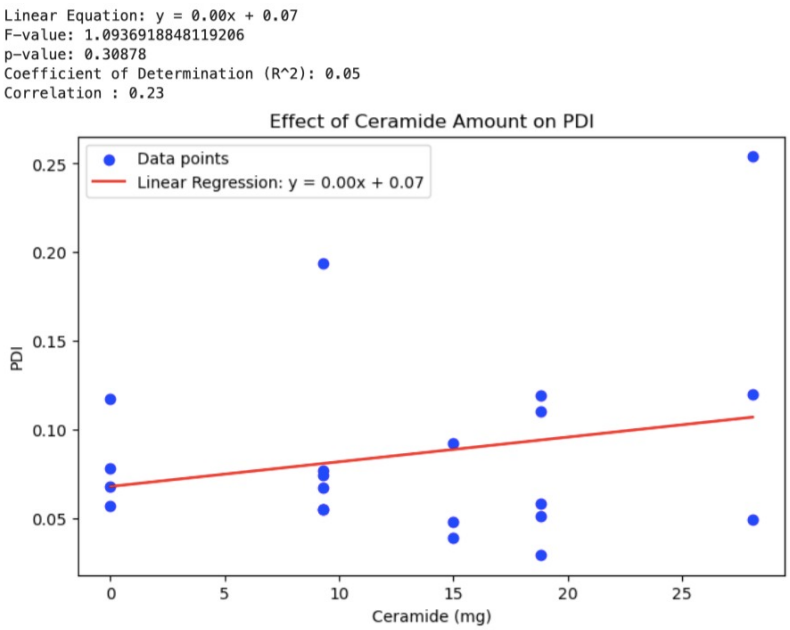

Figure 3.10. Statistical regression analysis showing no significant association between Cer3 increase and homogeneity results with a p-value of 0.309

After the introduction of 15:1.5:1.5:1.9 Cer3, a significant increase in PDI occurred, which might be attributed to the beginning of heterogeneity within the colloidal system. However, this homogeneity value was also within the approved range for mono-dispersion, which is less than 0.2 [91]. Despite the fact that TE12 formulation's mean size and PDI range fell within the permitted bounds, TE12 and TE13 formulations began to precipitate after two days of storage, and the formation of white, jelly aggregates was noted. One month stability results of these formulations with respect to mean size and PDI also demonstrated the arising impurities upon storage, both values increased dramatically. Due to instability problems with these formulations, all subsequent studies used a 15:1.5:1.5:1.5 mass ratio of Soy PC: Tween 80: cholesterol: Cer3, having a mean size of 80.17±8.60 nm and a PDI value of 0.06±0.03. This formulation also showed great stability upon one month of storage. The optical microscopy images and STEM results of this formulation, TE11, were shown in Figures 3.11 and 3.12, respectively and were in good agreement with the DLS results. Round-shaped TEs with diameters of about 90 nm were clearly seen in these pictures. Through this experiment, a TE formulation with Tween 80, cholesterol, and Cer3 was successfully obtained.

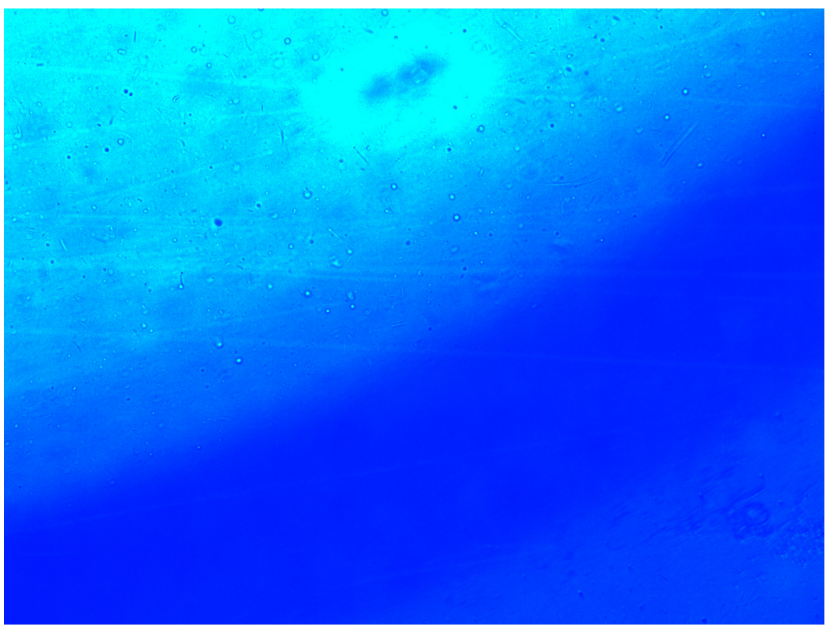

Figure 3.11. Optical microscopy image of TE11 sample under 50x magnification

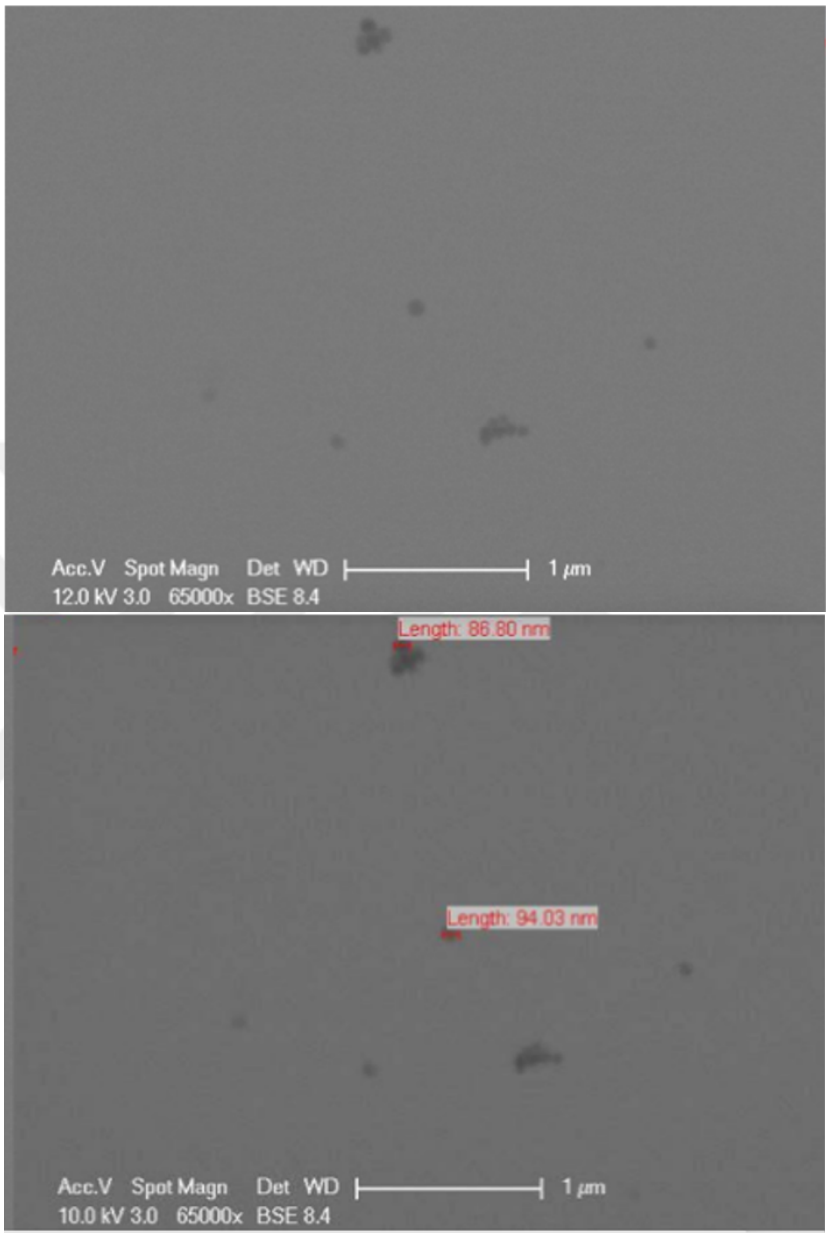

Figure 3.12. STEM images showing TE11 sample with and without size tags

Figure 3.13 and 3.14 summarize the size and homogeneity (PDI) comparisons upon Tween 80, cholesterol, cholestryl sulphate and Cer3 addition to the formulations. By analyzing these figures, also the effect of increasing these lipid concentrations on physical properties could be seen in terms of size and homogeneity.

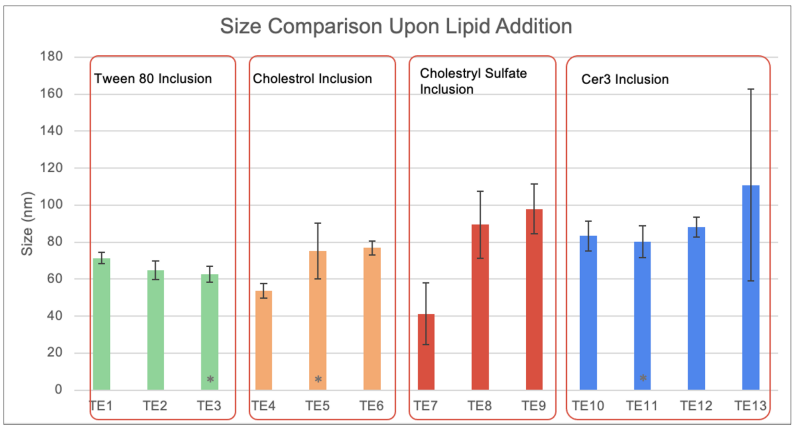

Figure 3.13. Effect of lipid additions and increase in lipid concentrations on size for various TE formulations

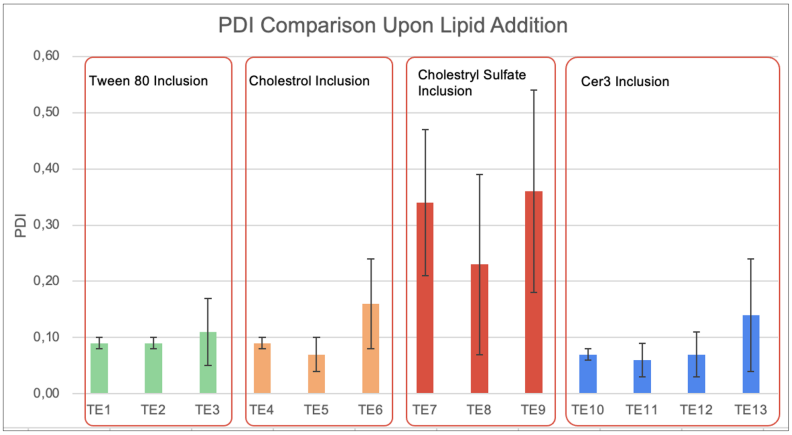

Figure 3.14. Effect of lipid additions and increase in lipid concentrations on homogeneity values for various TE formulations

3.3.1.5. Stability and Breakdown of the Final TE Formulation. One major problem for future applications of TEs in cosmeceutical formulations is the stability of the vesicular systems. All cosmeceutical products have a certain shelf life and the loaded components in these vesicles should last till the end of this shelf life without getting disrupted. There are of course some additives to prolong the stability of TEs within the products, but manufacturers would want to know the extends of stabilities of the isolated vesicular systems. To investigate one month storage stabilities, the mean size and homogeneity values of the TE5 and TE11 formulations were examined and compared 30 days after preparation, as can be seen in Table 3.6. Samples were kept in 4°C

fridge, wrapped in aluminum foil. The findings demonstrated that TE11 formulation was stable even after 30 days, very similar to TE5 formulation, neither the mean size nor the homogeneity of the samples were affected. After one month of storage, the size increase for both formulations was nearly the same, and there was no noticeable difference in their PDI values.

Table 3.6. One- month stability of TE5 (no Cer3) and TE11 (Cer3 containing) formulations with respect to mean size and PDI values

Sample	**Size (nm)**	**One-month size (nm)**	**PDI**	**One-month PDI**
TE5	75.28±15.17	80.46±18.66	0.07±0.03	0.06±0.04
TE11	80.17±8.60	85.12±6.51	0.06±0.03	0.09±0.03

After dilution of TE11 samples with 1:10 (v/v) ethanol and vigorous shaking with a vortex for 30 minutes, the freshly produced vesicles broke down, also confirmed by DLS findings. When the lipid bilayer was disrupted, broken vesicles did not exhibit any significant size peaks on DLS measurements, and distinctive bluish color of TEs vanished as well.

3.3.2. Cer3 Effect on Physical Properties of Ambora Extract and Chromabright Loaded TEs

As previously indicated, one hydrophilic and one lipophilic payload were selected in order to examine how Cer3 affected the physical properties of TEs in terms of mean size, homogeneity, and LE%. A series of studies were conducted; the results were presented in Table 3.7 and illustrated in Figures 3.15 and 3.16; showing that TE5 and TE11 did not include any loaded material, TE14 and TE15 contained 10% mass of hydrophobic chromabright by total lipid mass, and TE16 and TE17 contained 10% mass of hydrophilic ambora extract.

Table 3.7. Effect of Cer3 on physical properties of ambora extract or chromabright loaded TEs in terms of mean size, PDI and %LE and their one month stabilities

Sample	**Soy PC: Cer3**	**Cargo**	**Size (nm)**	**Size (nm) (One-month)**	**PDI**	**PDI (One-month)**	**%LE**	**%LE (One-month)**
TE11	15:1.5	-	80.17±8.60	85.20±6.51	0.06±0.03	0.09±0.03	-	-
TE5	-	-	75.28±15.17	80.47±18.66	0.07±0.03	0.06±0.04	-	-
TE14	15:1.5	Chromabright	86.62±7.99	84.68±4.54	0.09±0.02	0.11±0.03	96.60±2.79	87.79±13.70
TE15	-	Chromabright	81.88±9.13	83.47±12.19	0.06±0.01	0.06±0.02	95.12±4.01	88.48±16.33
TE16	15:1.5	Ambora Extract	116.95±12.36	116.50±9.88	0.12±0.02	0.13±0.02	58.82±7.84	66.90±11.13
TE17	-	Ambora Extract	127.05±13.52	130.67±8.81	0.13±0.02	0.09±0.04	60.38±9.30	69.34±16.58

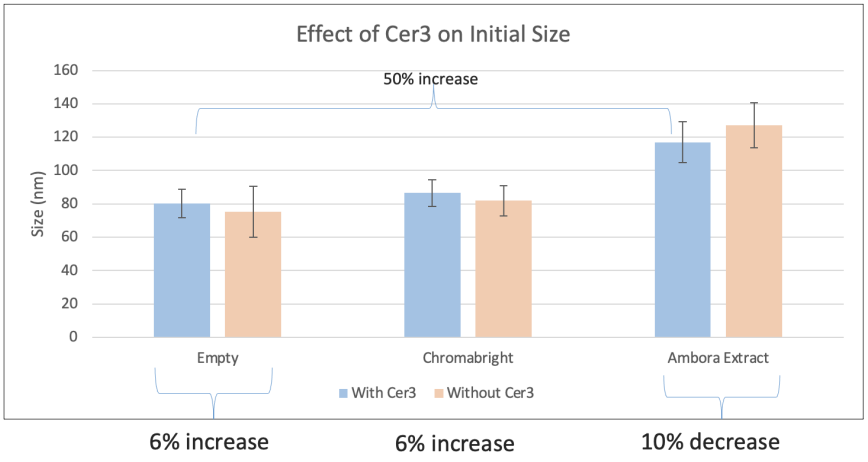

Figure 3.15. Effect of Cer3 addition on average size values for empty, chromabright or ambora extract loaded TEs

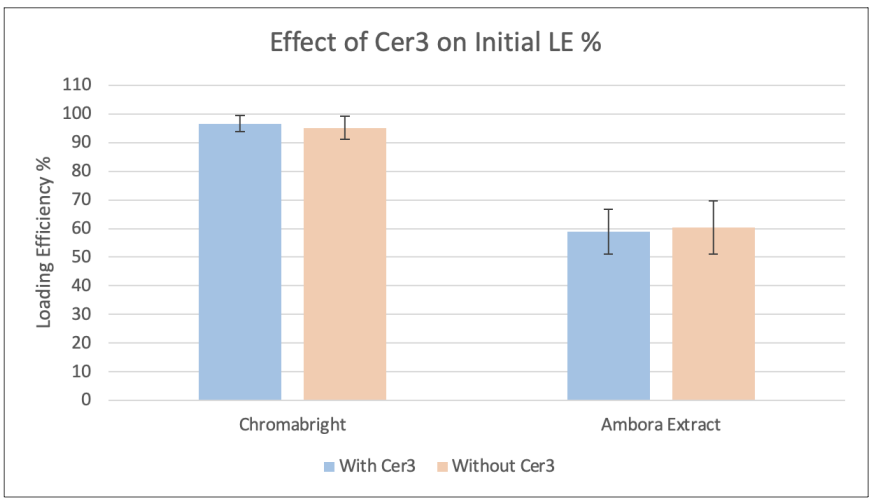

Figure 3.16. Effect of Cer3 addition on PDI values for empty, chromabright or ambora extract loaded TEs

A comparison of Cer3 containing TEs, TE 11, 14, and 16 as presented in Table 3.7, demonstrated that loading a lipophilic cargo within Cer3 containing TEs, resulted in nearly no change in size and homogeneity, whereas the introduction of a hydrophilic cargo caused a 68% rise in size and an almost 100% loss in homogeneity. One reasonable theory for that could be chromabright, as being a lipophilic molecule, was integrated into the bilayer structure where it acted as a constitutional lipid to reinforce the lipid wall of the vesicles. After a month of storage, lipophilic cargo did not appear

to significantly affect the size and homogeneity of the bilayer system; it might be due to reinforcing effect of chromabright to the lipid bilayer wall. This theory was further supported by loading studies, which showed that nearly all of the chromabright molecule entered the TE structures made with and without Cer3 and stayed quite stable for one month. Since hydrophobic molecules have higher affinity for multi-lamellar vesicles, it was very expected to obtain chromabright LE% values would be higher. Conversely, loading within the aqueous core of the TEs may account for the significant increase in size and PDI values of the TEs containing ambora extract. But the one month stability data showed hydrophilic cargo loaded vesicles preserved their stabilities as good as hydrophobic cargo loaded vesicles; neither the mean size nor the homogeneity values were corrupted. Percent size and LE% changes upon one-month storage time were summarized in Figures 3.17 and 3.18. One interesting result could be observed in the LE% of ambora extract, LE% of both TE16 and TE17 had an increase about 15% after one month of storage. The reason behind this phenomenon could be the bilayer structure of TE16 and TE17 might have swelled slightly and behaved like a sponge, causing an increase in the LE%. So, Cer3 had neither beneficial nor side effect on LE% of both cargos.

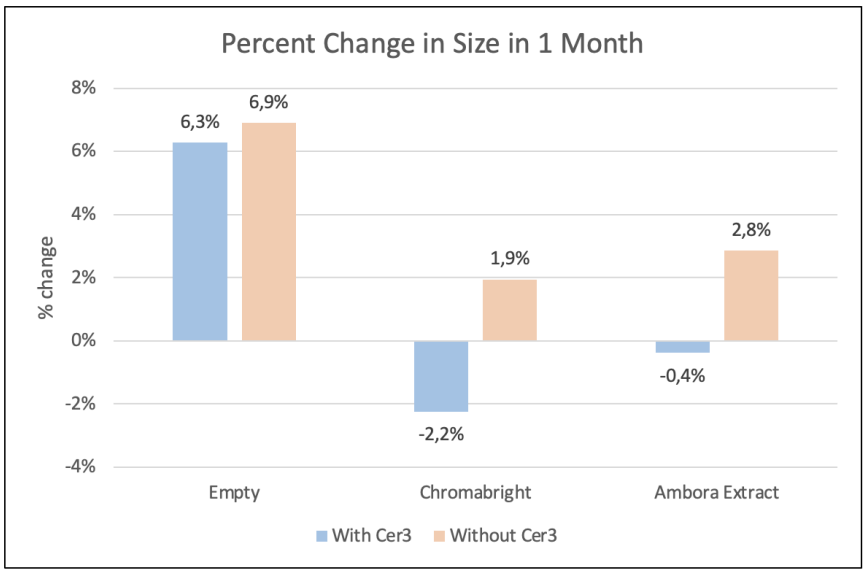

Figure 3.17. Effect of Cer3 addition on percent change in size after one month

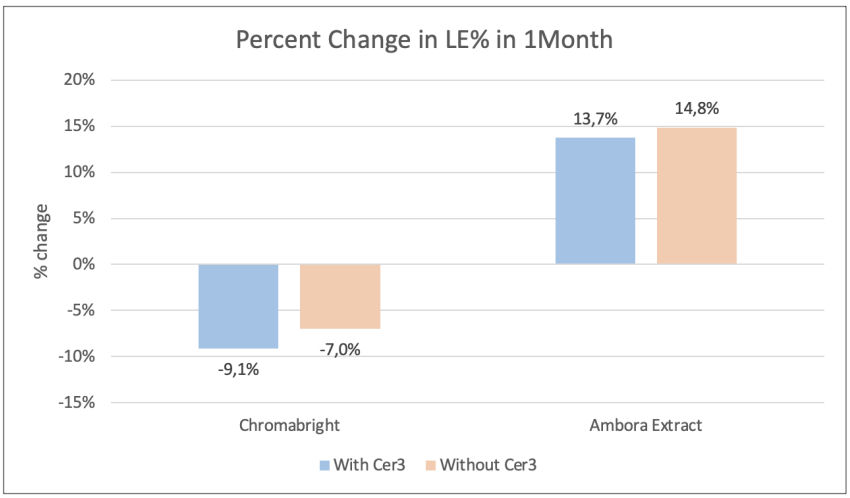

Figure 3.18. Effect of Cer3 addition on percent change in size after one month

As presented in Table 3.7, TEs 5, 15, and 17 that did not contain Cer3 were also compared. It could be seen that addition of Cer3 into the vesicular formulations caused an increase in the vesicle sizes for both lipophilic cargo; and no cargo containing vesicles. These results were parallel with the findings in section 3.3.1.4, which was increasing the mass ratio of Cer3 had an increase in vesicle mean size. But the results were opposite for hydrophlic cargo containing vesicles; Cer3 introduction had a size decrease within TE16 formulation. Cer3 could increase the stiffness of the bilayer and ambora extract could more easily arrange itself within the aqueous core without Cer3. This hypothesis could be supported by comparing the LE% data of TE16 and TE17, LE% of TE17 was slightly bigger than TE16. Once more, hydrophilic material in TE17 served as a cargo that entered the TE's aqueous core by increasing vesicle size and decreasing homogeneity as in TE16. Additionally, it appeared that hydrophilic cargo damaged the colloidal system's homogeneity. When TE16 and TE17 were compared to empty and lipophilic material containing vesicles, their PDI were much higher. This might have resulted from the fact that ambora extract was a mixture of chemicals and had a complex structure.

Figure 3.19 displayed the absorbance peaks of the TE's constituent parts (Soy PC, Tween 80, cholesterol, Cer3, Ambora extract and chromabright) as well as the

absorbance line of empty TE11, which was indicated in black bold. This image illustrated how the peak of the TE was separated from the peaks of the other elements once it was produced. Additionally, there was no lipid overlap at 274 or 286 nm, the maximum absorbance wavelengths of chromabright and ambora extract respectively, which allowed us to track the LE peak.

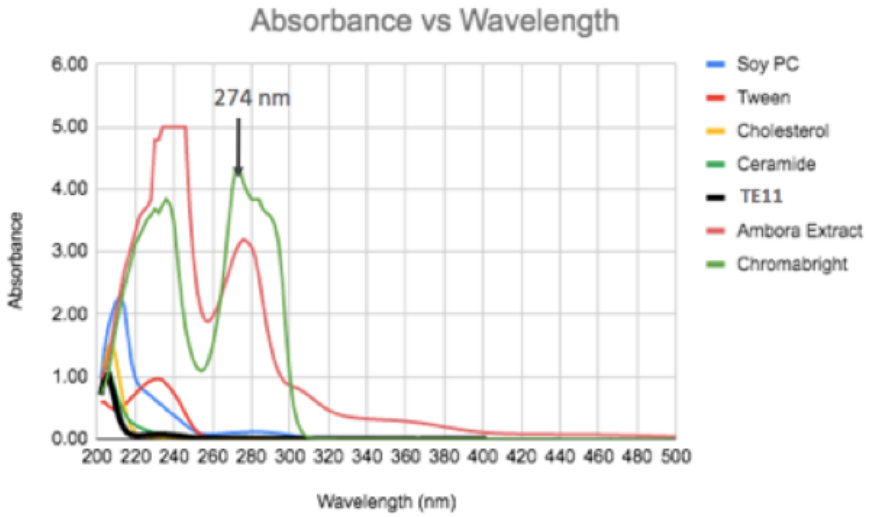

Figure 3.19. Maximum absorbance wavelengths of the lipids used in TE formation, TE11 and the payloads; Ambora extract and Chromabright

The following technique was the basis for the calculation of loading yields using the maximum absorbance wavelengths: After the preparation of the loaded TEs, a) they were placed under 50000 rpm ultra-centrifugation to eliminate all un-loaded free materials; b) the filtrate was analyzed at the maximum absorbance wavelengths using a UV/Vis spectrophotometer; and c) centrifugation was carried out repeatedly until the filtrate was free of free ambora extract or chromabright. Following the vesicles' disintegration, as detailed in section 3.3.1.5, absorbance and the quantity of the released substances were calculated by using the calibration curves as represented in Figure 3.20 for ambora extract and Figure 3.21 for chromabright with the displayed equations.

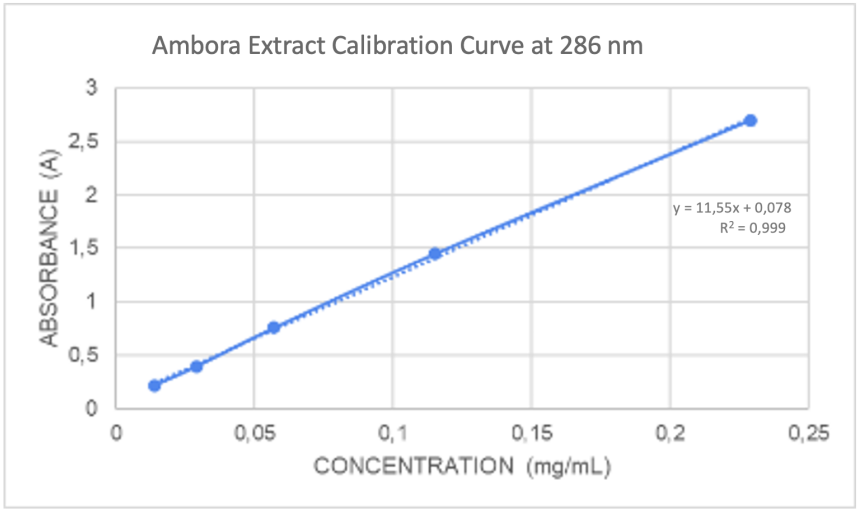

Figure 3.20. Absorbance versus concentration data of ambora extract measured at 286 nm

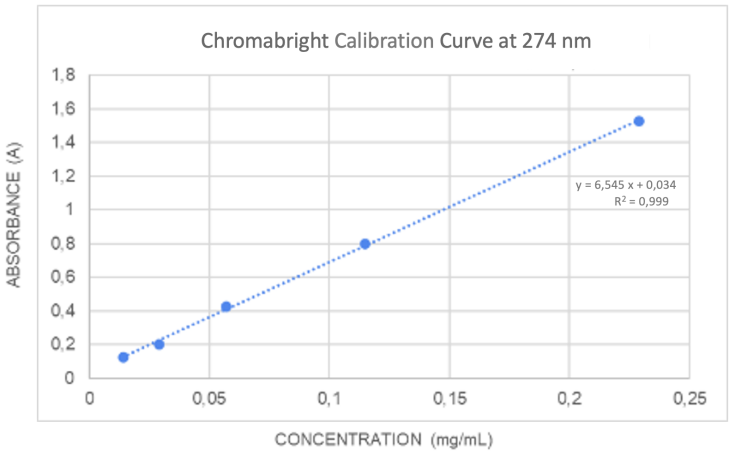

Figure 3.21. Absorbance versus concentration data of chromabright measured at 274 nm

The two-way ANOVA test was used to statistically assess the obtained data, as illustrated in Figures 3.22 and 3.23. The variance in size and homogeneity across various materials was evaluated through the utilization of a two-way ANOVA. This statistical approach enabled us to isolate the effect of material choice on size and PDI measurements. As shown in Figure 3.22, the ANOVA analysis indicated a statistically significant effect of material type on size ($p = 0.0011$). This important discovery

suggests that material choice had a major influence on the size variation observed among the investigated materials rather than being random. The p-value for Cer3,($p = 0.33$), was greater than the significance level, suggesting that Cer3 was not statistically significant in relation to size. The interaction between Cer3 and cargo material did not exhibit statistical significance in relation to size, as indicated by the p-value being bigger than the significance level ($p = 0.83$). In conclusion, size was statistically significantly influenced by the type of material selected, but not by Cer3 or the relationship between Cer3 and payload. The variance in size, which was ascribed to material selection, indicated innate variations in the physico-chemical characteristics of the materials, which subsequently impacted their stability and dispersion in a particular medium.

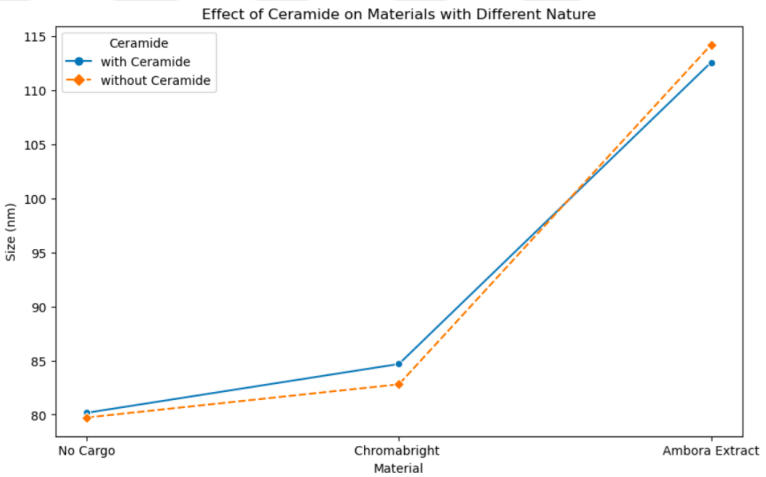

	df	sum_sq	mean_sq	F	PR(>F)
Material	2.0	0.014943	0.007472	10.441723	0.001102
Ceramide	1.0	0.000716	0.000716	1.001064	0.331083
Material:Ceramide	2.0	0.000264	0.000132	0.184545	0.833126
Residual	17.0	0.012164	0.000716	NaN	NaN

Figure 3.22. Statistical analysis on the effect of Cer3 existence on hydrophilic and hydrophobic payload containing TEs in terms of mean size

The p-value for material choice was 0.00021, less than the significance level which was 0.05, indicating that material type was statistically significant for homogeneity, as shown in Figure 3.23. Existence of Cer3 was not statistically significant in terms of homogeneity, according to the p-value of 0.99, which was higher than the significance

level. The interaction between Cer3 and material type was not statistically significant, as indicated by the p-value of 0.97, interaction being bigger than the significance level. Further investigations could expand on this foundation by examining the particular material characteristics influencing size and homogeneity and by including a wider range of materials to cover a wider spectrum of applications.

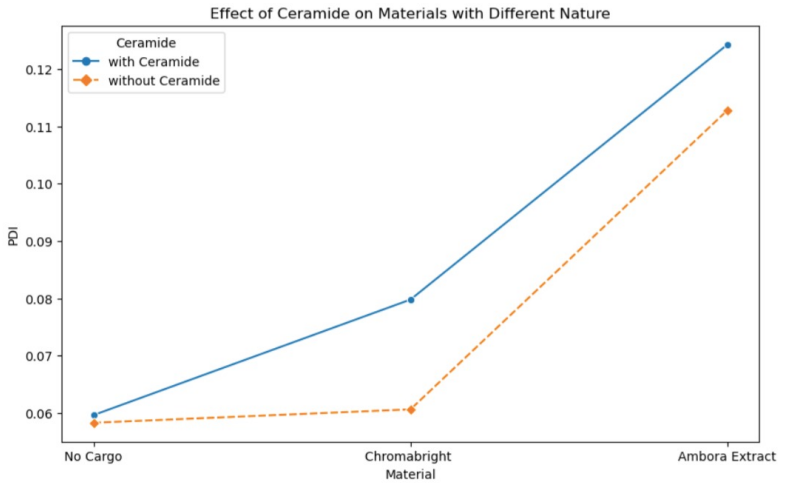

	df	sum_sq	mean_sq	F	PR(>F)
Material	2.0	5397.803140	2698.901570	14.590379	0.000205
Ceramide	1.0	0.056809	0.056809	0.000307	0.986222
Material:Ceramide	2.0	12.719914	6.359957	0.034382	0.966269
Residual	17.0	3144.628833	184.978167	NaN	NaN

Figure 3.23. Statistical analysis on the effect of Cer3 existence on hydrophilic and hydrophobic payload containing TEs in terms of homogeneity

Figures 3.24 and 3.25 demonstrated the physical differences between the loaded and empty TEs that were visible to naked eye. Distinct orange color of dissolved ambora extract seen in Figure 3.24(a), became cloudy after loading process (b), and further turned bluish upon extrusion (c). Vesicular suspensions like TEs, have a certain bluish color because of the scattering of light by the vesicles [100, 101]. Difference between (c) and (d) confirmed a successful loading of the hydrophilic cargo; whereas there was no trace of orange color in (d), it could be clearly seen a bluish-orange color in (c) demonstrating the presence of the orange colored cargo was within the vesicles.

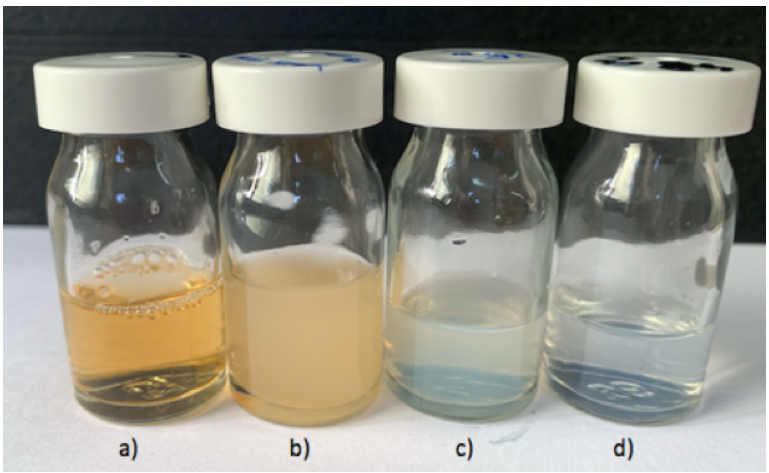

Figure 3.24. a) Ambora extract dissolved in water b) Ambora-extract-containing TEs prior to extrusion c) Ambora-extract-containing TEs after extrusion d) Empty TEs after extrusion

Similarly, colorless chromabright solution in Figure 3.25 (a), turned bluish upon loading (b), and further became more bluish after extrusion process (c). There was also an obvious color difference between empty TE sample (d) and chromabright containing TE sample (c).

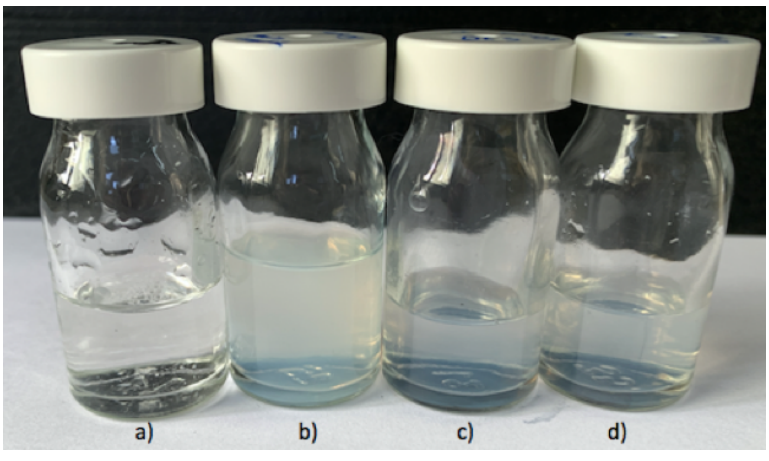

Figure 3.25. a) Chromabright dissolved in ethanol b) Chromabright-containing TEs prior to extrusion c) Chromabright-containing TEs after extrusion d) Empty TEs after extrusion

3.4. Conclusions

Despite the fact that many studies have documented the potential usage of liposomes as transdermal delivery vehicles, it appears that little is known about how to formulate a vesicular system with the best stability, homogeneity, and LE%. Thus, the primary goal of the this study was to construct a TE system that would be a superior skin delivery agent than liposomes by incorporating edge activators and ethanol into vesicular structures. Investigations were conducted to observe the effects of Cer3, cholesterol, cholesteryl sulphate and Tween 80 concentrations on the physical qualities of the TE formulations in terms of homogeneity, stability, and LE%. By adding ethanol, cholesterol, tween 80 and Cer3 to the vesicular system, an effective TE composition having a very narrow size distribution with the ideal size for skin applications was obtained. The LE% and one month LE% stabilities of the obtained TEs were examined.

Results showed that increasing Tween 80 concentrations caused a decrease in size while not affecting the homogeneity. This finding was also consistent with the literature data [102–104], which concluded that as the surfactant concentration increased, steric repulsion within the lipid bilayer was decreased that caused a reduction in vesicle aggregation and improvement in system stability.

Addition of cholesterol into the formulation caused a growth in size in agreement with the results stated by Shaker, S., *et al.* [103], but after 15:1.5:1.5 mass ratio of Soy PC:Tween 80:cholesterol a dramatic reduction in size distribution occurred. The possibility that more cholesterol molecules were dispersed throughout the phospholipid bilayer by increasing the membrane fluidity could be the cause of the rise in the mean size of the vesicles as the mass ratio of the cholesterol increases.

Cholesteryl sulphate added to the lipid composition with three different formulations of Soy PC:Tween 80:cholesterol:cholesteryl sulphate containing mass ratios of 15:1.5:1.5:0.37, 15:1.5:1.5:0.74 and 15:1.5:1.5:1.11 in order to create a vesicle system

that closely resembles the composition of the human skin. None of the formulations produced vesicles within the acceptable homogeneity range and they were all unstable upon two days of storage. These results were parallel with a previous study concluding that, lipid packing would be decreased because the bulkiness of the polar sulfate moiety of the cholesteryl sulphate would prevent the surrounding phospholipids from binding closely and form a proper vesicular structure [105]. Consequently, it was determined that adding cholesteryl sulphate to the vesicle medium using the cold method technique was not effective and was removed from later formulations.

Addition of Cer3 caused an increase in size and desired size and size distribution range was achived with using 15:1.5:1.5:1.5 mass ratio of Soy PC:Tween 80:cholesterol:Cer3. This formulation preserved its physical properties in terms of size and homogeneity upon one month of storage. LE% studies were performed with the achieved formulation using either ambora extract or chromabright as cargo materials. Effects of Cer3 and hydrophilic nature of the chosen material were studied and the results were analyzed statistically. According to the results LE% and LE% stability were more successful with the lipophilic cargo irrespective of the presence of the Cer3. Therefore, Cer3 had almost no effect on the LE% of the TEs but had an increase in vesicular size within lipophilic cargo containing TEs. All the TE formulations were within the acceptable size and PDI range with high LE% and were stable upon one month of storage in terms of size, homogeneity and LE%.

This research highlights the preparation of successful TE formulations containing Cer3 for transdermal delivery studies to be used in AD treatments which makes a valuable addition to the field of liposome research. These results suggest that Cer3 can be used in TE formulations and plays an important role in vesicle characteristics. Findings can be used in potential topical applications in AD curing studies. A future work can be done by examining the skin penetration characteristics and cyto-toxicity of the obtained TEs.

4. EFFECT OF SURFACTANT TYPE ON VITAMIN C AND VITAMIN E LOADED TRANSETHOSOMES AND A STUDY OF DUAL LOADING

4.1. Introduction

The human skin serves as the body's primary protective barrier against external agents. In order to efficiently deliver specific substances to the skin, topical treatments such as cosmeceuticals must first penetrate through the SC, the upper layer of the skin's structure. Agents with similar structure to this layer mimic the skin membrane and ease delivery [75]. As mentioned in the previous Chapter 3.1 in detail, TEs are very successful transdermal delivery agents containing ethanol and surfactants within their compositions.

The two primary categories of surfactant function in TE preparation are edge activating and penetration enhancing. Edge activators disrupt the phospholipid bilayer by penetrating into high-pressure areas of the vesicles while the vesicles are under stress and hence reduce the stiffness of the bilayers [20], [106]. Penetration enhancers have potential to diffuse into the SC and interact with its components to temporarily reduce the permeability barrier without causing significant damage to cellular structure. Alternatively, enhancers can change the characteristics of the formulation by promoting drug delivery with enhanced permeation. Many promising enhancers are amphiphilic compounds that have a polar head and hydrophobic chain [107].

Two of the surfactants that are most frequently utilized in dermo-cosmetics are Tween 80 and oleic acid. Tweens and oleic acids can also be employed to create TEs while creating vesicles. Tweens, for instance, are used in vesicular systems as edge activators at concentrations between 10% and 50% of the overall phospholipid concentration. Because of its solubilizing qualities, Tween 80, a nonionic water-soluble surfactant, has been specifically shown to improve skin penetration while enhancing

vesicle stability. Additionally, it keeps vesicles from aggregating, which boosts stability as well [47].

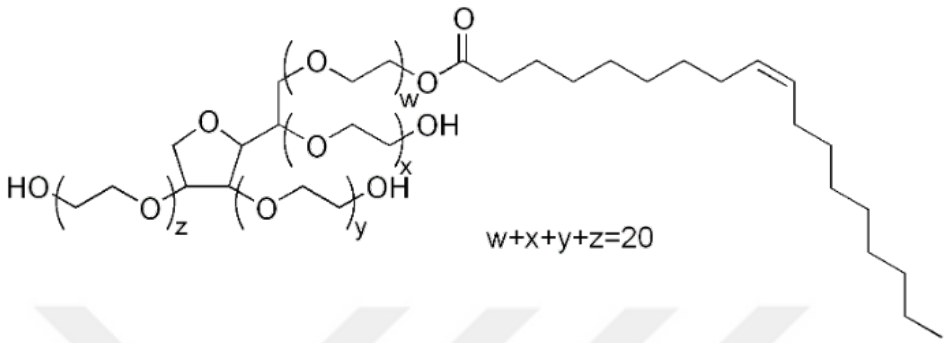

Figure 4.1. Structure of Tween 80 (Created with Chem Draw, accessed on June 2024)

Oleic acid, a naturally occurring anionic fatty acid, is being used in cosmeceuticals for a long time as a penetration enhancer. It is the most abundant fatty acid found within phospholipids that make cell membranes. Vesicles containing oleic acid have been reported previously to enhance drug absorption and used as carriers for several drugs in topical administration. They have been known to overcome the skin barrier, probably via lipid exchange between the SC layer and lipid carriers. After penetrating through the SC, they get washed out through the fusion of fatty acids around the skin. Hence, the ideal vesicle formulation for topical delivery could involve oleic acid within its composition [108, 109].

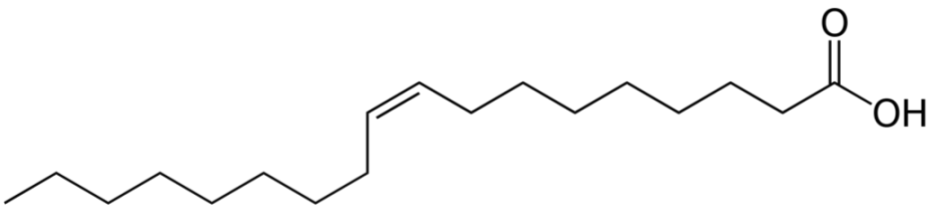

Figure 4.2. Structure of Oleic acid (Created with Chem Draw, accessed on June 2024)

Vitamin E, VitE, also known as alpha-tocopherol, is one of the essential lipid-soluble vitamins best known for its antioxidant ability against free radicals that are produced by UV radiation, drugs and pollutants. Studies have also shown that it

has anti-inflammatory qualities in addition to its powerful antioxidant benefits [110, 111]. Researchers are very interested in examining the medicinal potential of VitE for the prevention and treatment of many skin diseases but the low bioavailability of it continues to be a significant barrier for its therapeutic uses. Furthermore, as an antioxidant, VitE is very prone to oxidation in the presence of oxygen, light, and heat [112].

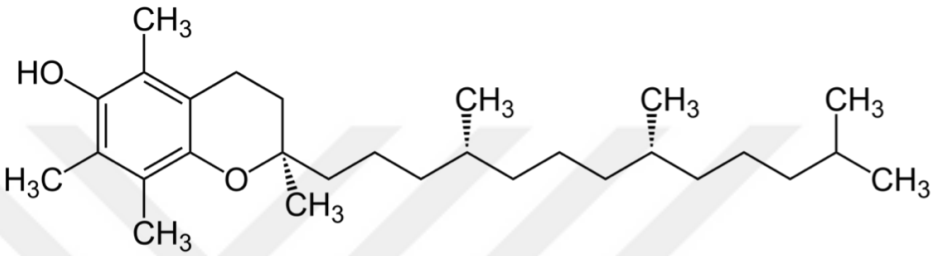

Figure 4.3. Structure of VitE (Created with Chem Draw, accessed on June 2024)

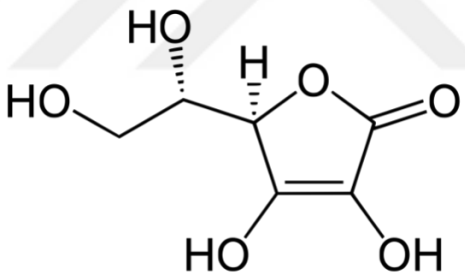

Figure 4.4. Structure of VitC (Created with Chem Draw, accessed on June 2024)

Vitamin C, VitC, also recognised as ascorbic acid, is a water-soluble vitamin and well-known antioxidant. It is used topically in dermatology to treat and prevent photo aging-related skin diseases like hyperpigmentation. It is also involved in tissue repair, collagen synthesis and enzymatic production of some neurotransmitters. VitC functions to shield the skin from oxidative stress by successively giving electrons to eliminate free radicals and its oxidized forms are relatively harmless. VitC is a weak, unstable organic acid that is easily oxidized or destroyed by light, oxygen and hot weather conditions. It is extremely sensitive to many physical and chemical factors such as pH, temperature, oxygen, and the presence of catalysts within the body. The lowest rate of oxidation is observed at pH 3 but the preservation solutions must resemble the physiological pH

of serum (7.35–7.45), at which VitC is unstable. So, the stabilization of ascorbic acid molecules and finding novel dermal delivery systems are the primary focuses of the current study [113, 114].

According to recent studies, reactive oxygen species like free radicals participate in the development of allergic inflammation. Large concentrations of reactive oxidants cause cellular damage in the epidermal keratinocytes through lipid oxidation. This creates an oxidative stress which causes tissue inflammation through activation of genes responsible for inflammatory cytokines. It has been suggested that inflammation and oxidative damage play a huge role in the emergence of AD. Urine 8-hydroxydeoxyguanosine levels which is the product of DNA oxidation by free radicals, are found to be higher in AD patients that demonstrate the interaction between the free radicals and AD [115, 116]. In the studies performed over AD patients, oral supplements of VitE showed contributing and beneficial effects in the treatment of AD [117, 118]. Another study done by Shin, J., *et al.* revealed that clinical severity of AD is strongly related to decreased levels of VitC in AD patients. VitC involves an important role in the activity of ceramide synthesis and improves overall skin barrier function [119]. Therefore, through transdermal delivery agents, antioxidant and anti-inflammatory properties of VitE and VitC could be utilized for a promising supplementary treatment of AD.

The aim of this study was to compare the effect of surfactant type on the physical properties and the LE% of the TEs loaded either with VitC or VitE to make an impact on AD treatment. Tween 80 and oleic acid were used as surfactants and effect of surfactant choice on size, homogeneity, morphology and LE% of the generated TEs was evaluated. Size and size distribution were followed by DLS whereas the morphologies were monitored via STEM. LE% was followed by UV/Vis spectrometer. All the formulations were also investigated upon one month storage in terms of physical property and LE% stabilities.

Effect of dual loading of both substances on the physical properties and the LE% were also a focus of this research to supply a synergistic effect between VitC and VitE. By regenerating the oxidized form of VitE to its natural form, VitC works synergistically with VitE and provides 4-fold protection against solar simulated irradiations superior to using either antioxidant alone [120, 121]. So, using these antioxidants together in a topical nano formulation can create an impressive treatment for AD. Dual loading studies were done to compare the LE% and physical properties of the obtained vesicles to the single cargo loaded ones.

4.2. Experimental

4.2.1. Materials

Soy PC with 94 % PC content, in light orange colored grease form, was kindly provided by Lipoid GmBH (Ludwigshafen, Germany) under the brand name of Lipoid S 100. Detailed information about Soy PC can be found in section 3.2.1.

Cholesterol, L-ascorbic acid (VitC) and 1,2-dimyristoyl-sn-glycero-3-phosphorac-(1-glycerol) (sodium salt) (DMPG) as an anionic lipid, were purchased from Sigma Aldrich in white powder form with more than %99 purity. DMPG is a minor component (1-2%) of most of cell membranes. Alpha-tocopherol (VitE) was also purchased from Sigma Aldrich in yellow viscous liquid form.

Tween®80 and oleic acid were purchased from Merck. Tween®80 was in the form of yellow liquid and used as an edge activator. Oleic acid was in the form of colorless liquid and used as a penetration enhancer.

Chitosan was purchased from Acros Organics in the form of off-white to beige powder with a molecular weight range of 60000-800000 Dalton.

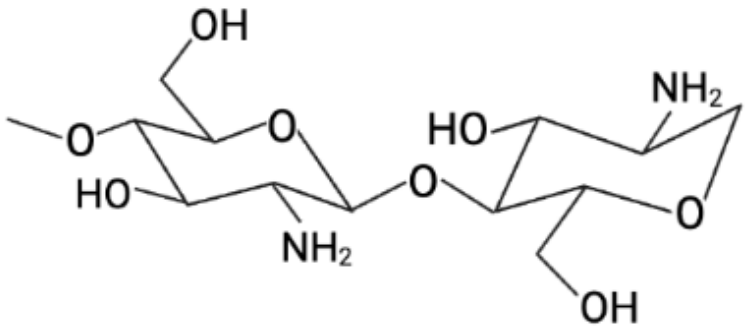

Figure 4.5. Structure of chitosan (Created with Chem Draw, accessed on June 2024)

4.2.2. Methods

4.2.2.1. Preparation of TEs. TEs were prepared with the cold method as mentioned in section 3.2.2.1. VitC was dissolved in aqueous phase and heated separately to 35°C. The aqueous phase was added to the ethanol solution drop by drop using a 1 mL syringe with a speed of 250 µL/min. In dual loading studies VitE was mixed into the ethanolic solution with other lipids while VitC was again in the aqueous part. The lipid mass ratios and cargo types used in different TE formulations can be found in Table 4.1, presented as Soy PC:cholesterol:Tween 80:oleic acid mass ratios. In all the cargo loaded formulations Soy PC:VitC mass ratio was 15:0.75 and Soy PC:VitE mass ratio was 15:3 mg VitE. These concentrations were chosen such that they could be followed by UV/Vis spectroscopy. In all the formulations, total lipid concentration in the final TE dispersion was preserved constant as 10 mg lipid per ml of total dispersion and ethanol:water volume ratio was fixed as 3:7. Chitosan solution (1.25 mg/ml) was prepared with 1% glacial acetic acid aqueous solution, and final vesicular dispersions contained chitosan at a concentration of 0.83 mg/mL. The coating procedure was performed as previously described in the literature [122]. Briefly, chitosan coated TEs were prepared by adding the pre-prepared TE dispersions drop wise (0.25 mL/min) to the chitosan solution (1:1, v/v), followed by incubation for 1 hour with gentle stirring.

Table 4.1. The mass ratios of Soy PC:cholesterol:Tween 80 or oleic acid and cargo types in different TE formulations coded under the abbreviation of "Dual"

Sample	**Soy PC**	**Cholesterol**	**Tween 80**	**Oleic acid**	**Cargo**
Dual1	15	1.5	1.5	-	-
Dual2	15	1.5	1.5	-	VitC
Dual3	15	1.5	1.5	-	VitE
Dual4	15	1.5	1.5	-	Dual
Dual5	15	1.5	-	1.5	-
Dual6	15	1.5	-	1.5	VitC
Dual7	15	1.5	-	1.5	VitE
Dual8	15	1.5	-	1.5	Dual

4.2.2.2. Characterization of TEs. Characterization of TEs were performed as mentioned in section 3.2.2.2.

4.2.2.3. Loading Efficiency Studies. Calculation of LE% was followed as described in section 3.2.2.3. Maximum absorbance wavelength for VitC was detected as 258 nm whereas it was determined as 287 nm for VitE. There was no interference observed between the maximum absorbance wavelenghts of the loaded components and the other lipid compounds. After they had all been removed from their external media, the loaded TEs were broken down and their released cargo was measured using a UV/Vis spectrophotometer with the equations shown in Figures 4.7 and 4.8. Alternative detection of non-capsulated VitC amount was achieved with iodometric titration method. As the iodine solution was added during the titration, un-loaded VitC within the samples was oxidized to dehydroascorbic acid, while the iodine was reduced to iodide ions and gave a purple-like color at the end point. Two different solutions were used in this method; 0.001M iodine solution and 0.5% starch indicator solution as indicated in the literature [123]. Briefly; 1 mL of the sample solution was pipetted into a 10 mL glass vial, 6 ml of Type 1 water was added onto it, followed by addition of 3 drops of starch

indicator solution. Then the sample solution was titrated with 0.001M iodine solution. Endpoint was identified as the first permanent trace of a dark blue - purple color due to the starch-iodide complex. The titration was repeated three times and average data was used.



Figure 4.6. End point color of the iodometric titration

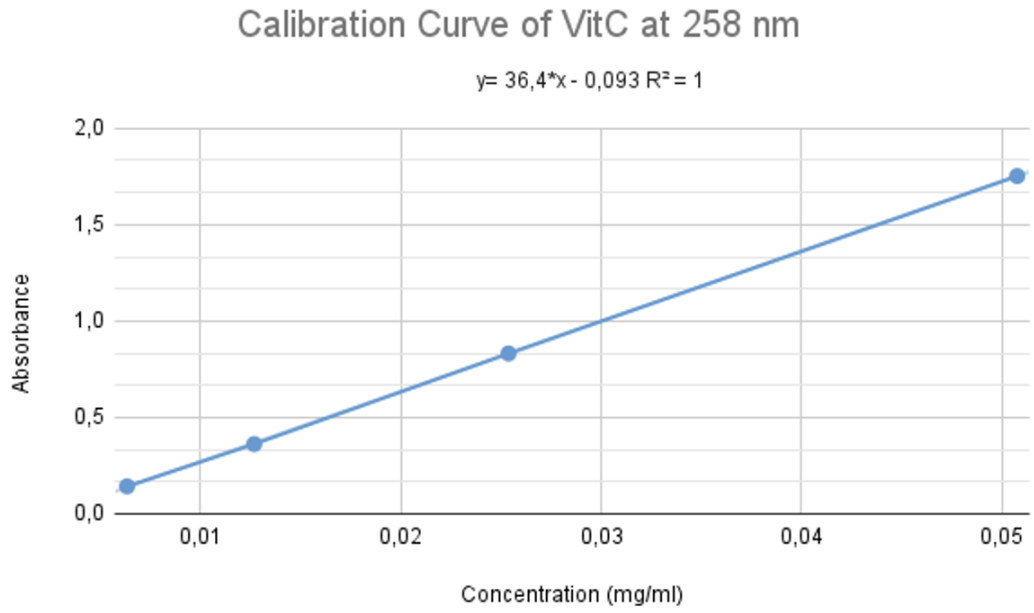

Figure 4.7. Calibration curve of VitC at 258 nm

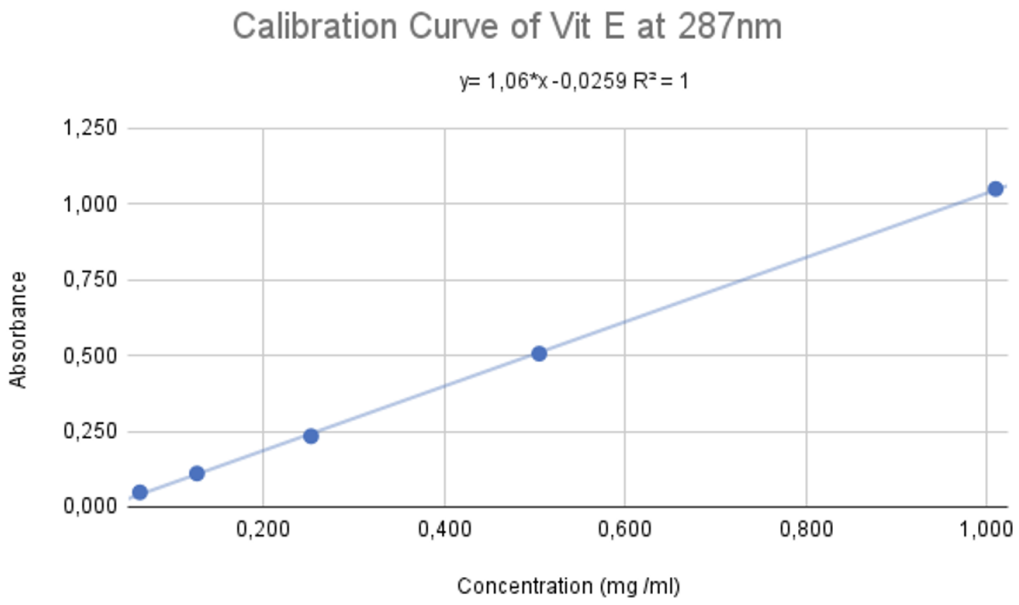

Figure 4.8. Calibration curve of VitE at 258 nm

4.3. Results and Discussion

4.3.1. Effect of Surfactant Type on Physical Properties of TEs

According to the results presented in Table 4.2 and summarized in Figures 4.9 and 4.10, if the formulations Dual 1,2 and 3 were compared, it could be seen that addition of both VitC and VitE cargos did not much changed the size and homogeneity values of tween containing vesicles. Also, they were all stable upon one month of storage in terms of size and homogeneity as seen in Figure 4.11. However, VitC containing vesicles (Dual 2) were lost homogeneity and got bigger after six months even though empty and VitE containing formulations (Dual 1 and 3) preserved their physical stabilities. It could be caused from the fact that hydrophobic cargos like VitE tend to behave as a constitutional lipid within the TE bilayer structure. LE% data also could be evidence for this such that almost all the VitE was incorporated within the vesicles with a 93% of LE% whereas it was 58% for the loading of VitC.

Table 4.2. Effect of surfactant type on physical properties of VitC or VitE loaded TEs in terms of mean size, PDI and %LE and their one month stabilities

Sample	**Surfactant**	**Cargo**	**Size (nm)**	**Size (nm) (One-month)**	**PDI**	**PDI (One-month)**	**%LE**	**%LE (One-month)**
Dual1	Tween 80	-	89.50±7.15	90.33±10.17	0.05±0.01	0.06±0.03	-	-
Dual2	Tween 80	VitC	84.94±8.26	86.96±13.08	0.08±0.06	0.13±0.08	58.29±20.97	38.53±22.09
Dual3	Tween 80	VitE	92.52±1.70	94.06±5.12	0.06±0.03	0.07±0.03	93.92±3.08	97.73±0.34
Dual4	Tween 80	Dual	112.88±31.23	111.75±1.77	0.16±0.15	0.09±0.01	59.43±9.30 89.67±5.38	47.45±13.65 76.38±29.31
Dual5	Oleic Acid	-	102.68±0.92	102.60±0.28	0.08±0.01	0.08±0.04	-	-
Dual6	Oleic Acid	VitC	104.26±10.00	107.04±13.10	0.10±0.03	0.11±0.06	71.92±26.14	63.55±28.33
Dual7	Oleic Acid	VitE	124.84±36.53	130.39±38.67	0.10±0.03	0.12±0.02	98.66±1.59	97.66±1,98
Dual8	Oleic Acid	Dual	334.32±98.60	302.40±77.57	0.38±0.12	0.37±0.06	68.49±16.12 81.91±12.69	42.23±19.24 65.72±15.65

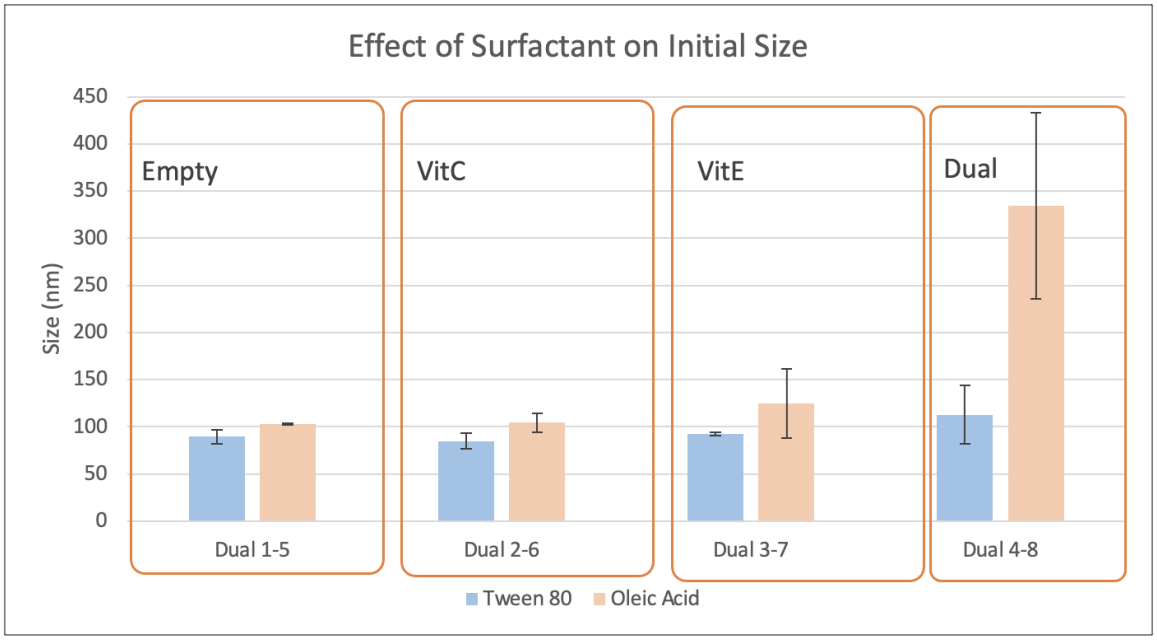

Figure 4.9. Effect of surfactant type on mean sizes of various TE formulations

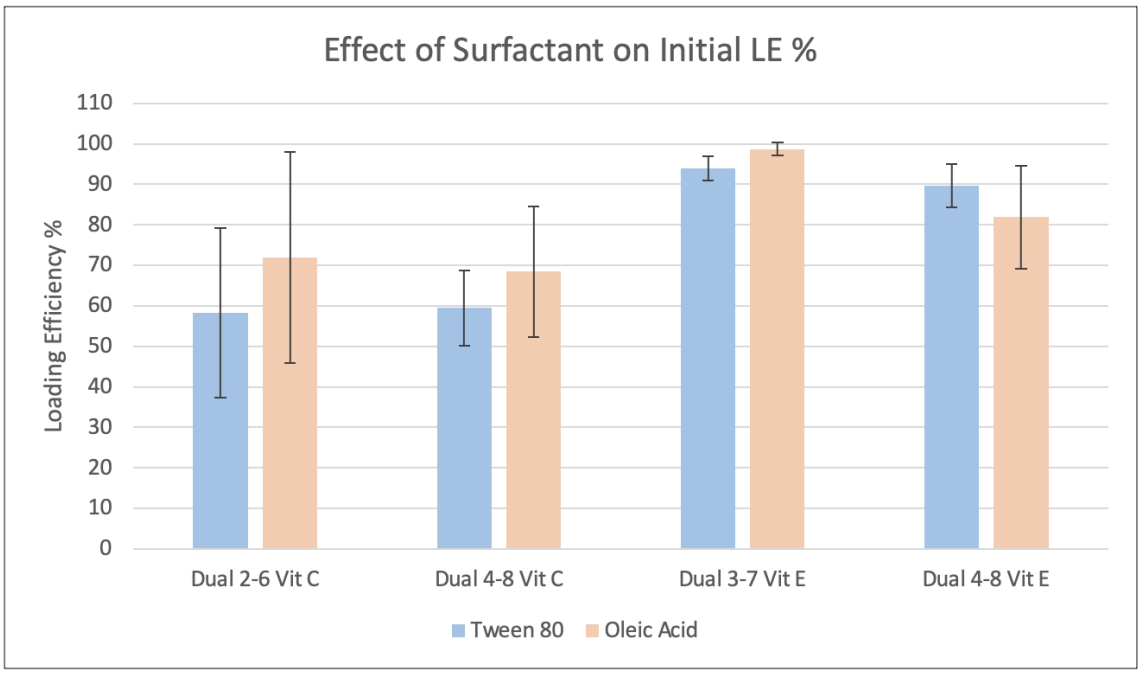

Figure 4.10. Effect of surfactant type on LE% of various TE formulations

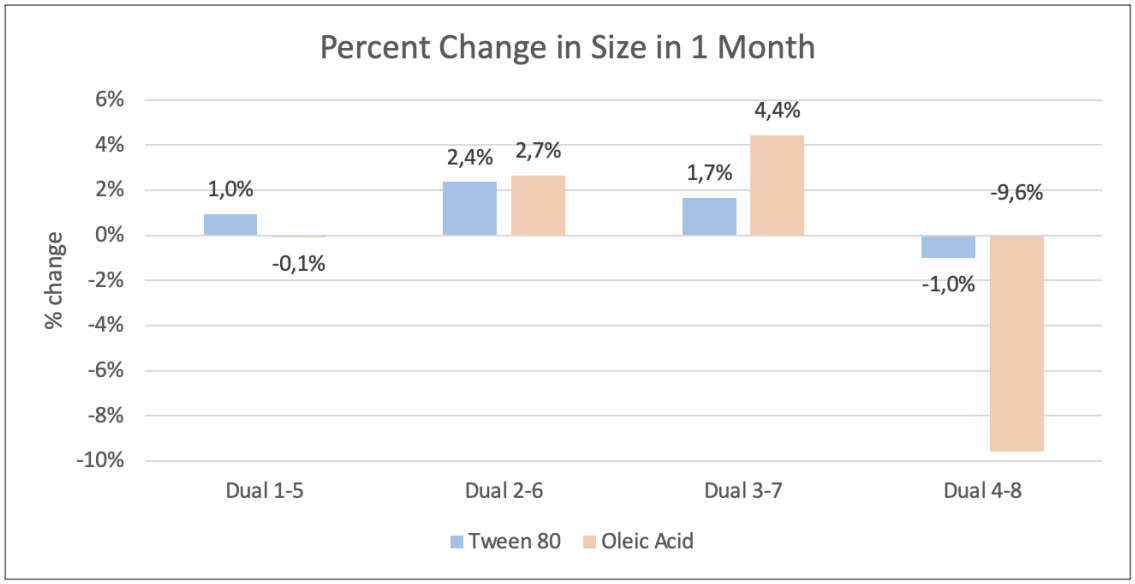

Figure 4.11. Effect of surfactant type on percent change in sizes upon one month of storage

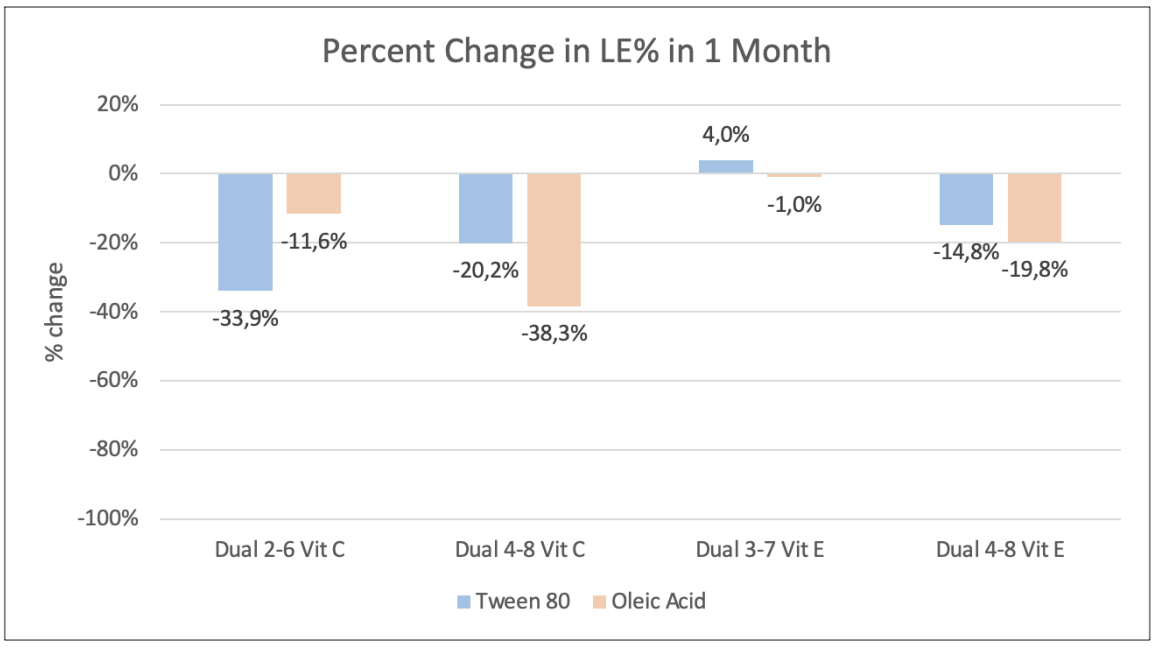

Figure 4.12. Effect of surfactant type on percent change in LE% upon one month of storage for various TE formulations

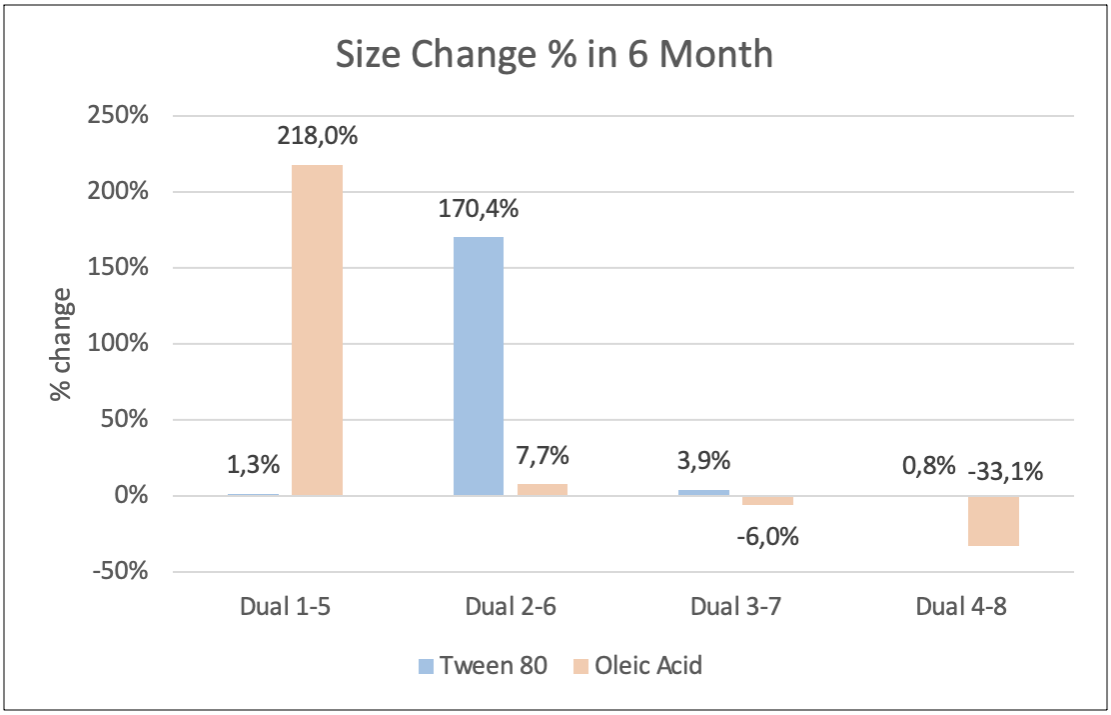

Figure 4.13. Effect of surfactant type on percent change in size upon six month of storage for various TE formulations

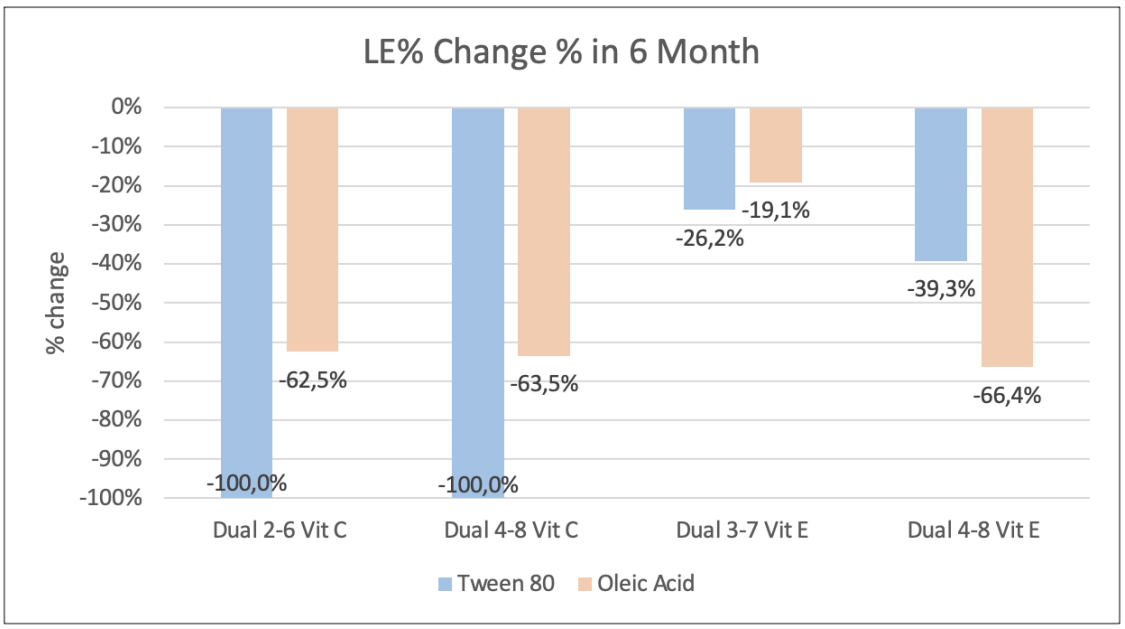

Figure 4.14. Effect of surfactant type on percent change in LE% upon six month of storage for various TE formulations

One month loading studies showed that loading stability was better for VitE (Dual 3) as being a hydrophobic cargo than VitC (Dual 2) as shown in Figure 4.12. Lipids that made up the TE structure could solubilize and interact with VitE better which lead to better loading yields than VitC. Leakages within the TE structure could be the cause of the decreased LE% of VitC upon one month of storage. Dual loading of both VitC and VitE (Dual4) yielded bigger sized TE structures with a lower homogeneity than singly VitC and VitE loaded TEs (Dual 2 and 3) but these formulation kept its stability upon 6 months of storage which was way better than VitC containing vesicles (Dual 2) as presented in Figures 4.13 and 4.14. STEM images belonging to Dual 4 formulation could be seen in Figure 4.15.

VitC LE% in co-loaded vesicles (Dual 4) attained better success in loading of VitC than Dual 2 samples that contain solely VitC not only in terms of LE% but also by giving a better size and size distribution value. In singly VitC loaded formulations, VitC LE% was decreased 35% after one month whereas the decrease was 20% in dual loaded ones (Dual 2 vs Dual 4).This may be stem from the fact that VitE could protect VitC from oxidation as mentioned in the literature before [120,121] and this was one of the main targets of this chapter of the study. Controversially, in Dual 4 formulations VitE LE% and LE% stability was worsen. As a result, dual loading of VitC and VitE together showed better performance in terms of preserving LE% and physical properties than single loading of VitC but the results were reverse for VitE loading.

If the formulations Dual 5,6 and 7 were compared as presented in Table 4.2, again same pattern observed in the size and homogeneities of the vesicles; addition of VitC and VitE separately did not much had an effect on size and size distribution. Slight increase in size and size distrıbution of Dual 7 formulation was caused by addition of a hydrophobic cargo attaining the bilayer structure of the vesicles. LE% data again proved this, almost all of the VitE had loaded with a 98% efficiency. All the vesicles kept their size and homogeneity stabilities upon one month of storage but after 6 months they started to be deteriorated. Empty vesicles were collapsed more than vitamin loaded ones. Oleic acid is a saturated fatty acid and prone to oxidation at a

remarkably fast rate [124]. Being a strong anti-oxidant agent, VitC could preserved oleic acid from oxidation because the best results were with VitC loaded vesicles in terms of size and size distribution stability after six months. Once again, anti-oxidant ability of VitE could preserve oleic acid vesicles from degradation; co-loading of VitC and VitE within oleic acid containing vesicles yielded way bigger vesicles (Dual 8) with a low homogeneity value, but these vesicles were successful in keeping their stabilities even after six months of storage. STEM images belonging to Dual 8 formulation could be seen in Figure 4.16.

LE% for Dual 8 formulation decreased in comparison to singly loaded ones in terms of both VitC and VitE loading. Especially, LE% and LE% stability for VitE decreased dramatically upon co-loading. Even though dual loading of both vitamins made a good impact on vesicle properties in terms of size, homogeneity and stability, it was bad for loading yields. However, the results were quite good to promote a dual loaded commercial skin product containing such valuable skin lipids and vitamins that work synergistically great.

When Tween 80 and oleic acid containing vesicles were compared, all the Tween 80 containing vesicles were smaller than oleic acid containing formulations either with or without cargo. Tweens in liposome research are known for their tendency to form highly curved structures by reducing vesicle sizes and increasing the storage stabilities [125]. So the use of Tween 80 as a surfactant could cause vesicles to be smaller and more stable than oleic acid containing vesicles. Tween 80 containing vesicles were more stable in terms of size and homogeneity upon six months of storage except with VitC loaded ones (Dual 2). The six months stability results were the reverse for VitC containing vesicles; there was a dramatic increase in size and PDI in Dual 2 formulations, whereas they were preserved quite well in Dual 6 ones. Also, adding VitC to the formulations had no significant effect on size and size distribution within both Tween 80 and oleic acid containing TEs, whereas adding VitE increased the size without changing size distribution in both. This may be due to the long hydrophobic chain and chain volume of VitE and hydrophobic cargos like VitE tend to behave as a constitutional lipid

within the TE bilayer structure by causing a slight size increase.

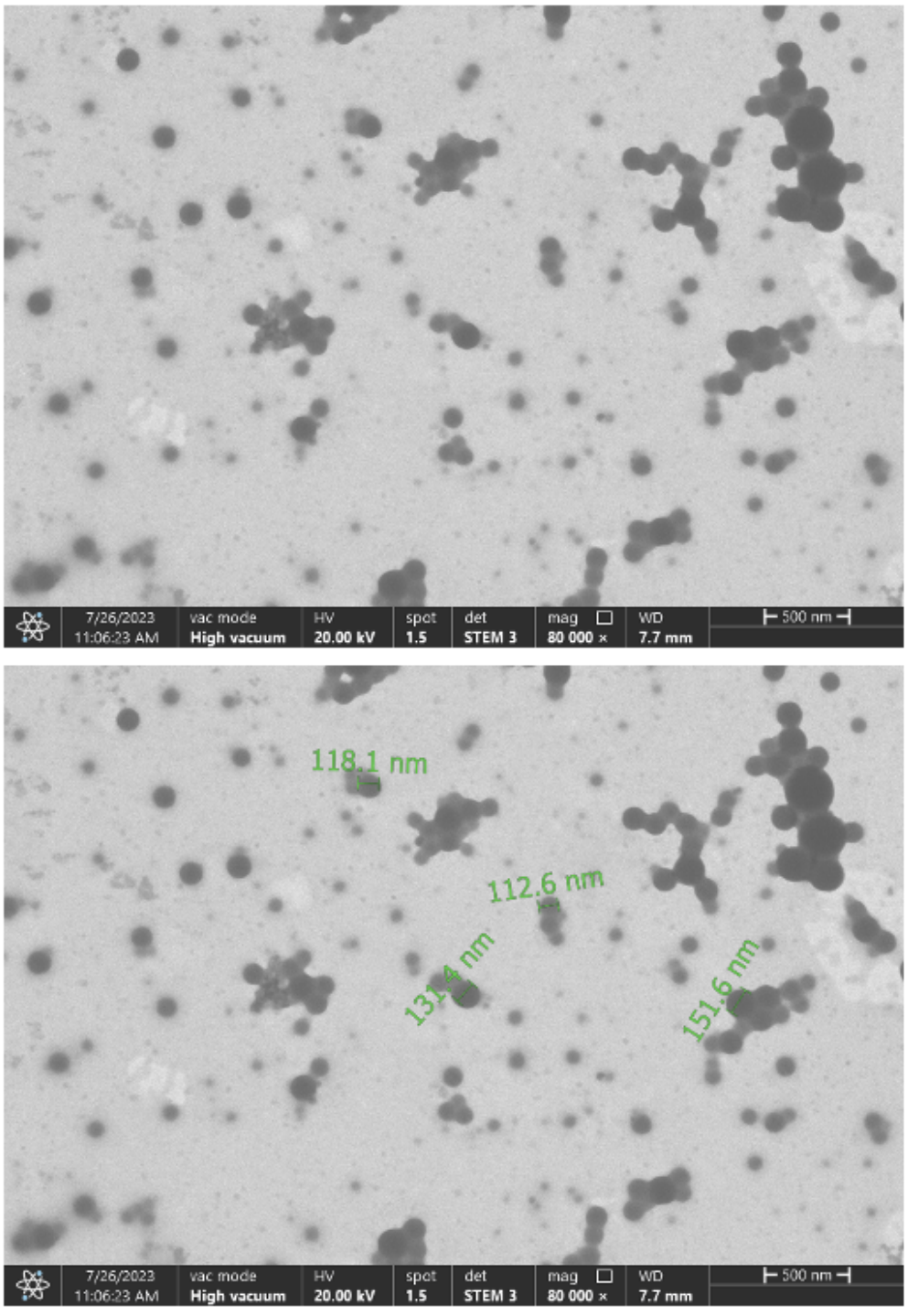

Figure 4.15. STEM image of a sample from Dual 4 formulation set with and without size tags

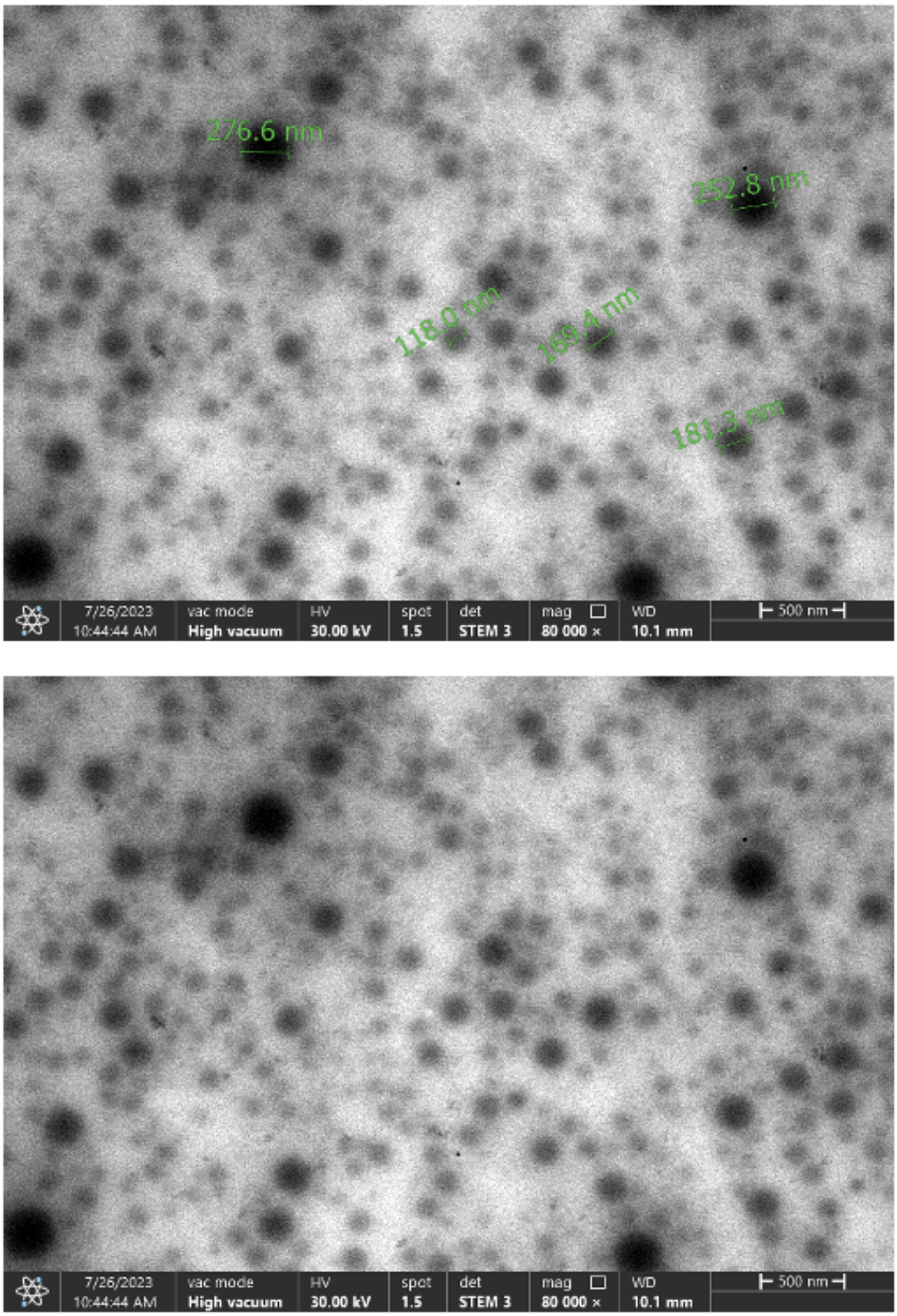

Figure 4.16. STEM image of a sample from Dual 8 formulation set with and without size tags

4.3.2. Chitosan Coating Studies

In literature, some bio-polymers are used to modify the surface of nano-particles like liposomes to protect the stability of the structure and increase the LE%. Chitosan is a naturally occuring cationic polysaccharide and have been widely used in industry due to its biocompatibility, nontoxic, biodegradable and fungistatic properties. In aqueous solutions, the amine moiety of chitosan stays protonated at pH values below 6.5 and becomes a cationic polymer. As a result, it has been regarded as a special biological polymer that can be appropriate for a wide range of required applications such as antibacterial, antioxidant, wound healing and bone formation studies. The cosmetic industry has shown a great deal of interest in chitosan because of its intriguing qualities like being a natural humectant, moisturizer, and rheology modifier for the skin. It is an ingredient approved for use in cosmetics by the FDA and the EU. The main advantage of chitosan is its polycationic nature, thanks to which it can be absorbed by negatively charged skin membranes and support the penetration of actives. Oral administration of chitosan alone is also a treatment option. It has been demonstrated to lower triglyceride and cholesterol levels as well as lower the risk of cardiovascular illnesses. Chitosan is also being used widely for active food ingredient encapsulation in various oral drug delivery applications to protect them from microbial organism attacks and increase their nutritional value [126, 127]. In this part of the study, these unique properties of the chitosan was tried to be utilized by enhancing the application areas of the TEs containing VitC and VitE with the coating studies. With this study, obtained vesicles could be used not only in transdermal delivery applications but also in oral delivery of the selected vitamins. So it could be a wise move to incorporate chitosan coating to the obtained TEs with the advantages of making them more stable and enlarging the application areas. Also, by the presence of chitosan coating, enhancing the transdermal delivery efficiency of VitC and VitE was aimed [128].

DMPG is an anionic lipid and essential component of the membrane bilayers across diverse biological systems. It is found at higher concentrations in lung surfactants and its presence in amniotic fluid indicates fetal lung maturity and fetal fit-

ness [129]. So it was a naturally occurring lipid that can be incorporated into our TE formulations to increase the coating efficiency by creating a charge attraction between the vesicles and the chitosan polymer. Because the lipid composition changed by adding an extra lipid, DMPG containing TEs were generated at first as a preliminary study as summarized in Table 4.3.

Table 4.3. Size, size distribution and 6 month stability comparisions of DMPG containing non-coated (DMPG 1 and 5) and chitosan coated (CHIT1 and 5) vesicles

Sample	**Content**	**Size (nm)**	**PDI**	**6-mo size**	**6-mo PDI**
CHIT0	Chitosan particles	184.36±9.54	0.17±0.08	-	-
DMPG1	Tween TEs	82.21±4.14	0.07±0.01	175.19±62.00	0.25±0.25
CHIT1	Coated Tween TEs	139.36±67.55	0.22±0.06	130.3±42.48	0.22±0.05
DMPG5	O.Acid TEs	94.82±3.25	0.11±0.02	181.80±86.85	0.08±0.02
CHIT5	Coated O.Acid TEs	176.53±44.58	0.24±0.14	162.40±47.06	0.17±0.08

CHIT0 was just chitosan dissolved in 1% acetic acid solution and dropped in ethanol as in cold method production of vesicles just to see if chitosan itself was capable of forming nano-particles or not. To all the formulations except CHIT0, 10:1 mass ratio of Soy PC: DMPG was added. DMPG was dissolved in appropriate amount of ethanol and used with other lipid soluble substances. Chitosan coating was achieved as mentioned in the section 4.2.2.1. Chitosan coated vesicles were coded as CHIT. According to the data in 4.3, chitosan itself was capable of forming nano-particles with a size around 185 nm. DMPG incorporation decreased the 6 month vesicle stability drastically for both tween 80 and oleic acid containing TEs with compared to non DMPG containing Dual 1 and Dual 5 vesicles. However, chitosan coating increased the stability of the vesicles as expected. Chitosan incorporation caused approximately 50% size increase for both DMPG 1 and 5 which indicated a successful coating. Both CHIT 1 and 3 were bigger than non coated vesicles and smaller than the nano-particles created by chitosan itself. Interestingly, while the non coated vesicle sizes were getting bigger after six months, chitosan coated vesicles got smaller upon time. The reason

for that could be degradation of chitosan coating layers upon time but the size and homogeneity data showed the 6-month stability of the coating was good enough as only 6% of a size decrease occurred for both CHIT1 and 5. To be concluded, chitosan coating achieved more stable vesicles as hypothesised at the beginning of the study due to creating more rigid structure by preventing aggregations and direct water exposure.

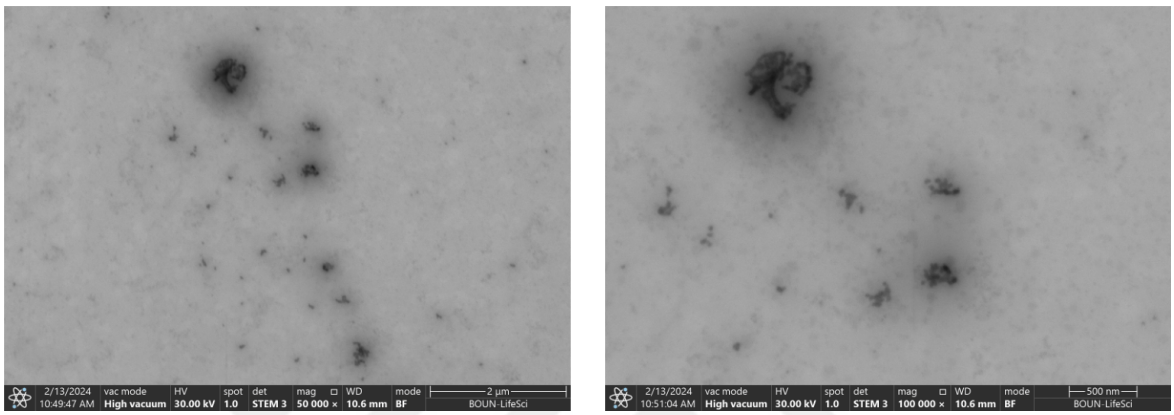

Figure 4.17. STEM of CHIT0, only chitosan nano-particles

Comparison of STEM images of the CHIT 0, DMPG1 and CHIT1 formulations also proved a successful coating. In Figure 4.17, there could be seen the fine nano-particles of chitosan but they were not round shaped vesicular structures like Figure 4.18. TEs were seen as finely rounded shapes. Chitosan coating was also clearly seen around the vesicles in Figure 4.19. Brighter colored circles around dark vesicles were obvious within the approximate size ranges taken by DLS analysis.

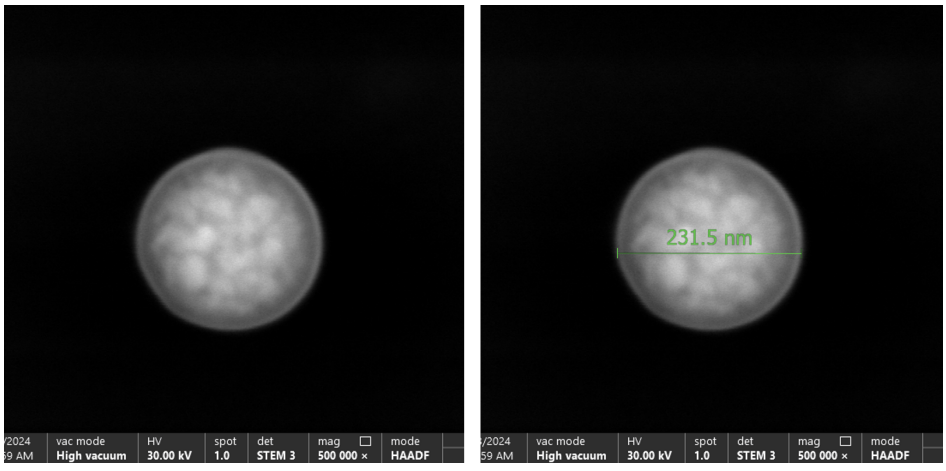

Figure 4.18. STEM of DMPG1, non-coated TE nano-particles

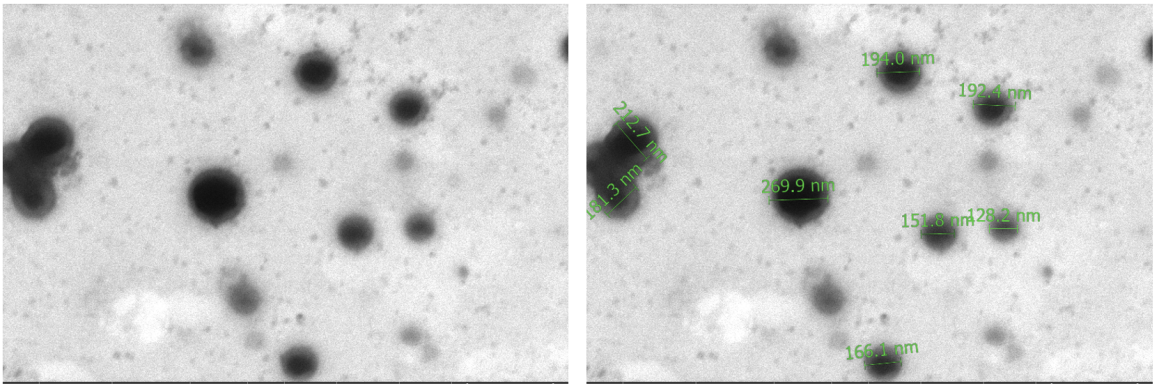

Figure 4.19. STEM of CHIT5, chitosan coated TEs

To test the effect of loading on size and size distribution of the chitosan coated vesicles and study the LE%, following formulations were prepared as presented in Table 4.4. Soy PC:Cholesterol:DMPG:Tween80/Oleic acid:Chitosan mass ratios and the cargo types were specified in the table.

Table 4.4. Mass ratios of Soy PC:cholesterol (Chol.):Tween 80 or oleic acid (O. acid) and chitosan in different TE formulations coded under the abbreviation of CHIT

Sample	**Soy PC**	**Chol.**	**DMPG**	**Tween 80**	**O. acid**	**Chitosan**	**Cargo**
CHIT1	15	1.5	1.5	1.5	-	0.8	-
CHIT2	15	1.5	1.5	1.5	-	0.8	VitC
CHIT3	15	1.5	1.5	1.5	-	0.8	VitE
CHIT4	15	1.5	1.5	1.5	-	0.8	Dual
CHIT5	15	1.5	1.5	-	1.5	0.8	-
CHIT6	15	1.5	1.5	-	1.5	0.8	VitC
CHIT7	15	1.5	1.5	-	1.5	0.8	VitE
CHIT8	15	1.5	1.5	-	1.5	0.8	Dual

All the formulations contained Soy PC, cholesterol and DMPG whereas some of them prepared with tween 80 and others contained oleic acid. Results of this study helped to compare the efficiency of chitosan coating on different surfactant and cargo

containing vesicles.

As the data in Table 4.6 was analyzed, it could be seen that all the vesicles had a more bigger size and lower homogeneity values than non coated versions as demonstrated in Figure 4.20. In this figure, green bars represented chitosan coated vesicles whereas orange bars represented non-coated vesicles and the effect of surfactant could also be observed. Chitosan incorporation made an obvious increase in sizes which may indicate coating layers.

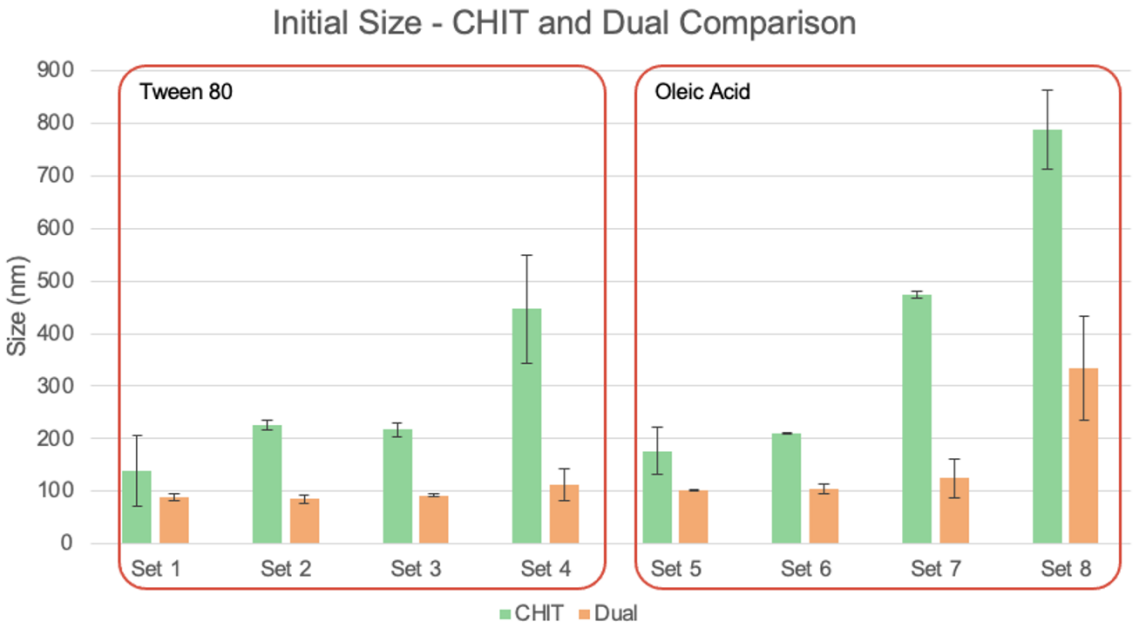

Figure 4.20. Effect of chitosan coating on mean size with respect to non coated vesicles

To better understand the reason behind this difference, a closer look at the solubility, molar weight and ionic properties of the materials used in TE composition were needed to be compared as in Table 4.5. When tween 80 containing chitosan coated vesicles were compared, size and PDI values of VitC cargo containing TEs (CHIT2) were bigger than VitE ones (CHIT3). Being all Tween 80, VitC and chitosan structures hydrophilic, they could solubilize within each other more, and anionic VitC could attract chitosan better due to having opposite charges.

Table 4.5. The solubility, charge and molar weight comparison of the used materials

Material	**Solubility**	**Charge at pH:7**	**Molar weight**
Tween 80	Hydrophilic	Nonionic	1310.0
VitE	Hydrophobic	Nonionic	430.7
VitC	Hydrophilic	Anionic	176.1
Oleic acid	Hydrophobic	Anionic	282.5
DMPG	Hydrophobic	Anionic	688.9
Chitosan	Hydrophilic	Cationic	60000.0

If Dual 2 and CHIT 2 LE% was compared as in Table 4.7 and Figure 4.21, it seemed that this hypothesis was true because without chitosan coating, VitC LE% was lower. Being a non-ionic and hydrophobic cargo, LE% decreased upon chitosan coating, if Dual 3 and CHIT 3 was compared. Co-loading under chitosan coating again was more successful with VitC when Dual 4 and CHIT 4 was compared whereas coating had almost no effect on VitE cargo loading. So hydrophilic compounds could help to be dissolved within each other and chitosan could increase the LE% of VitC again. When oleic acid containing vesicles were compared, this time VitE containing vesicles had bigger size value as expected because being an hydrophobic surfactant, oleic acid solubilized VitE and helped it to incorporate within vesicle structure that could cause an increase in size. LE% of Dual 7 and CHIT 7 were near 98% which proved the hypothesis. Being an hydrophobic surfactant, oleic acid had increased the LE% of VitE as we compare Dual3 and CHIT3 with Dual7 and CHIT7. Co-loading of both vitamins created way bigger vesicles with a very low homogeneity value, so STEM images were needed to be analyzed to be sure that chitosan coating and vesicle formation were successful. In Figure 4.24, STEM image of CHIT8 sample could be seen. Brighter colored circles were quite observable around vesicle structures even though the fine round shape of the vesicles changed a bit.

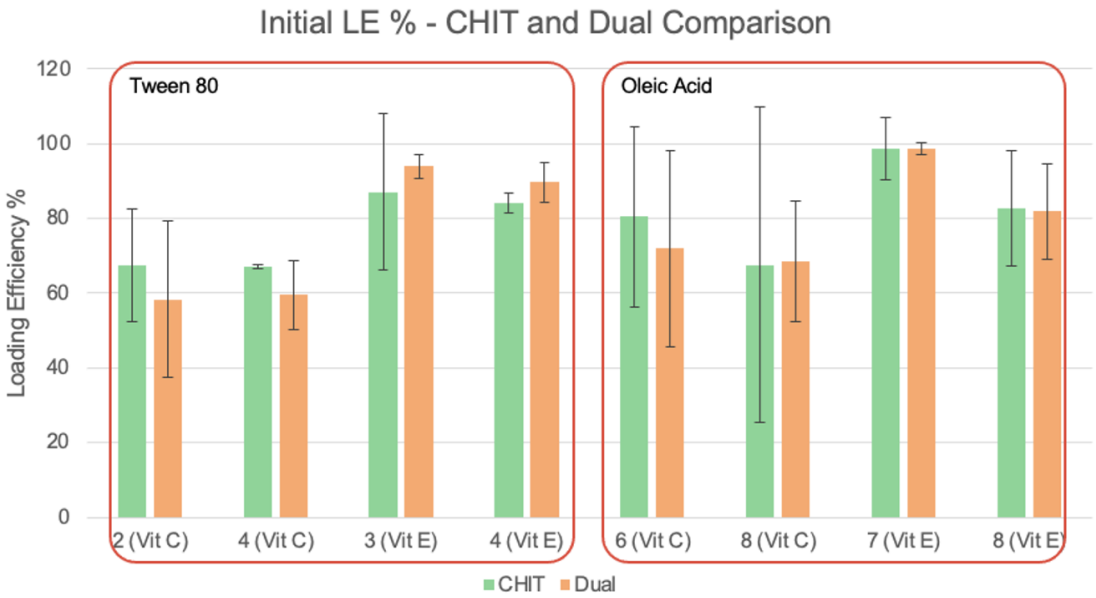

Figure 4.21. Effect of chitosan coating on LE%

Also chitosan coating caused an increase in the one month LE% within co-loaded vesicles for both VitC and VitE. Table 4.7, Figures 4.22 and 4.23 were combined and rearranged forms of the data presented in Tables 4.2 and 4.6 to make an easy comparison of the effect of chitosan coating on physical properties and one month stabilities of them. From these table and figures, all groups could clearly be seen to distinguish the effect of coating. To further observe and correlate the effect of chitosan coating on physical stability and LE% stability, six-month stability results were attempted to be compared. Since only one-month stability results of the chitosan coated TEs were available at the time of the presentation of this dissertation, six-month stability results were not included. However, six-month stability results of the non-coated TEs were presented in Table 4.8.

Lastly, all the PDI values of the coated vesicles were above 0.4 which was normally unacceptable for liposome studies but when the chitosan coating studies were analyzed, it could be seen that chitosan coating resulted PDIs with a range between 0.3 and 0.9 [130–132]. Compared with the literature data, it could be seen that all the chitosan coated vesicles were within the acceptable size range.

With this study, TEs with good physicochemical properties were prepared and embedded within the chitosan network.

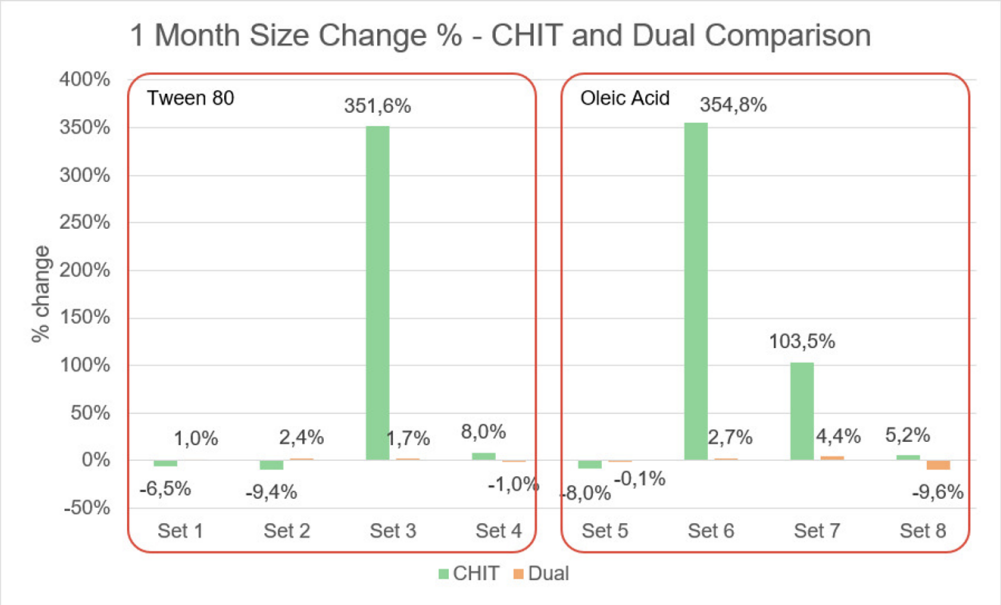

Figure 4.22. Effect of chitosan coating on mean size upon one month storage with respect to non coated vesicles

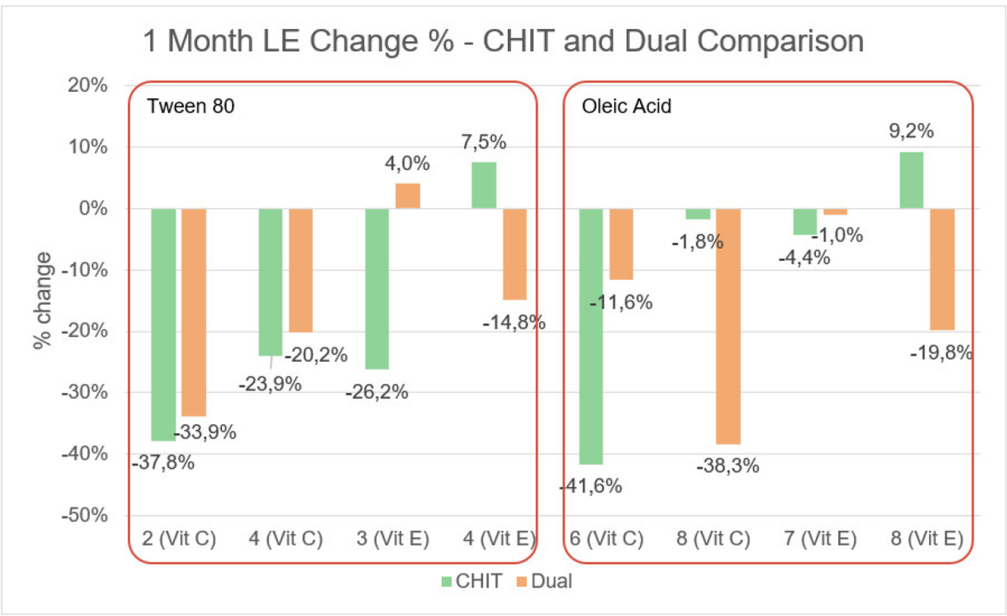

Figure 4.23. Effect of chitosan coating on LE% upon one month storage with respect to non coated vesicles

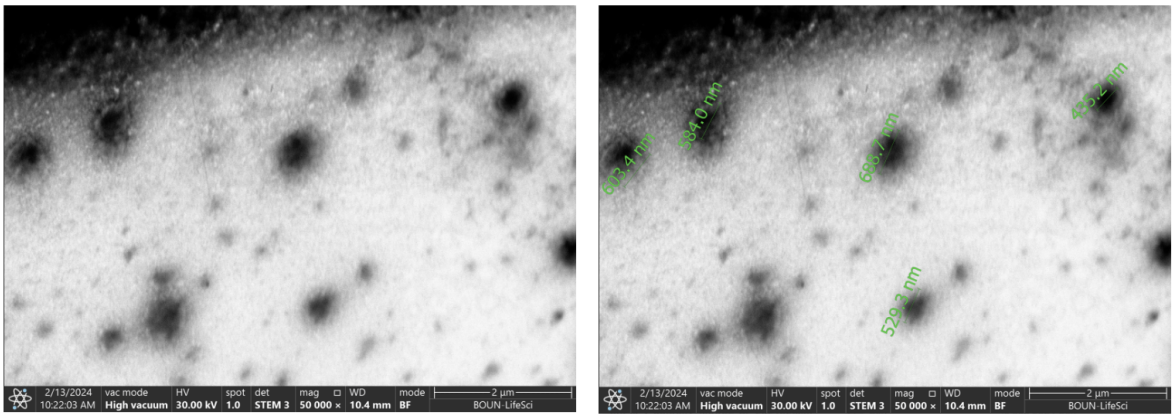

Figure 4.24. STEM of CHIT8, chitosan coated dual loaded TEs

Table 4.6. Effect of surfactant type on physical properties of VitC or VitE loaded, chitosan coated TEs in terms of mean size, PDI and %LE and their one month stabilities

Sample	**Surfactant**	**Cargo**	**Size (nm)**	**Size (nm) (One-month)**	**PDI**	**PDI (One-month)**	**%LE**	**%LE (One-month)**
CHIT1	Tween 80	-	139.36±67.55	130.31±42.48	0.22±0.06	0.22±0.05	-	-
CHIT2	Tween 80	VitC	226.70±8.58	205.40±2.54	0.45±0.02	0.40±0.03	67.50±15.07	42.00±5.38
CHIT3	Tween 80	VitE	217.00±14.34	980.00±129.20	0.40±0.04	0.98±0.02	87.08±20.91	64.25±1.63
CHIT4	Tween 80	Dual	446.80±102.54	482.67±175.11	0.41±0.09	0.49±0.03	67.06±0.63 84.02±2.62	51.00±2.97 90.33±0.45
CHIT5	Oleic Acid	-	176.53±44.58	162.40±47.06	0.24±0.14	0.17±0.08	-	-
CHIT6	Oleic Acid	VitC	211.00±1.38	959.70±75.37	0.16±0.02	0.59±0.36	80.50±24.18	47.00±24.81
CHIT7	Oleic Acid	VitE	475.10±6.65	966.90±81.90	0.35±0.05	0.68±0.18	98.72±8.38	94.42±10.48
CHIT8	Oleic Acid	Dual	787.73±76.05	828.66±104.51	0.59±0.31	0.57±0.25	67.51±42.24 82.66±15.38	66.30±15.84 90.29±2.31

Table 4.7. Comparison of coated and non-coated vesicles in terms of mean size, PDI and %LE and their one month stabilities

Sample	**Surfactant**	**Cargo**	**Size (nm)**	**Size (nm) (One-month)**	**PDI**	**PDI (One-month)**	**%LE**	**%LE (One-month)**
Dual2	Tween 80	VitC	84.94±8.26	86.96±13.08	0.08±0.06	0.13±0.08	58.29±20.97	38.53±22.09
CHIT2	Tween 80	VitC	226.70±8.58	205.40±2.54	0.45±0.02	0.40±0.03	67.50±15.07	42.00±5.38
Dual3	Tween 80	VitE	92.52±1.70	94.06±5.12	0.06±0.03	0.07±0.03	93.92±3.08	97.73±0.34
CHIT3	Tween 80	VitE	217.00±14.34	980.00±129.20	0.40±0.04	0.98±0.02	87.08±20.91	64.25±1.63
Dual4	Tween 80	Dual	112.88±31.23	111.75±1.77	0.16±0.15	0.09±0.01	59.43±9.30 89.67±5.38	47.45±13.65 76.38±29.31
CHIT4	Tween 80	Dual	446.80±102.54	482.67±175.11	0.41±0.09	0.49±0.03	67.06±0.63 84.02±2.62	51.00±2.97 90.33±0.45
Dual6	Oleic Acid	VitC	104.26±10.00	107.04±13.10	0.10±0.03	0.11±0.06	71.92±26.14	63.55±28.33
CHIT6	Oleic Acid	VitC	211.00±1.38	959.70±75.37	0.16±0.02	0.59±0.36	80.50±24.18	47.00±24.81
Dual7	Oleic Acid	VitE	124.84±36.53	130.39±38.67	0.10±0.03	0.12±0.02	98.66±1.59	97.66±1,98
CHIT7	Oleic Acid	VitE	475.10±6.65	966.90±81.90	0.35±0.05	0.68±0.18	98.72±8.38	94.42±10.48
Dual8	Oleic Acid	Dual	334.32±98.60	302.40±77.57	0.38±0.12	0.37±0.06	68.49±16.12 81.91±12.69	42.23±19.24 65.72±15.65
CHIT8	Oleic Acid	Dual	787.73±76.05	828.66±104.51	0.59±0.31	0.57±0.25	67.51±42.24 82.66±15.38	66.30±15.84 90.29±2.31

Table 4.8. Comparison of coated and non-coated vesicles in terms of mean size, PDI and %LE and their 6-month stabilities

Sample	**Surfactant**	**Cargo**	**Size (nm)**	**Size (nm) (6-month)**	**PDI**	**PDI (6-month)**	**%LE**	**%LE (6-month)**
Dual2	Tween 80	VitC	84.94±8.26	229.65±195.29	0.08±0.06	0.23±0.22	58.29±20.97	0
CHIT2	Tween 80	VitC	226.70±8.58	Not Available	0.45±0.02	Not Available	67.50±15.07	Not Available
Dual3	Tween 80	VitE	92.52±1.70	96.17±5.42	0.06±0.03	0.08±0.01	93.92±3.08	69.36
CHIT3	Tween 80	VitE	217.00±14.34	Not Available	0.40±0.04	Not Available	87.08±20.91	Not Available
Dual4	Tween 80	Dual	112.88±31.23	113.80±13.86	0.16±0.15	0.07±0.01	59.43±9.30 89.67±5.38	0 54.44±7.58
CHIT4	Tween 80	Dual	446.80±102.54	Not Available	0.41±0.09	Not Available	67.06±0.63 84.02±2.62	Not Available Not Available
Dual6	Oleic Acid	VitC	104.26±10.00	112.30±8.06	0.10±0.03	0.29±0.02	71.92±26.14	27.00
CHIT6	Oleic Acid	VitC	211.00±1.38	Not Available	0.16±0.02	Not Available	80.50±24.18	Not Available
Dual7	Oleic Acid	VitE	124.84±36.53	117.30±8.54	0.10±0.03	0.12±0.02	98.66±1.59	79.79
CHIT7	Oleic Acid	VitE	475.10±6.65	Not Available	0.35±0.05	Not Available	98.72±8.38	Not Available
Dual8	Oleic Acid	Dual	334.32±98.60	223.50±71.56	0.38±0.12	0.46±0.04	68.49±16.12 81.91±12.69	25.00±2.32 27.50±9.65
CHIT8	Oleic Acid	Dual	787.73±76.05	Not Available	0.59±0.31	Not Available	67.51±42.24 82.66±15.38	Not Available Not Available

4.4. Conclusions

The human skin acts as a protective barrier, allowing topical treatments like cosmeceuticals to penetrate the SC selectively. Agents like TEs that can mimic the skin membrane, make transdermal delivery more successful. Surfactants in TE preparation serve two main functions: edge activating and penetration enhancing. Tween 80 and oleic acid are common surfactants in dermo-cosmetics, used to create TEs and vesicles. Tween 80 improves skin penetration and stability, while oleic acid enhances penetration and drug absorption. Both surfactants can overcome skin barriers, making them effective in enhancing drug absorption and carrier delivery in topical administration. So in this study, effect of surfactant choice on physical properties of the vesicles in terms of size, homogeneity and LE% was analyzed.

For loading studies VitC and VitE were chosen. VitC, also known as ascorbic acid, is a water-soluble antioxidant used in dermatology to treat skin diseases like hyperpigmentation and is involved in tissue repair, collagen synthesis, and neurotransmitter production. However, it is sensitive to pH, temperature, oxygen, and catalysts, and its stability is crucial for preservation solutions. ViE, also known as alpha-tocopherol, is a lipid-soluble vitamin known for its antioxidant properties against free radicals and anti-inflammatory properties. However, its low bioavailability and oxidation resistance make it a significant barrier for therapeutic use in skin disease prevention and treatment. Recent studies suggest that reactive oxygen species, such as free radicals, contribute to allergic inflammation and oxidative stress, leading to the development of AD. Oral VitE and VitC supplements have shown beneficial effects in treating AD disease. The antioxidant and anti-inflammatory properties of VitE and VitC, when delivered through transdermal agents, could be a promising supplementary treatment for AD skin disease.

To summarize, dual loading of VitC and VitE within TEs either containing Tween 80 or oleic acid was successful for both formulations to be used in transdermal delivery studies. Tween 80 containing vesicles were smaller in size (around 95 nm) with better

homogeneity values (around 0.07 PDI) in general. Oleic acid formulations had a size around 160 nm in average with a PDI of 0.17. Also six month stability values of the tween 80 containing vesicles were better. Tween 80 vesicles were around 132 nm with 0.12 PDI whereas oleic acid containing vesicles had 220 nm size in average with 0.27 PDI upon six months of storage.

For both formulations, VitE caused a size increase with better LE% values indicating that it was used as a constitutional lipid within the vesicle bilayers. For both tween 80 and oleic acid vesicles VitE LE% was above 90% even after one month of storage. Oleic acid vesicles were better in loading VitC by having a 70% of LE% in contrast to tween 80 vesicles that had a 60% VitC LE% roughly. One month VitC LE% results were also better for oleic acid vesicles; they yielded 63% LE% whereas it was 38% for tween 80 containing ones.

Co-loading of VitC and VitE caused a dramatic size and PDI increase for both formulations but they both kept their physical stabilities well even after six months of storage. LE% of VitC was best achieved with Dual 8 TE formulations that contained oleic acid whereas tween80 TEs were better in loading VitE within dual loading. Dual 8 vesicles contained around 68% of VitC and 82% of VitE where Dual 4 vesicles the values were 59% for VitC and 90% for VitE.

With chitosan coating the aim was to broaden the application areas of the obtained TEs and to increase the stability in terms of LE%. With CHIT 8 formulation this aim was achieved. Even though bigger size and lower homogeneity having vesicles, LE% and loading stability was quite successful than non coated vesicles. CHIT 8 had an LE% of 67% for VitC and 82% for VitE which was stable even after one month without any change in loading percentages. Size and PDI values were all bigger for chitosan coated vesicles which was around 257 nm for tween 80 containing ones and 400 nm for oleic acid formulations. PDI values were varied between 0.2 and 0.6 which was an acceptable range for chitosan coating studies.

With this study, successful formulations loading either VitC, VitE or both were obtained by using Soy PC, cholesterol, tween 80 and oleic acid. Chitosan coating studies to extend the application areas of the obtained vesicles were also achieved. All the TEs were characterized in terms of size, size distribution, morphology, stability and LE%. All the vesicles were capable in using AD treatment studies but future work is needed to be done in terms of transdermal delivery studies. A future work can be done by examining the skin penetration characteristics and cyto-toxicity of the obtained TEs.

5. PROTEIN LOADING STUDIES WITHIN TRANSETHOSOMES

5.1. Introduction

Proteins are one of the most complicated bio-molecular structures found in living organisms. They are formed when amino acid chains are covalently bonded with peptide bonds and function mostly in catalytic processes, metabolism, signal transduction, storage, transport, defense, and structural support. Each protein has its unique structure and function due to the arrangement of the 20 amino acids that are employed in the creation of proteins. Proteins have four structural levels which can be divided as primary, secondary, tertiary and quaternary structure as illustrated in Figure 5.1.

Primary structure stands for the straight polypeptide chains formed by amino acids with peptide bonds. The formation of secondary structure involves the repeated folding of these chains and divided into two subgroups: α-helix and β-sheet. In the conformation of the α-helix, each backbone N-H group forms a hydrogen bond with the backbone C=O group of the amino acid located four residues ahead in the protein sequence, while β-sheets are formed when the parallel hydrogen bonds fuse together by creating a generally twisted, pleated sheet. 3D arrangement that a single protein molecule can form by folding into a compact globular structure is referred as tertiary structure. These conformations are driven by a variety of non-covalent interactions like hydrophobic collapse, hydrogen bonding, ionic interactions and Van der Waals forces. Hydrophobic collapse cause the hydrophobic parts of the protein to fold inward and ensure that the hydrophilic parts remain outside, turning the proteins into hydrophilic structures. It is very crucial to determine the tertiary structure of proteins to understand how they operate at the molecular level. Lastly, quaternary structure is made up of the accumulation of two or more distinct polypeptide chains (subunits), that work together to form a single functional unit [133].

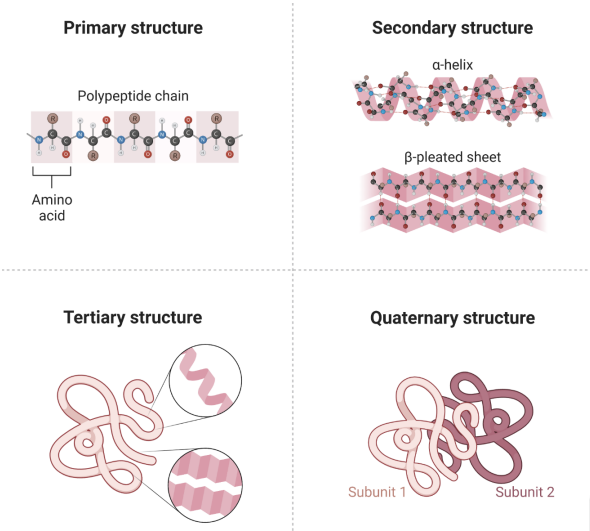

Figure 5.1. Four levels of protein structure (Created with BioRender.com, accessed on June 2024)

Proteins can be introduced into the body by mouth, catheter, needle injection, or locally transmitted from the skin surface. The term "first pass mechanism" refers to the process when a drug enters the body and passes through the digestive system, it is broken down in the liver. So most of the substances taken orally or through the vessels are metabolized by the liver, and very few can get into the circulatory system. Transdermal delivery has advantage of transmitting the active substance directly into the circulation or transferring it to the target organ, by overcoming this mechanism [134, 135]. The biggest problem with the proteins delivered transdermally is their large volume and mass (57 kDa on average). In addition, due to having a hydrophilic structure, proteins find it difficult to pass through the lipophilic SC. Furthermore, even if the proteins can pass under the skin, they are at risk of deterioration due to their low stability and half-life.

Thanks to the developments in nanotechnology, successful transmission of these macro-molecular structures through the skin has begun to be achieved with the help of nano and micro carriers, and transdermal delivery has gained popularity. Lipid vesicles are one of the most promising tools that is used lately in skin delivery studies to carry and utilize proteins [136, 137]. As previous writers have examined and documented in

the literature, the high molecular weight and 3D shape of the proteins make protein loading into lipid vesicles difficult. Either passive loading or active loading techniques, or a mix of the two, can be employed to carry out the procedure. In brief, protein internalization occurs during the vesicle formation and assembly stages in the passive approach. Drug molecules that can only diffuse one way are added to premade liposomes using the active-loading technique [138]. In order to boost skin permeability and establish new pathways for the vesicles to pass through the skin, the TE type of vesicles were used in this study, as a passive loading strategy. These vesicles contained proteins; filaggrin, caspase-14 and protein-arginine-deiminase-type-1 (PAD-1) that had been selected for use in the treatment of AD skin disease.

Filaggrin is a 37kDa protein that supports the mechanical integrity of the skin by keeping the keratin filaments together. Since the dryness of human skin is related to the proper functioning of the keratin filaments, the amount of filaggrin present in the skin is also directly related to skin water retention and preventing water loss. When the corneocyte layer that provides the skin barrier is not formed properly, the skin cells dry up, causing cracks in the lipid layer. With the decrease of the water gradient in the outer layers of the epidermis, filaggrin hydrolysis occurs in hygroscopic amino acids such as arginine, glutamine and histidine and also to their derivatives, such as pyrrolidone carboxylic acid and uraconic acid as illustared in Figure 5.2. They generate natural moisturizing factor which is responsible for maintaining skin hydration and water retention within the SC in conditions of low environmental humidity. Recent studies have found that loss-of-function mutations in FLG, the gene encoding the filaggrin, is the main cause of AD [139–142]. An additional notable study showed that increasing filaggrin levels in FLG deficient mice can reduce the mice's development of the AD phenotype. Consequently, transdermal delivery of this protein might be an effective strategy to enhance AD [143].

Filaggrin is a key protein for the epidermal barrier function and deimination is a major step in its metabolism. Deimination is the process by which the amino acid citrulline is created from the amino acid arginine inside a peptide sequence. A

class of enzymes known as peptidylarginine deiminases catalyzes this post-translational alteration. In order to utilize filaggrin, PAD-1 enzyme must break down it into free amino acids by deiminating it. Unprocessed filaggrin cannot continue working while attached to keratin filaments [144]. So, abnormalities in the metabolic process of filaggrin can result in a malfunctioning skin barrier and SC dehydration and it may be a wise move to deliver PAD-1 enzyme through skin to boost this metabolic process.

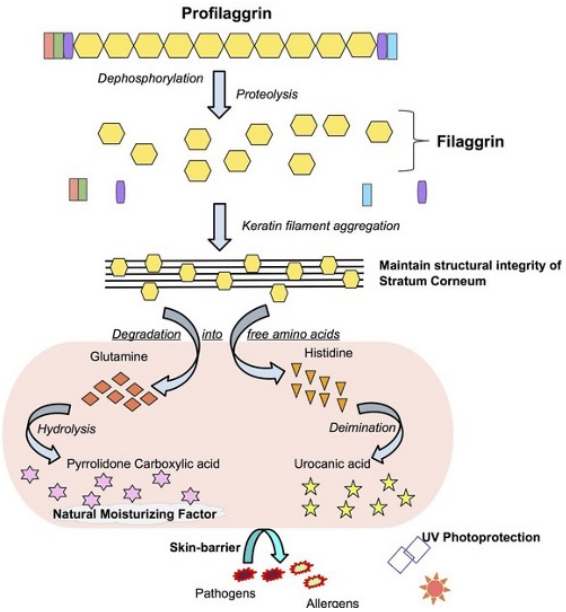

Figure 5.2. Illustrated scheme of filaggrin working pathway [145]

Further degradation of deiminated filaggrin monomers into smaller fragments, that are pyrrolidone carboxylic acid and uraconic acid, is facilitated by the actions of three enzymes: bleomycin hydrolase, calpain-1, and caspase-14. In 2007, a study done by Denecker, et al., proved the importance of caspase-14 presence for maintenance of a healthy skin by observing reduced epidermal hydration and increased trans-epidermal water loss in caspase-14 deficient mice. They suggested that may be caused by the absence of filaggrin conversion into free hygroscopic amino acids. The study showed that filaggrin was expressed in the lower cornified layer in wild-type skin whereas in caspase-14–deficient skin, additional filaggrin fragments were detected in the upper layers of the SC. This research provided evidence that caspase-14 enzyme is absolutely needed for the degradation of filaggrin protein [146,147]. Moreover, caspase-14 participates in the process of the formation of lipid water-repelling coat for the skin and plays

a crucial role for the protection against outer stress factors like transdermal water loss and UV radiation [148].

A randomized controlled trial of an emollient with ceramide and filaggrin associated amino acids for the primary prevention of AD showed that daily application of the emollient therapy had a protective impact on the development of the disease and gives promising results for transdermal delivery of the proteins [149]. Ceramides are branch of sphingolipids that are responsible for intra-cellular signal mediators in cell differentiation, growth inhibition, and apoptosis. Importance of ceramides for AD patients was already discussed in Section 3.1. In this study, Cer3 was also included within TE formulation for its upregulation effect on caspase-14. The native caspase-14 protein is not catalytically active and it is activated somewhere between the granular and cornified layers which both are within epidermis. High activity levels of caspase-14 are particularly demonstrated in existence of ceramides. So, the upregulation of caspase-14 has been confirmed to be stimulated by ceramides [150].

Denaturation is the disruption of a protein's tertiary structure and biological activity and can occur at high temperatures, acidic environments and upon interaction with organic solvents. Since the proteins attempted to be loaded in this project were exposed to an environment containing ethanol, their tertiary structures and biological activities had to be monitored. For this reason, the 3D structures and activities of the proteins were monitored with circular dichroism (CD) spectrometry during the loading process. The basis of CD is the difference in the absorption of left and right circularly polarized light by chromophores that possess intrinsic chirality. As the peptide bonds absorb the light, proteins contain a number of chromophores which can give rise to CD signals. Regular secondary structural characteristics like α-helix and β-sheet can be found in the CD spectra by analyzing the far UV region (240-180 nm), which correlates to the peptide bond absorption. Tertiary structure analysis can be done within the near UV region (320–260 nm), which is reflected by the environments of the aromatic amino acid side chains [151].

By taking into account how the skin barrier contributes to the onset of AD, delivery strategies of filaggrin, PAD-1 and caspase-14 proteins were investigated to strengthen the barrier function, and to treat and/or prevent the disease. So, the aim of the current study was loading of these proteins within vesicles, i.e. TEs, containing Soy PC, Tween 80, Cer3 and cholesterol and follow their stabilities after a six months of storage range. Oleic acid was not preferred as an edge activator due to its a negative charge. It has been studied that negatively charged vesicles obtained either by passive or active loading methods resulted in low LE% [138]. Obtained vesicles were characterized in terms size and size distribution, LE% and morphology. Size and size distribution were followed by DLS whereas the morphologies were monitored via STEM. Protein LE% studies were monitored via UV/Vis spectroscopy. Loaded proteins were analyzed to see if they were retaining the proper secondary and tertiary structures during and after the vesicle formation or not. CD was used to assay structures of the proteins.

5.2. Experimental

5.2.1. Materials

Soy PC with 94 % PC content, in light orange colored grease form, was kindly provided by Lipoid GmBH (Ludwigshafen, Germany) under the brand name of Lipoid S 100. Detailed information about Soy PC can be found in section 3.2.1.

Cholesterol was purchased from Sigma Aldrich in white powder form with more than %99 purity. Detailed information about this lipid can be found in section 3.2.1.

Tween®80 and ethanol with 99 % purity were purchased from Merck. Tween®80 was in the form of yellow liquid and used as an edge activator. Ethanol was used to solubilize the hydrophobic materials used in the formulation.

Water was used as the main solvent for the proteins. All the experiments were performed using ultrapure Milli-Q water (Type 1) from Millipore instrument. 1:2

ethanol:water volume ratio is kept constant for all the vesicular dispersions.

Cer3 was kindly provided by Novodist Turkey in white solid form.

Recombinant mouse filaggrin and recombinant human PAD-1 with histidine tags were purchased from mybiosource.com with 85% purity as freeze-dried powder. Reconstituted filaggrin protein solution was prepared with 20 mM Tris containing 150 mM NaCl with a pH of 8.0 to a concentration of 1.0 mg/mL. This 37 kDa positively charged protein contains mostly arginine and histidine residues and has a β-sheet secondary structure. Reconstituted PAD-1 protein solution was prepared with water to a concentration of 0.2 mg/mL. This 75 kDa protein catalyzes the deimination of arginine residues of filaggrin and maintains hydration of the SC.

Recombinant human caspase-14 with histidine tag was purchased from Elabscience Biotechnology Inc. with 95% purity as lyophilized powder. Reconstituted protein solution was prepared with 20mM PBS containing 150mM NaCl with a pH of 7.4 to a concentration of 0.2 mg/mL. This 28 kDa enzyme is found in SC and plays an important role in regulating maturation of the epidermis by processing filaggrin.

5.2.2. Methods

5.2.2.1. Preparation and Characterization of TEs. TEs were prepared with the cold method as mentioned in section 3.2.2.1. Proteins were dissolved in aqueous phase and heated separately to 35°C. The aqueous phase was added to the ethanol solution drop by drop using a 1 mL syringe with a speed of 250 µL/min. The lipid mass ratios and proteins used in different TE formulations can be found in Table 5.1, presented as Soy PC:cholesterol:Tween 80:Cer3 mass ratios. In all the cargo loaded formulations 10 µg/ml of protein is used. These concentrations were chosen such that they could be followed by UV/Vis spectroscopy. In all the formulations, total lipid concentration in the final TE dispersion was preserved constant as 10 mg lipid per ml of total dispersion and ethanol:water volume ratio was fixed as 1:2. Characterization of TEs were

performed as mentioned in section 3.2.2.2.

Table 5.1. The mass ratios of Soy PC, cholesterol, Tween 80 and Cer3 with the indicated cargo types in different TE formulations coded as FLG, PAD and CAS

Sample	**Soy PC**	**Cholesterol**	**Tween 80**	**Cer3**	**Cargo Type**
FLG	15	1.5	1.5	1.5	Filaggrin
PAD	15	1.5	1.5	1.5	PAD-1
CAS	15	1.5	1.5	1.5	Caspase-14

5.2.2.2. Loading Efficiency Studies. To separate the loaded vesicles from the bulk solution, the ultracentrifugation technique was used as a quick and effective option. The Vivascience Vivaspin 2 mL concentrator and the Rotafix 32 Hettich centrifuge were used in conjunction to filter the loaded vesicle suspensions. Every sample was centrifuged at room temperature at 6000 rpm. Periodically, solutions at the bottom of the filtration tube were inspected using UV/Vis spectrophotometer, and by this way any excess payload was removed. Un-loaded free proteins had all been removed from their external vesicle containing media with ultra-centrifugation under 6000 rpm, for 30 minutes and the resultant filtrates that contain free cargo were measured using a UV/Vis spectrophotometer.

5.2.2.3. Following the Stability of the Protein Structures. With CD spectroscopy, the difference between the absorption of left- and right-handed circularly polarized light is measured. Every chemical that is optically active will exhibit the CD phenomena but this method is applied significantly for detection of secondary structure of the proteins which contains chirality. So, percentages of alpha helices, beta sheets and random coils can be calculated with the help of CD analysis at different physical conditions (temp, pH, salt, concentration, ligands, etc.) as illustrated in Figure 5.3. For a pure alpha helical structure, the CD spectrum obtained between 190 and 250 nm shows a greater maximum at 191–193 nm and a typical double minimum at 208 and 222 nm. Similar

to this, the beta-sheet structure has a maximum at 198 nm and a typical minimum at 215 nm. Protein random coil segments, on the other hand, typically show a maximum and a minimum that are practically the reverse of those of alpha-helical and beta-sheet structures [152]. By CD spectroscopy, one can also determine if a protein is folded or not by measuring the structural integrity and the stability of domain structures. Visual inspection of the spectra suggests largely unfolded proteins if there is a negative maximum near 200 nm [153].

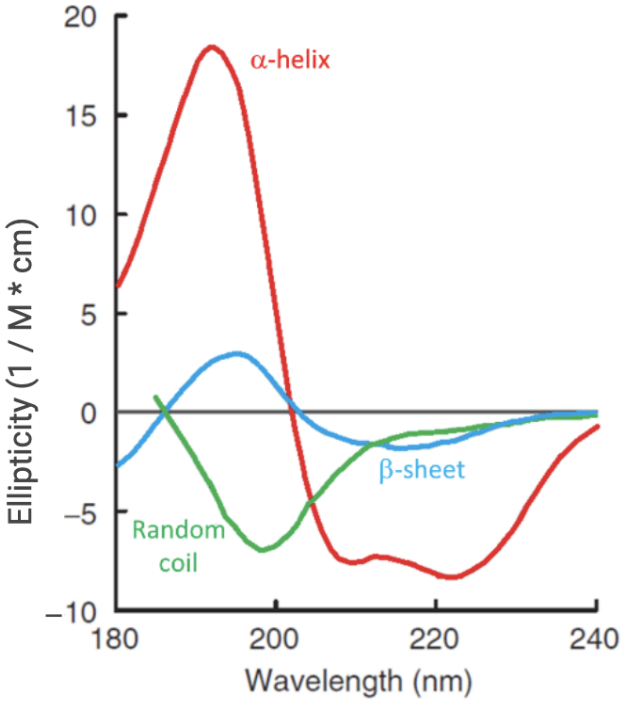

Figure 5.3. Typical CD spectra of proteins (Created with BioRender.com, accessed on June 2024)

The Jasco Model J-810 spectro-polarimeter instrument was used to detect protein stabilies. CD signal arises from the peptide bonds and so, larger proteins will give stronger signals at the same concentrations in contrast to smaller proteins. So before the analysis the size of the proteins were entered to the CD software to determine the molar ellipticity values. Protein concentrations for CD scans with a 1 mm path-length should be between 10 and 30 µg/ml, with a total volume of about 2 ml. For filaggrin, 4 µg/ml protein was prepared in 2:1 water:ethanol solvent and CD data was

taken before and after shaking vigorously for 30 min with vortex. The concentration was lower than others because it was giving strong elipticity values. For caspase-14 and PAD-1, 20 µg/ml protein was prepared in 2:1 water:ethanol solvent and CD data was taken before and after shaking vigorously for 30 min with vortex. Ellipticity was reported in millidegrees (mdeg).

5.3. Results and Discussion

5.3.1. Preparation and Characterization of Protein Loaded TEs

According to the results presented in Table 5.2, all the protein loaded vesicles were within the acceptable size and PDI range to be utilized in transdermal delivery studies.

Table 5.2. Mean size and homogeneity values of TEs (number of trials, n=3)

Sample	**Size (nm)**	**6-month size (nm)**	**PDI**	**6-month PDI**
FLG	89.50±0.28	127.13±1.92	0.03±0.02	0.40±0.01
CAS	89.58±14.65	94.50±15.63	0.07±0.01	0.12±0.08
PAD	82.42±8.88	83.87±9.09	0.07±0.00	0.10±0.01

TEs that have sizes smaller than 100 nm are stated as good candidates for subcutaneous cargo material delivery. PDI index results showed that the obtained vesicles were quite homogeneous and upon six month of storage the size and homogeneity values were preserved successfully. However, even though the mean size and PDI results were similar for the freshly prepared vesicles, size and PDI increment upon six months of storage was highest for FLG vesicles. This could be due to the fact that filaggrin was a positively charged histidine-rich protein and those charges might affect the stability of the vesicular system. CAS and PAD formulations showed similar stability values after six months of storage.

In Figure 5.4, round and bilayer structures of the resultant FLG vesicles could distinctly be observed through STEM images. Measured size values were consistent with the data obtained from DLS results. It could also be confirmed that homogeneity of the dispersion media was in agreement with the PDI outcomes; there were nearly same sized particles all over the sample.

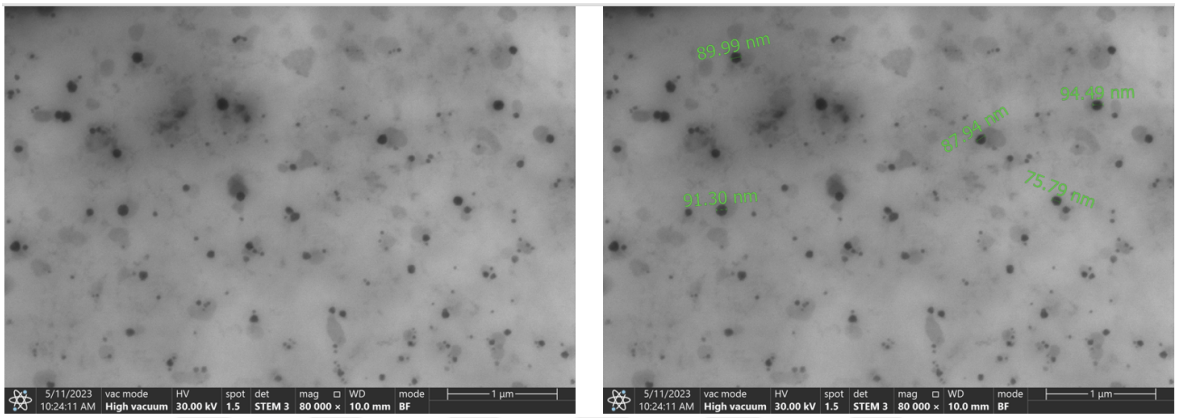

Figure 5.4. STEM images of the vesicles belonging to the data set of FLG

In Figure 5.5, STEM images of pure caspase-14 protein could be seen. There were distinct line shaped structures similar to polymers all over the sample. If the structural analysis of this image was compared to the Figure 5.6, which belonged to the vesicles loaded with caspase-14 protein, it could be clearly seen that there were no traces of protein and ellipse shaped, protein containing shiny vesicles were formed and even the proteins could be seen within the vesicles. Observed size and homogeneity ranges were consistent with the calculated DLS results.

In Figure 5.7, STEM images of pure PAD-1 protein could be seen. There were accumulations of fibrillary structures which were bigger than caspase-14 proteins that was consistent with the molecular weight data. Caspase-14 was a 28 kDa protein whereas PAD-1 was 75kDa and this could clearly be observed from the STEM images. If the protein structures were compared to the Figure 5.8, which belonged to the vesicles loaded with PAD-1 protein, it could also be clearly seen that there were no traces of protein and oval shaped, protein containing vesicles were formed with the proteins

visible within the vesicles. Observed size and homogeneity ranges were also consistent with the calculated DLS results.

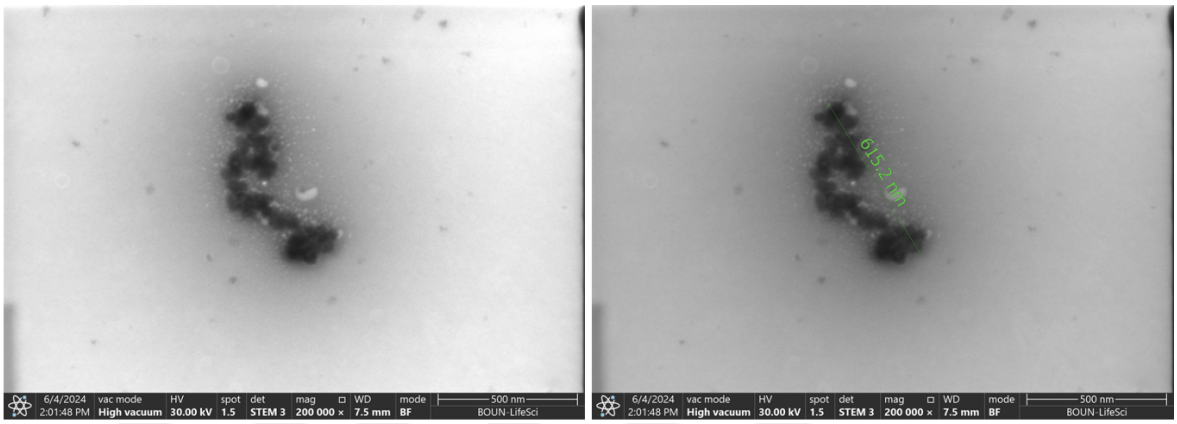

Figure 5.5. STEM images of caspase-14 proteins

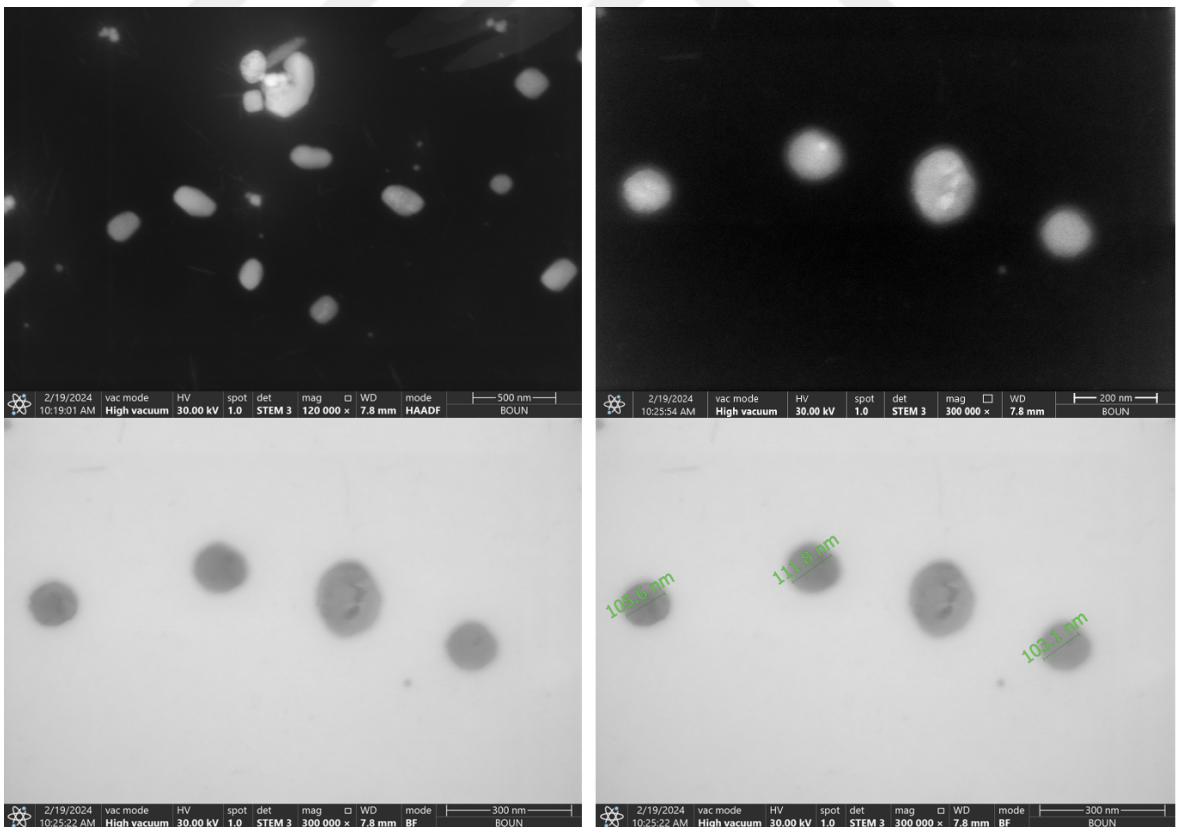

Figure 5.6. STEM images of the vesicles belonging to the data set of CAS

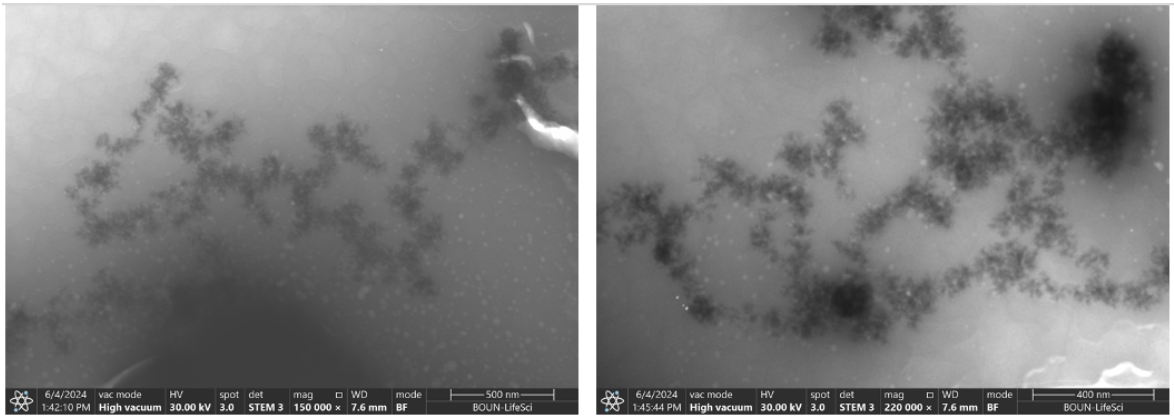

Figure 5.7. STEM images of PAD-1 proteins

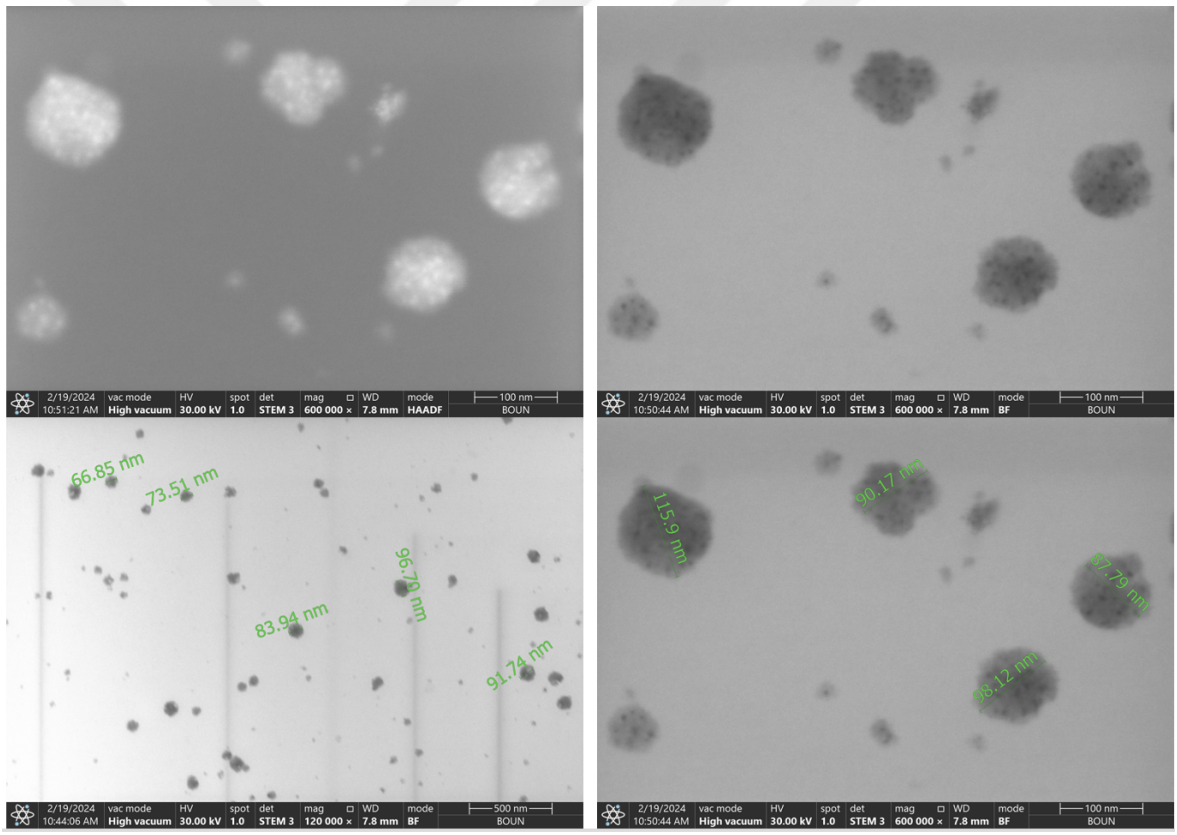

Figure 5.8. STEM images of the vesicles belonging to the data set of PAD

5.3.2. The Stability of the Protein Structures During Vesicle Preparation

To examine the effect of using 1:2 ethanol:water as solvent and long term mixing process upon preparation of the protein containing vesicles, proteins were subjected

to 30 min vigorous shaking under vortex in 1:2 ethanol containing solution. The aim was to compare and contrast the effect of the preparation process on the secondary structures of the proteins and to observe if any destruction on the proper folding of the proteins occurred or not. As seen in Figure 5.9, the secondary structure of the filaggrin protein was mostly preserved but there was a 33% decrease in the intensity of the peak came around 198 nm which meant a decrease in the concentration of beta sheets. However, peaks around 208 and 222 nm were stayed exactly the same that showed the alpha helix content of the protein was conserved upon vesicle preparation process. According to protein data bank with a code of 4pcw, filaggrin has a total of 8 histidine residues which 4 of them are in alpha helices and the others are found in random coils. So it could be concluded that histidine residues were not affected from the ethanolic process.

In order to investigate the impact of utilizing a 1:2 ethanol:water solvent and a prolonged mixing procedure during the formation of protein-containing vesicles, caspase-14 and PAD-1 proteins were also vigorously shaken for 30 minutes under a vortex in a 1:2 ethanol solution. As seen in Figures 5.10 and 5.11, the secondary structure and the folding pattern of the caspase-14 protein was mostly preserved whereas PADI-1 protein's structure changed from beta sheet to random coil distinctly and folding pattern of the substance was disturbed. According to protein data bank with 5HP5 code, there are 34 histidine residues in PAD-1 protein which are mostly located in alpha helices and beta sheets. So, histidine residues were affected from the ethanolic process and an alternative procedure for passive loading of PAD-1 protein needs to be developed. There was a 6% of change in beta sheet content in caspase-14 structure whereas alpha helices just changed 2%. According to the data obtained from Uniprot under the code of 089094-1, there are 5 histidine residues within the caspase-14 protein which are all located within random coils. So it could be concluded that histidine residues in caspase-14 did not affected from the ethanolic process.

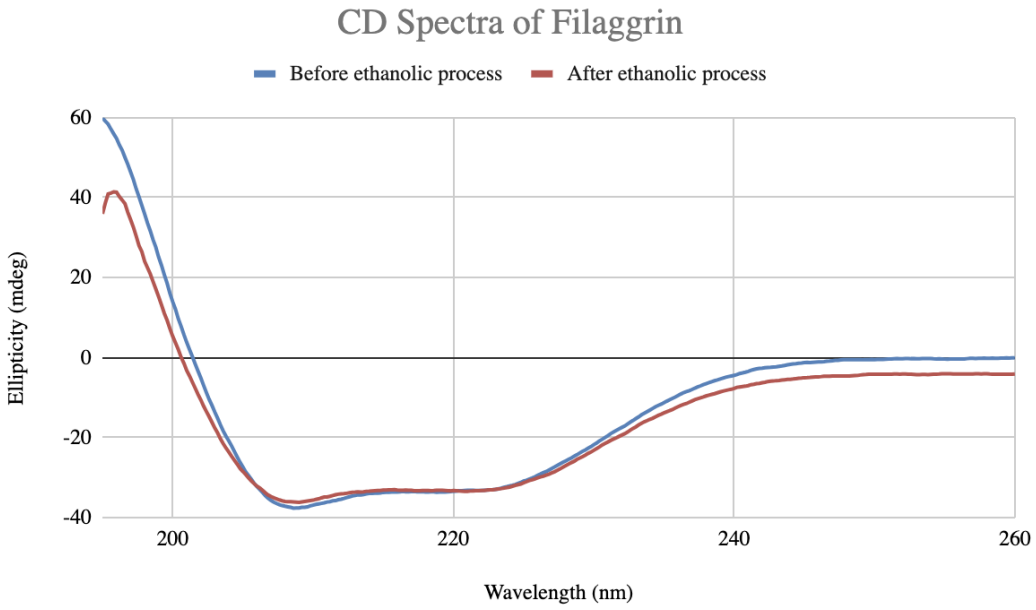

Figure 5.9. CD results of Filaggrin before (blue) and after (red) ethanolic process

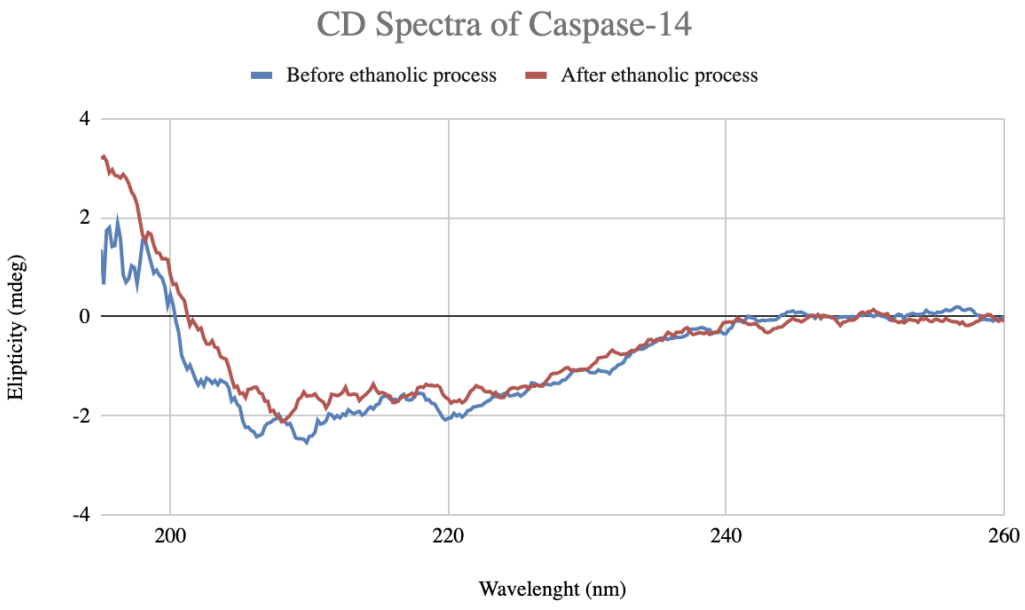

Figure 5.10. CD results of Caspase-14 before (blue) and after (red) ethanolic process

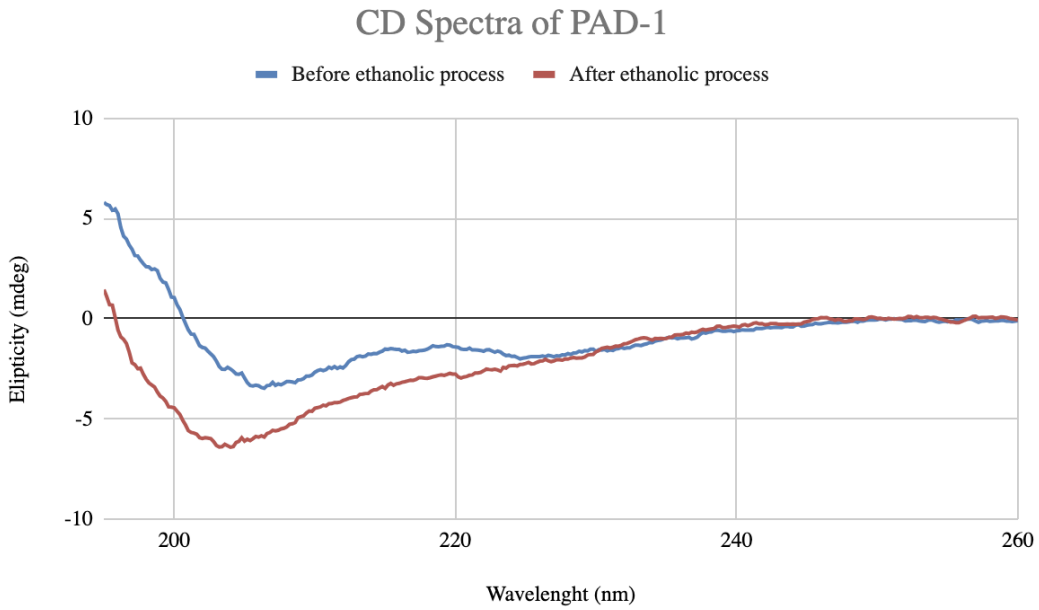

Figure 5.11. CD results of PAD-1 before (blue) and after (red) ethanolic process

5.3.3. Protein Loading Efficiency Studies

To examine the LE%, UV spectrophotometry was used. Maximum absorbance wavelengths for filaggrin, PAD-1 and caspase-14 were detected as 280 nm, 278 nm and 280 nm respectively. They all gave similar maximum absorbance wavelengths due to their histidine tags. As shown in Figure 5.12, there was no interference observed between the maximum absorbance wavelenghts of the loaded components and the other lipid compounds. All the lipids and vesicles gave peaks around 200 nm as previously shown in Figure 3.19. Peaks around 220 nm were more intense but they were not appropriate for following up the LE% because the lipids used in the vesicle composition also gave maximum absorbance wavelength peaks around 200-230 nm and could cause overlaps during calculations.

For filaggrin calibration curve; from 40 µg/ml to 2.5 µg/ml protein containing samples were analyzed and a calibration curve was generated with R2 value of 1 at 280 nm as shown in Figure 5.13.

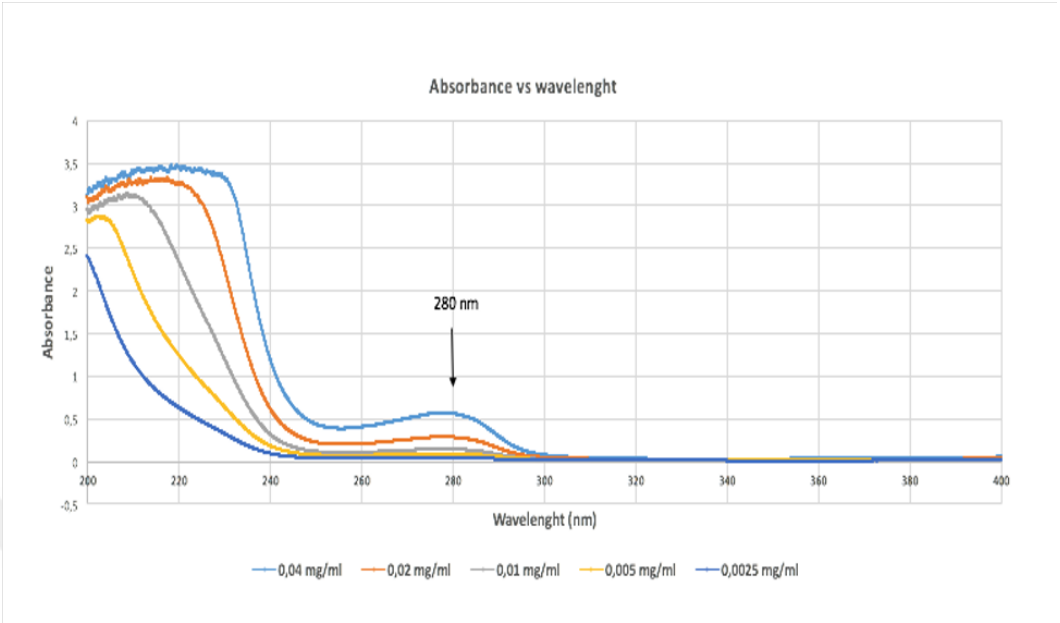

Figure 5.12. Maximum absorbance wavelength of Filaggrin protein

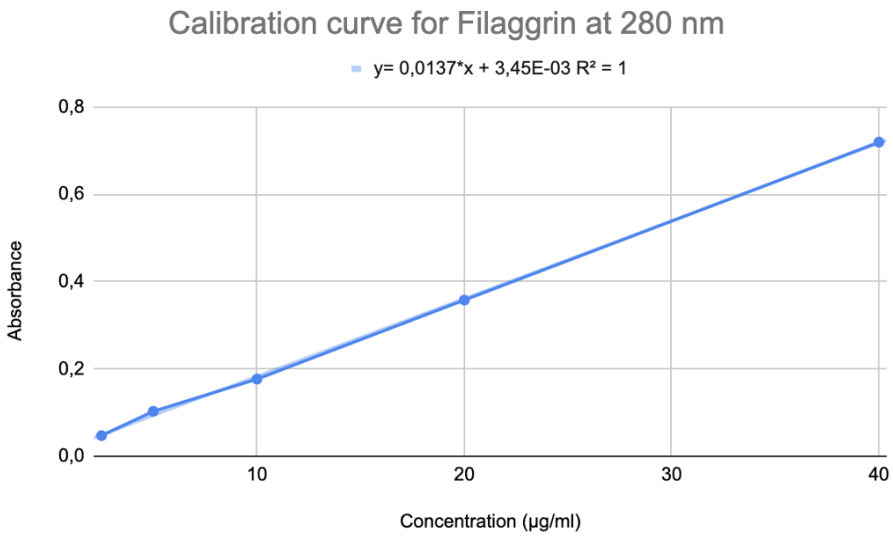

Figure 5.13. Calibration curve of Filaggrin protein

For PAD-1 and caspase-14; from 20 µg/ml to 1.25 µg/ml protein containing samples were analyzed and calibration curves were generated with R2 value of 0.99 at 278 nm and 280 nm respectively as given in Figures 5.14 and 5.15. Unfortunately, LE% calculations could not be finalized due to the lack of equipment that was ultra-centrifugation tubes with pore sizes bigger than 30 kDa to eliminate the excess, un-

loaded protein samples from vesicles. Expected protein LE% is around 5 to 10% according to the literature data but these are yet to be determined in the future [138].

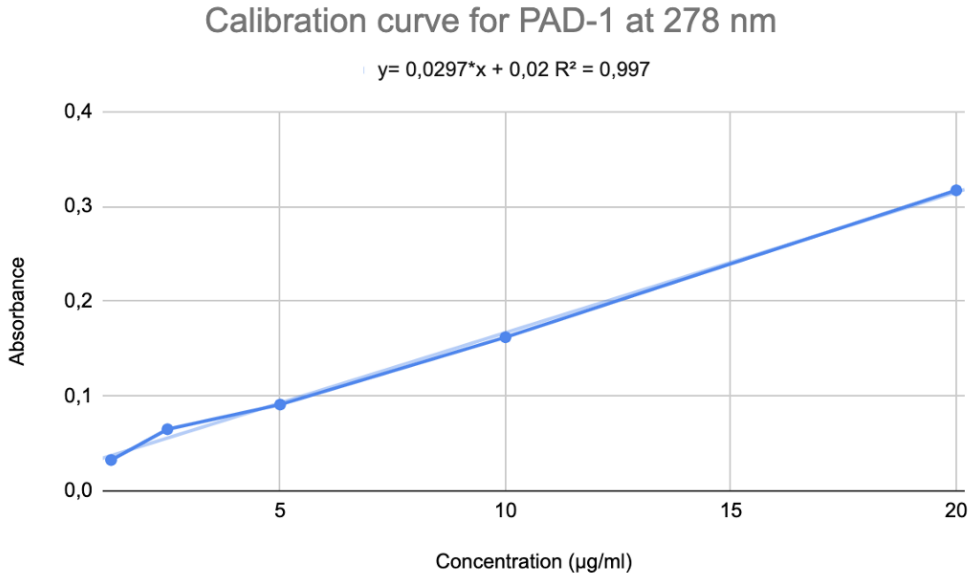

Figure 5.14. Calibration curve of PAD-1 protein

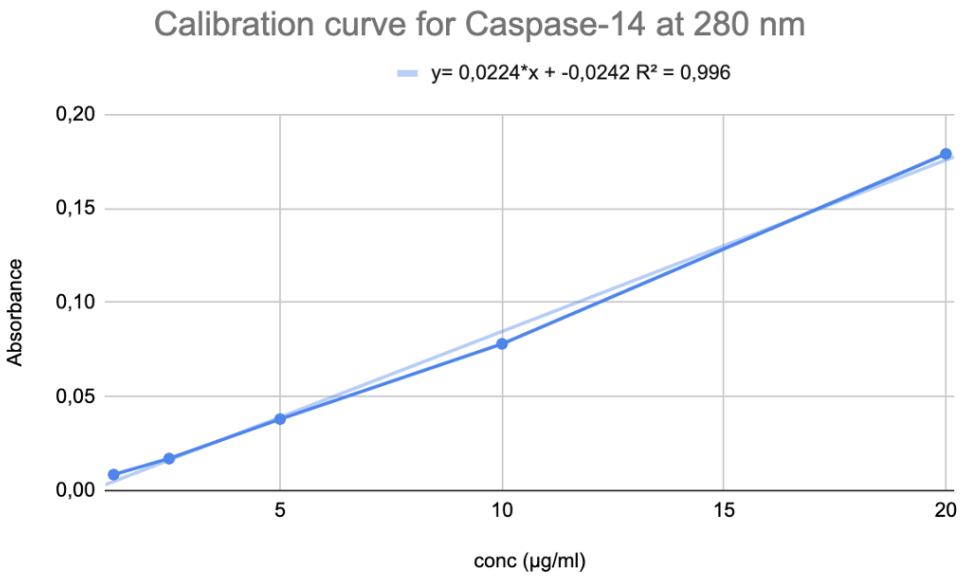

Figure 5.15. Calibration curve of caspase-14 protein

5.4. Conclusions

Proteins are complex bio-molecular structures in living organisms, formed by covalent bonding of amino acids. They can enter the body by the skin surface, through the mouth, via a catheter, or by injection using a needle. First pass mechanism restricts their circulation through the body and decreases the dose utility. Although transdermal delivery addresses this, it still confronts difficulties because of the hydrophilic nature, large volume and mass, limited stability, and short half-life of the proteins. Although they can go through the skin, proteins run the risk of degrading. Lipid vesicles are a promising tool for skin delivery studies, but their high molecular weight and 3D shape make loading proteins difficult. In this study, TE type vesicles containing Soy PC, cholesterol, Tween 80 and Cer3 were used as a passive loading strategy for proteins. These vesicles contained proteins; filaggrin, caspase-14 and PAD-1 that had been selected for use in the treatment of AD skin disease. Studies found that daily application of emollients with ceramides and filaggrin amino acids supplied primary prevention of AD and had a protective impact on disease development. So with Cer3 inclusion within the vesicles, a promising treatment of AD with transdermal protein delivery was targeted.

Filaggrin is a crucial protein for skin mechanical integrity and water retention. Its presence prevents skin cell dryness and cracks in the lipid layer. Studies showed loss-of-function mutations in the FLG gene, producing filaggrin protein, cause AD. So, transdermal delivery of this protein may be a solution for AD treatment. The filaggrin protein must be de-iminated by the PAD-1 enzyme in order to work properly. Unprocessed filaggrin cannot continue working, abnormalities in the metabolic process of this protein can result in a disturbed skin barrier and SC dehydration. So, it may be a wise move to deliver PAD-1 enzyme through transdermal delivery to boost this metabolic process. Also, deiminated filaggrin monomers are further broken down into smaller fragments by caspase-14 enzymes. Studies highlighted the importance of caspase-14 for maintaining a healthy skin and formation of lipid water-repelling coat for the protection against outer stress factors like transdermal water loss and UV radiation.

So, loading of caspase-14 within vesicles may help to enhance AD disease.

Protein denaturation caused by high temperatures, acidic environments, and organic solvent interactions disrupts tertiary structure and biological activity. In this project ethanol was used as an organic solvent and there was a vigorous shaking within the vesicle formation process. To monitor proteins' tertiary structures and activities CD spectrometry was used.

The study investigated one of the passive delivery strategies of filaggrin, PAD-1, and caspase-14 proteins through TEs to strengthen the skin barrier and treat or prevent AD. The proteins were loaded into vesicles containing Soy PC, Tween 80, Cer3 and cholesterol. Obtained vesicles were characterized in terms size, size distribution, LE% and morphology. Size and size distribution were followed by DLS whereas the morphologies were monitored via STEM. Protein LE% studies were monitored via UV/Vis spectroscopy. Proteins were analyzed whether they were achieving the proper secondary and tertiary structures during and after the vesicle formation or not. Size and homogeneity stabilities were monitored after six months of storage.

The study found that all protein loaded vesicles were within acceptable size and PDI range for transdermal delivery studies. TEs smaller than 100 nm are good candidates for subcutaneous cargo material delivery. However, FLG vesicles showed the highest size and PDI increment after six months of storage, possibly due to histidine-rich protein charges. STEM images showed distinct shaped protein loaded vesicles and were consistent with DLS data and PDI outcomes for all the three proteins. The study investigated the impact of a 1:2 ethanol:water solvent and long-term mixing process on protein vesicles preparation. Results showed mostly preserved secondary structures, with a decrease in alpha helix concentration for filaggrin and caspase-14 proteins. Proper protein foldings were also preserved. However, PADI-1 protein's secondary and tertiary structure changed from beta sheet to random coil distinctly and folding pattern of the substance was disturbed. Therefore, a different method for passively loading the PAD-1 protein must be created. UV spectrophotometry was used

to analyze the LE% of filaggrin, PAD-1, and caspase-14. Maximum absorbance wavelengths were found to be 280 nm, 278 nm, and 280 nm, with no interference between loaded components and other lipid compounds.

With this study, successful formulations loading caspase-14, PAD-1 and filaggrin were obtained by using Soy PC, cholesterol, tween 80 and Cer3. All the TEs were characterized in terms of size, size distribution, morphology, six-month stability and LE%. All the vesicles were promising for usage in AD treatment studies but future work needs to be done in terms of transdermal delivery studies, by examining the skin penetration characteristics and cyto-toxicity of the obtained TEs.

6. CONCLUSIONS

In this dissertation, the design and fabrication of TEs to be used in treatment of AD was achieved. TEs are type of vesicles that are better than ordinary liposomes in terms of flexibility, permeability, loading capacity, and efficiency. They contain ethanol and an edge activator such Tween 80 in their compositions. Formulation of three distinct TEs, which comprise proteins, vitamins, and ceramides, has allowed for the achievement of this goal. To promote improved skin delivery for AD, TE-based nano-particles were employed in each design. The methods included loading filaggrin, caspase-14, PAD-1, Cer3, and VitE and VitC within TEs. TEs with Soy PC, cholesterol, Tween 80 or oleic acid and ethanol were created for this investigation. TEs have been widely used for transdermal administration of drugs and cosmetics, showing encouraging outcomes for anti-inflammatory compounds, antifungal drugs, and vaccinations.

Due to critical function in regulating trans epidermal water loss, which is a result of the skin barrier's water permeability, the initial attempt was including Cer3 within TEs formulations. Cer3 containing TEs were successful to be used in transdermal delivery studies and they were capable of loading both hydrophilic and hydrophobic cargo. TEs were analyzed in terms of size, homogeneity, morphology and LE%. Addition of Cer3 caused an increase in size and desired size and size distribution range was achived. Effects of Cer3 and hydrophilic nature of the chosen material were studied and the results were analyzed statistically. According to the results LE% and LE% stability were more successful with the lipophilic cargo irrespective of the presence of the Cer3. All the TE formulations were within the acceptable size and PDI range with high LE% and were stable upon one month of storage in terms of size, homogenity and LE%. Cer3 inclusion findings can be used in potential topical applications in AD curing studies.

In the second strategy, VitC and VitE were utilized to treat AD, and the impact of surfactant type on loading efficiency was examined. Dual loading of both vitamins was also in the scope of this study. The antioxidant and anti-inflammatory properties of VitE and VitC, when delivered through transdermal agents, could be a promising supplementary treatment for AD skin disease. Dual loading of VitC and VitE within TEs either containing Tween 80 or oleic acid was successful for both formulations to be used in transdermal delivery studies. The goal of the chitosan coating was to increase the application regions of the produced TEs, including as face masks and oral pills. All the TEs were characterized in terms of size, size distribution, morphology, stability and LE% and they were capable in using AD treatment studies. VitC and VitE were successfully loaded within TEs with reinforced stability and LE% with chitosan.

The third strategy made use of proteins because of their ability to improve AD therapy. The goal of the trial was to cure or prevent AD by strengthening the skin barrier by means of a passive delivery technique that delivered filaggrin, PAD-1, and caspase-14 proteins through TEs. The proteins were added to vesicles that contain cholesterol, Cer3, Tween 80, and Soy PC. According to the study results, every protein was successfully loaded within vesicles that were inside the permissible limit in terms of both size and PDI for transdermal distribution experiments.

In summary, design and production of TEs for application in the treatment of AD were accomplished in this dissertation. When it comes to flexibility, permeability, loading capacity, and efficiency, TEs are superior to regular liposomes. The development of three unique TEs consisting of ceramides, proteins, and vitamins has made this objective possible. In every design, TE-based nanoparticles were used to facilitate better skin delivery for AD. Filaggrin, caspase-14, PAD-1, Cer3, and VitE and VitC were among the techniques loaded into TEs. Further studies to develop cosmetic products by implementing the obtained systems could be future work for these studies.

REFERENCES

1. Menon, G. K., "New Insights Into Skin Structure: Scratching the Surface", *Advanced Drug Delivery Reviews*, Vol. 54, pp. 3–17, 2002.

2. Zaenglein, A. L., "Acne Vulgaris", *New England Journal of Medicine*, Vol. 379, No. 14, pp. 1343–1352, 2018.

3. Hay, R., S. E. Bendeck, S. Chen, R. Estrada, A. Haddix, T. McLeod and A. Mahé, *Disease Control Priorities in Developing Countries. 2nd Edition*, Oxford University Press, New York, 2006.

4. Chan, L. S., C. J. Vanderlugt, T. Hashimoto, T. Nishikawa, J. J. Zone, M. M. Black, F. Wojnarowska, S. R. Stevens, M. Chen, J. A. Fairley *et al.*, "Epitope Spreading: Lessons From Autoimmune Skin Diseases", *Journal of Investigative Dermatology*, Vol. 110, No. 2, pp. 103–109, 1998.

5. Alam, M. and D. Ratner, "Cutaneous Squamous-cell Carcinoma", *New England Journal of Medicine*, Vol. 344, No. 13, pp. 975–983, 2001.

6. Domingues, B., J. M. Lopes, P. Soares and H. Pópulo, "Melanoma Treatment in Review", *Immunotargets and Therapy*, Vol. 7, No. 7, pp. 35–49, 2018.

7. Burgdorf, W. *et al.*, *Braun-falco's Dermatology*, Springer, Berlin, 2009.

8. Hanifin, J. M., M. L. Reed, E. Prevalence and I. W. Group, "A Population-based Survey of Eczema Prevalence in the United States", *Derm*, Vol. 18, No. 2, pp. 82–91, 2007.

9. Berke, R., A. Singh and M. Guralnick, "Atopic Dermatitis: An Overview", *American Family Physician*, Vol. 86, No. 1, pp. 35–42, 2012.

10. Saeki, H., Y. Ohya, J. Furuta, H. Arakawa, S. Ichiyama, T. Katsunuma, N. Katoh, A. Tanaka, Y. Tsunemi, T. Nakahara *et al.*, "Clinical Practice Guidelines for the Management of Atopic Dermatitis", *The Journal of Dermatology*, Vol. 49, No. 10, pp. 315–375, 2022.

11. Olbrich, H., C. D. Sadik, R. J. Ludwig, D. Thaçi and K. Boch, "Dupilumab in Inflammatory Skin Diseases: A Systematic Review", *Biomolecules*, Vol. 13, No. 4, p. 634, 2023.

12. Morganti, P. and M.-B. Coltelli, "A New Carrier for Advanced Cosmeceuticals", *Cosmetics*, Vol. 6, No. 1, p. 10, 2019.

13. Choi, C. M. and D. S. Berson, "Cosmeceuticals", *Seminars in Cutaneous Medicine and Surgery*, Vol. 25, pp. 163–168, Elsevier, 2006.

14. Juncan, A. M., D. G. Moisă, A. Santini, C. Morgovan, L.-L. Rus, A. L. Vonica-Țincu and F. Loghin, "Advantages of Hyaluronic Acid and Its Combination With Other Bioactive Ingredients in Cosmeceuticals", *Molecules*, Vol. 26, No. 15, p. 4429, 2021.

15. Ahmad, A. and H. Ahsan, "Lipid-based Formulations in Cosmeceuticals and Biopharmaceuticals", *Biomedical Dermatology*, Vol. 4, pp. 1–10, 2020.

16. Crous, C., J. Pretorius and A. Petzer, "Overview of Popular Cosmeceuticals in Dermatology", *Skin Health and Disease*, Vol. 4, No. 2, p. e340, 2024.

17. Paudel, K. S., M. Milewski, C. L. Swadley, N. K. Brogden, P. Ghosh and A. L. Stinchcomb, "Challenges and Opportunities in Dermal/Transdermal Delivery", *Therapeutic Delivery*, Vol. 1, No. 1, pp. 109–131, 2010.

18. Singh Malik, D., N. Mital and G. Kaur, "Topical Drug Delivery Systems: A Patent Review", *Expert Opinion on Therapeutic Patents*, Vol. 26, No. 2, pp. 213–228, 2016.

19. Lou, J., H. Duan, Q. Qin, Z. Teng, F. Gan, X. Zhou and X. Zhou, "Advances in Oral Drug Delivery Systems: Challenges and Opportunities", *Pharmaceutics*, Vol. 15, No. 2, p. 484, 2023.

20. Sala, M., R. Diab, A. Elaissari and H. Fessi, "Lipid Nanocarriers as Skin Drug Delivery Systems: Properties, Mechanisms of Skin Interactions and Medical Applications", *International Journal of Pharmaceutics*, Vol. 535, No. 1-2, pp. 1–17, 2018.

21. Prausnitz, M. R., "Microneedles for Transdermal Drug Delivery", *Advanced Drug Delivery Reviews*, Vol. 56, No. 5, pp. 581–587, 2004.

22. Dhote, V., P. Bhatnagar, P. K. Mishra, S. C. Mahajan and D. K. Mishra, "Iontophoresis: A Potential Emergence of a Transdermal Drug Delivery System", *Scientia Pharmaceutica*, Vol. 80, No. 1, pp. 1–28, 2012.

23. Gowda, A., B. Healey, H. Ezaldein and M. Merati, "A Systematic Review Examining the Potential Adverse Effects of Microneedling", *The Journal of Clinical and Aesthetic Dermatology*, Vol. 14, No. 1, p. 45, 2021.

24. Chantasart, D. and S. K. Li, "Structure Enhancement Relationship of Chemical Penetration Enhancers in Drug Transport Across the Stratum Corneum", *Pharmaceutics*, Vol. 4, No. 1, pp. 71–92, 2012.

25. Tanwar, H. and R. Sachdeva, "Transdermal Drug Delivery System: A Review", *International Journal of Pharmaceutical Sciences and Research*, Vol. 7, No. 6, p. 2274, 2016.

26. Souto, E. B., J. F. Fangueiro, A. R. Fernandes, A. Cano, E. Sanchez-Lopez, M. L. Garcia, P. Severino, M. O. Paganelli, M. V. Chaud and A. M. Silva, "Physicochemical and Biopharmaceutical Aspects Influencing Skin Permeation and Role of SLN and NLC for Skin Drug Delivery", *Heliyon*, Vol. 8, No. 2, p. 8938, 2022.

27. Liu, P., G. Chen and J. Zhang, "A Review of Liposomes as a Drug Delivery System: Current Status of Approved Products, Regulatory Environments, and Future Perspectives", *Molecules*, Vol. 27, No. 4, p. 1372, 2022.

28. Akbarzadeh, A., R. Rezaei-Sadabady, S. Davaran, S. W. Joo, N. Zarghami, Y. Hanifehpour, M. Samiei, M. Kouhi and K. Nejati-Koshki, "Liposome: Classification, Preparation, and Applications", *Nanoscale Research Letters*, Vol. 8, pp. 1–9, 2013.

29. Nayak, D. and V. K. Tippavajhala, "A Comprehensive Review on Preparation, Evaluation and Applications of Deformable Liposomes", *Iranian Journal of Pharmaceutical Research*, Vol. 20, No. 1, pp. 186–205, 2021.

30. Ohsawa, T., H. Miura and K. Harada, "Evaluation of a New Liposome Preparation Technique: The Freeze-thawing Method, Using L-asparaginase as a Model Drug", *Chemical and Pharmaceutical Bulletin*, Vol. 33, No. 7, pp. 2916–2923, 1985.

31. Batzri, S. and E. D. Korn, "Single Bilayer Liposomes Prepared Without Sonication", *Biochimica Et Biophysica Acta (bba)-biomembranes*, Vol. 298, No. 4, pp. 1015–1019, 1973.

32. Charcosset, C., A. Juban, J.-P. Valour, S. Urbaniak and H. Fessi, "Preparation of Liposomes at Large Scale Using the Ethanol Injection Method: Effect of Scale-up and Injection Devices", *Chemical Engineering Research and Design*, Vol. 94, pp. 508–515, 2015.

33. Ingebrigtsen, L. and M. Brandl, "Determination of the Size Distribution of Liposomes by Sec Fractionation, and PCS Analysis and Enzymatic Assay of Lipid Content", *AAPS Pharmscitech*, Vol. 3, pp. 9–15, 2002.

34. Chibowski, E. and A. Szcześ, "Zeta Potential and Surface Charge of DPPC and DOPC Liposomes in the Presence of PLC Enzyme", *Adsorption*, Vol. 22, pp.

755–765, 2016.

35. Brgles, M., D. Jurašin, M. D. Sikirić, R. Frkanec and J. Tomašić, "Entrapment of Ovalbumin Into Liposomes—factors Affecting Entrapment Efficiency, Liposome Size, and Zeta Potential", *Journal of Liposome Research*, Vol. 18, No. 3, pp. 235–248, 2008.

36. Abd-El-Azim, H., A. Ramadan, N. Nafee and N. Khalafallah, "Entrapment Efficiency of Pyridoxine Hydrochloride in Unilamellar Liposomes: Experimental Versus Model-generated Data", *Journal of Liposome Research*, Vol. 28, No. 2, pp. 112–116, 2018.

37. Vemuri, S. and C. Rhodes, "Separation of Liposomes by a Gel Filtration Chromatographic Technique: a Preliminary Evaluation", *Pharmaceutica Acta Helvetiae*, Vol. 69, No. 2, pp. 107–113, 1994.

38. Taylor, T. M., S. Gaysinsky, P. M. Davidson, B. D. Bruce and J. Weiss, "Characterization of Antimicrobial-bearing Liposomes by Zeta Potential, Vesicle Size and Encapsulation Efficiency", *Food Biophysics*, Vol. 2, pp. 1–9, 2007.

39. Solomon, D., N. Gupta, N. S. Mulla, S. Shukla, Y. A. Guerrero and V. Gupta, "Role of in Vitro Release Methods in Liposomal Formulation Development: Challenges and Regulatory Perspective", *The AAPS Journal*, Vol. 19, pp. 1669–1681, 2017.

40. Munir, M., M. Zaman, M. A. Waqar, H. Hameed and T. Riaz, "A Comprehensive Review on Transethosomes as a Novel Vesicular Approach for Drug Delivery Through Transdermal Route", *Journal of Liposome Research*, Vol. 34, No. 1, pp. 203–218, 2024.

41. Smith, E. A. and P. K. Dea, *Applications of Calorimetry in a Wide Context—differential Scanning Calorimetry, Isothermal Titration Calorimetry and*

Microcalorimetry, InTech Rijeka, Croatia, 2013.

42. Wang, S., Y. Chen, J. Guo and Q. Huang, "Liposomes for Tumor Targeted Therapy: A Review", *International Journal of Molecular Sciences*, Vol. 24, No. 3, p. 2643, 2023.

43. Bulbake, U., S. Doppalapudi, N. Kommineni and W. Khan, "Liposomal Formulations in Clinical Use: An Updated Review", *Pharmaceutics*, Vol. 9, No. 2, p. 12, 2017.

44. Beltrán-Gracia, E., A. López-Camacho, I. Higuera-Ciapara, J. B. Velázquez-Fernández and A. A. Vallejo-Cardona, "Nanomedicine Review: Clinical Developments in Liposomal Applications", *Cancer Nanotechnology*, Vol. 10, No. 1, pp. 1–40, 2019.

45. Touitou, E., N. Dayan, L. Bergelson, B. Godin and M. Eliaz, "Ethosomes—Novel Vesicular Carriers for Enhanced Delivery: Characterization and Skin Penetration Properties", *Journal of Controlled Release*, Vol. 65, No. 3, pp. 403–418, 2000.

46. Abdulbaqi, I. M., Y. Darwis, N. A. K. Khan, R. A. Assi and A. A. Khan, "Ethosomal Nanocarriers: The Impact of Constituents and Formulation Techniques on Ethosomal Properties, in Vivo Studies, and Clinical Trials", *International Journal of Nanomedicine*, Vol. 11, pp. 2279–2304, 2016.

47. Song, C. K., P. Balakrishnan, C.-K. Shim, S.-J. Chung, S. Chong and D.-D. Kim, "A Novel Vesicular Carrier, Transethosome, for Enhanced Skin Delivery of Voriconazole: Characterization and in Vitro/in Vivo Evaluation", *Colloids and Surfaces B: Biointerfaces*, Vol. 92, pp. 299–304, 2012.

48. Hmingthansanga, V., N. Singh, S. Banerjee, S. Manickam, R. Velayutham and S. Natesan, "Improved Topical Drug Delivery: Role of Permeation Enhancers and Advanced Approaches", *Pharmaceutics*, Vol. 14, No. 12, p. 2818, 2022.

49. Ascenso, A., S. Raposo, C. Batista, P. Cardoso, T. Mendes, F. G. Praça, M. V. L. B. Bentley and S. Simões, "Development, Characterization, and Skin Delivery Studies of Related Ultradeformable Vesicles: Transfersomes, Ethosomes, and Transethosomes", *International Journal of Nanomedicine*, Vol. 10, pp. 5837–5851, 2015.

50. Anwar, E., D. Ramadon and G. D. Ardi, "Novel Transethosome Containing Green Tea (Camellia Sinensis L. Kuntze) Leaf Extract for Enhanced Skin Delivery of Epigallocatechin Gallate: Formulation and in Vitro Penetration Test", *International Journal of Applied Pharmaceuticals*, Vol. 10, No. 1, pp. 299–302, 2018.

51. Kim, J.-E., G.-H. Oh, G.-H. Jang, Y.-M. Kim and Y.-J. Park, "Transformerethosomes With Palmitoyl Pentapeptide for Improved Transdermal Delivery", *Journal of Drug Delivery Science and Technology*, Vol. 52, pp. 460–467, 2019.

52. Barge, K., S. Tank, B. Parab, M. Nagarsenker and S. Shidhaye, "Liposomal Cosmeceuticals as Skin Protectives and Curatives", *Indian Journal of Pharmaceutical Education and Research*, Vol. 58, No. 1, pp. 34–44, 2024.

53. Eroğlu, İ., M. Aslan, Ü. Yaman, M. Gultekinoglu, S. Çalamak, D. Kart and K. Ulubayram, "Liposome-based Combination Therapy for Acne Treatment", *Journal of Liposome Research*, Vol. 30, No. 3, pp. 263–273, 2020.

54. Castro, G. A. and L. A. Ferreira, "Novel Vesicular and Particulate Drug Delivery Systems for Topical Treatment of Acne", *Expert Opinion on Drug Delivery*, Vol. 5, No. 6, pp. 665–679, 2008.

55. Nešić, I., V. Savić and A. Kolarević, "Investigation of Efficacy of Anti-aging Liposomal Intimate Gel: An in Vivo Long-term Study", *Acta Facultatis Medicae Naissensis*, Vol. 37, No. 1, pp. 48–56, 2020.

56. Varjão Mota, A. d. C., Z. M. Faria de Freitas, E. R. Júnior, G. M. Dellamora-Ortiz,

R. Santos-Oliveira, R. A. Ozzetti, A. L. Vergnanini, V. L. Ribeiro, R. S. Silva and E. P. dos Santos, "In Vivo and in Vitro Evaluation of Octyl Methoxycinnamate Liposomes", *International Journal of Nanomedicine*, Vol. 8, pp. 4689–4701, 2013.

57. Lee, Y. S., S. H. Jeon, H. J. Ham, H. P. Lee, M. J. Song and J. T. Hong, "Improved Anti-inflammatory Effects of Liposomal Astaxanthin on a Phthalic Anhydride-induced Atopic Dermatitis Model", *Frontiers in Immunology*, Vol. 11, p. 565285, 2020.

58. Montanari, J., C. Maidana, M. I. Esteva, C. Salomon, M. J. Morilla and E. L. Romero, "Sunlight Triggered Photodynamic Ultradeformable Liposomes Against Leishmania Braziliensis Are Also Leishmanicidal in the Dark", *Journal of Controlled Release*, Vol. 147, No. 3, pp. 368–376, 2010.

59. Maestrelli, F., M. González-Rodríguez, A. Rabasco, C. Ghelardini and P. Mura, "New "Drug-in Cyclodextrin-in Deformable Liposomes" Formulations to Improve the Therapeutic Efficacy of Local Anaesthetics", *International Journal of Pharmaceutics*, Vol. 395, No. 1-2, pp. 222–231, 2010.

60. Dubey, V., D. Mishra, A. Asthana and N. K. Jain, "Transdermal Delivery of a Pineal Hormone: Melatonin Via Elastic Liposomes", *Biomaterials*, Vol. 27, No. 18, pp. 3491–3496, 2006.

61. Imokawa, G., A. Abe, K. Jin, Y. Higaki, M. Kawashima and A. Hidano, "Decreased Level of Ceramides in Stratum Corneum of Atopic Dermatitis: an Etiologic Factor in Atopic Dry Skin?", *Journal of Investigative Dermatology*, Vol. 96, No. 4, pp. 523–526, 1991.

62. Di Nardo, A., P. Wertz, A. Giannetti, S. Seidenari *et al.*, "Ceramide and Cholesterol Composition of the Skin of Patients With Atopic Dermatitis", *Acta Dermato-Venereologica*, Vol. 78, pp. 27–30, 1998.

63. Coderch, L., O. López, A. de la Maza and J. L. Parra, "Ceramides and Skin Function", *American Journal of Clinical Dermatology*, Vol. 4, pp. 107–129, 2003.

64. Meckfessel, M. H. and S. Brandt, "The Structure, Function, and Importance of Ceramides in Skin and Their Use as Therapeutic Agents in Skin-care Products", *Journal of the American Academy of Dermatology*, Vol. 71, No. 1, pp. 177–184, 2014.

65. Uchida, Y. and K. Park, "Ceramides in Skin Health and Disease: an Update", *American Journal of Clinical Dermatology*, Vol. 22, No. 6, pp. 853–866, 2021.

66. Choi, M. J. and H. I. Maibach, "Role of Ceramides in Barrier Function of Healthy and Diseased Skin", *American Journal of Clinical Dermatology*, Vol. 6, No. 4, pp. 215–223, 2005.

67. Emmert, H., H. Baurecht, F. Thielking, D. Stölzl, E. Rodriguez, I. Harder, E. Proksch and S. Weidinger, "Stratum Corneum Lipidomics Analysis Reveals Altered Ceramide Profile in Atopic Dermatitis Patients Across Body Sites With Correlated Changes in Skin Microbiome", *Experimental Dermatology*, Vol. 30, No. 10, pp. 1398–1408, 2021.

68. Berkers, T., D. Visscher, G. S. Gooris and J. A. Bouwstra, "Topically Applied Ceramides Interact With the Stratum Corneum Lipid Matrix in Compromised Ex Vivo Skin", *Pharmaceutical Research*, Vol. 35, pp. 1–13, 2018.

69. Danby, S. G., P. V. Andrew, K. Brown, J. Chittock, L. J. Kay and M. J. Cork, "An Investigation of the Skin Barrier Restoring Effects of a Cream and Lotion Containing Ceramides in a Multi-vesicular Emulsion in People With Dry, Eczema-prone, Skin: the Restore Study Phase 1", *Dermatology and Therapy*, Vol. 10, pp. 1031–1041, 2020.

70. Şahin Bektay, H., A. A. Sağıroğlu, K. Bozali, E. M. Güler and S. Güngör, "The

Design and Optimization of Ceramide Np-loaded Liposomes to Restore the Skin Barrier", *Pharmaceutics*, Vol. 15, No. 12, p. 2685, 2023.

71. Joo, K.-M., J.-H. Hwang, S. Bae, D.-H. Nahm, H.-S. Park, Y.-M. Ye and K.-M. Lim, "Relationship of Ceramide and Free Fatty Acid and Cholesterol Ratios in the Stratum Corneum With Skin Barrier Function of Normal, Atopic Dermatitis Lesional and Non-lesional Skins", *Journal of Dermatological Science*, Vol. 77, No. 1, pp. 71–74, 2015.

72. Uche, L. E., G. S. Gooris, J. A. Bouwstra and C. M. Beddoes, "Barrier Capability of Skin Lipid Models: Effect of Ceramides and Free Fatty Acid Composition", *Langmuir*, Vol. 35, No. 47, pp. 15376–15388, 2019.

73. Imura, T., H. Sakai, H. Yamauchi, C. Kaise, K. Kozawa, S. Yokoyama and M. Abe, "Preparation of Liposomes Containing Ceramide 3 and Their Membrane Characteristics", *Colloids and Surfaces B: Biointerfaces*, Vol. 20, No. 1, pp. 1–8, 2001.

74. Čuříková-Kindlová, B. A., A. Vovesná, A. Nováčková and J. Zbytovská, "In Vitro Modeling of Skin Barrier Disruption and Its Recovery by Ceramide-based Formulations", *AAPS Pharmscitech*, Vol. 23, pp. 1–15, 2022.

75. Murthy, S. N., "Approaches for Delivery of Drugs Topically", *Aaps Pharmscitech*, Vol. 21, pp. 1–2, 2020.

76. Cevc, G., "Rational Design of New Product Candidates: the Next Generation of Highly Deformable Bilayer Vesicles for Noninvasive, Targeted Therapy", *Journal of Controlled Release*, Vol. 160, No. 2, pp. 135–146, 2012.

77. Ghasemiyeh, P. and S. Mohammadi-Samani, "Potential of Nanoparticles as Permeation Enhancers and Targeted Delivery Options for Skin: Advantages and Disadvantages", *Drug Design, Development and Therapy*, Vol. 14, pp. 3271–3289, 2020.

78. Patzelt, A., W. C. Mak, S. Jung, F. Knorr, M. C. Meinke, H. Richter, E. Rühl, K. Y. Cheung, N. B. N. N. Tran and J. Lademann, "Do Nanoparticles Have a Future in Dermal Drug Delivery?", *Journal of Controlled Release*, Vol. 246, pp. 174–182, 2017.

79. Cevc, G. and G. Blume, "Lipid Vesicles Penetrate Into Intact Skin Owing to the Transdermal Osmotic Gradients and Hydration Force", *Biochimica Et Biophysica Acta: Biomembranes*, Vol. 1104, No. 1, pp. 226–232, 1992.

80. Albash, R., A. A. Abdelbary, H. Refai and M. A. El-Nabarawi, "Use of Transethosomes for Enhancing the Transdermal Delivery of Olmesartan Medoxomil: in Vitro, Ex Vivo, and in Vivo Evaluation", *International Journal of Nanomedicine*, Vol. 14, pp. 1953–1968, 2019.

81. Pleguezuelos-Villa, M., I. Castangia, O. Diez-Sales, M. L. Manca, M. Manconi, A. R. Sauri, R. Taléns-Visconti and A. Nácher, "Control of Skin Damages Caused by Oxidative Stress Using Mangiferin and Naringin Co-loaded in Phospholipid Vesicles", *Journal of Drug Delivery Science and Technology*, Vol. 91, pp. 1052–1061, 2024.

82. Fitoussi, J., S. Virassamynaïk, S. Callejon, S. Weber, E. Collet, J. Scalia, M. Chavagnac-Bonneville, S. Trompezinski and M. Sayag, "Inhibition of Thymic Stromal Lymphopoietin Production to Improve Pruritus and Quality of Life in Infants and Children With Atopic Dermatitis", *Journal of Cosmetic Dermatology*, Vol. 19, No. 8, pp. 2061–2069, 2020.

83. Mangues, M., C. Carreño, J. Cebrián and N. Almiñana, "Development of a New Cosmetic Active for Safe Skin Brightening", *International Journal of Cosmetic Science*, Vol. 32, No. 4, pp. 318–319, 2010.

84. Nara, E., K. Miyashita and T. Ota, "Oxidative Stability of Liposomes Prepared From Soybean Pc, Chicken Egg Pc, and Salmon Egg Pc", *Bioscience, Biotech-*

nology, and Biochemistry, Vol. 61, No. 10, pp. 1736–1738, 1997.

85. Thomas, A. H., Á. Catalá and M. Vignoni, "Soybean Phosphatidylcholine Liposomes as Model Membranes to Study Lipid Peroxidation Photoinduced by Pterin", *Biochimica Et Biophysica Acta -Biomembranes*, Vol. 1858, No. 1, pp. 139–145, 2016.

86. Rheinstädter, M. C. and O. G. Mouritsen, "Small Scale Structure in Fluid Cholesterol: Lipid Bilayers", *Current Opinion in Colloid & Interface Science*, Vol. 18, No. 5, pp. 440–447, 2013.

87. Mouritsen, O. G. and M. J. Zuckermann, "What's So Special About Cholesterol?", *Lipids*, Vol. 39, No. 11, pp. 1101–1113, 2004.

88. Bhattacharya, S. and S. Haldar, "Interactions Between Cholesterol and Lipids in Bilayer Membranes: Role of Lipid Headgroup and Hydrocarbon Chain and Backbone Linkage", *Biochimica Et Biophysica Acta: Biomembranes*, Vol. 1467, No. 1, pp. 39–53, 2000.

89. Bouwstra, J., F. Dubbelaar, G. Gooris and M. Ponec, "The Lipid Organisation in the Skin Barrier", *Acta Dermato-Venereologica*, Vol. 208, pp. 23–30, 2000.

90. Shaji, J. and S. Garude, "Transethosomes and Ethosomes for Enhanced Transdermal Delivery of Ketorolac Tromethamine: a Comparative Assessment", *Int J Curr Pharm Res*, Vol. 6, No. 4, pp. 88–93, 2014.

91. Verma, D. D., S. Verma, G. Blume and A. Fahr, "Particle Size of Liposomes Influences Dermal Delivery of Substances Into Skin", *International Journal of Pharmaceutics*, Vol. 258, No. 1-2, pp. 141–151, 2003.

92. Robson, A.-L., P. C. Dastoor, J. Flynn, W. Palmer, A. Martin, D. W. Smith, A. Woldu and S. Hua, "Advantages and Limitations of Current Imaging Techniques for Characterizing Liposome Morphology", *Frontiers in Pharmacology*,

Vol. 9, p. 80, 2018.

93. Simões, S., J. Tapadas, C. Marques, M. Cruz, M. Martins and G. Cevc, "Permeabilisation and Solubilisation of Soybean Phosphatidylcholine Bilayer Vesicles, as Membrane Models, by Polysorbate, Tween 80", *European Journal of Pharmaceutical Sciences*, Vol. 26, No. 3-4, pp. 307–317, 2005.

94. Jain, S., P. Jain, R. Umamaheshwari and N. Jain, "Transfersomes — A Novel Vesicular Carrier for Enhanced Transdermal Delivery: Development, Characterization, and Performance Evaluation", *Drug Development and Industrial Pharmacy*, Vol. 29, No. 9, pp. 1013–1026, 2003.

95. Mkam Tsengam, I. K., M. Omarova, E. G. Kelley, A. McCormick, G. D. Bothun, S. R. Raghavan and V. T. John, "Transformation of Lipid Vesicles Into Micelles by Adding Nonionic Surfactants: Elucidating the Structural Pathway and the Intermediate Structures", *The Journal of Physical Chemistry B*, Vol. 126, No. 11, pp. 2208–2216, 2022.

96. Feingold, K. R., "Thematic Review Series: Skin Lipids; the Role of Epidermal Lipids in Cutaneous Permeability Barrier Homeostasis", *Journal of Lipid Research*, Vol. 48, No. 12, pp. 2531–2546, 2007.

97. Lee, S.-C., K.-E. Lee, J.-J. Kim and S.-H. Lim, "The Effect of Cholesterol in the Liposome Bilayer on the Stabilization of Incorporated Retinol", *Journal of Liposome Research*, Vol. 15, No. 3-4, pp. 157–166, 2005.

98. Wang, R., C. Ma, H. Yan, H. Zhao, P. Wang, S. Zhang, J. Ju, S. Yu and Z. Yin, "Lecithin/Cholesterol/Tween 80 Liposomes for Co-encapsulation of Vitamin C and Xanthoxylin", *ACS Applied Nano Materials*, Vol. 7, No. 6, pp. 5982–5995, 2024.

99. Mir-Palomo, S., A. Nácher, O. Díez-Sales, M. O. V. Busó, C. Caddeo, M. L.

Manca, M. Manconi, A. M. Fadda and A. R. Saurí, "Inhibition of Skin Inflammation by Baicalin Ultradeformable Vesicles", *International Journal of Pharmaceutics*, Vol. 511, No. 1, pp. 23–29, 2016.

100. Thompson, B. R., B. C. Zarket, E. H. Lauten, S. Amin, S. Muthukrishnan and S. R. Raghavan, "Liposomes Entrapped in Biopolymer Hydrogels Can Spontaneously Release Into the External Solution", *Langmuir*, Vol. 36, No. 26, pp. 7268–7276, 2020.

101. Anwekar, H., S. Patel and A. Singhai, "Liposomes as Drug Carriers", *International Journal of Pharmacy and Life Sciences*, Vol. 2, No. 7, pp. 945–951, 2011.

102. Xia, S. and S. Xu, "Ferrous Sulfate Liposomes: Preparation, Stability and Application in Fluid Milk", *Food Research International*, Vol. 38, No. 3, pp. 289–296, 2005.

103. Shaker, S., A. R. Gardouh and M. M. Ghorab, "Factors Affecting Liposomes Particle Size Prepared by Ethanol Injection Method", *Research in Pharmaceutical Sciences*, Vol. 12, No. 5, p. 346, 2017.

104. Bnyan, R., I. Khan, T. Ehtezazi, I. Saleem, S. Gordon, F. O'Neill and M. Roberts, "Surfactant Effects on Lipid-based Vesicles Properties", *Journal of Pharmaceutical Sciences*, Vol. 107, No. 5, pp. 1237–1246, 2018.

105. Schofield, M., L. J. Jenski, A. C. Dumaual and W. Stillwell, "Cholesterol Versus Cholesterol Sulfate: Effects on Properties of Phospholipid Bilayers Containing Docosahexaenoic Acid", *Chemistry and Physics of Lipids*, Vol. 95, No. 1, pp. 23–36, 1998.

106. Kumar, A., K. Pathak and V. Bali, "Ultra-adaptable Nanovesicular Systems: A Carrier for Systemic Delivery of Therapeutic Agents", *Drug Discovery Today*, Vol. 17, No. 21-22, pp. 1233–1241, 2012.

107. Kováčik, A., M. Kopečná and K. Vávrová, "Permeation Enhancers in Transdermal Drug Delivery: Benefits and Limitations", *Expert Opinion on Drug Delivery*, Vol. 17, No. 2, pp. 145–155, 2020.

108. Sales-Campos, H., P. Reis de Souza, B. Crema Peghini, J. Santana da Silva and C. Ribeiro Cardoso, "An Overview of the Modulatory Effects of Oleic Acid in Health and Disease", *Mini Reviews in Medicinal Chemistry*, Vol. 13, No. 2, pp. 201–210, 2013.

109. Verma, S., A. Bhardwaj, M. Vij, P. Bajpai, N. Goutam and L. Kumar, "Oleic Acid Vesicles: a New Approach for Topical Delivery of Antifungal Agent", *Artificial Cells, Nanomedicine, and Biotechnology*, Vol. 42, No. 2, pp. 95–101, 2014.

110. Peh, H. Y., W. D. Tan, W. Liao and W. F. Wong, "Vitamin E Therapy Beyond Cancer: Tocopherol Versus Tocotrienol", *Pharmacology & Therapeutics*, Vol. 162, pp. 152–169, 2016.

111. Chin, K.-Y., K.-L. Pang and I.-N. Soelaiman, "Tocotrienol and Its Role in Chronic Diseases", *Anti-inflammatory Nutraceuticals and Chronic Diseases*, Vol. 928, pp. 97–130, 2016.

112. Sabliov, C. M., C. Fronczek, C. Astete, M. Khachaturyan, L. Khachatryan and C. Leonardi, "Effects of Temperature and Uv Light on Degradation of α-tocopherol in Free and Dissolved Form", *Journal of the American Oil Chemists' Society*, Vol. 86, pp. 895–902, 2009.

113. Traikovich, S. S., "Use of Topical Ascorbic Acid and Its Effects on Photodamaged Skin Topography", *Archives of Otolaryngology–head & Neck Surgery*, Vol. 125, No. 10, pp. 1091–1098, 1999.

114. Janda, K., M. Kasprzak and J. Wolska, "Vitamin C: Structure, Properties, Occurrence and Functions", *Pomeranian Journal of Life Sciences*, Vol. 61, No. 4,

pp. 419–425, 2015.

115. Tsuboi, Kouda, Takeuchi, Takigawa, Masamoto, Takeuchi and Ochi, "8-hydroxydeoxyguanosine in Urine as an Index of Oxidative Damage to Dna in the Evaluation of Atopic Dermatitis", *British Journal of Dermatology*, Vol. 138, No. 6, pp. 1033–1035, 1998.

116. Teo, C. W. L., S. H. Y. Tay, H. L. Tey, Y. W. Ung and W. N. Yap, "Vitamin E in Atopic Dermatitis: From Preclinical to Clinical Studies", *Dermatology*, Vol. 237, No. 4, pp. 553–564, 2021.

117. Javanbakht, M. H., S. A. Keshavarz, M. Djalali, F. Siassi, M. R. Eshraghian, A. Firooz, H. Seirafi, A. H. Ehsani, M. Chamari and A. Mirshafiey, "Randomized Controlled Trial Using Vitamins E and D Supplementation in Atopic Dermatitis", *Journal of Dermatological Treatment*, Vol. 22, No. 3, pp. 144–150, 2011.

118. Jaffary, F., G. Faghihi, A. Mokhtarian and S. M. Hosseini, "Effects of Oral Vitamin E on Treatment of Atopic Dermatitis: A Randomized Controlled Trial", *Journal of Research in Medical Sciences*, Vol. 20, No. 11, pp. 1053–1057, 2015.

119. Shin, J., Y. J. Kim, O. Kwon, N.-I. Kim and Y. Cho, "Associations Among Plasma Vitamin C, Epidermal Ceramide and Clinical Severity of Atopic Dermatitis", *Nutrition Research and Practice*, Vol. 10, No. 4, p. 398, 2016.

120. Hamilton, I. M., W. S. Gilmore, I. F. Benzie, C. W. Mulholland and J. Strain, "Interactions Between Vitamins C and E in Human Subjects", *British Journal of Nutrition*, Vol. 84, No. 3, pp. 261–267, 2000.

121. Lin, J.-Y., M. A. Selim, C. R. Shea, J. M. Grichnik, M. M. Omar, N. A. Monteiro-Riviere and S. R. Pinnell, "Uv Photoprotection by Combination Topical Antioxidants Vitamin C and Vitamin E", *Journal of the American Academy of Dermatology*, Vol. 48, No. 6, pp. 866–874, 2003.

122. Liu, W., W. Liu, A. Ye, S. Peng, F. Wei, C. Liu and J. Han, "Environmental Stress Stability of Microencapsules Based on Liposomes Decorated With Chitosan and Sodium Alginate", *Food Chemistry*, Vol. 196, pp. 396–404, 2016.

123. Satpathy, L., N. Pradhan, D. Dash, P. P. Baral and S. P. Parida, "Quantitative Determination of Vitamin C Concentration of Common Edible Food Sources by Redox Titration Using Iodine Solution", *Letters in Applied Nanobioscience*, Vol. 10, No. 3, pp. 2361–2369, 2021.

124. Leyton, J., P. Drury and M. Crawford, "Differential Oxidation of Saturated and Unsaturated Fatty Acids in Vivo in the Rat", *British Journal of Nutrition*, Vol. 57, No. 3, pp. 383–393, 1987.

125. Sopyan, I., D. Gozali *et al.*, "A Review: A Novel of Efforts to Enhance Liposome Stability as Drug Delivery Approach", *Systematic Reviews in Pharmacy*, Vol. 11, No. 6, p. 555, 2020.

126. Joy, J. M., P. Amruth, P. K. Dara, V. Renuka, R. Anandan *et al.*, "Liposome Mediated Encapsulation and Role of Chitosan on Modulating Liposomal Stability to Deliver Potential Bioactives - A Review", *Food Hydrocolloids for Health*, Vol. 4, p. 100142, 2023.

127. Kulka, K. and A. Sionkowska, "Chitosan Based Materials in Cosmetic Applications: A Review", *Molecules*, Vol. 28, No. 4, p. 1817, 2023.

128. Furlani, F., A. Rossi, M. A. Grimaudo, G. Bassi, E. Giusto, F. Molinari, F. Lista, M. Montesi and S. Panseri, "Controlled Liposome Delivery From Chitosan-based Thermosensitive Hydrogel for Regenerative Medicine", *International Journal of Molecular Sciences*, Vol. 23, No. 2, p. 894, 2022.

129. Furse, S., "Is Phosphatidylglycerol Essential for Terrestrial Life?", *Journal of Chemical Biology*, Vol. 10, No. 1, pp. 1–9, 2017.

130. Tai, K., M. Rappolt, L. Mao, Y. Gao, X. Li and F. Yuan, "The Stabilization and Release Performances of Curcumin-loaded Liposomes Coated by High and Low Molecular Weight Chitosan", *Food Hydrocolloids*, Vol. 99, p. 105355, 2020.

131. Hemmingsen, L. M., B. Giordani, A. K. Pettersen, B. Vitali, P. Basnet and N. Škalko-Basnet, "Liposomes-in-chitosan Hydrogel Boosts Potential of Chlorhexidine in Biofilm Eradication in Vitro", *Carbohydrate Polymers*, Vol. 262, p. 117939, 2021.

132. Sebaaly, C., A. Trifan, E. Sieniawska and H. Greige-Gerges, "Chitosan-coating Effect on the Characteristics of Liposomes: A Focus on Bioactive Compounds and Essential Oils: a Review", *Processes*, Vol. 9, No. 3, p. 445, 2021.

133. Branden, C. I. and J. Tooze, *Introduction to Protein Structure*, Garland Science, New York, 1998.

134. Mitragotri, S., P. A. Burke and R. Langer, "Overcoming the Challenges in Administering Biopharmaceuticals: Formulation and Delivery Strategies", *Nature Reviews Drug Discovery*, Vol. 13, No. 9, pp. 655–672, 2014.

135. Chaulagain, B., A. Jain, A. Tiwari, A. Verma and S. K. Jain, "Passive Delivery of Protein Drugs Through Transdermal Route", *Artificial Cells, Nanomedicine, and Biotechnology*, Vol. 46, No. sup1, pp. 472–487, 2018.

136. Kalluri, H. and A. K. Banga, "Transdermal Delivery of Proteins", *AAPS Pharmscitech*, Vol. 12, pp. 431–441, 2011.

137. Peña-Juárez, M. C., O. R. Guadarrama-Escobar and J. J. Escobar-Chávez, "Transdermal Delivery Systems for Biomolecules", *Journal of Pharmaceutical Innovation*, Vol. 17, No. 2, pp. 319–332, 2022.

138. Pisani, S., D. Di Martino, S. Cerri, I. Genta, R. Dorati, G. Bertino, M. Benazzo and B. Conti, "Investigation and Comparison of Active and Passive Encapsu-

lation Methods for Loading Proteins Into Liposomes", *International Journal of Molecular Sciences*, Vol. 24, No. 17, p. 13542, 2023.

139. Rawlings, A. and C. Harding, "Moisturization and Skin Barrier Function", *Dermatologic Therapy*, Vol. 17, pp. 43–48, 2004.

140. Smith, F. J., A. D. Irvine *et al.*, "Loss-of-function Mutations in the Gene Encoding Filaggrin Cause Ichthyosis Vulgaris", *Nature Genetics*, Vol. 38, No. 3, pp. 337–342, 2006.

141. Harding, C., S. Aho and C. Bosko, "Filaggrin–Revisited", *International Journal of Cosmetic Science*, Vol. 35, No. 5, pp. 412–423, 2013.

142. Deddy, D., M. Devi *et al.*, "Epidermal Proliferation and Differentiation in Ichthyosis Vulgaris", *Bioscientia Medicina: Journal of Biomedicine and Translational Research*, Vol. 5, No. 2, pp. 235–247, 2021.

143. Otsuka, A., H. Doi, G. Egawa, A. Maekawa, T. Fujita, S. Nakamizo, C. Nakashima, S. Nakajima, T. Watanabe, Y. Miyachi *et al.*, "Possible New Therapeutic Strategy to Regulate Atopic Dermatitis Through Upregulating Filaggrin Expression", *Journal of Allergy and Clinical Immunology*, Vol. 133, No. 1, pp. 139–146, 2014.

144. Méchin, M.-C., H. Takahara and M. Simon, "Deimination and Peptidylarginine Deiminases in Skin Physiology and Diseases", *International Journal of Molecular Sciences*, Vol. 21, No. 2, p. 566, 2020.

145. Eaaswarkhanth, M., D. Xu, C. Flanagan, M. Rzhetskaya, M. G. Hayes, R. Blekhman, N. G. Jablonski and O. Gokcumen, "Atopic Dermatitis Susceptibility Variants in Filaggrin Hitchhike Hornerin Selective Sweep", *Genome Biology and Evolution*, Vol. 8, No. 10, pp. 3240–3255, 2016.

146. Denecker, G., E. Hoste, B. Gilbert, T. Hochepied, P. Ovaere, S. Lippens,

C. Van den Broecke, P. Van Damme, K. D'Herde, J.-P. Hachem *et al.*, "Caspase-14 Protects Against Epidermal Uvb Photodamage and Water Loss", *Nature Cell Biology*, Vol. 9, No. 6, pp. 666–674, 2007.

147. Denecker, G., P. Ovaere, P. Vandenabeele and W. Declercq, "Caspase-14 Reveals Its Secrets", *The Journal of Cell Biology*, Vol. 180, No. 3, pp. 451–458, 2008.

148. Markiewicz, A., D. Sigorski, M. Markiewicz, A. Owczarczyk-Saczonek and W. Placek, "Caspase-14—from Biomolecular Basics to Clinical Approach: A Review of Available Data", *International Journal of Molecular Sciences*, Vol. 22, No. 11, p. 5575, 2021.

149. McClanahan, D., A. Wong, S. Kezic, A. Samrao, T. Hajar, E. Hill and E. Simpson, "A Randomized Controlled Trial of an Emollient With Ceramide and Filaggrin-associated Amino Acids for the Primary Prevention of Atopic Dermatitis in High-risk Infants", *Journal of the European Academy of Dermatology and Venereology*, Vol. 33, No. 11, pp. 2087–2094, 2019.

150. Jiang, Y. J., P. Kim, Y. Uchida, P. M. Elias, D. D. Bikle, C. Grunfeld and K. R. Feingold, "Ceramides Stimulate Caspase-14 Expression in Human Keratinocytes", *Experimental Dermatology*, Vol. 22, No. 2, pp. 113–118, 2013.

151. Kelly, S. M. and N. C. Price, "The Use of Circular Dichroism in the Investigation of Protein Structure and Function", *Current Protein and Peptide Science*, Vol. 1, No. 4, pp. 349–384, 2000.

152. Wei, Y., A. A. Thyparambil and R. A. Latour, "Protein Helical Structure Determination Using CD Spectroscopy for Solutions With Strong Background Absorbance From 190 to 230 nm", *Biochimica Et Biophysica Acta -Proteins and Proteomics*, Vol. 1844, No. 12, pp. 2331–2337, 2014.

153. Miles, A., R. W. Janes and B. A. Wallace, "Tools and Methods for Circular

Dichroism Spectroscopy of Proteins: A Tutorial Review", *Chemical Society Reviews*, Vol. 50, No. 15, pp. 8400–8413, 2021.

APPENDIX A: DLS RESULTS OF THE TEs IN CHAPTER 3

Size and PDI results of the vesicles obtained in chapter 3 can be found here.

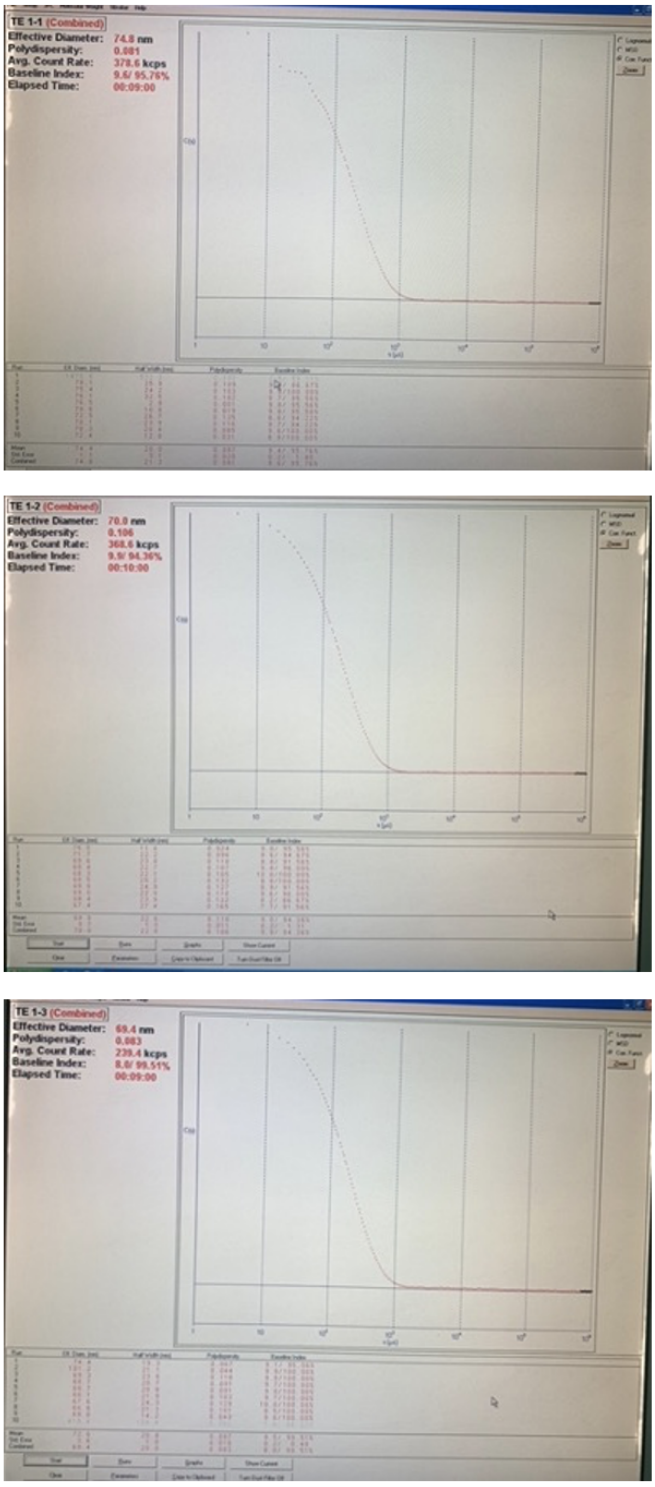

Figure A.1. DLS results belonging to the three trials of TE1 samples

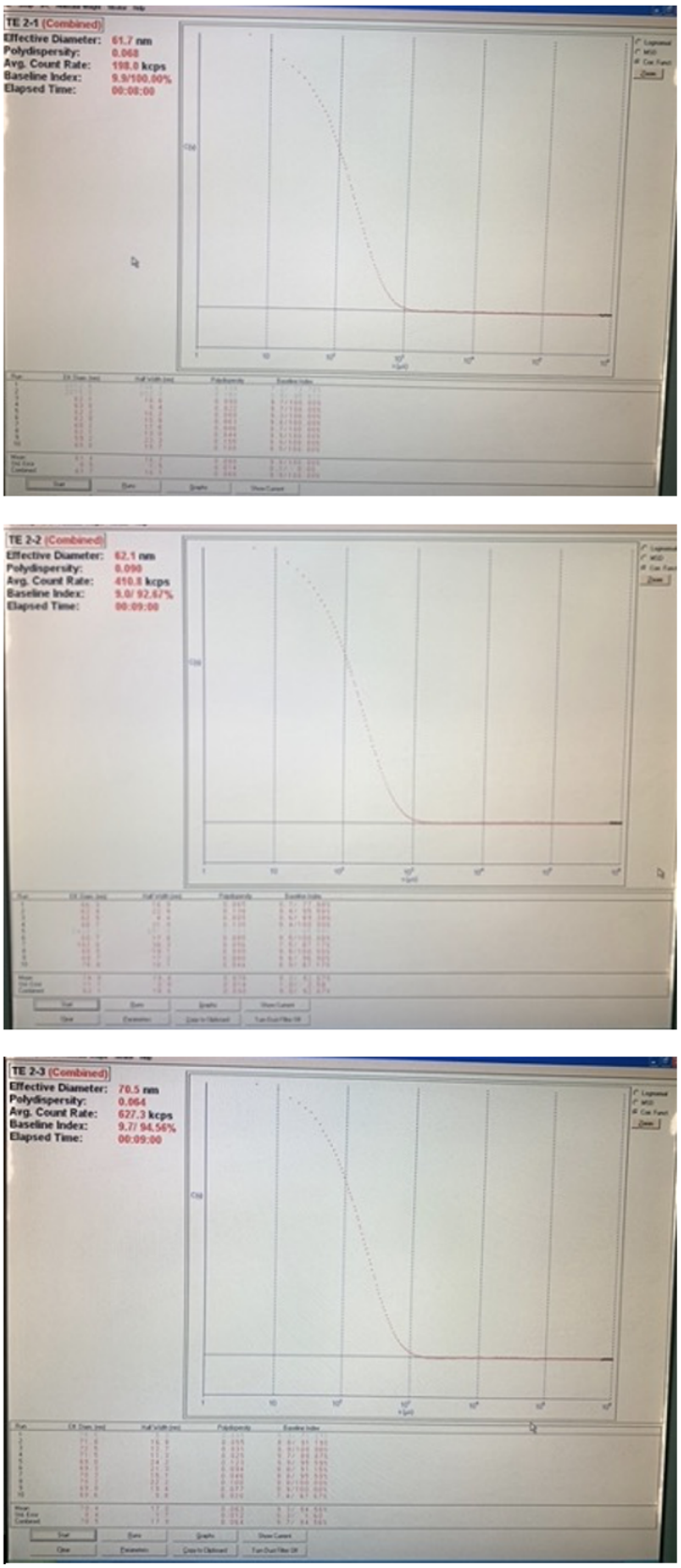

Figure A.2. DLS results belonging to the three trials of TE2 samples

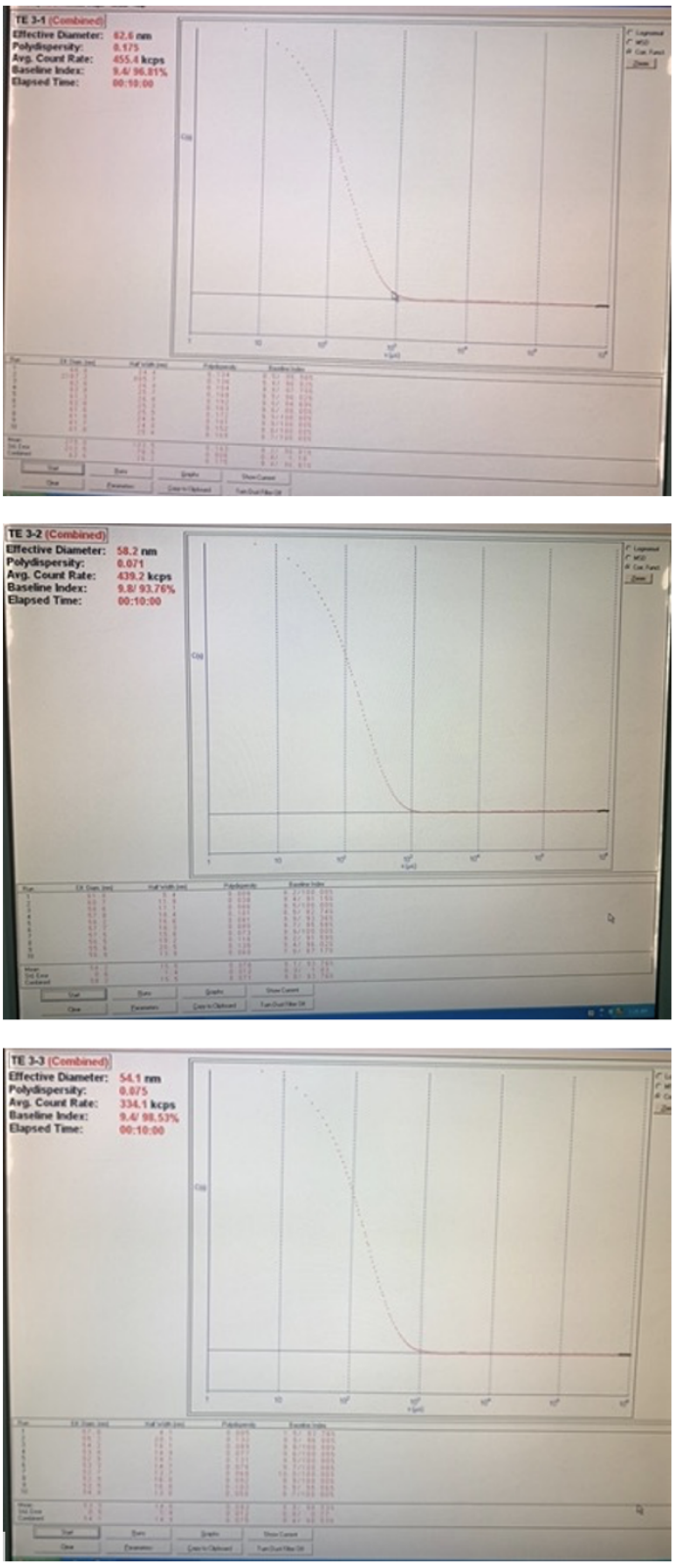

Figure A.3. DLS results belonging to the three trials of TE3 samples

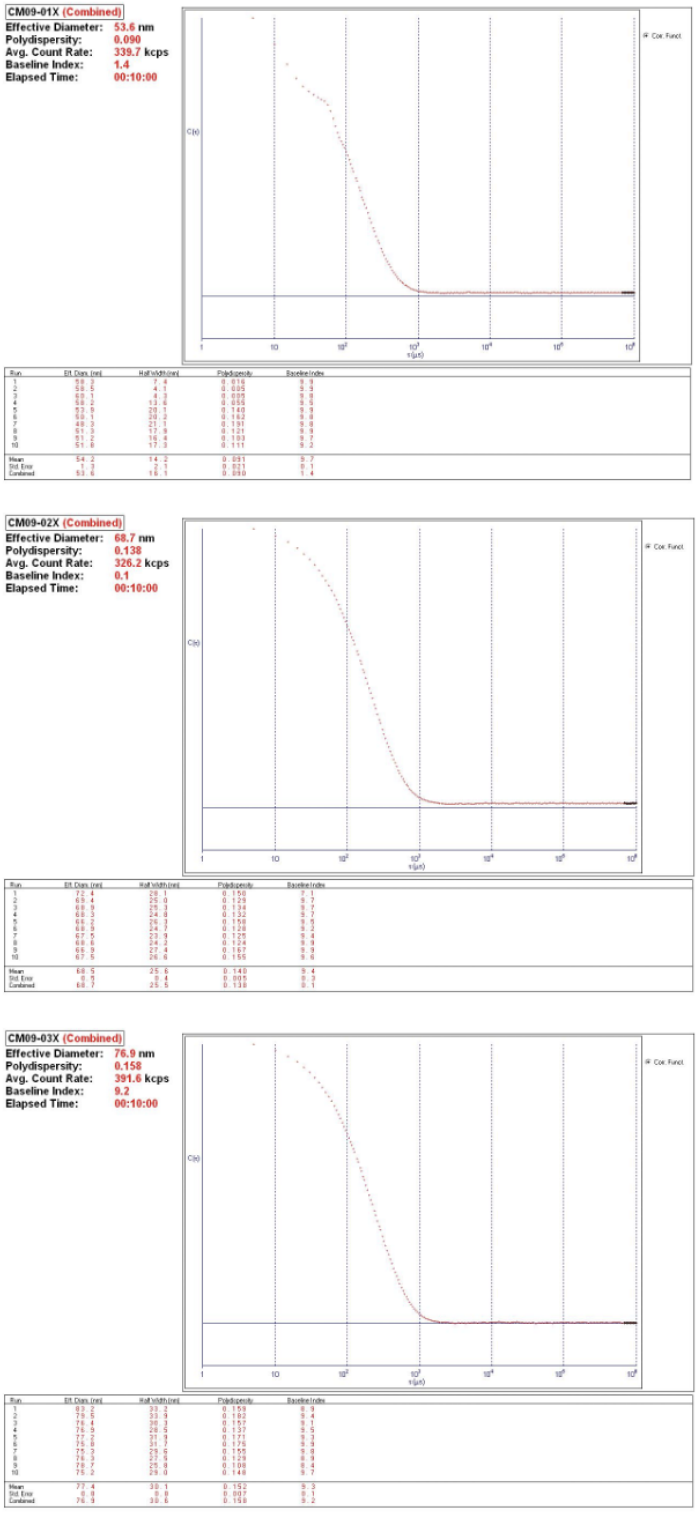

Figure A.4. DLS results belonging to the samples of TE4, TE5 and TE6

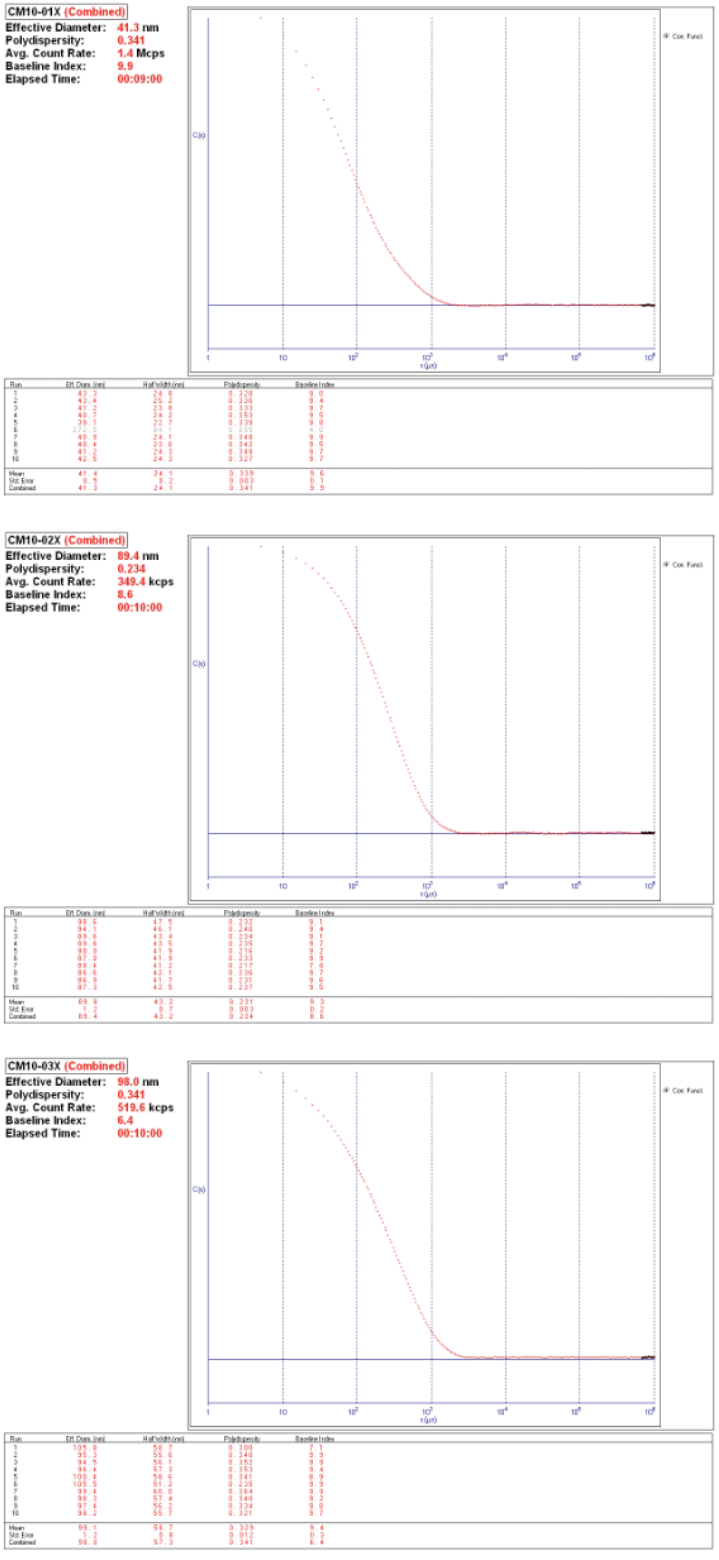

Figure A.5. DLS results belonging to the samples of TE7, TE8 and TE9

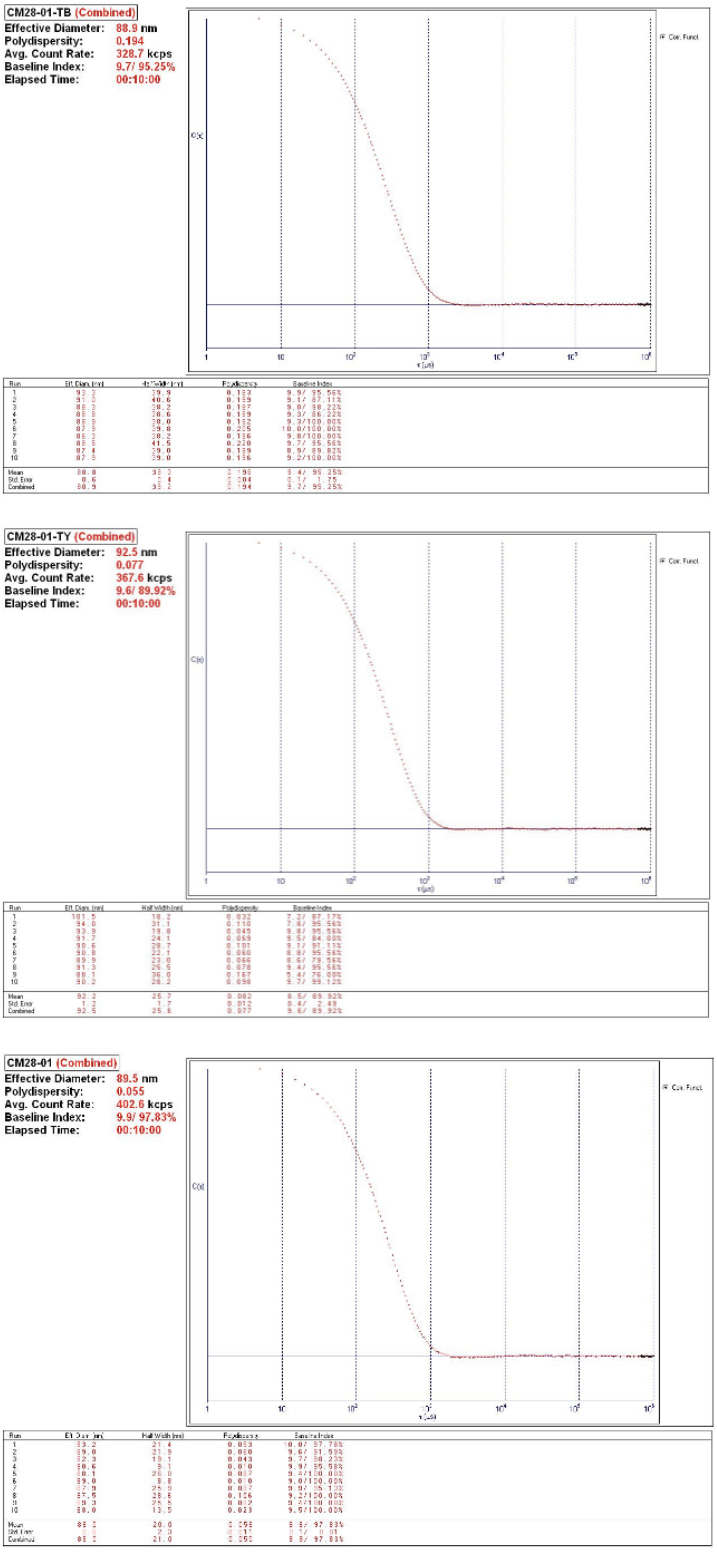

Figure A.6. DLS results belonging to the three trials of TE10 samples

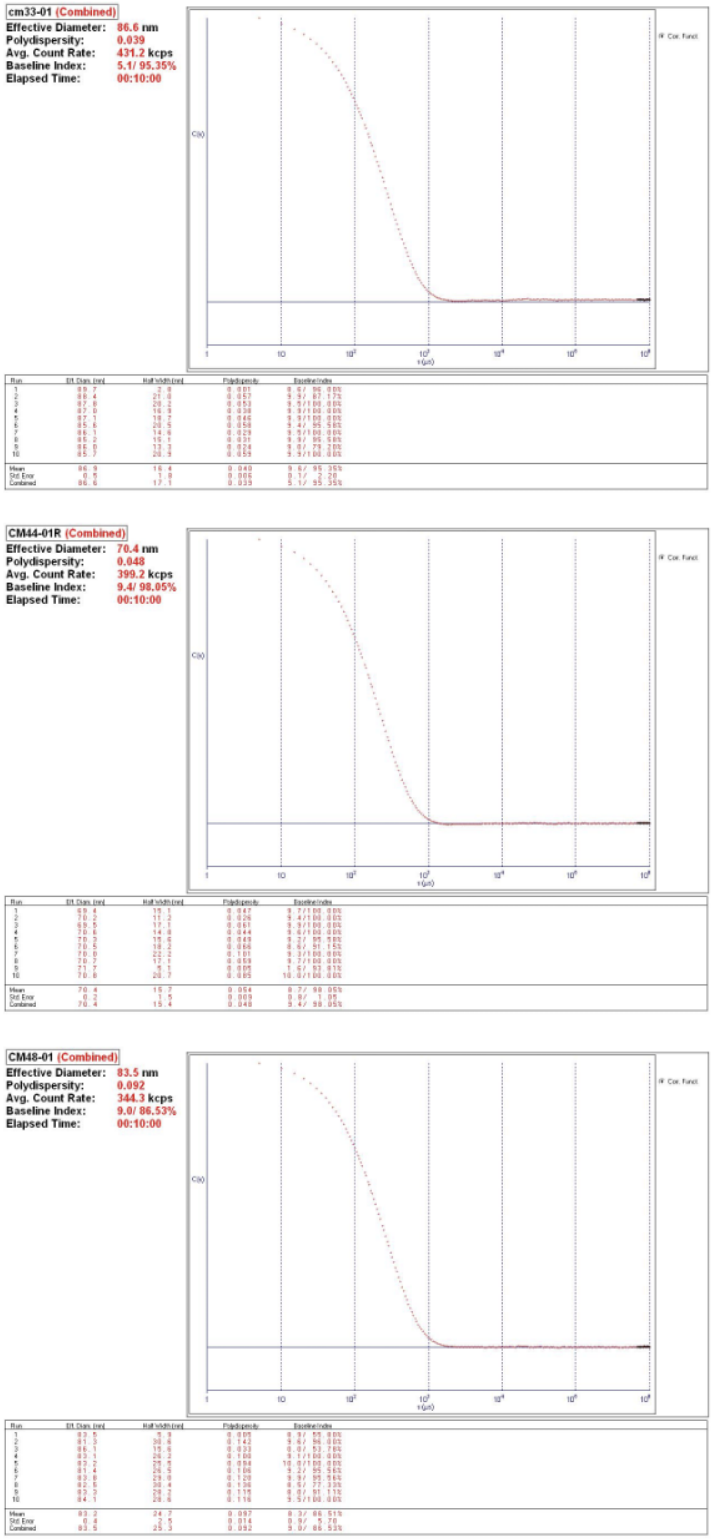

Figure A.7. DLS results belonging to the three trials of TE11 samples

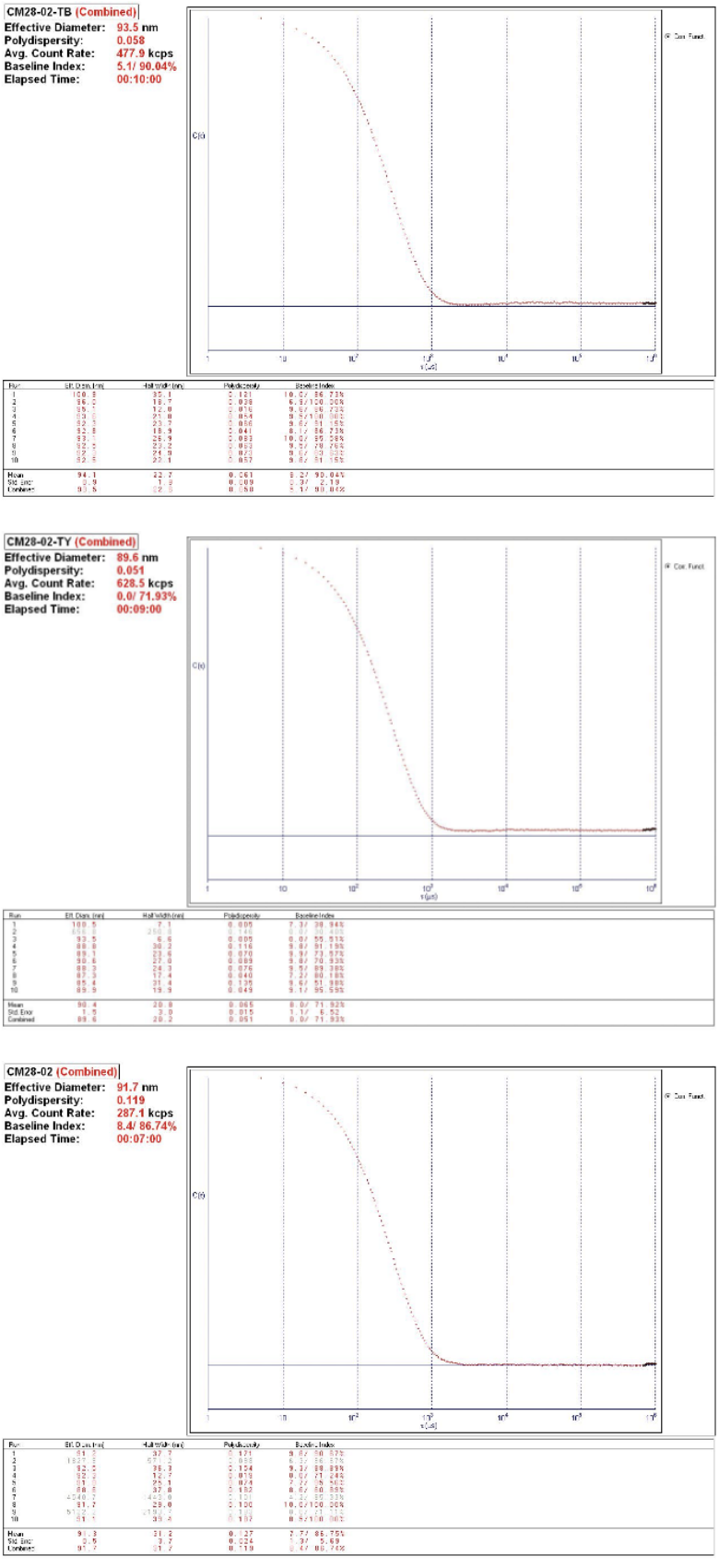

Figure A.8. DLS results belonging to the three trials of TE12 samples

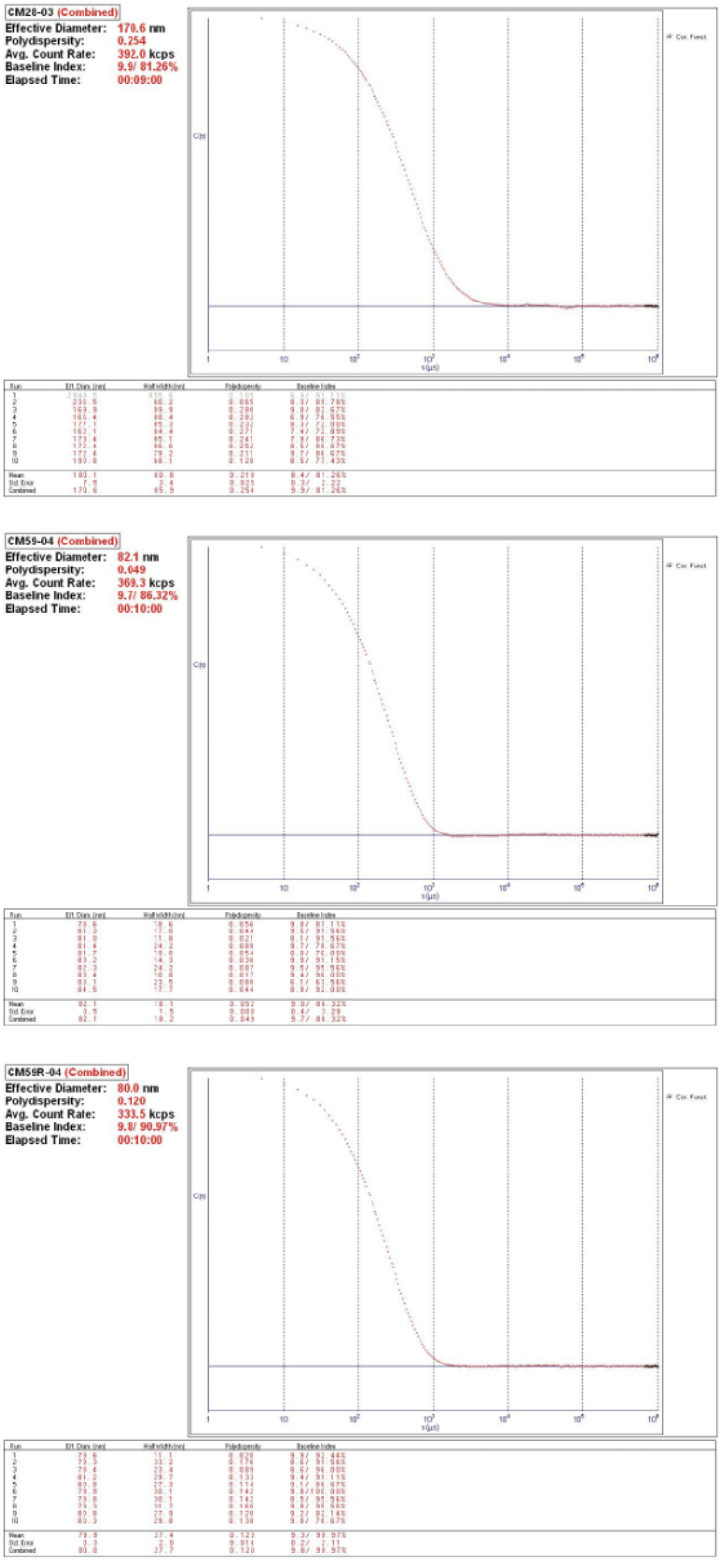

Figure A.9. DLS results belonging to the three trials of TE13 samples

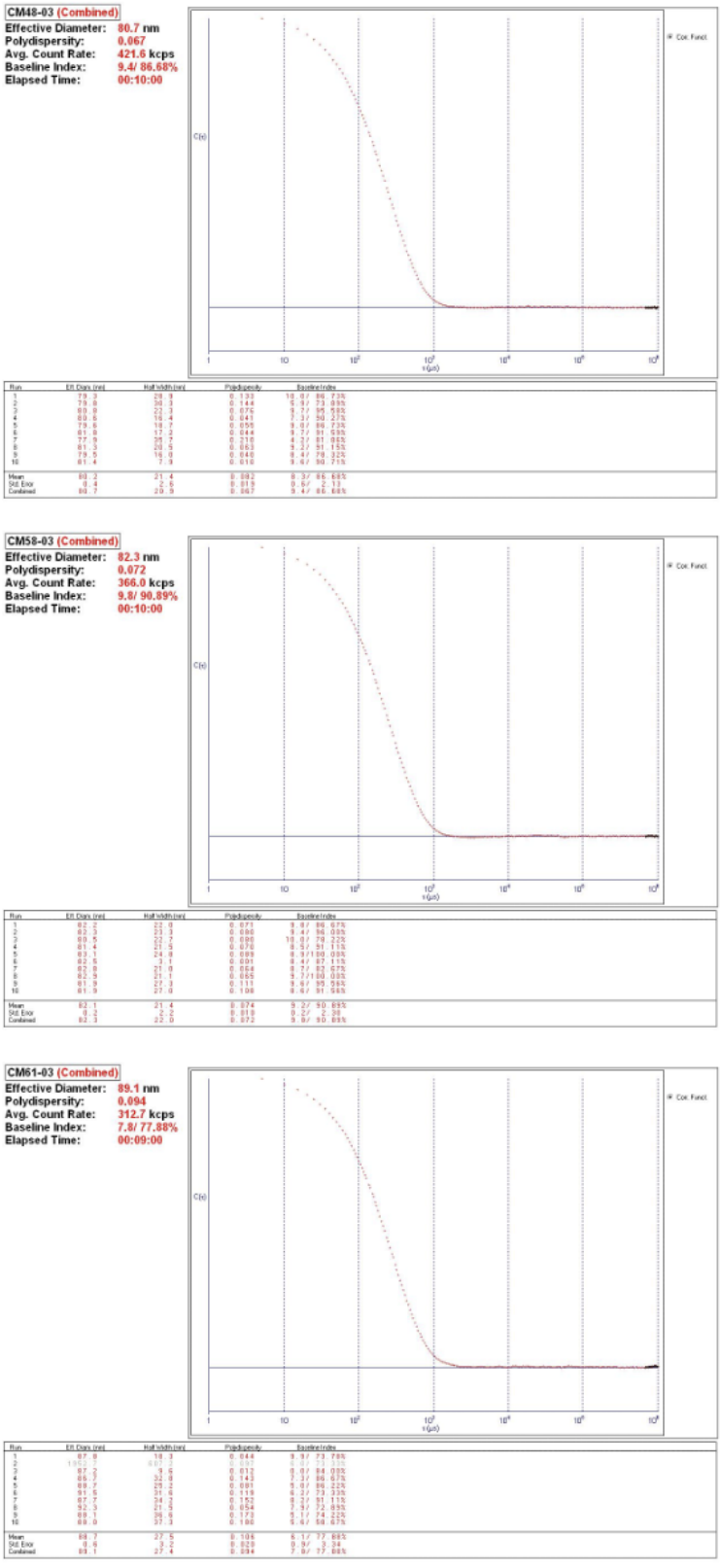

Figure A.10. DLS results belonging to the three trials of TE14 samples

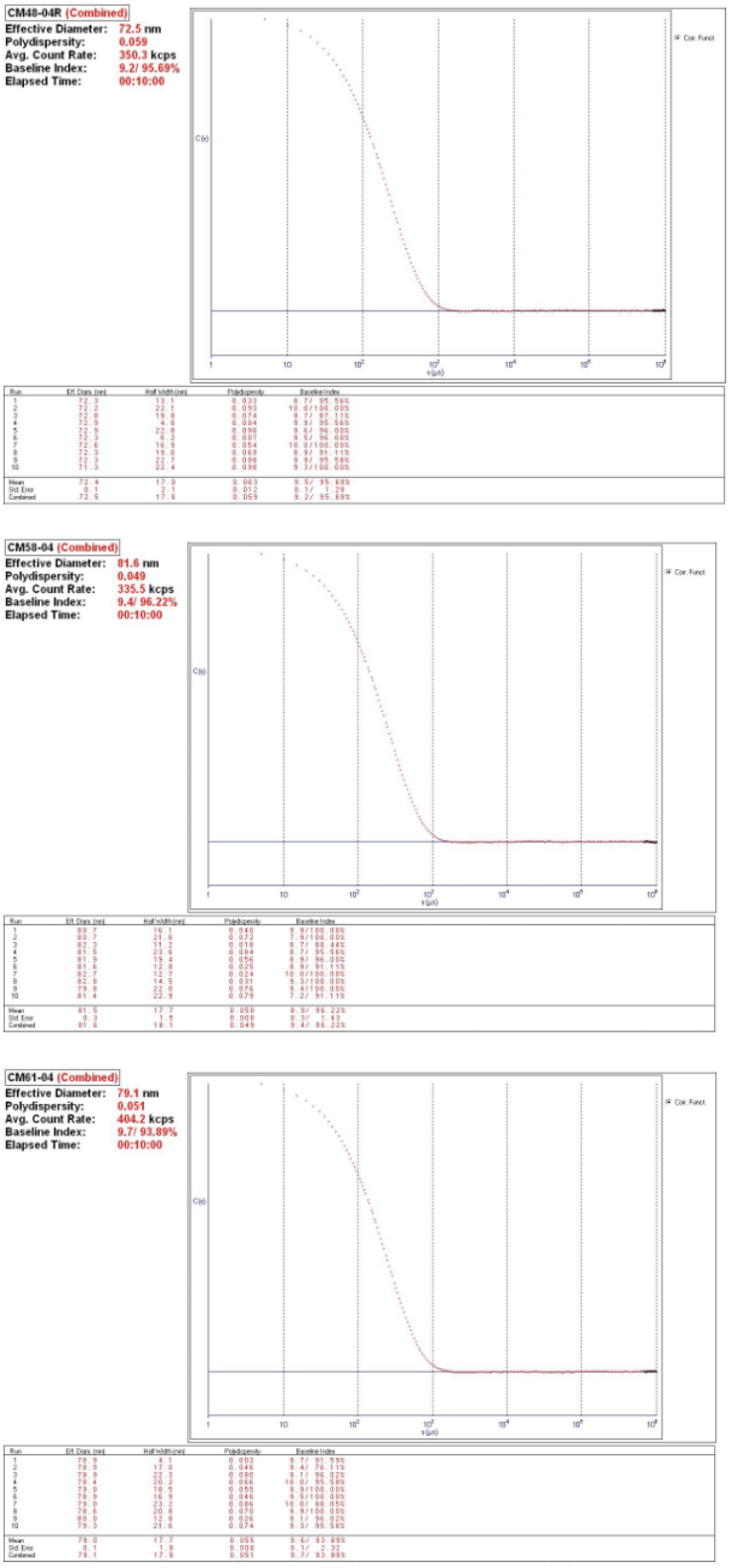

Figure A.11. DLS results belonging to the three trials of TE15 samples

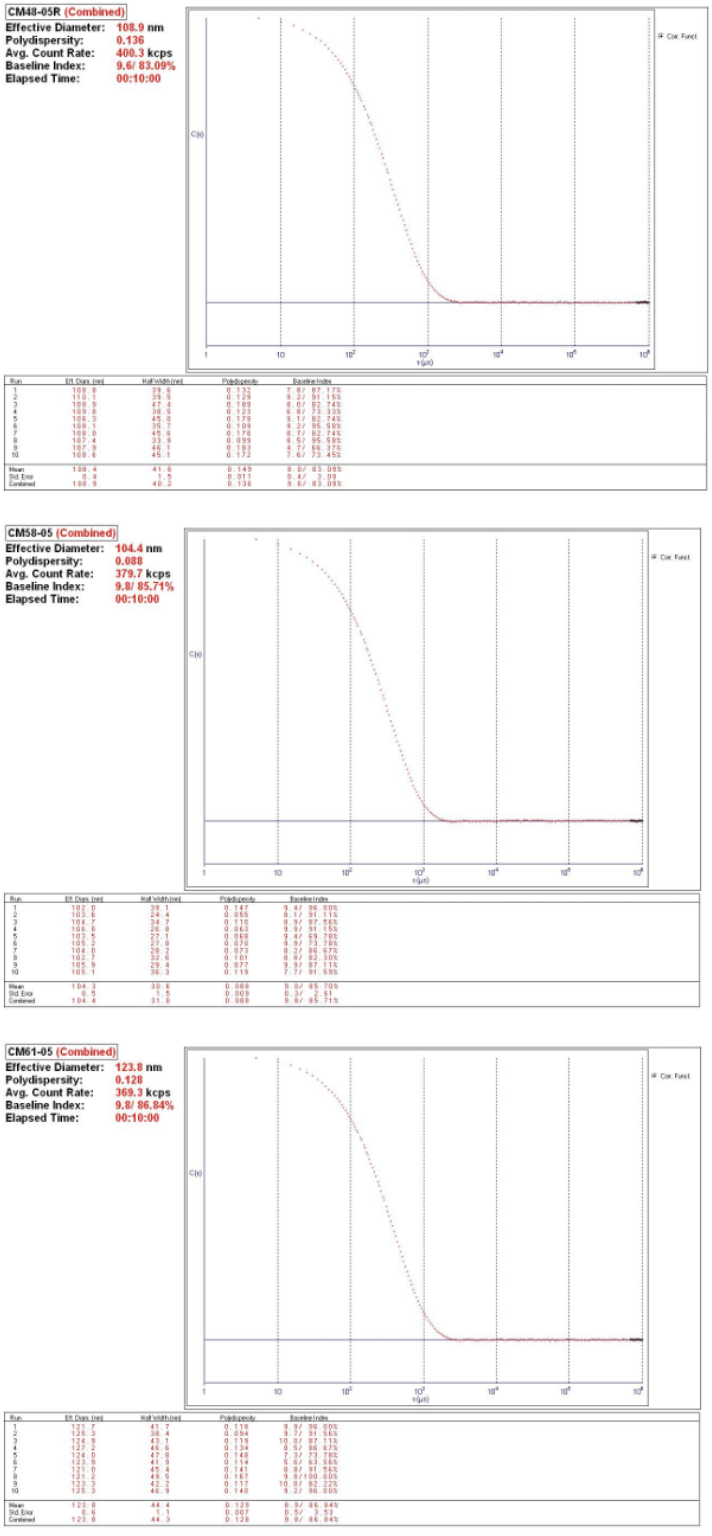

Figure A.12. DLS results belonging to the three trials of TE16 samples

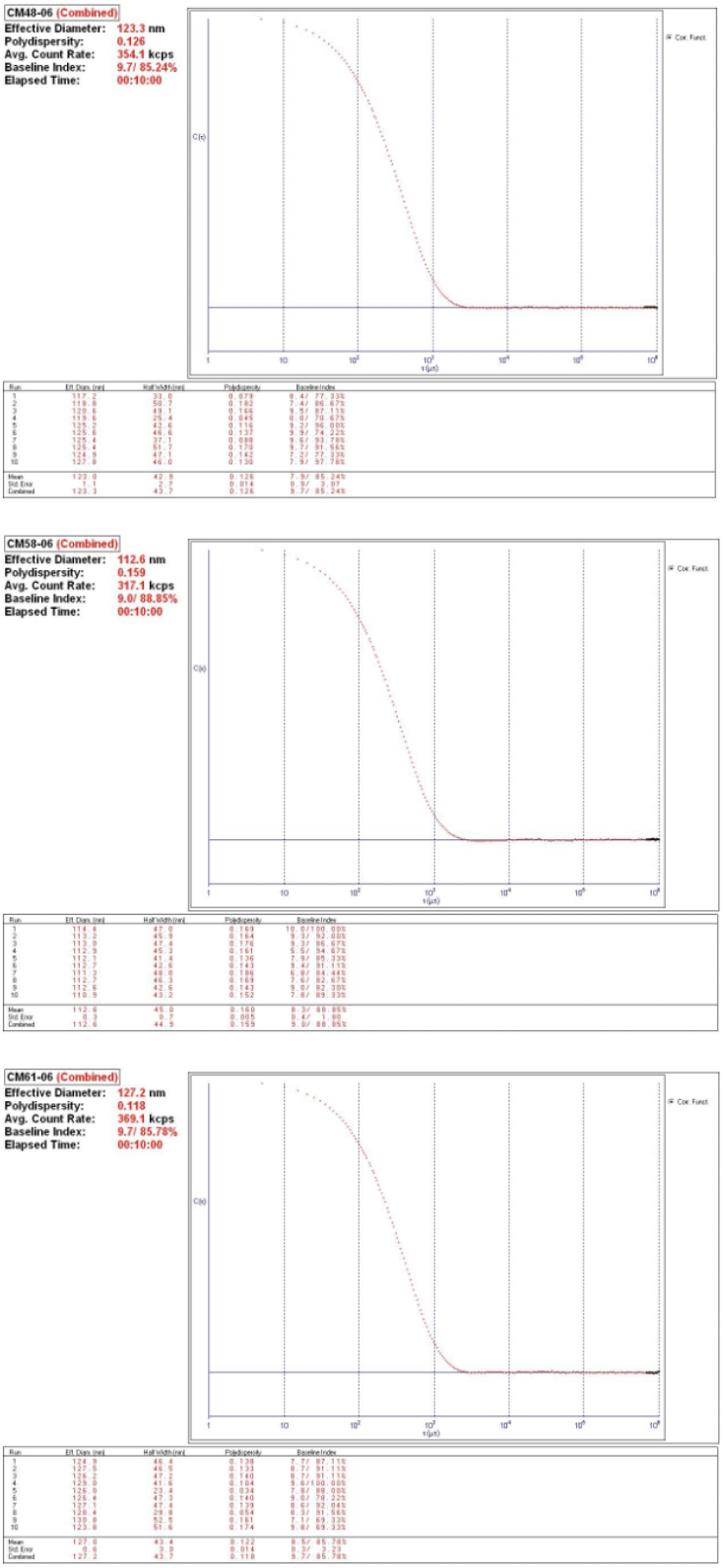

Figure A.13. DLS results belonging to the three trials of TE17 samples

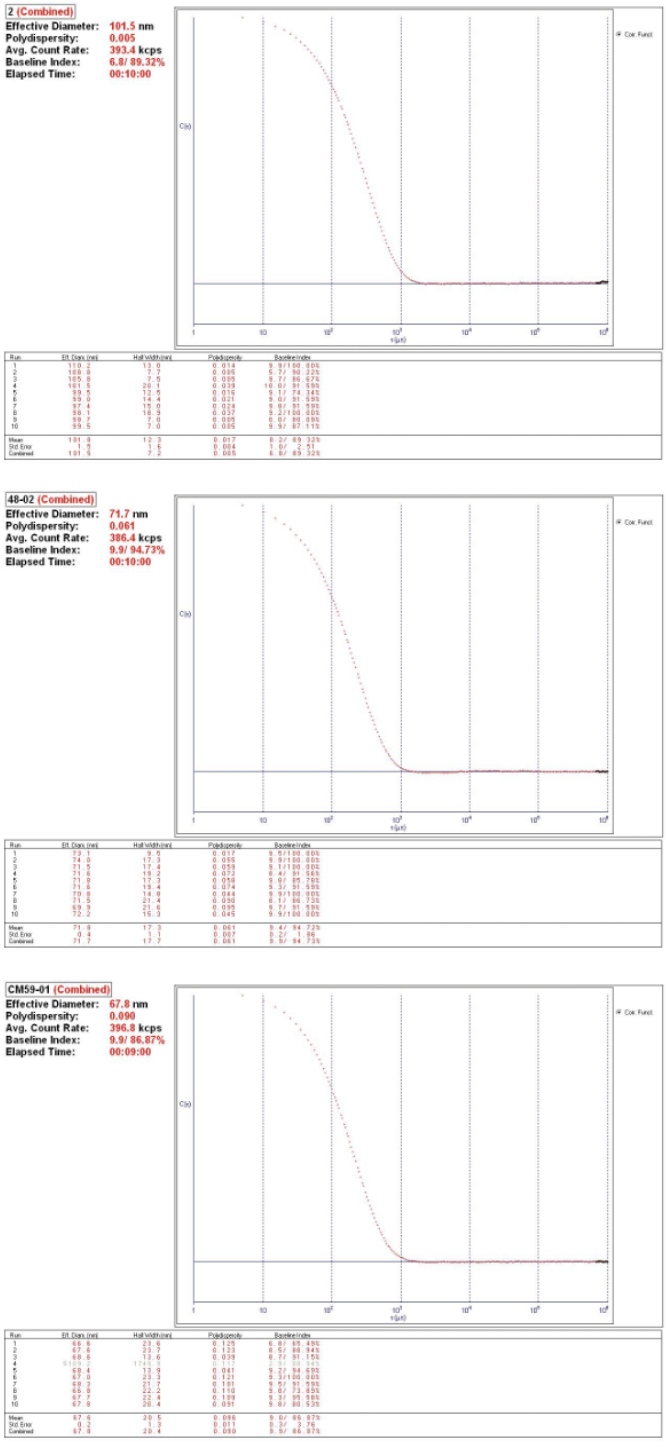

Figure A.14. DLS results showing one month stabilities of the TE5 samples

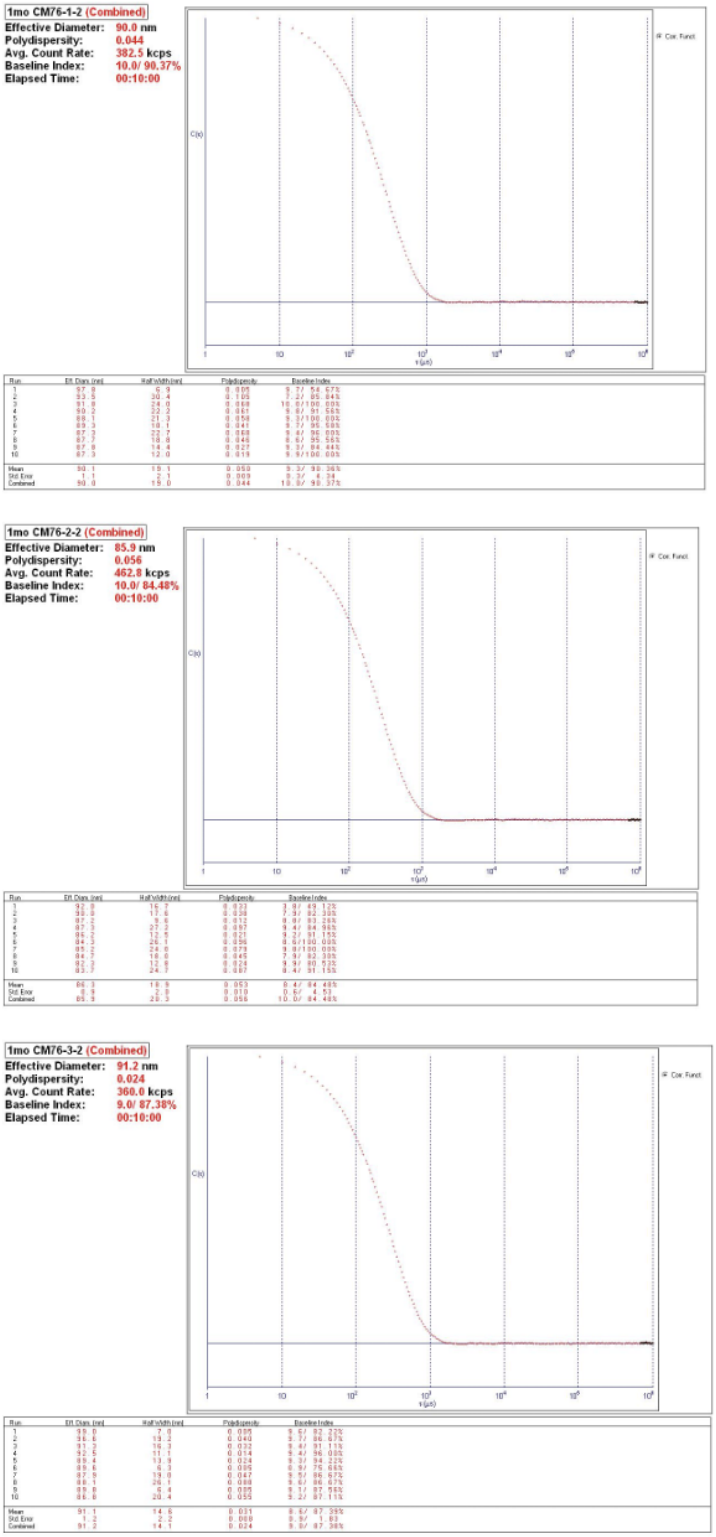

Figure A.15. DLS results showing one month stabilities of the TE11 samples

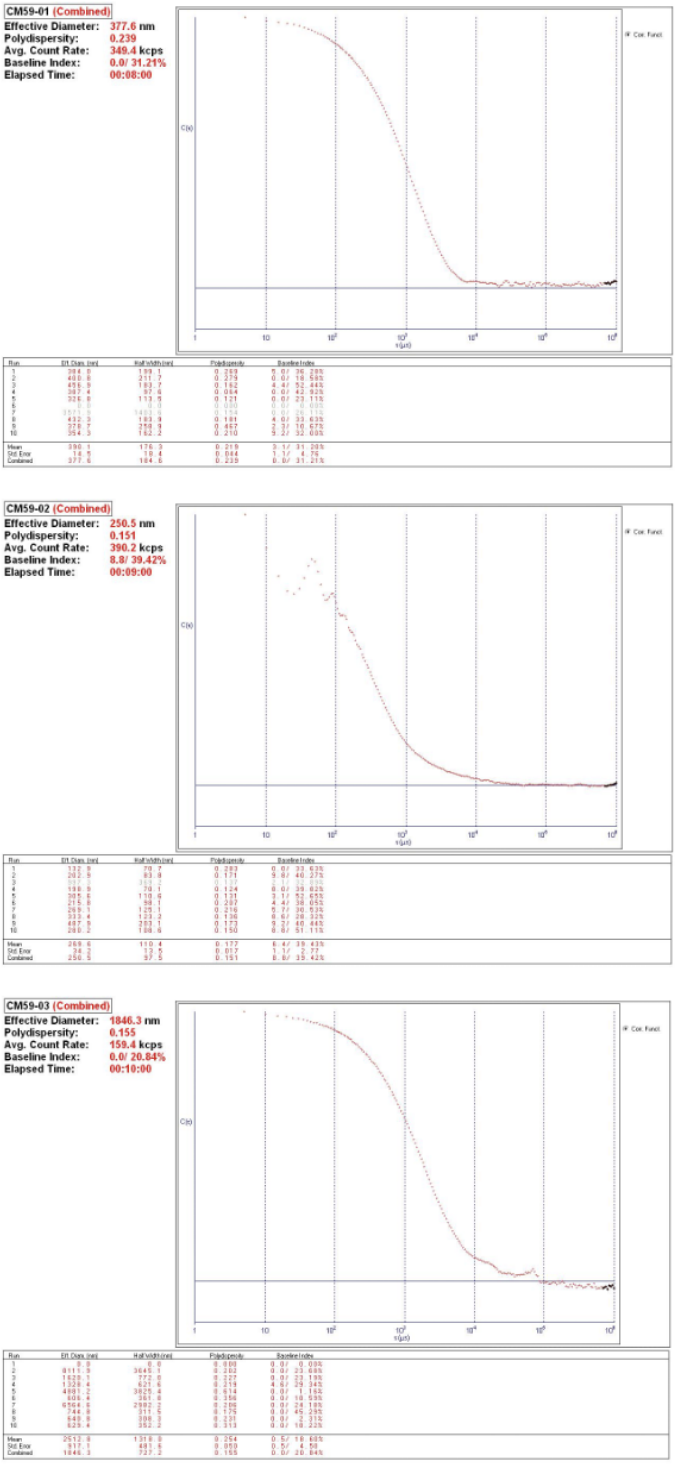

Figure A.16. DLS results showing one month stabilities of the TE 10, 12 and 13 samples

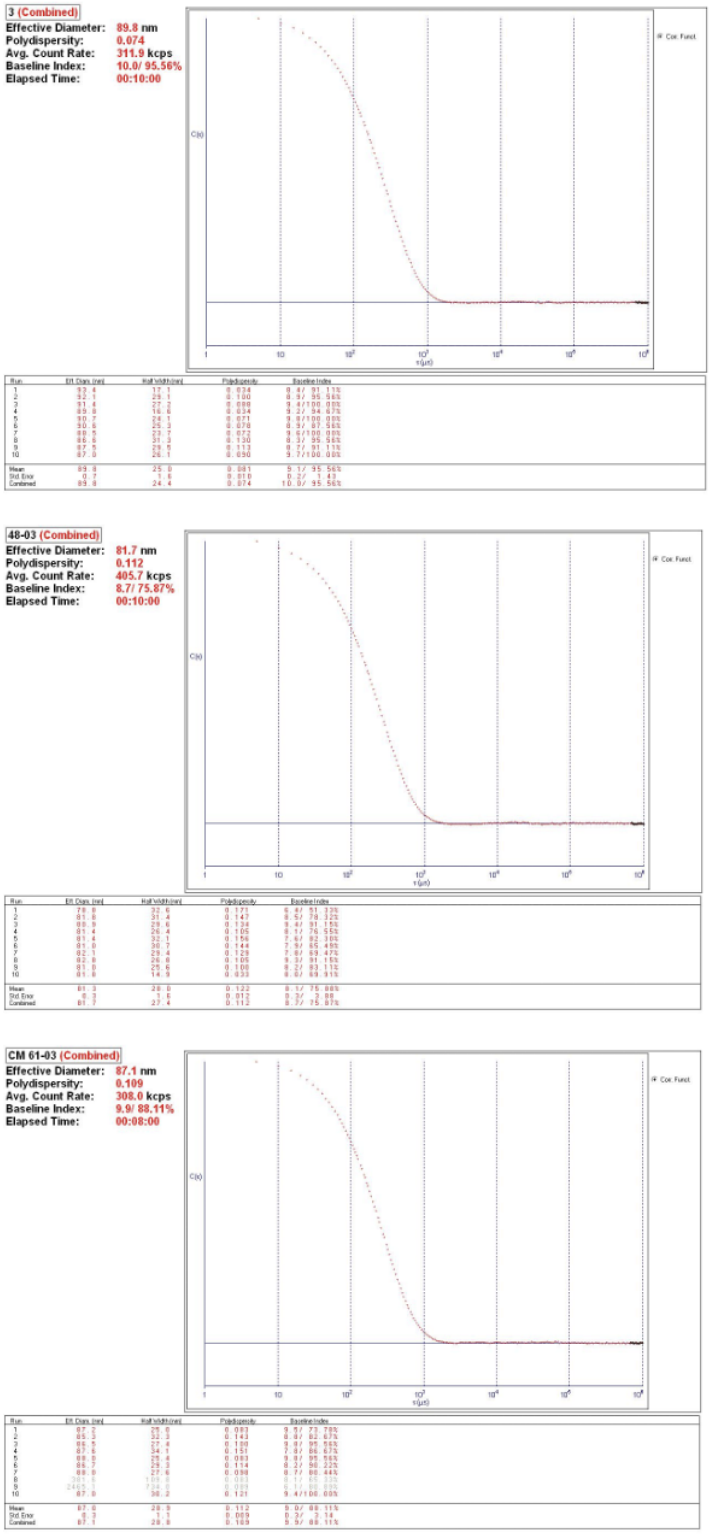

Figure A.17. DLS results showing one month stabilities of the TE14 samples

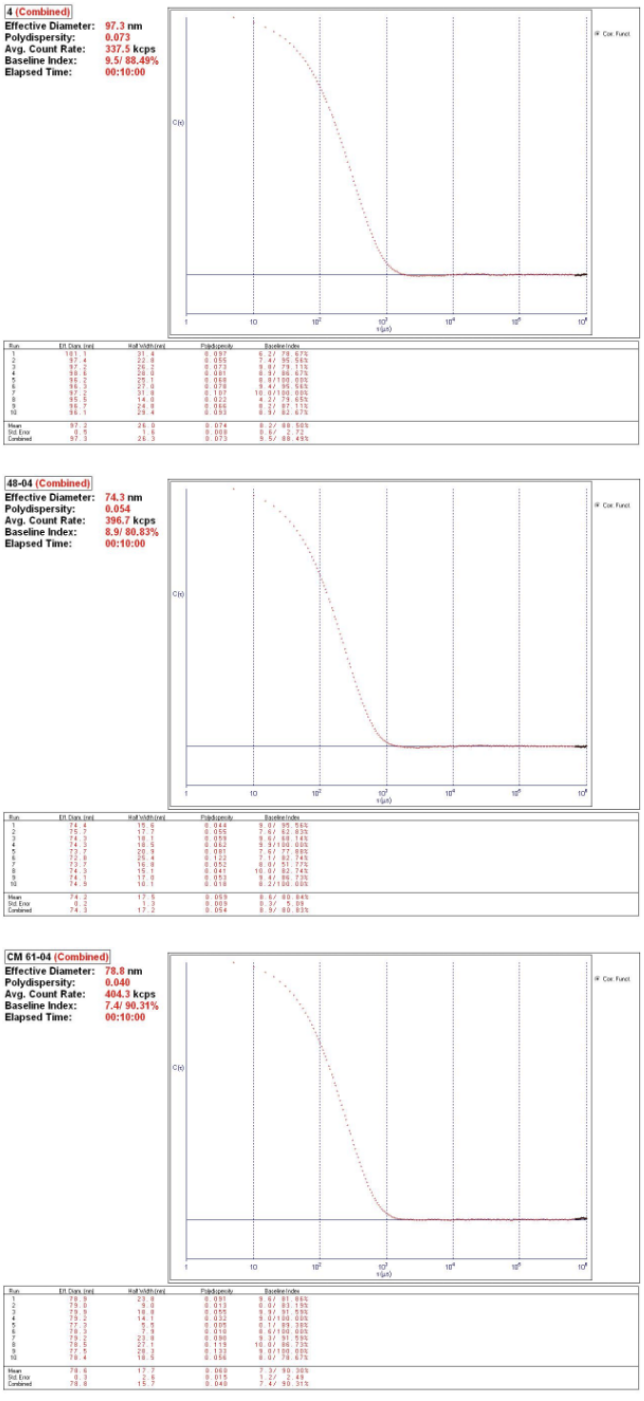

Figure A.18. DLS results showing one month stabilities of the TE15 samples

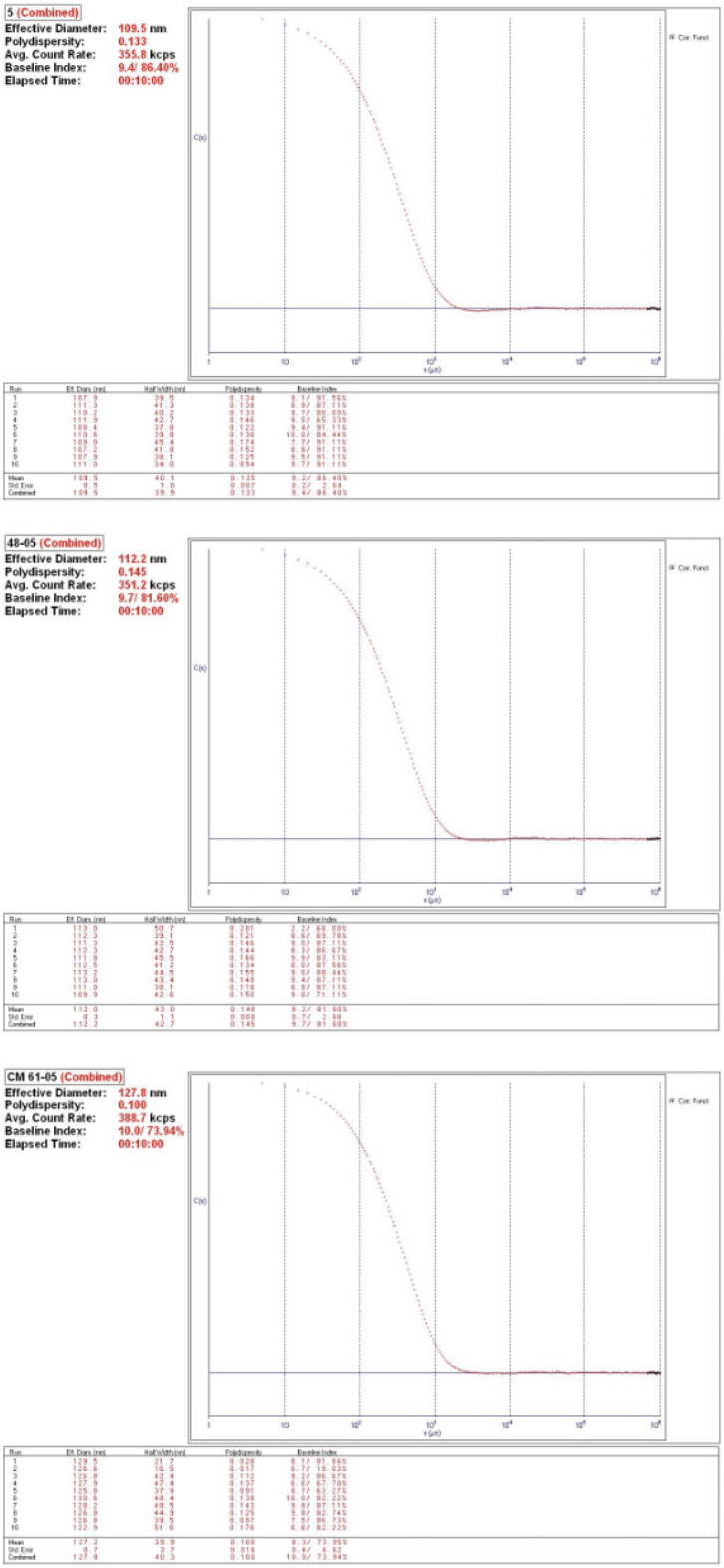

Figure A.19. DLS results showing one month stabilities of the TE16 samples

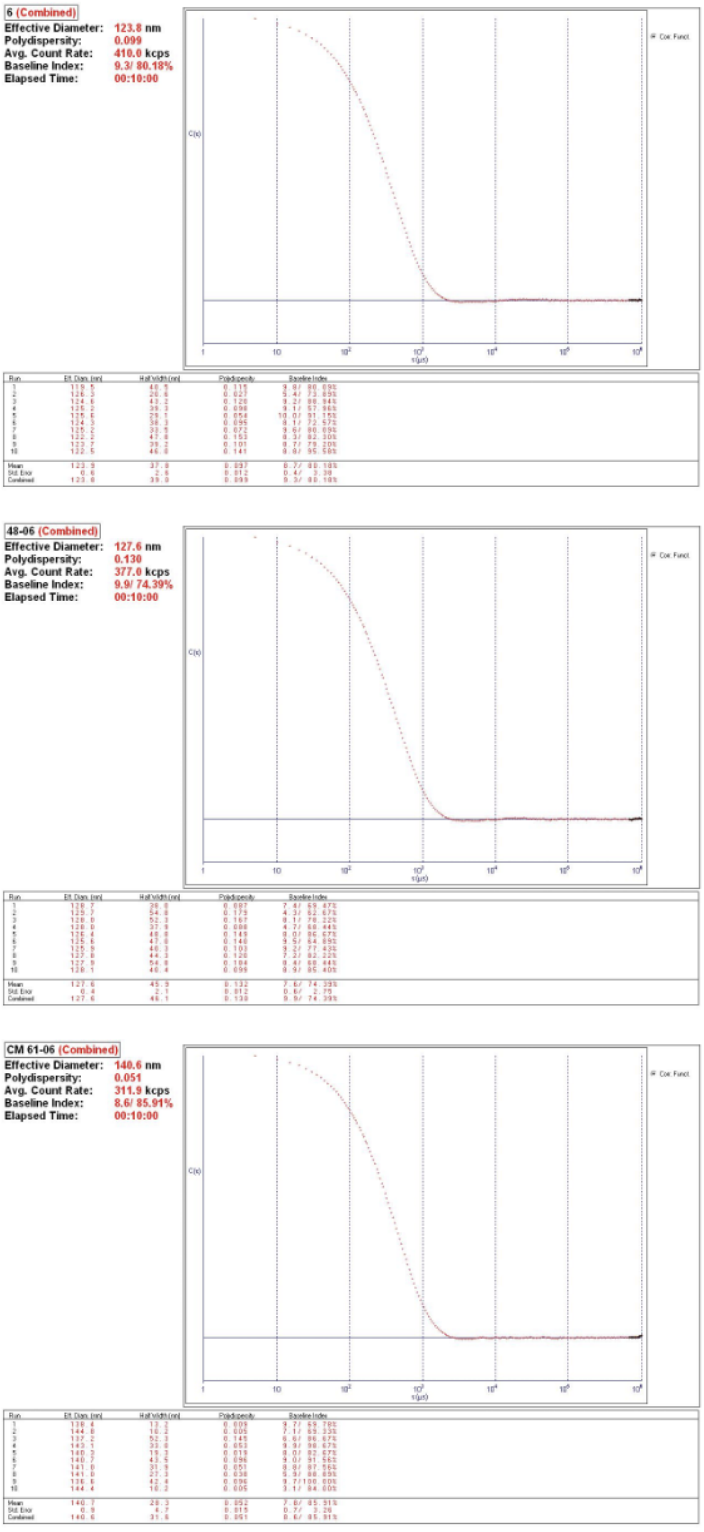

Figure A.20. DLS results showing one month stabilities of the TE17 samples

APPENDIX B: DLS RESULTS OF THE TEs IN CHAPTER 4

Size and PDI results of the vesicles obtained in chapter 4 can be found here.

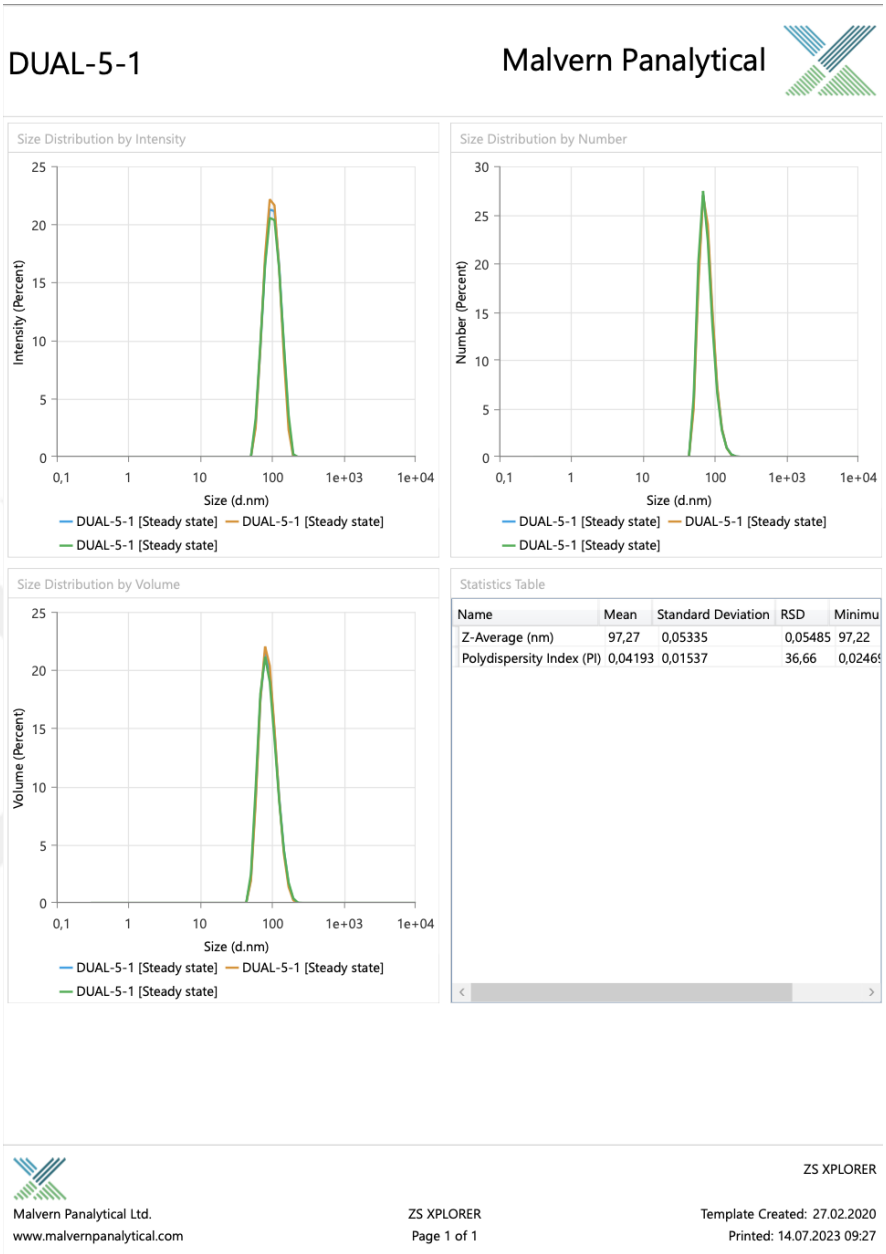

Figure B.1. DLS results of sample 5-1, belongs to the data set of Dual 1

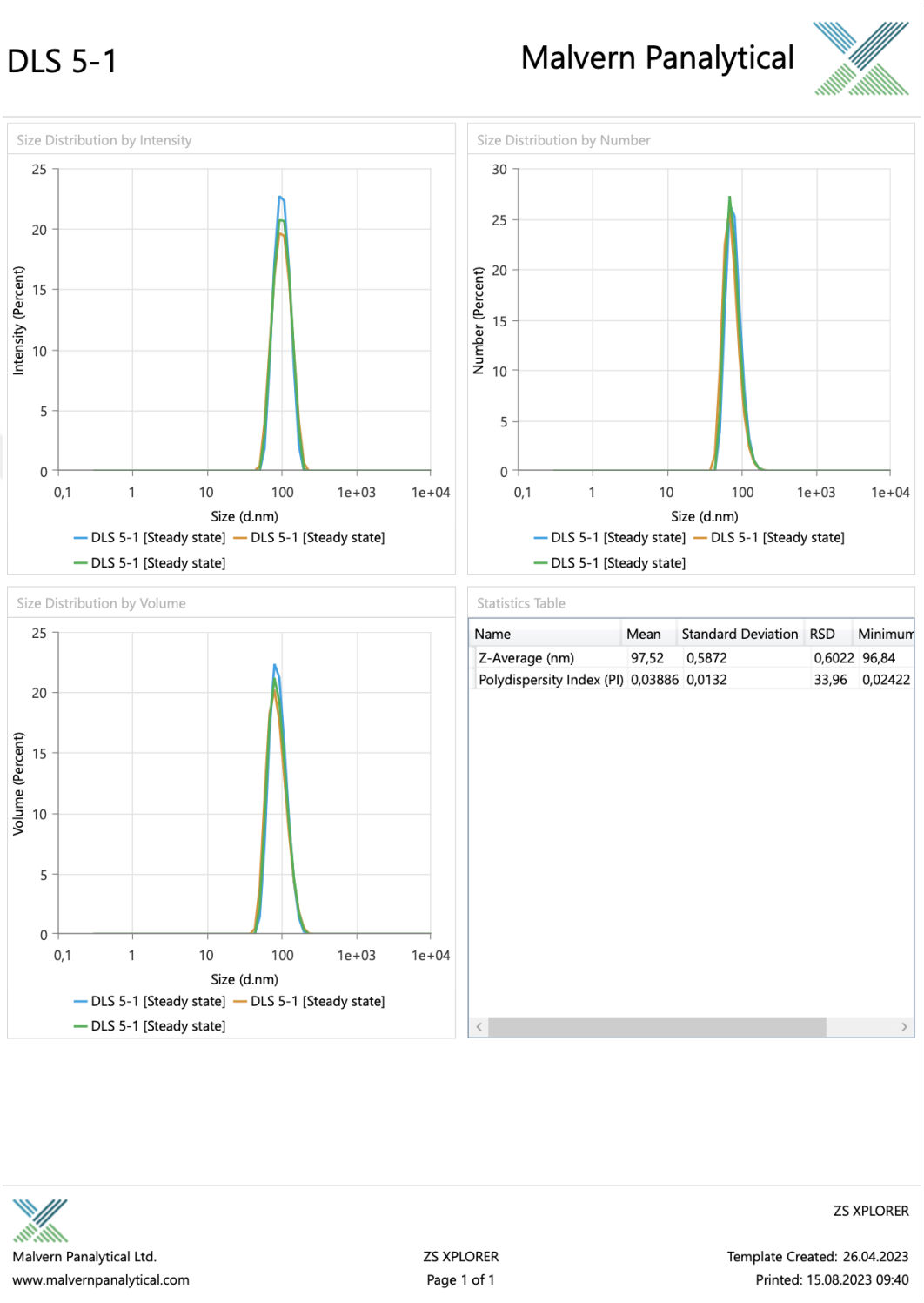

Figure B.2. 1-month DLS results of sample 5-1, belongs to the data set of Dual 1

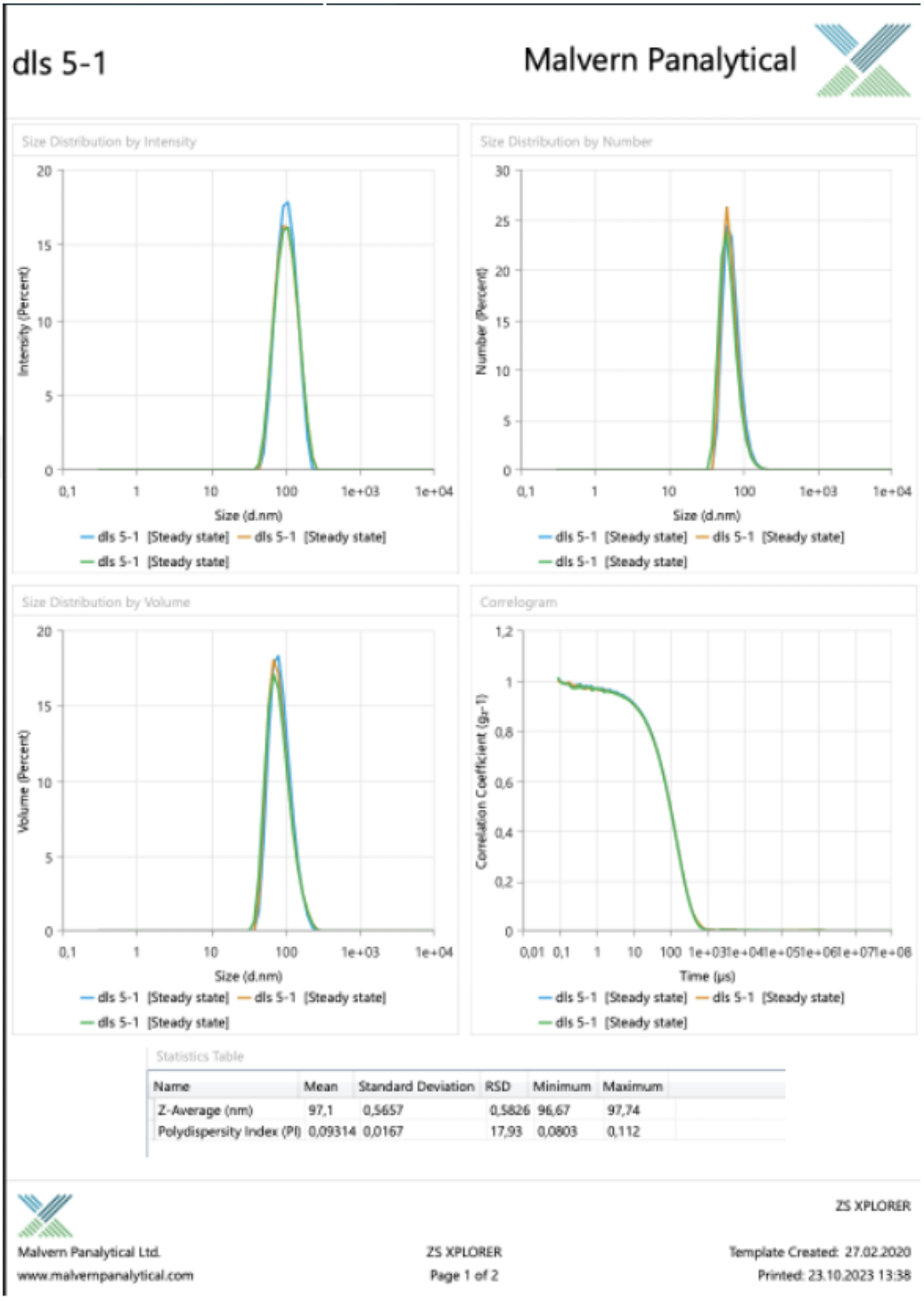

Figure B.3. 3-month DLS results of sample 5-1, belongs to the data set of Dual 1

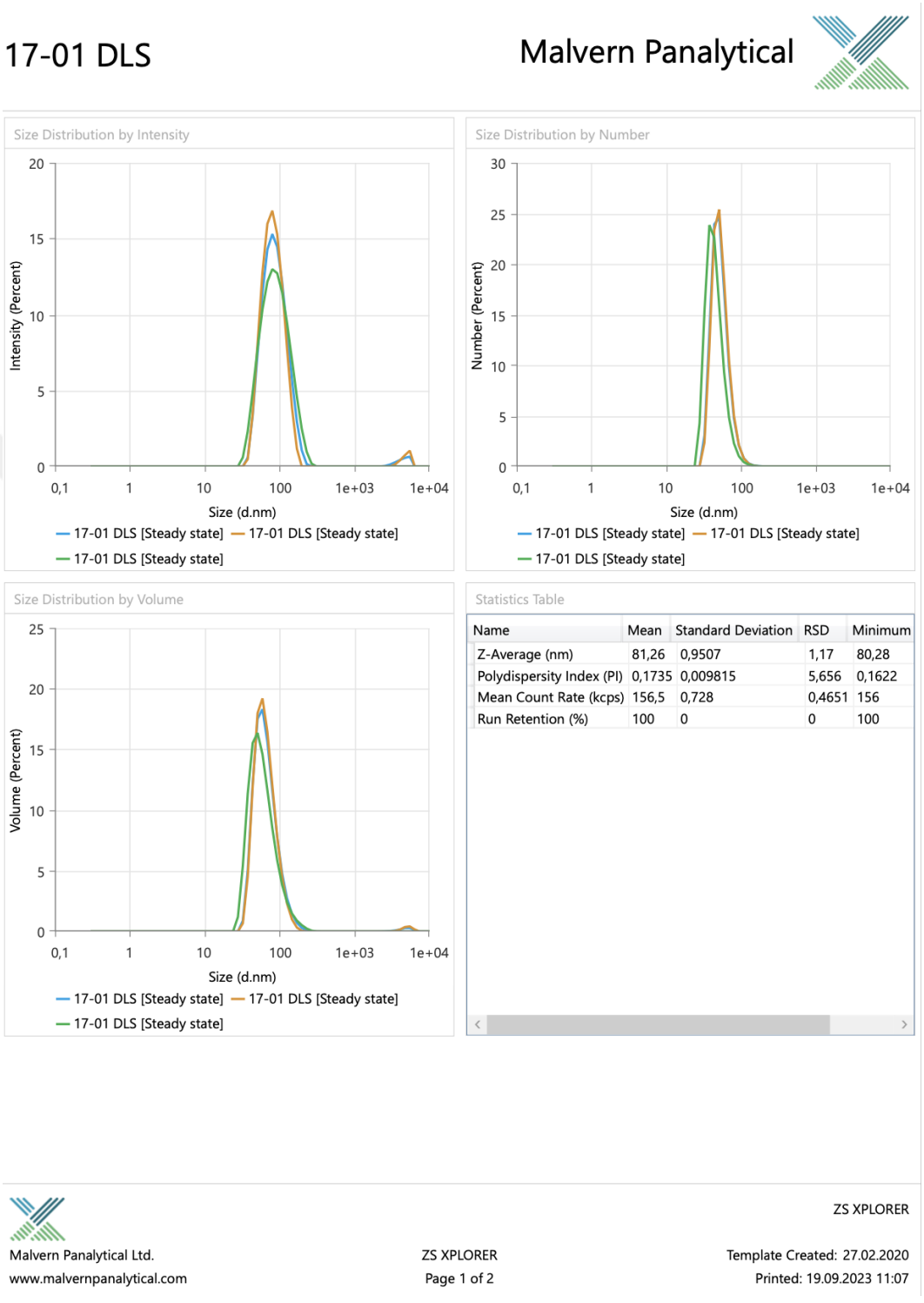

Figure B.4. DLS results of sample 17-1, belongs to the data set of Dual 2

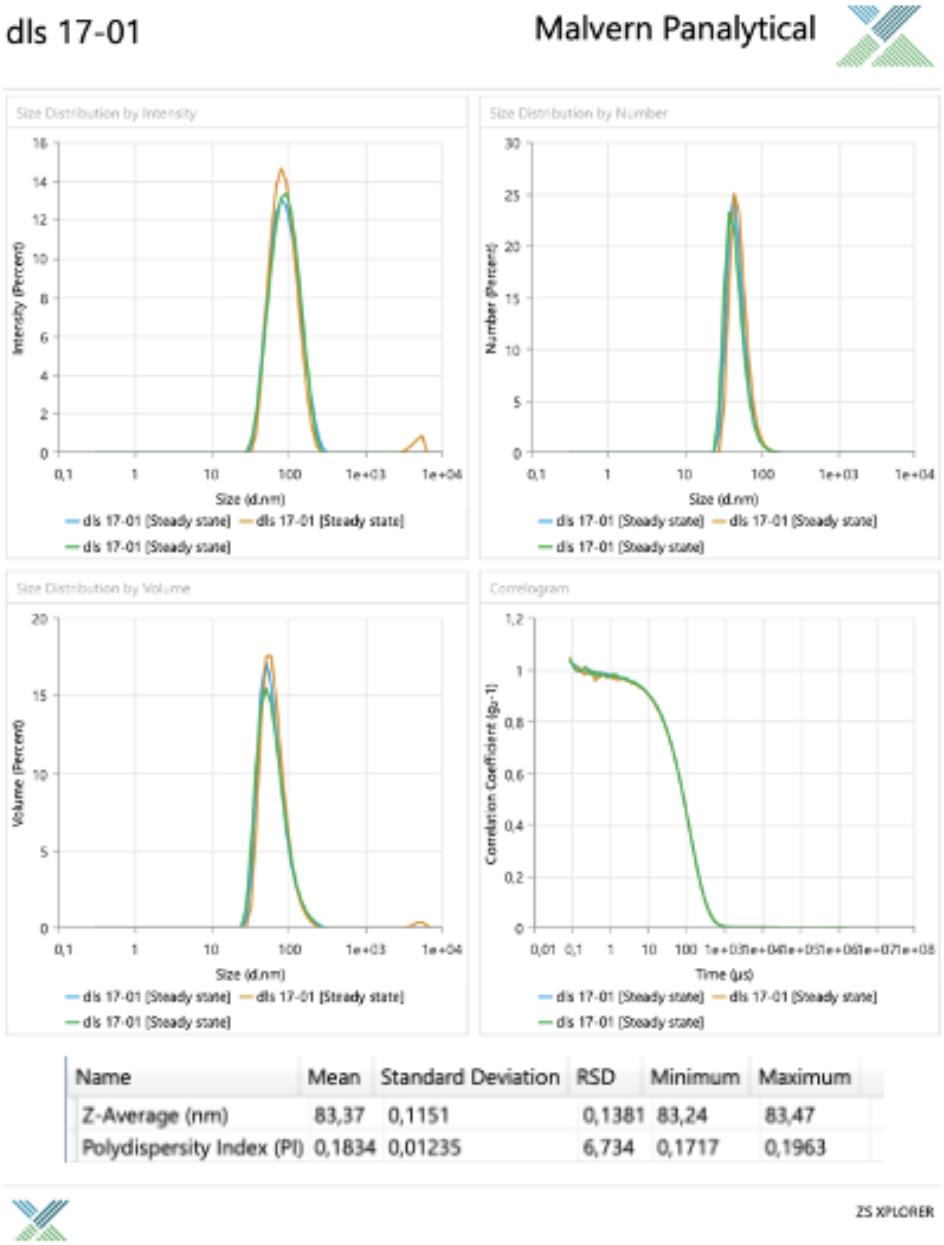

Name	Mean	Standard Deviation	RSD	Minimum	Maximum
Z-Average (nm)	83,37	0,1151	0,1381	83,24	83,47
Polydispersity Index (PI)	0,1834	0,01235	6,734	0,1717	0,1963

Figure B.5. 1-month DLS results of sample 17-1, belongs to the data set of Dual 2

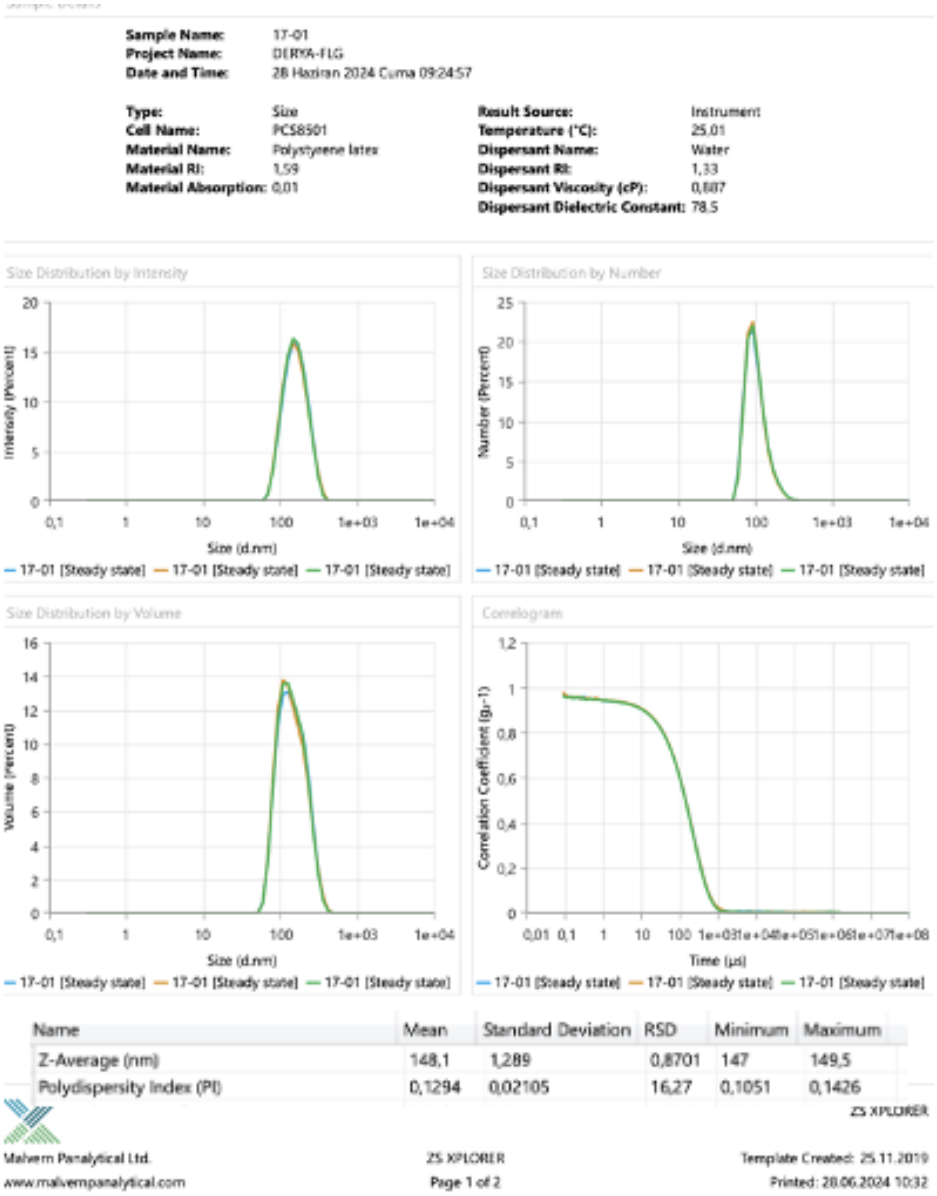

Figure B.6. 6-month DLS results of sample 17-1, belongs to the data set of Dual 2

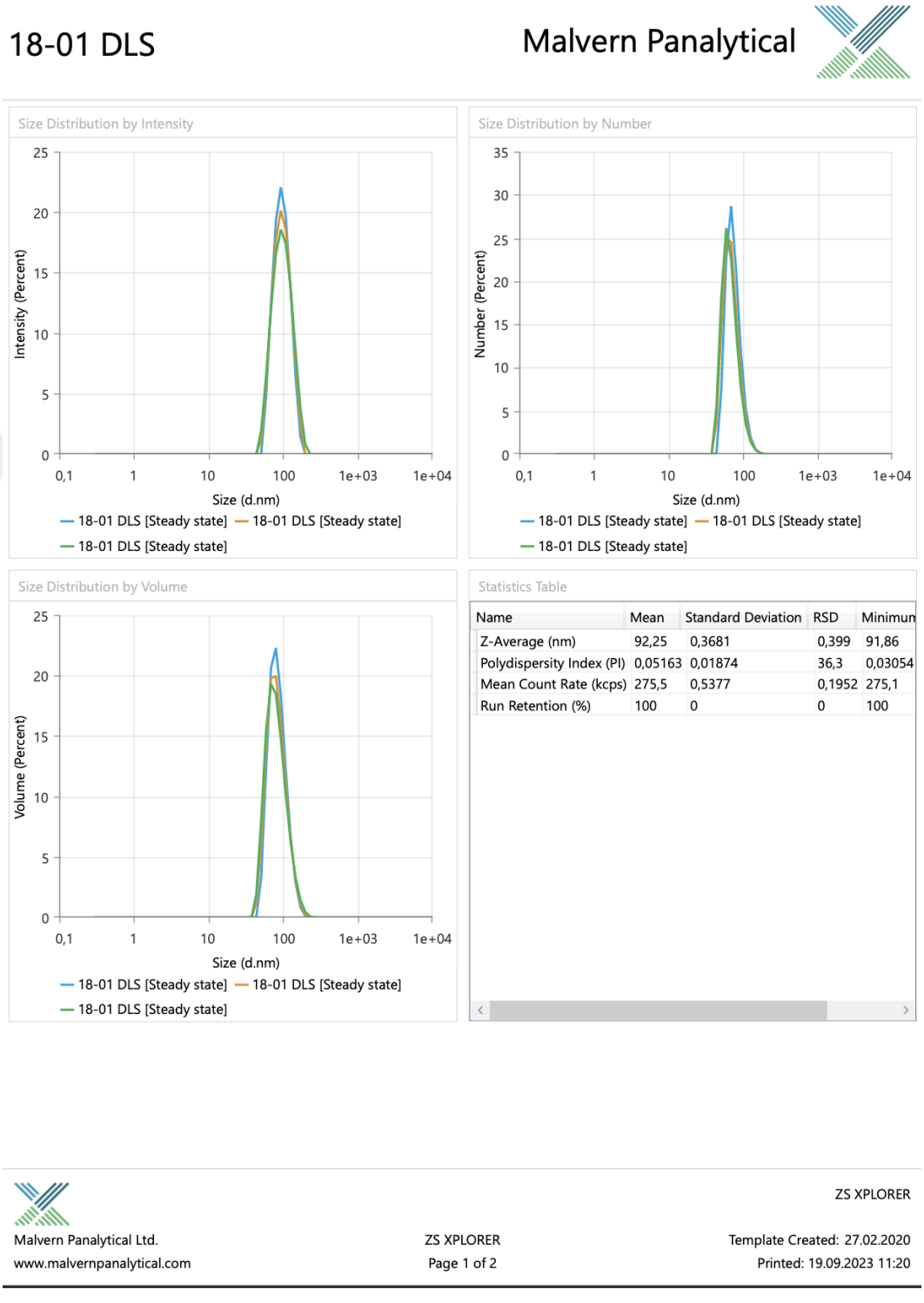

Figure B.7. DLS results of sample 18-1, belongs to the data set of Dual 3

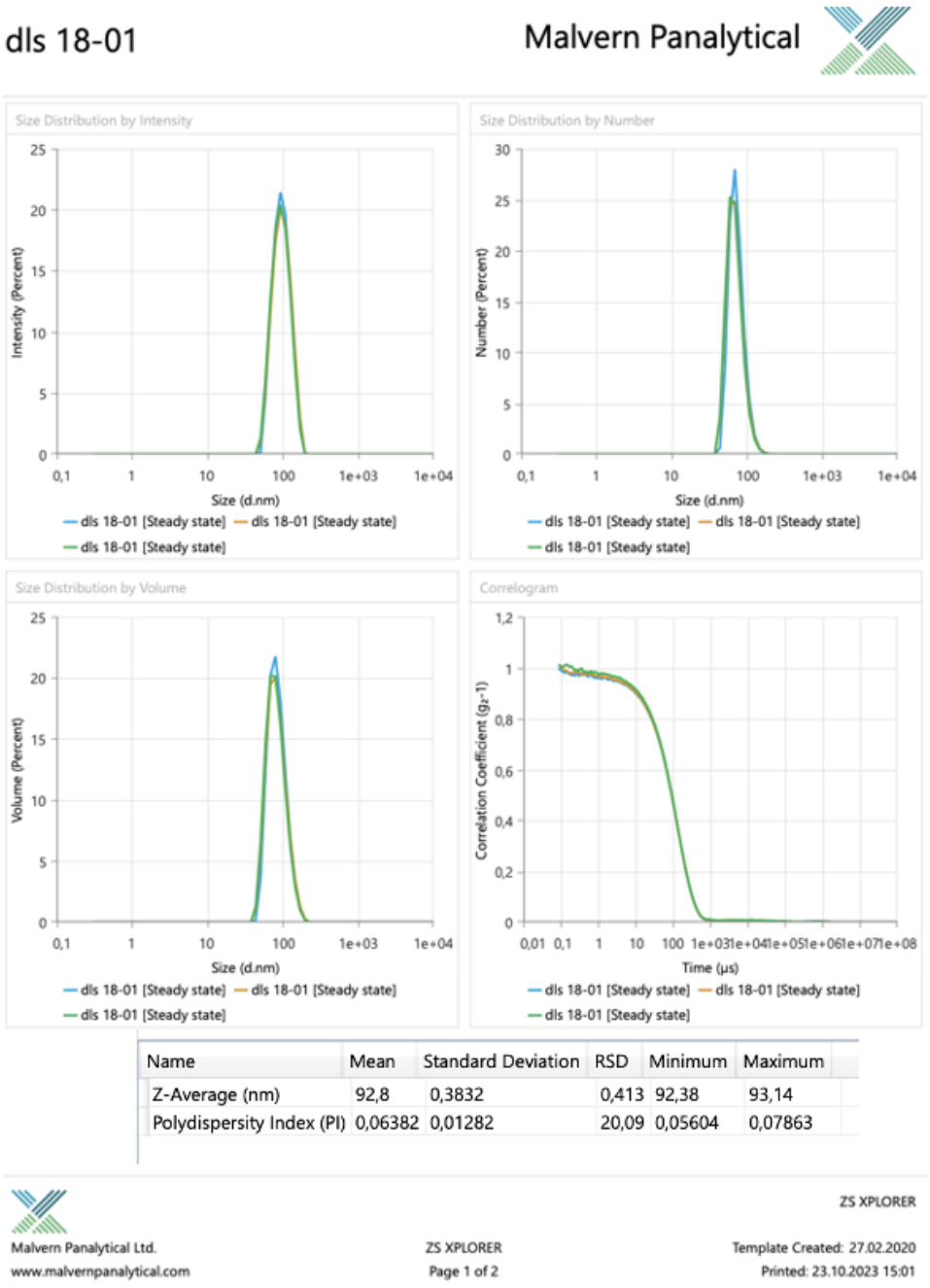

Figure B.8. 1-month DLS results of sample 18-1, belongs to the data set of Dual 3

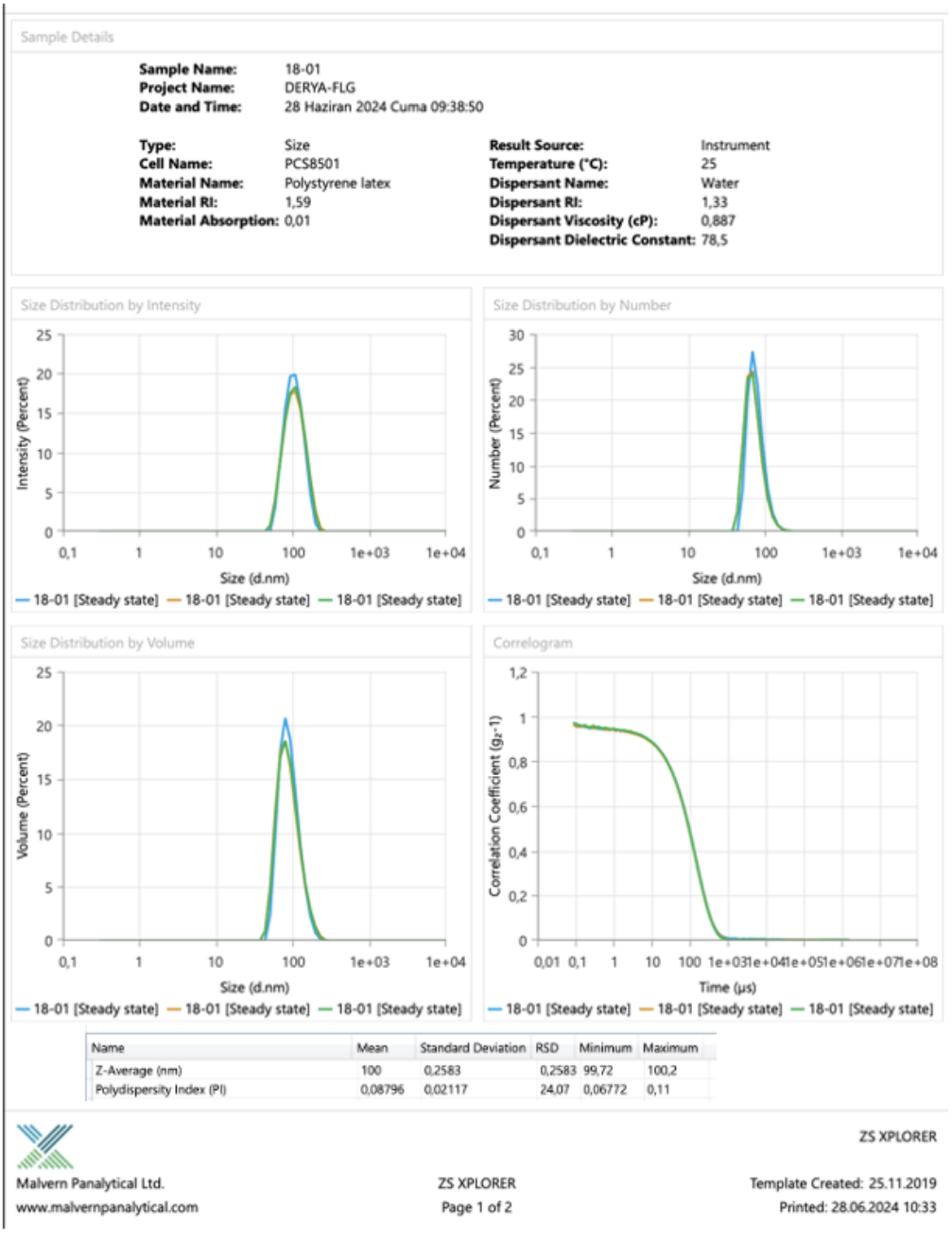

Figure B.9. 6-month DLS results of sample 18-1, belongs to the data set of Dual 3

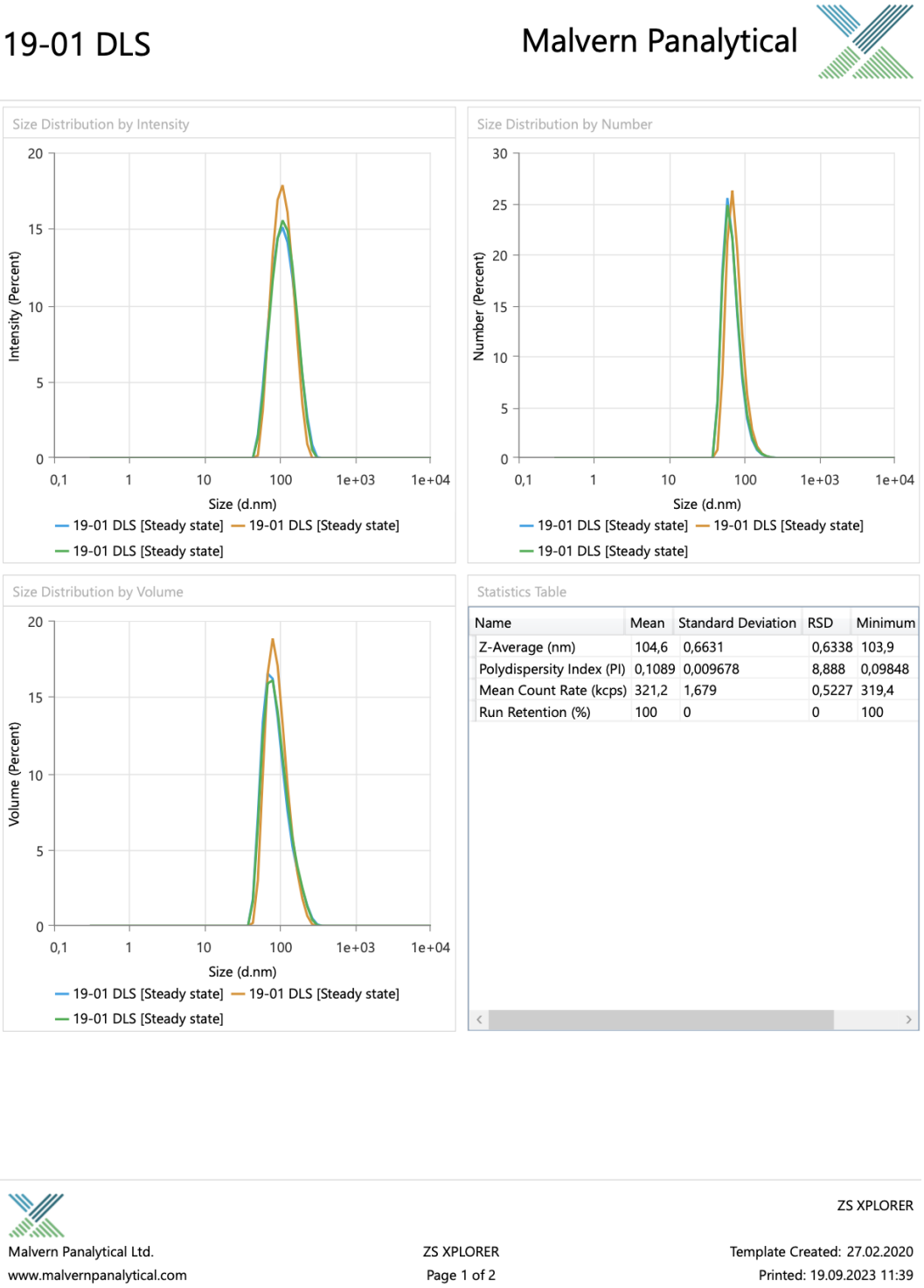

Figure B.10. DLS results of sample 19-1, belongs to the data set of Dual 4

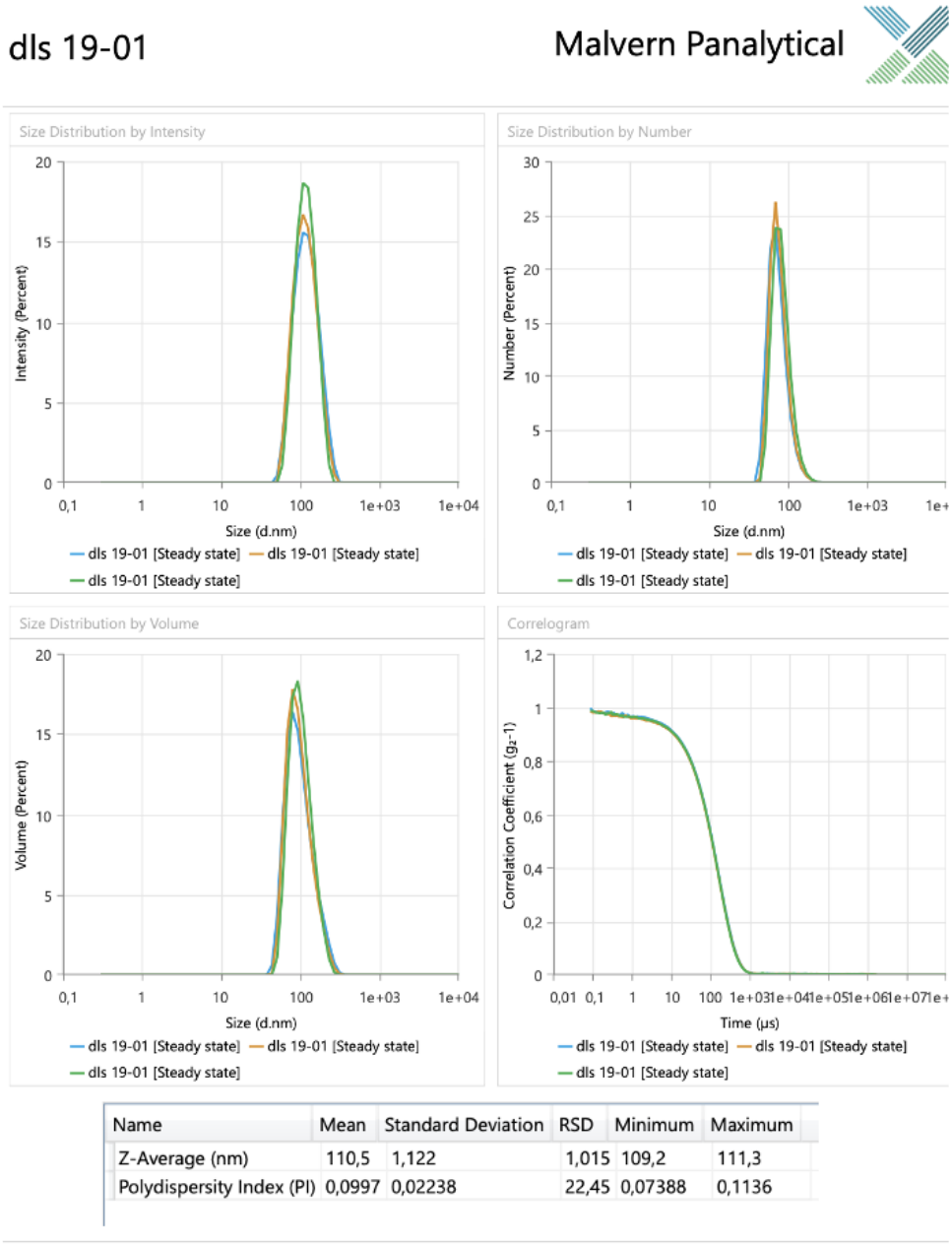

Name	Mean	Standard Deviation	RSD	Minimum	Maximum
Z-Average (nm)	110,5	1,122	1,015	109,2	111,3
Polydispersity Index (PI)	0,0997	0,02238	22,45	0,07388	0,1136

Figure B.11. 1-month DLS results of sample 19-1, belongs to the data set of Dual 4

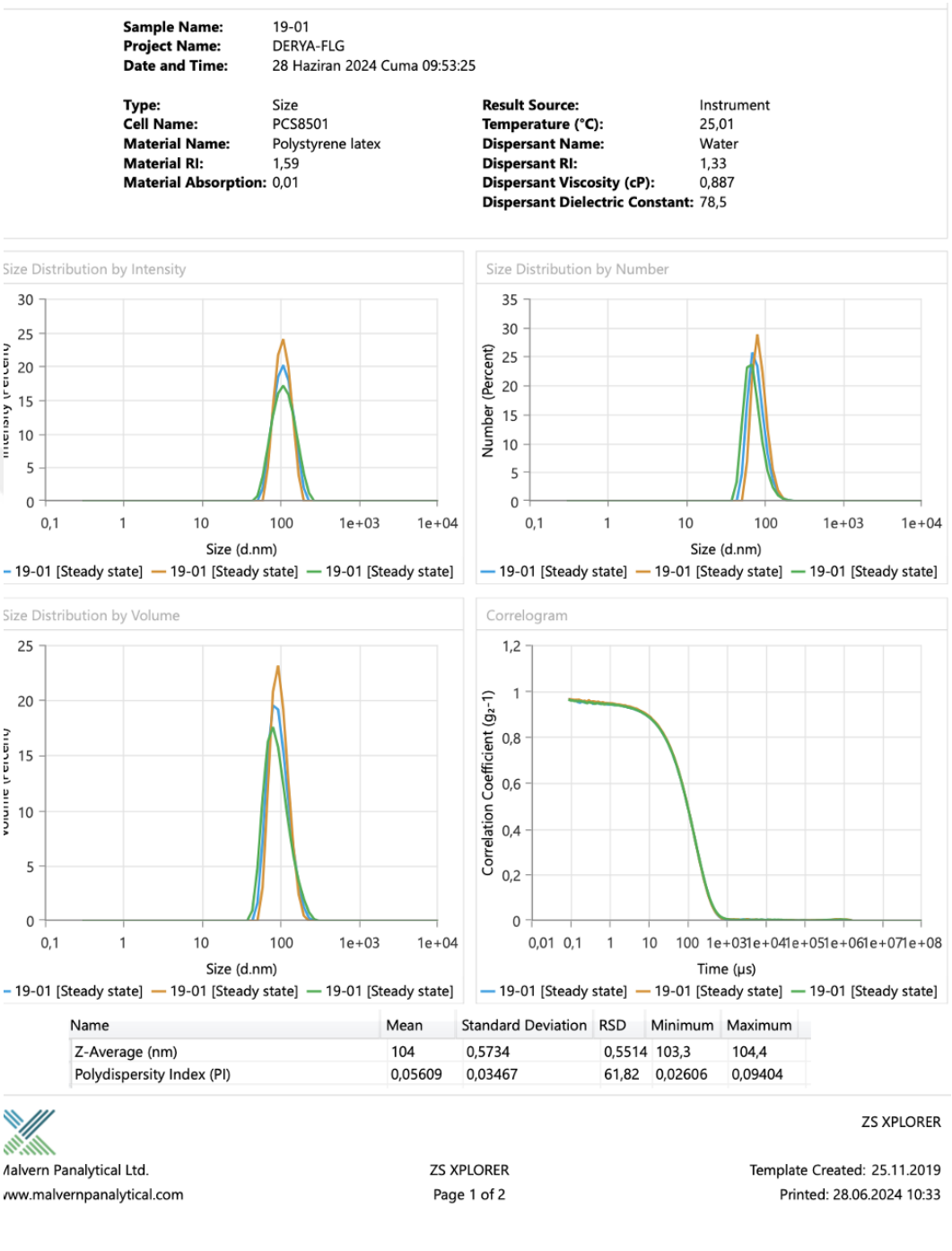

Figure B.12. 6-month DLS results of sample 19-1, belongs to the data set of Dual 4

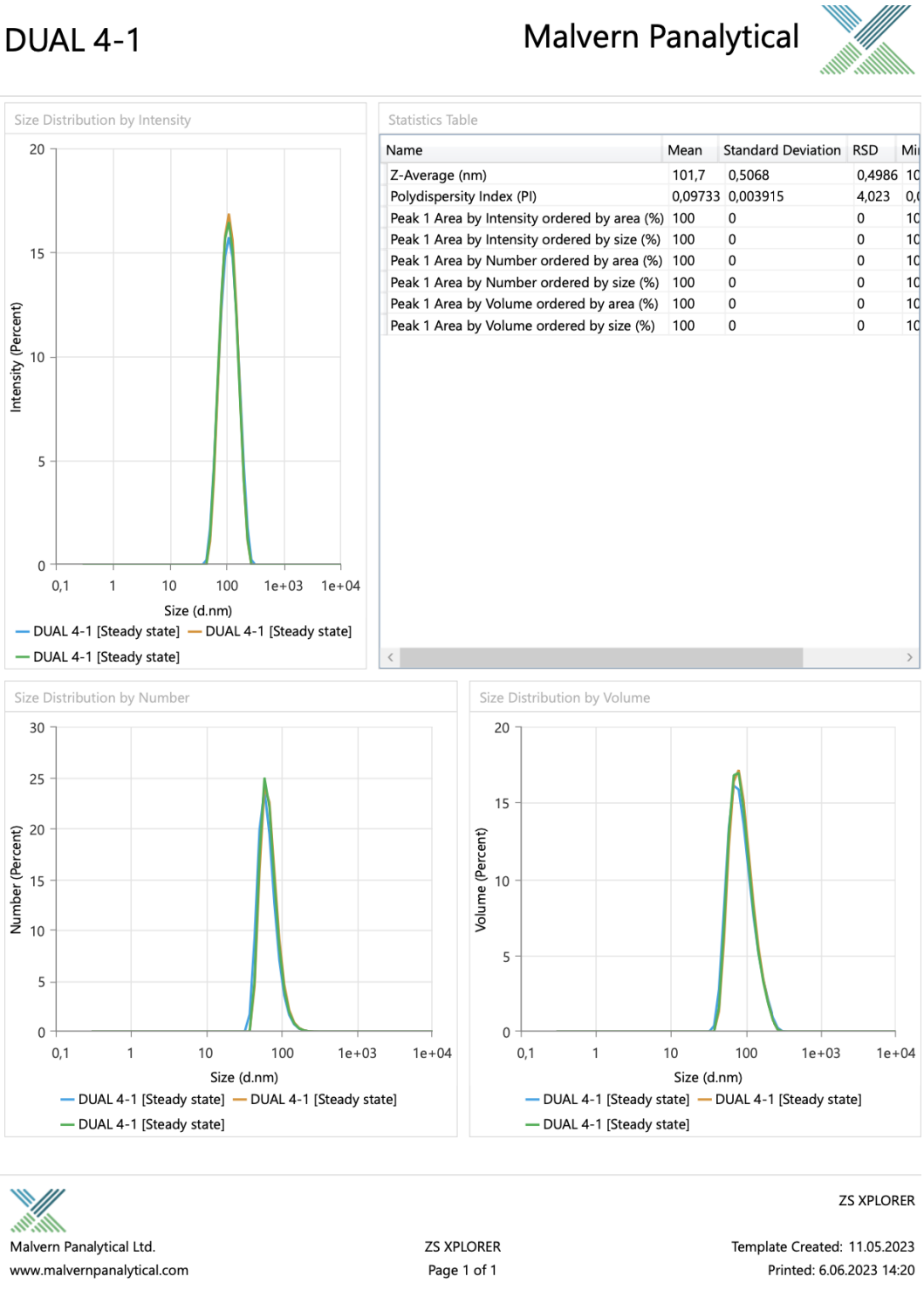

Figure B.13. DLS results of sample 4-1, belongs to the data set of Dual 5

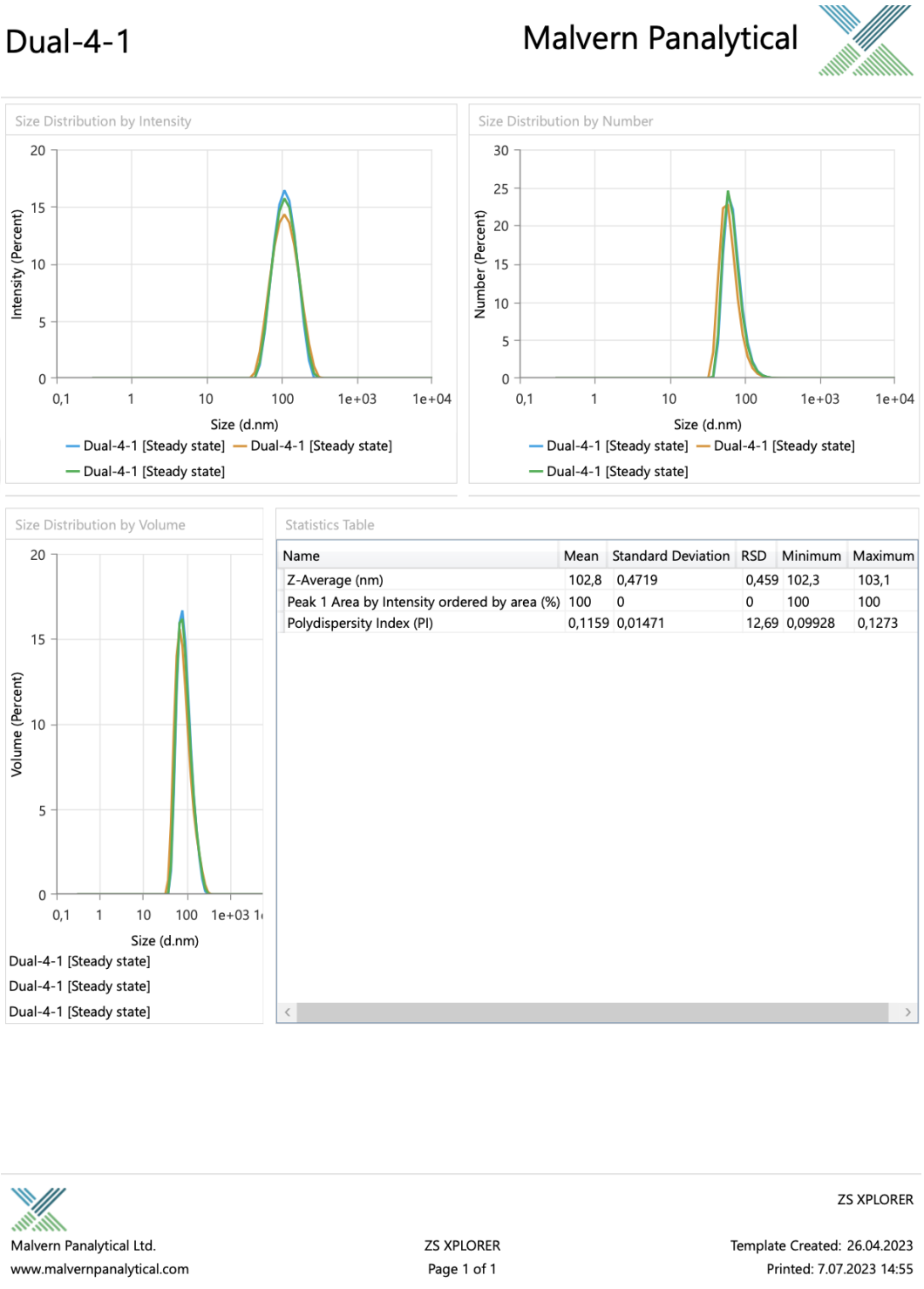

Figure B.14. 1-month DLS results of sample 4-1, belongs to the data set of Dual 5

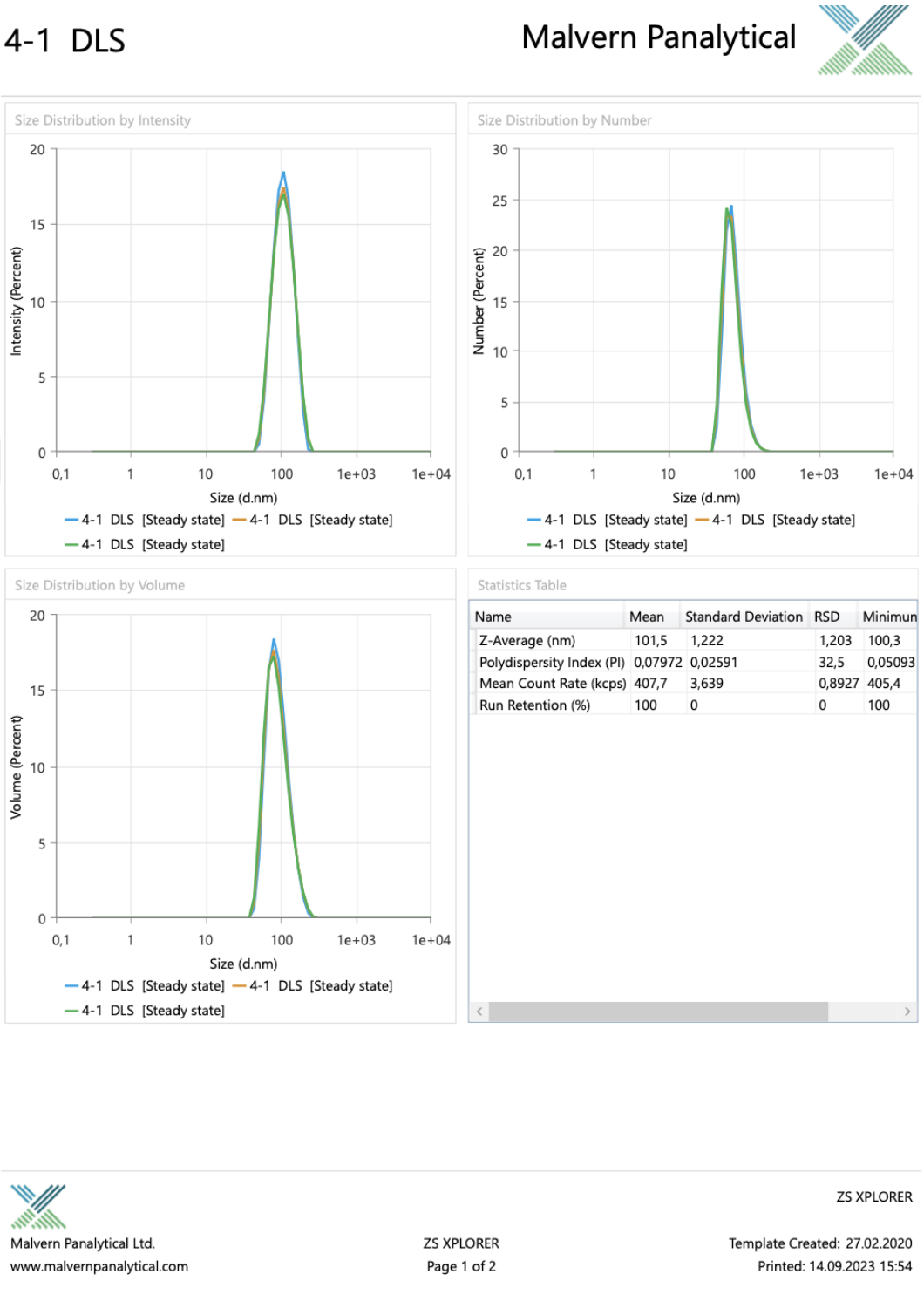

Figure B.15. 3-month DLS results of sample 4-1, belongs to the data set of Dual 5

17-02 DLS

Malvern Panalytical

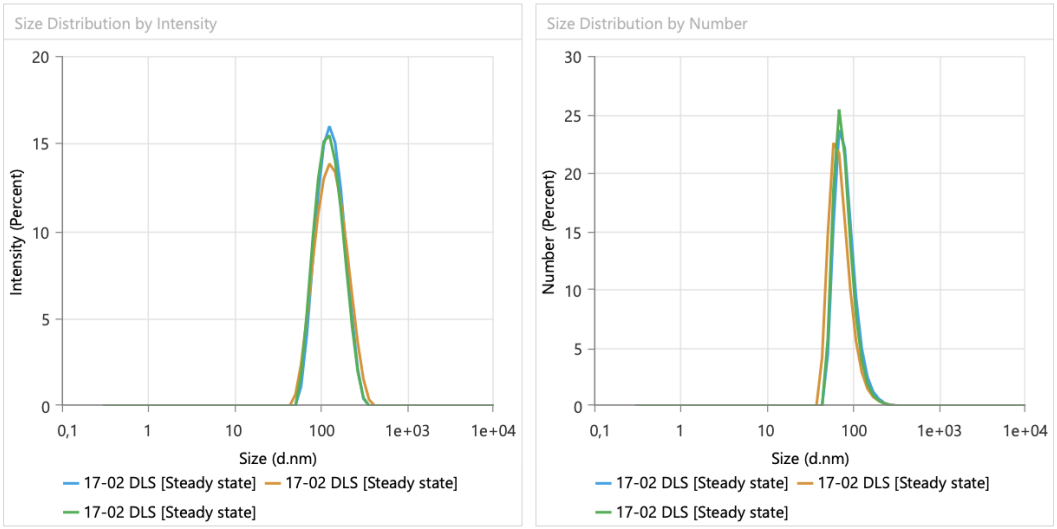

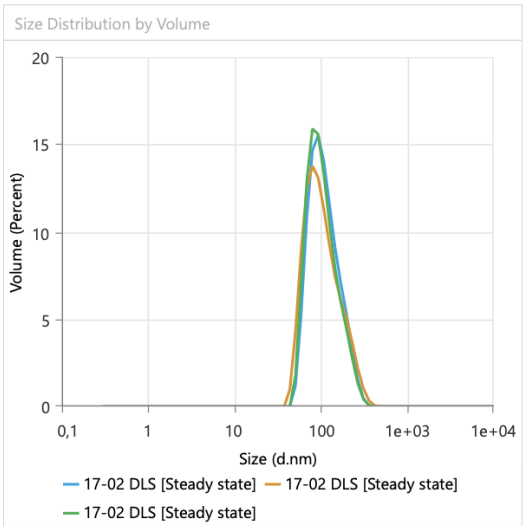

Statistics Table

Name	Mean	Standard Deviation	RSD	Minimum
Z-Average (nm)	120,5	1,049	0,8706	119,3
Polydispersity Index (PI)	0,1256	0,02173	17,3	0,1007
Mean Count Rate (kcps)	255,7	0,999	0,3908	255
Run Retention (%)	100	0	0	100

Figure B.16. DLS results of sample 17-2, belongs to the data set of Dual 6

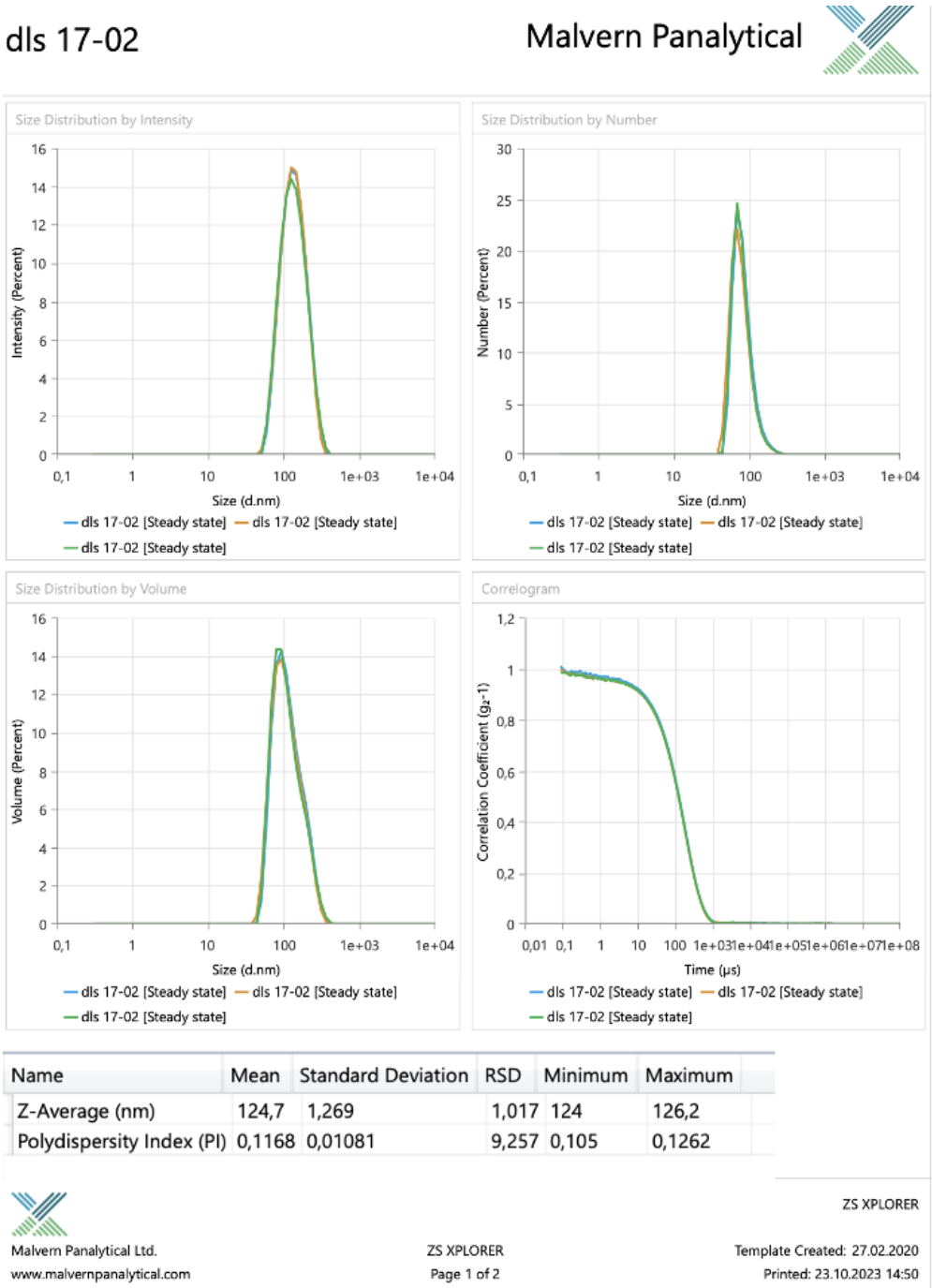

Figure B.17. 1-month DLS results of sample 17-2, belongs to the data set of Dual 6

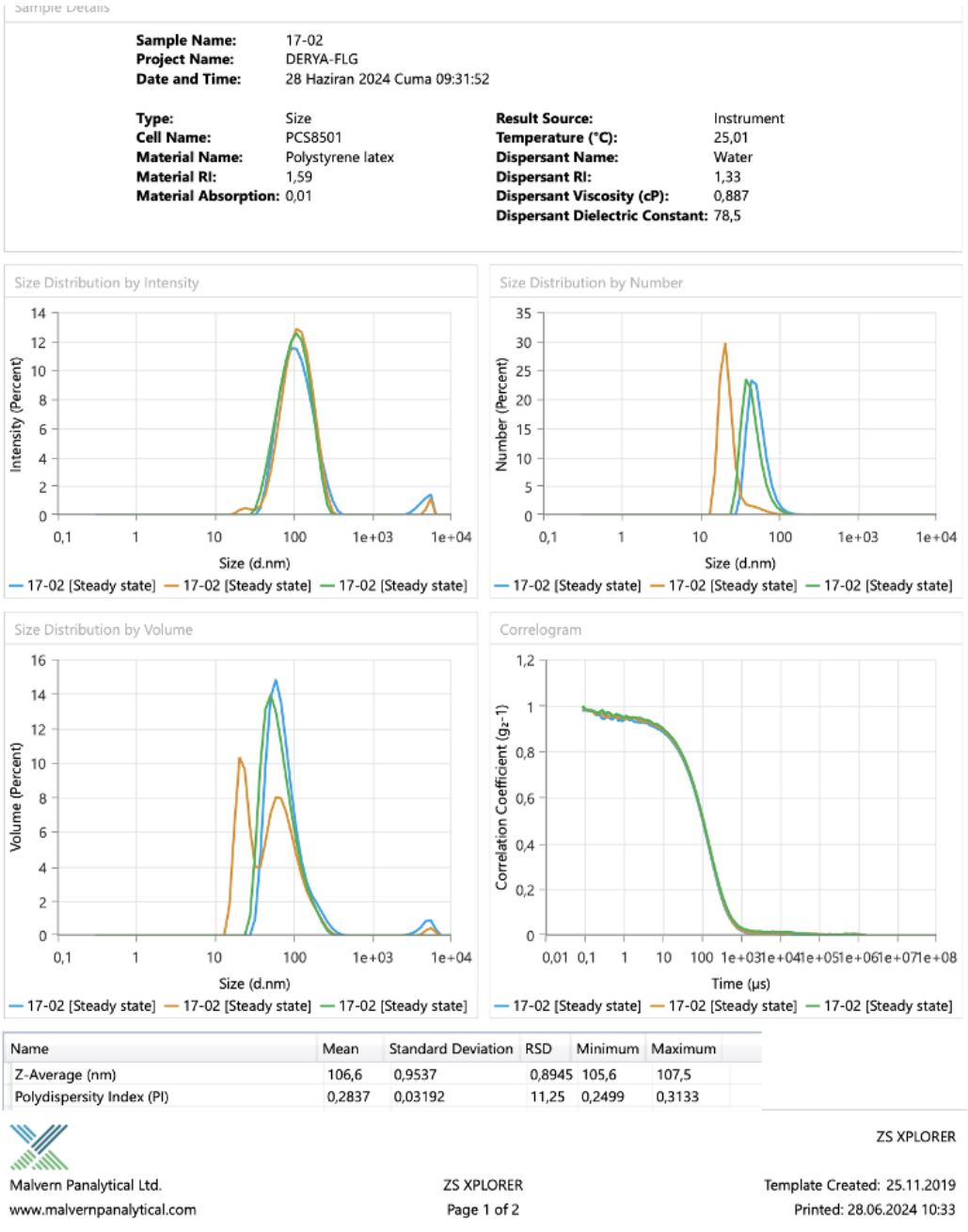

Figure B.18. 6-month DLS results of sample 17-2, belongs to the data set of Dual 6

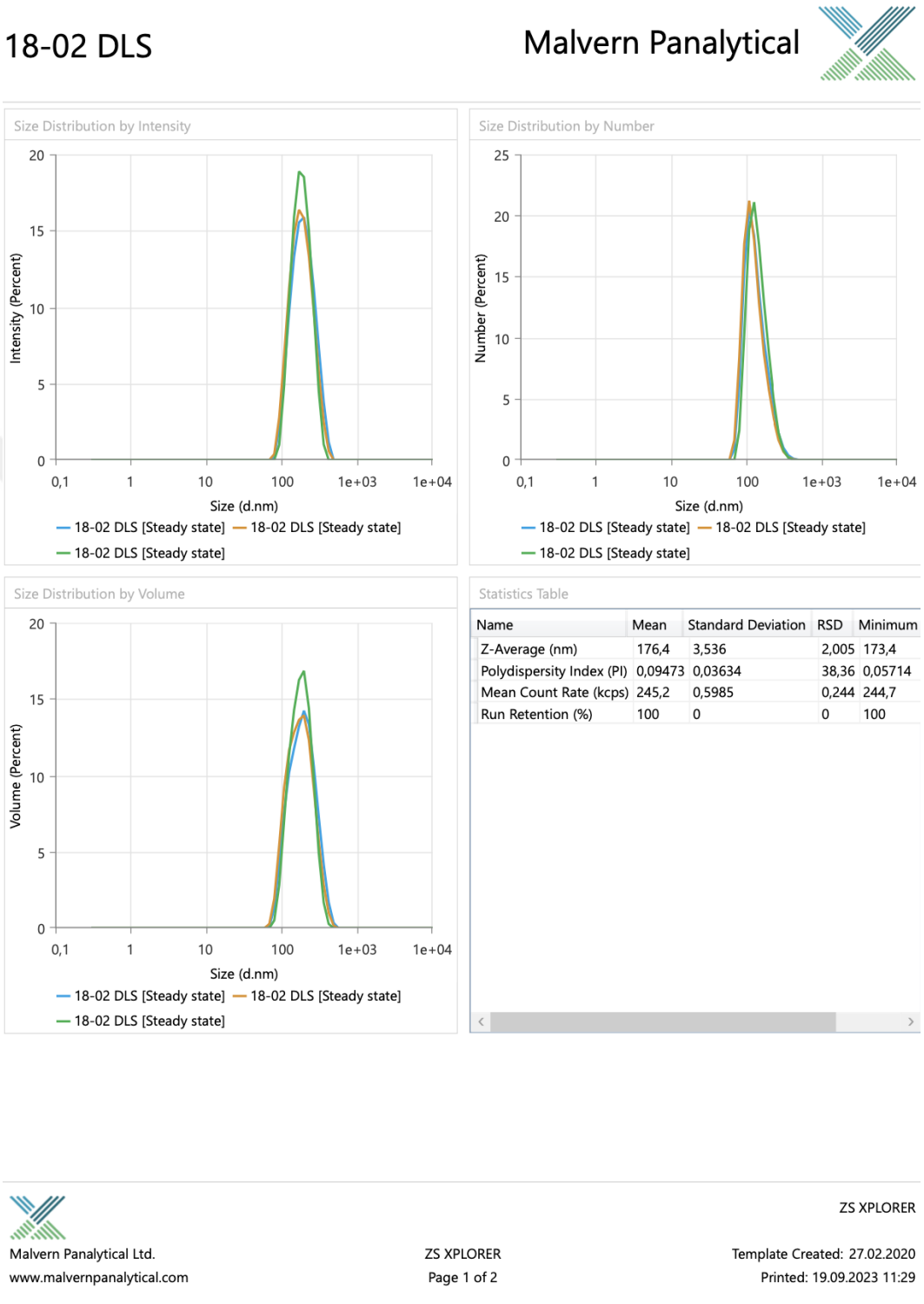

Figure B.19. DLS results of sample 18-2, belongs to the data set of Dual 7

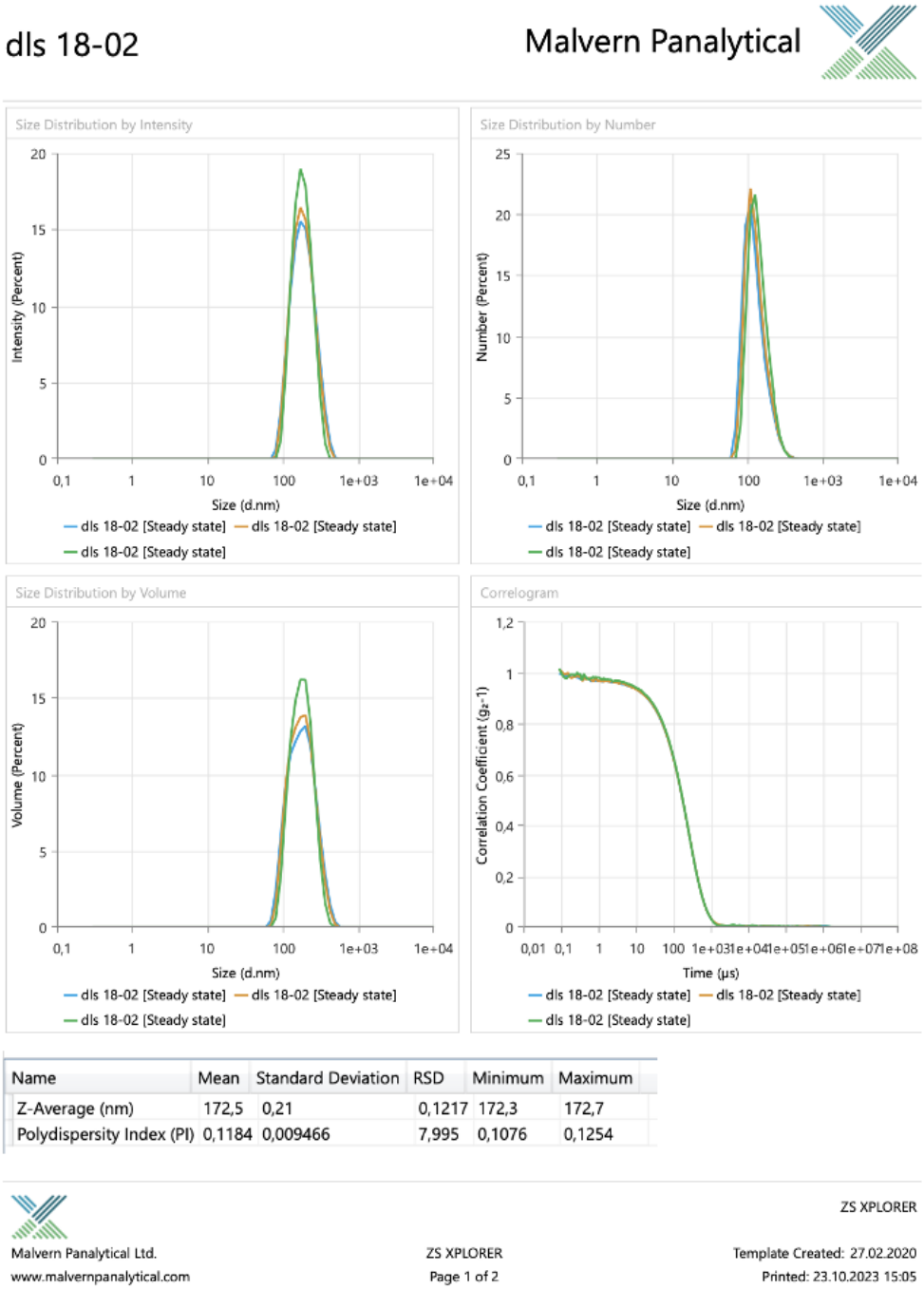

Name	Mean	Standard Deviation	RSD	Minimum	Maximum
Z-Average (nm)	172,5	0,21	0,1217	172,3	172,7
Polydispersity Index (PI)	0,1184	0,009466	7,995	0,1076	0,1254

Figure B.20. 1-month DLS results of sample 18-2, belongs to the data set of Dual 7

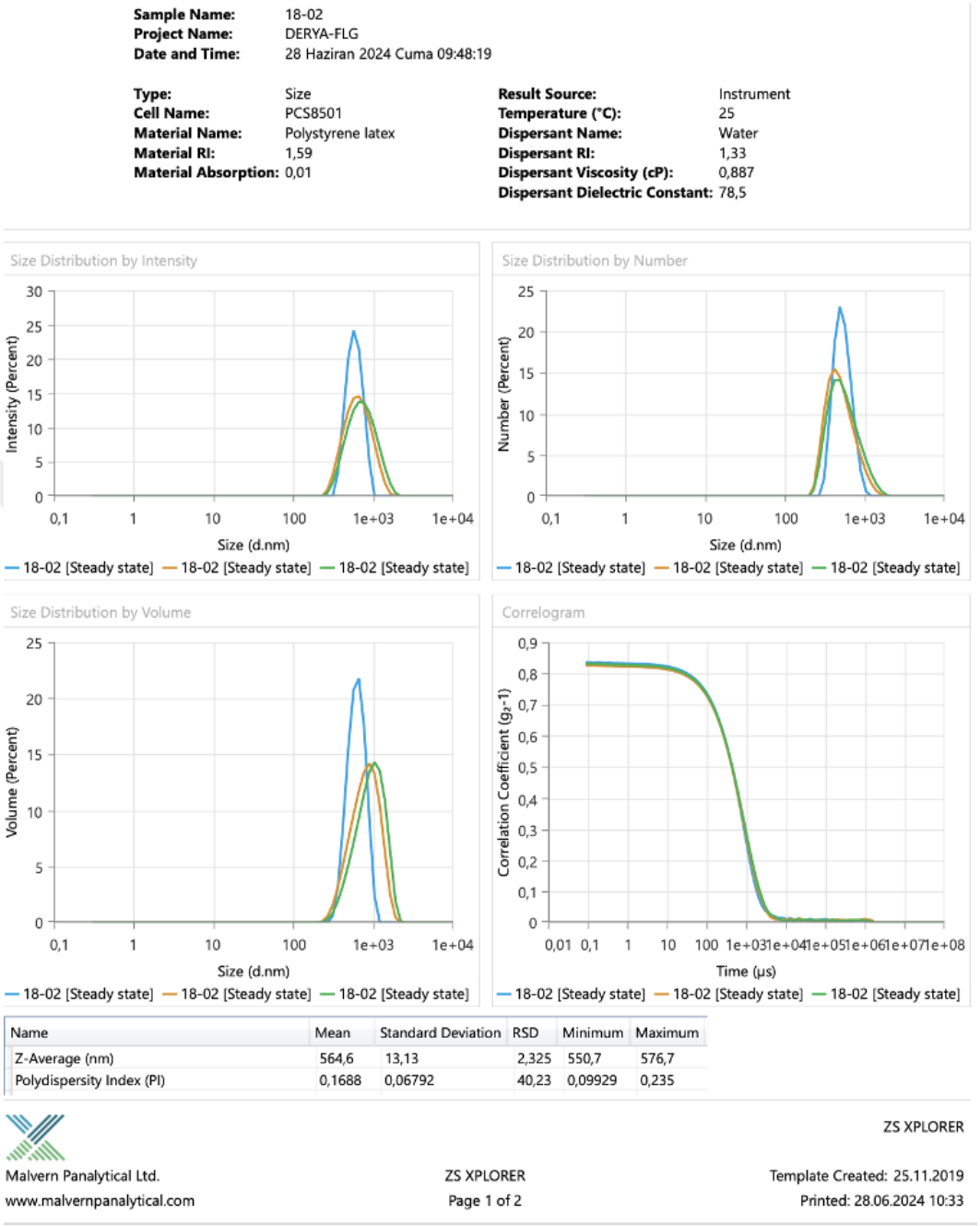

Figure B.21. 6-month DLS results of sample 18-2, belongs to the data set of Dual 7

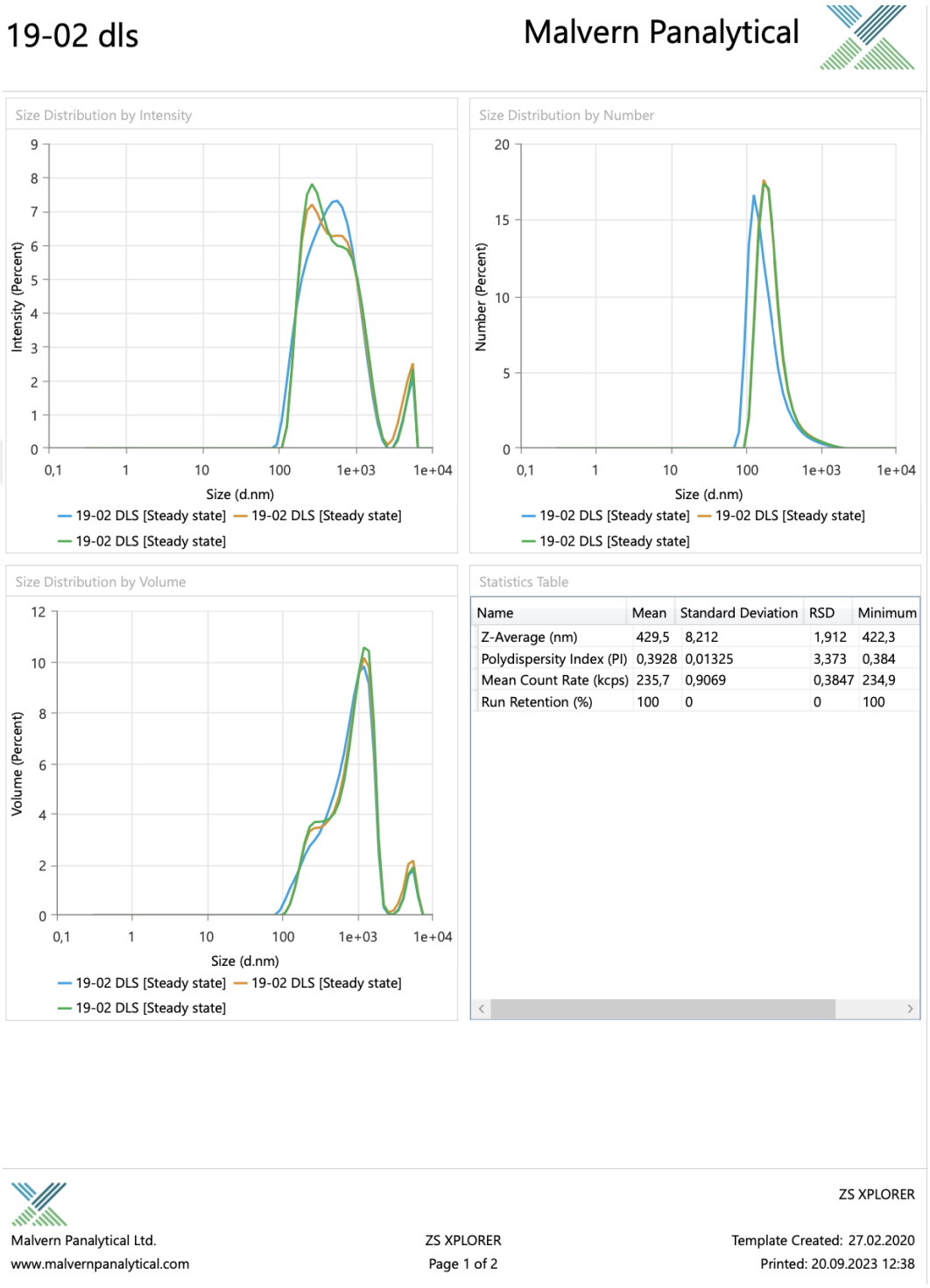

Figure B.22. DLS results of sample 19-2, belongs to the data set of Dual 8

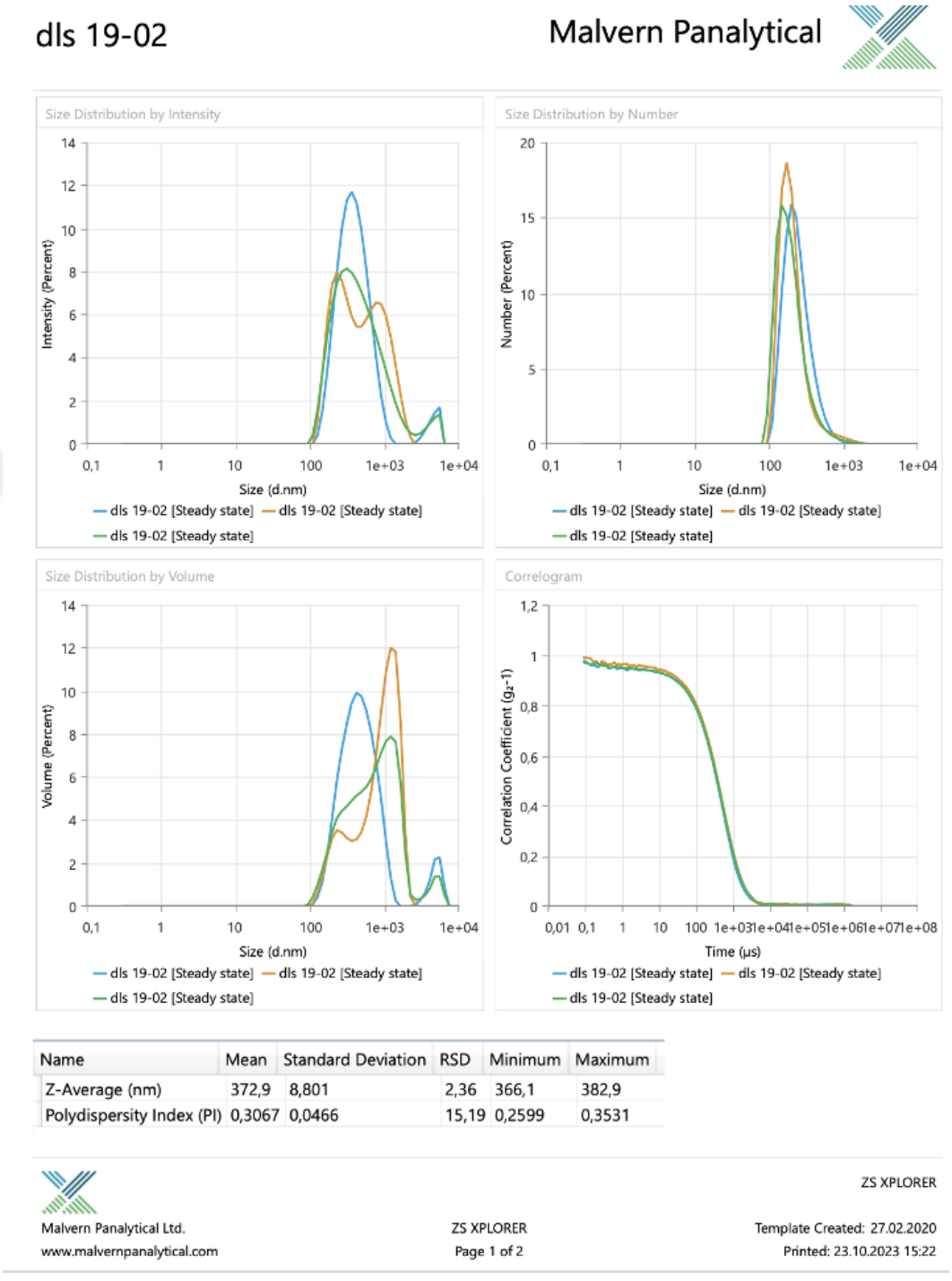

Figure B.23. 1-month DLS results of sample 19-2, belongs to the data set of Dual 8

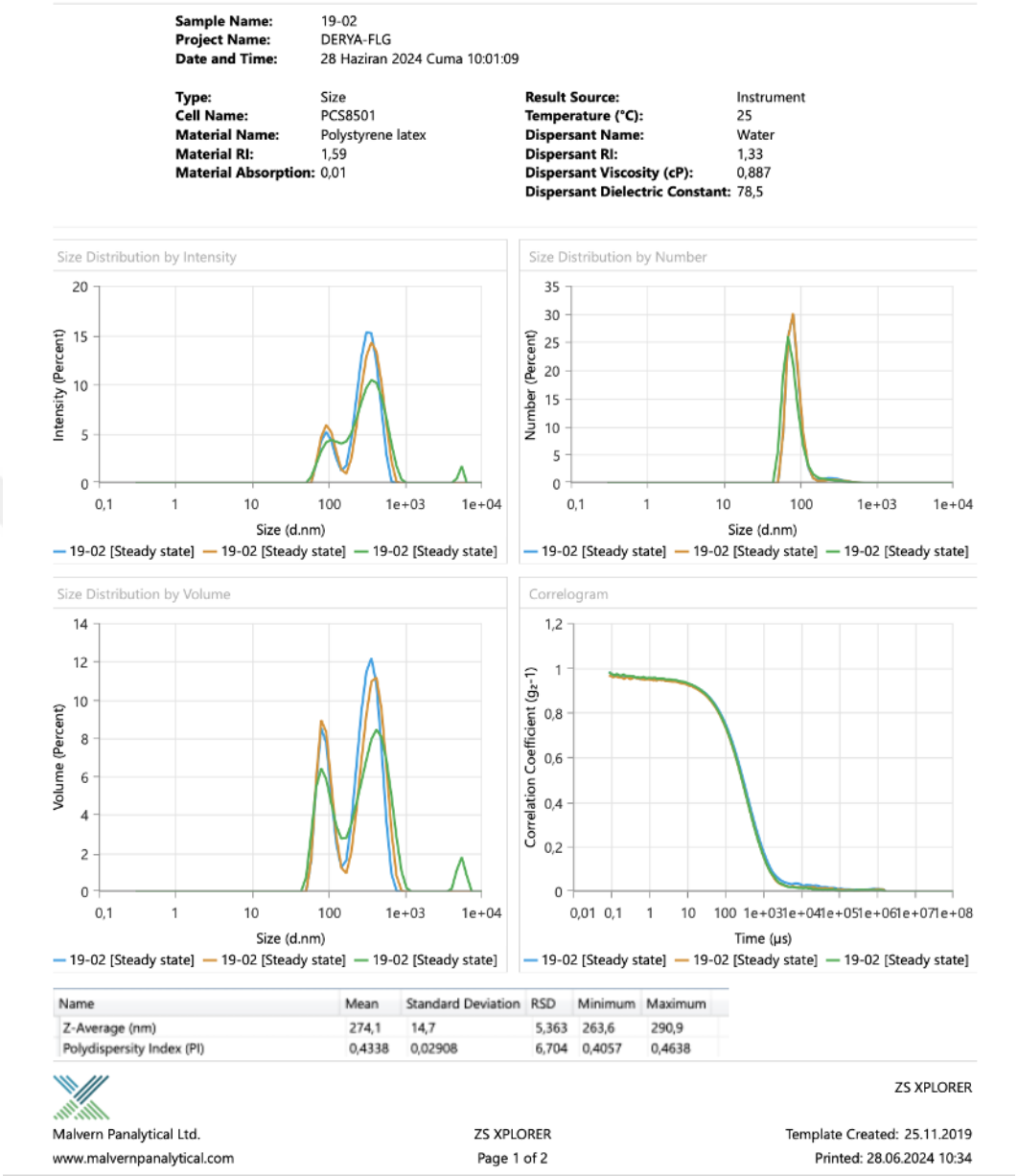

Figure B.24. 6-month DLS results of sample 19-2, belongs to the data set of Dual 8

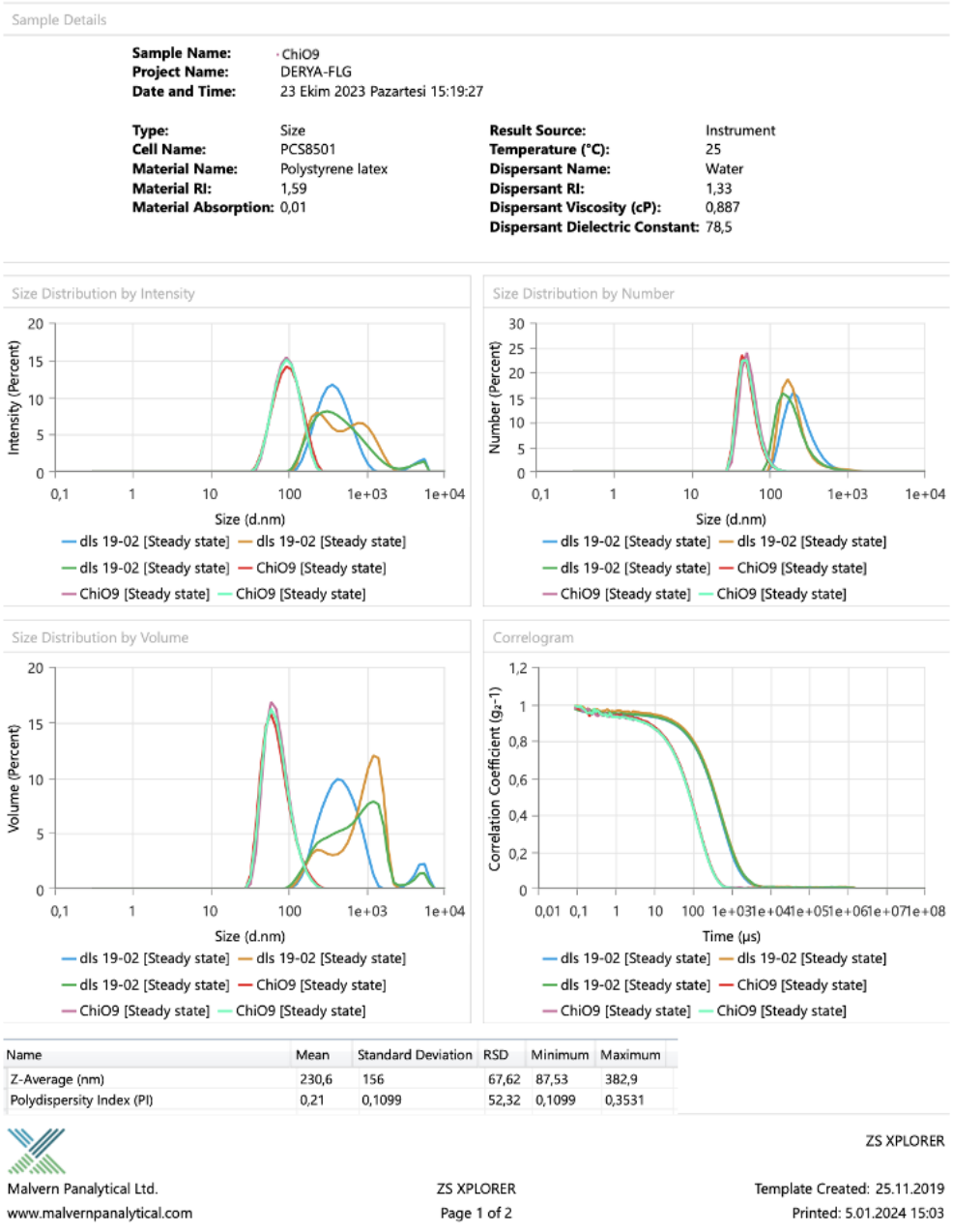

Figure B.25. DLS results of sample CHIT9, belongs to the data set of CHIT1

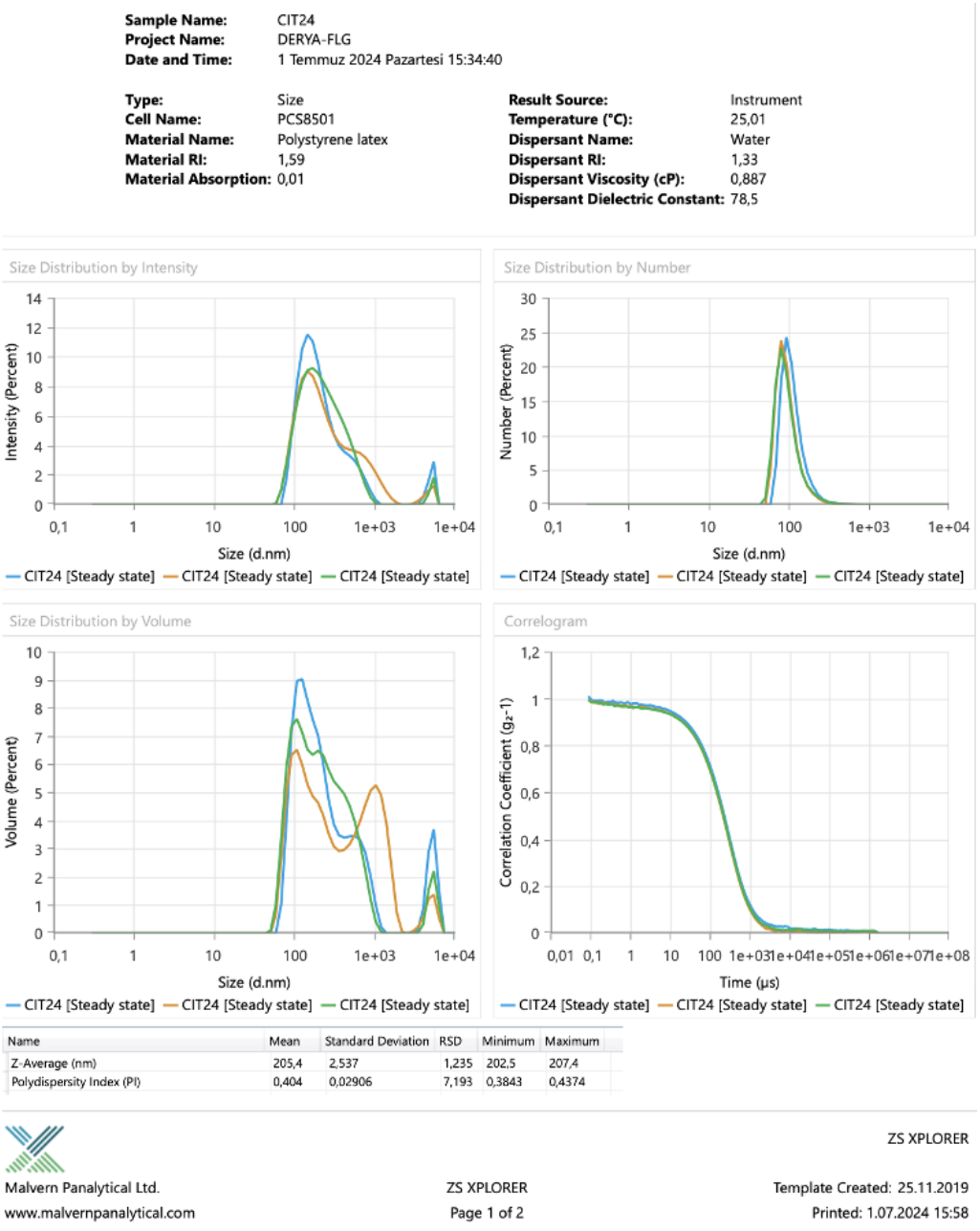

Figure B.26. 1-month DLS results of sample CHIT24, belongs to the data set of CHIT2

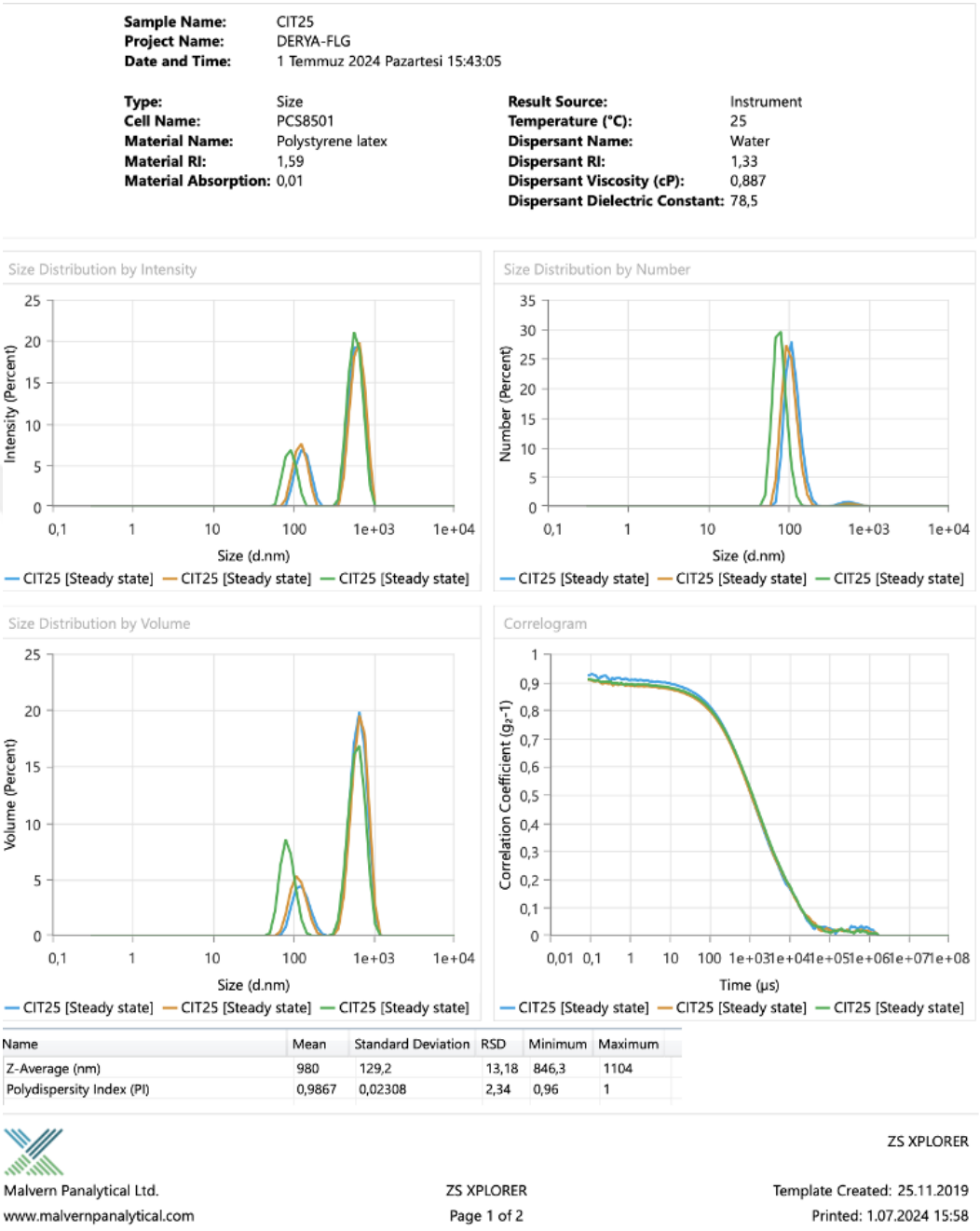

Figure B.27. 1-month DLS results of sample CHIT25, belongs to the data set of CHIT3

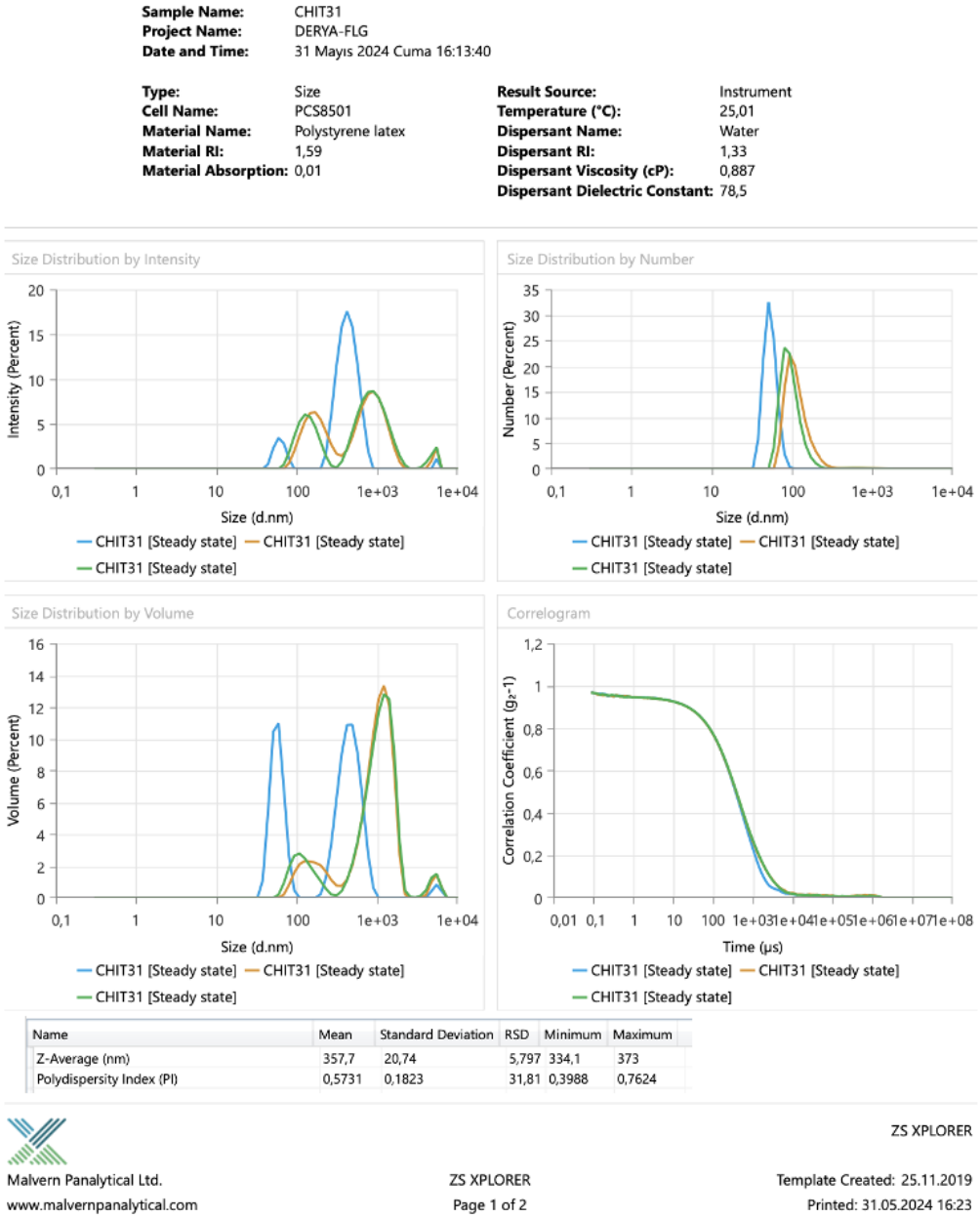

Figure B.28. DLS results of sample CHIT31, belongs to the data set of CHIT4

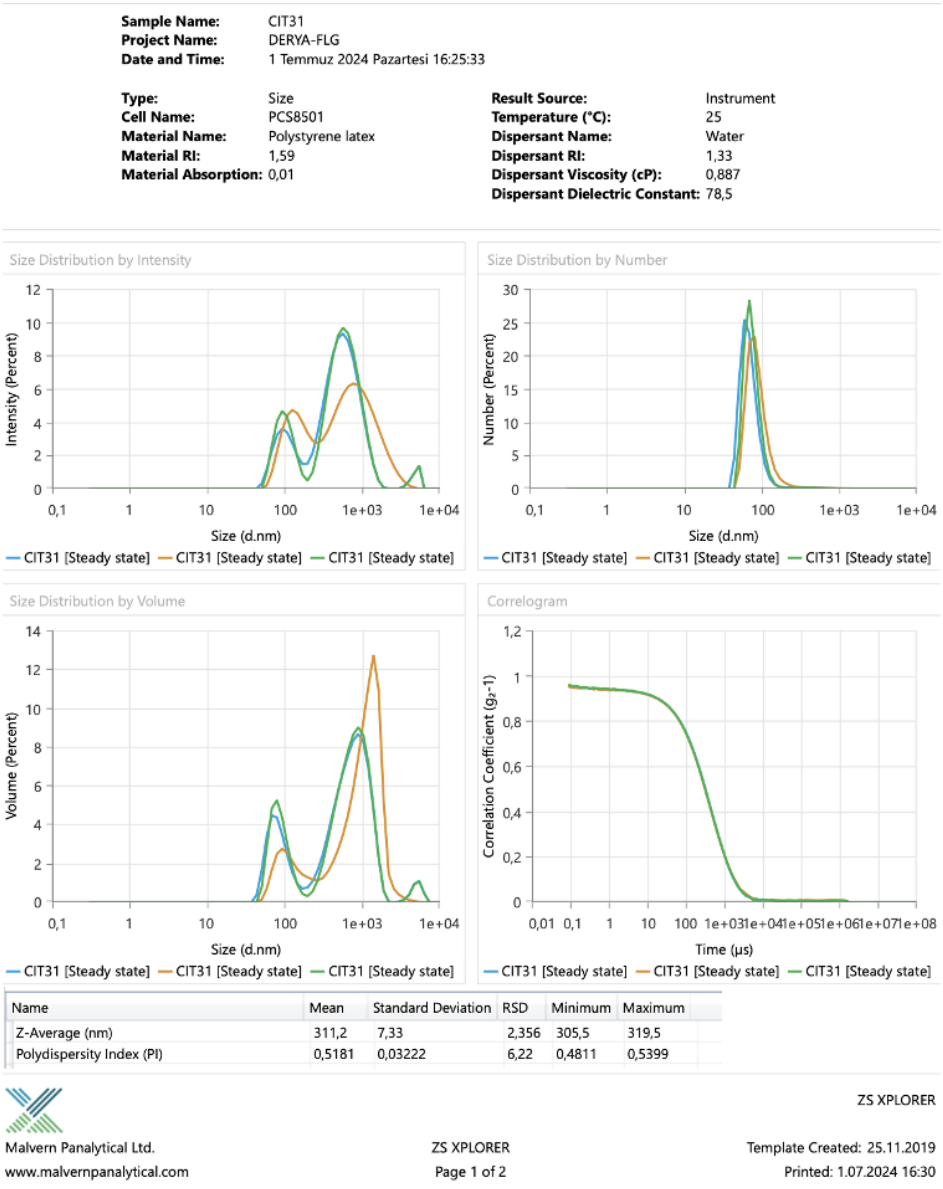

Figure B.29. 1-month DLS results of sample CHIT31, belongs to the data set of CHIT4

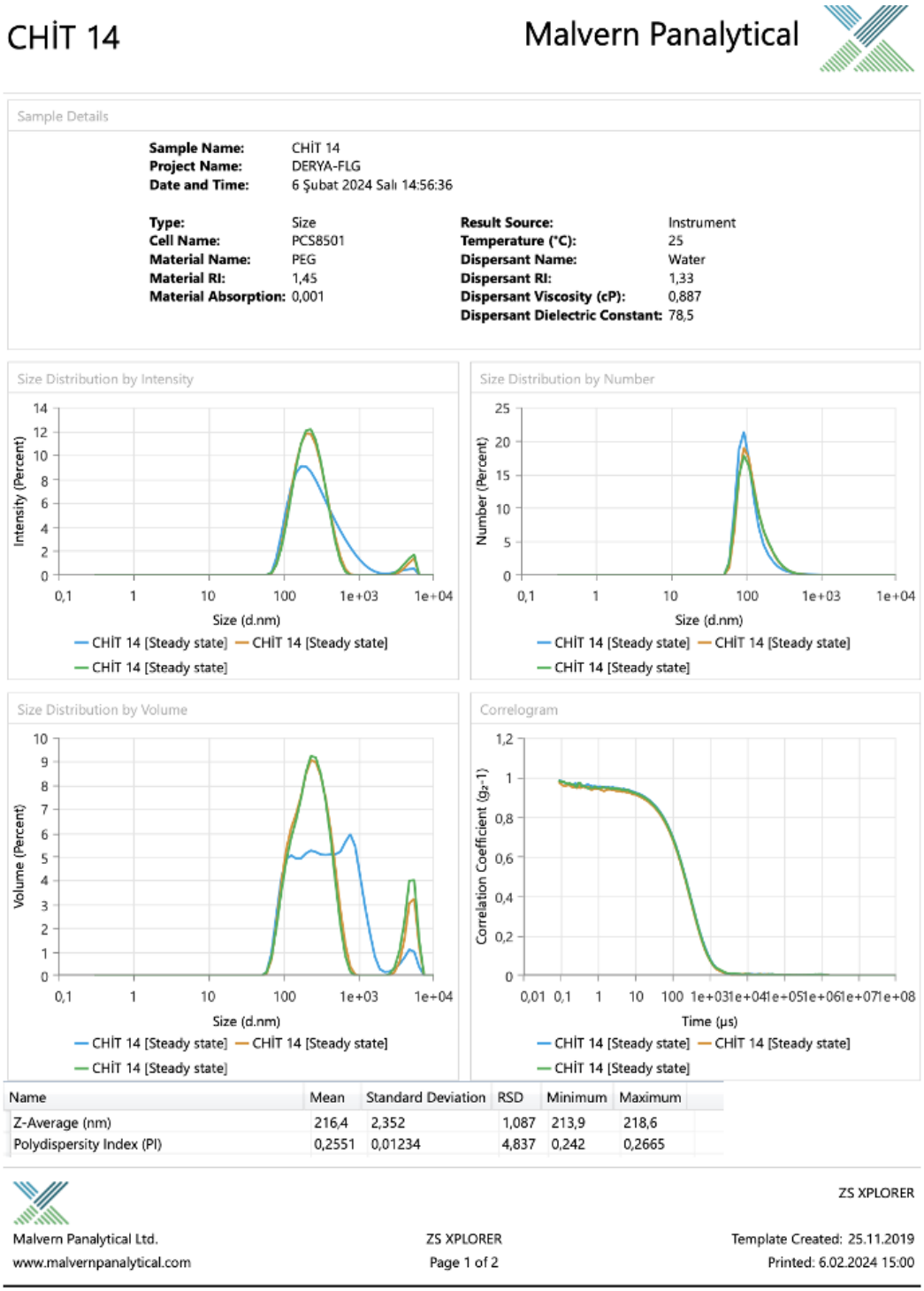

Figure B.30. DLS results of sample CHIT14, belongs to the data set of CHIT5

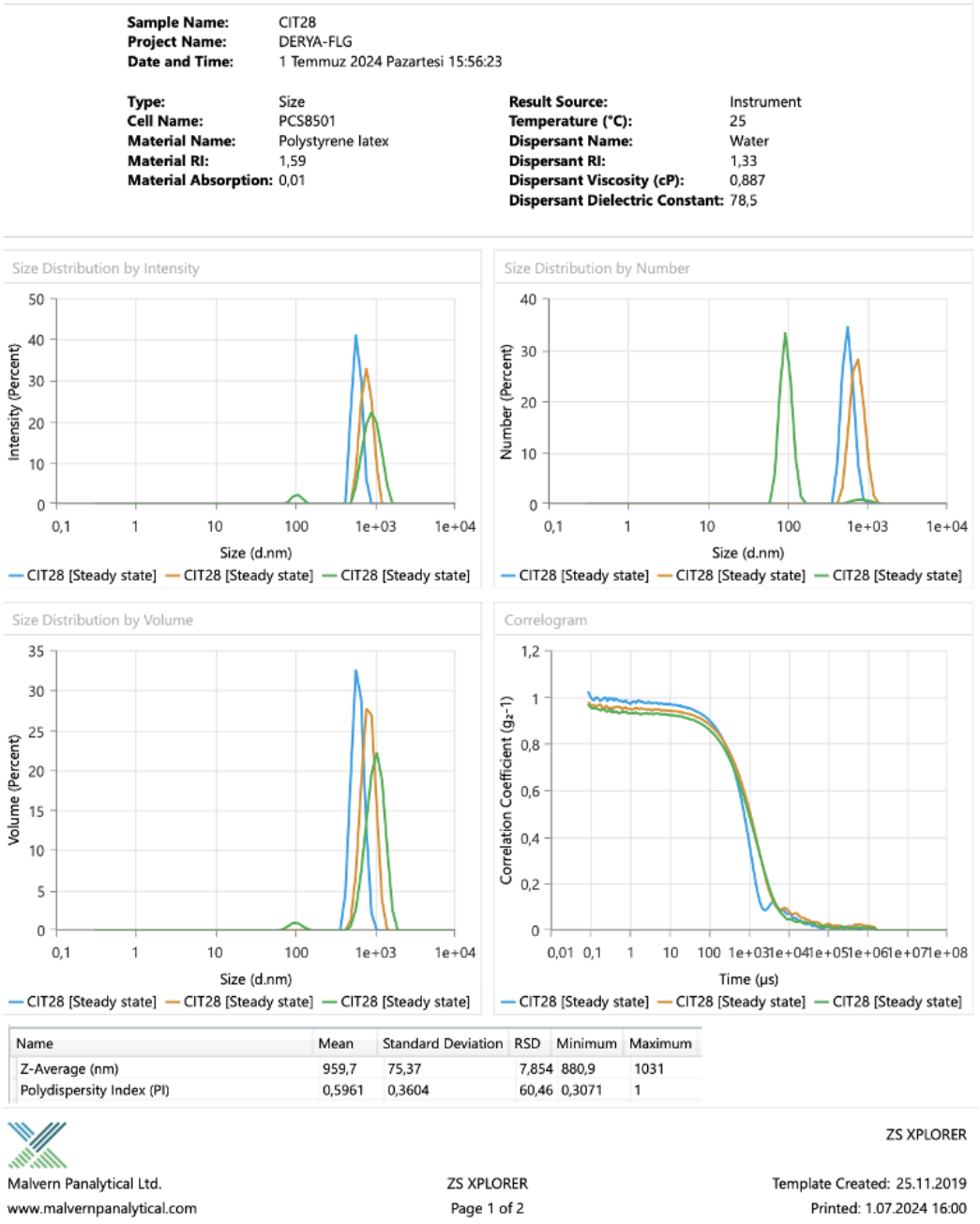

Figure B.31. 1-month DLS results of sample CHIT28, belongs to the data set of CHIT6

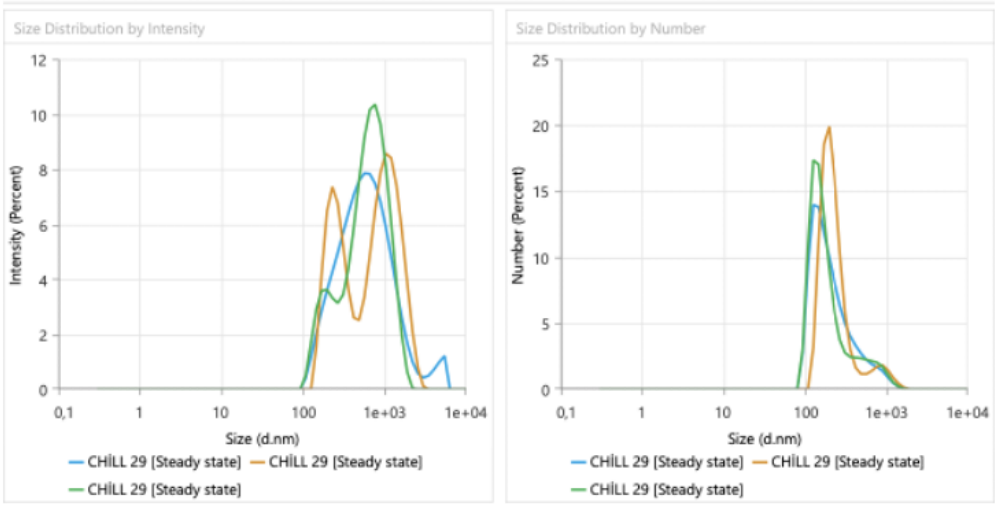

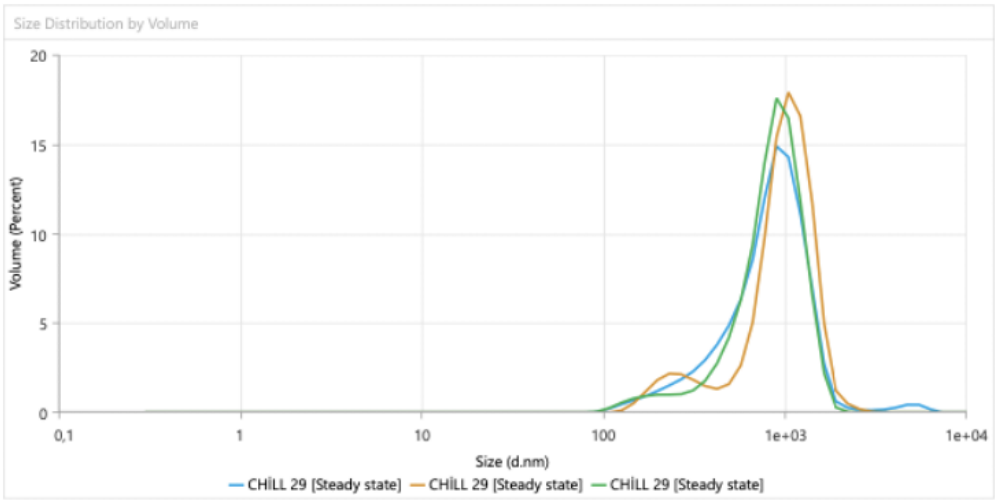

Name	Mean	Standard Deviation	RSD	Minimum	Maximum
Z-Average (nm)	475,1	6,646	1,399	470,8	482,7
Polydispersity Index (PI)	0,3547	0,05017	14,14	0,2968	0,3853

Figure B.32. DLS results of sample CHIT29, belongs to the data set of CHIT7

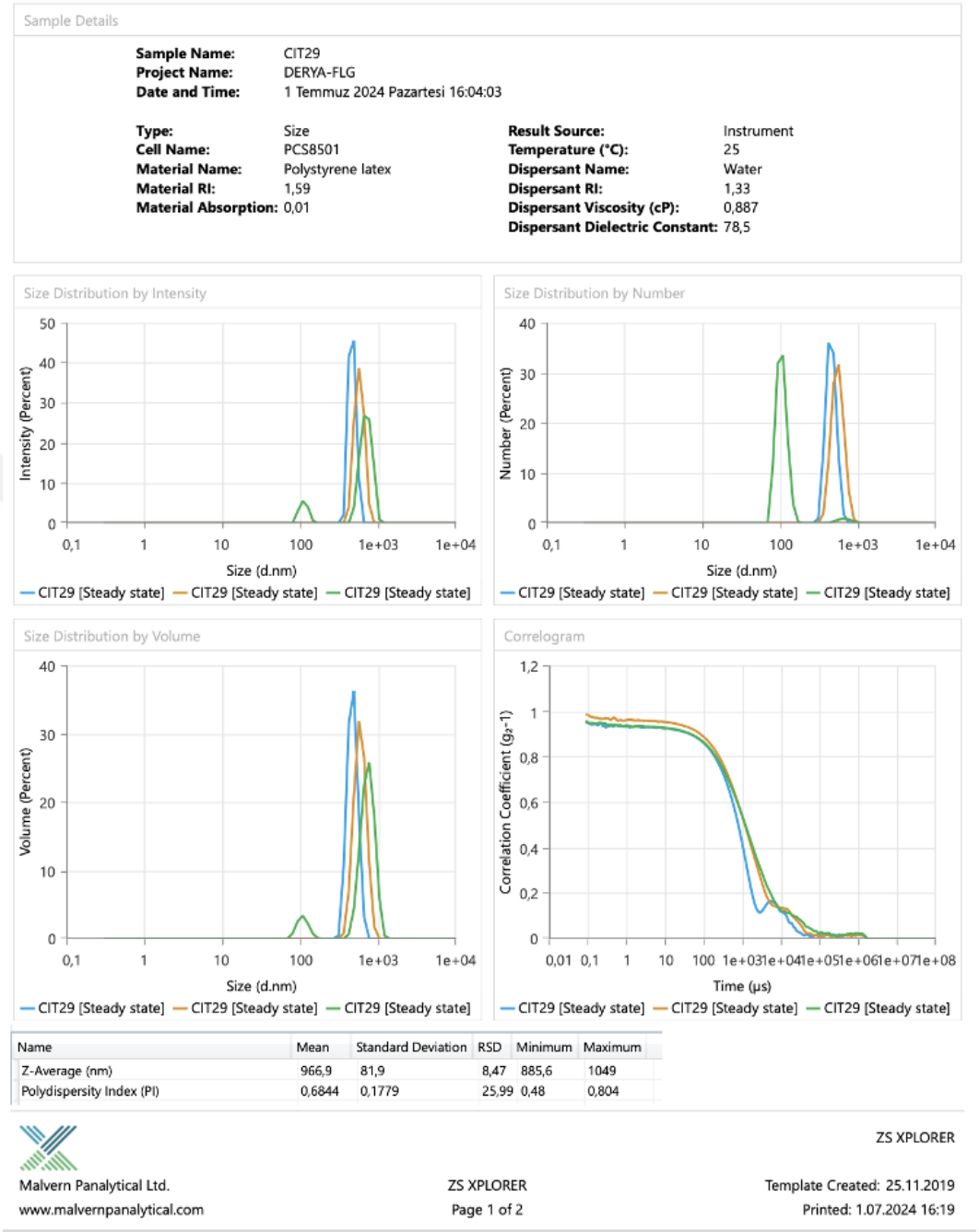

Figure B.33. 1-month DLS results of sample CHIT29, belongs to the data set of CHIT7

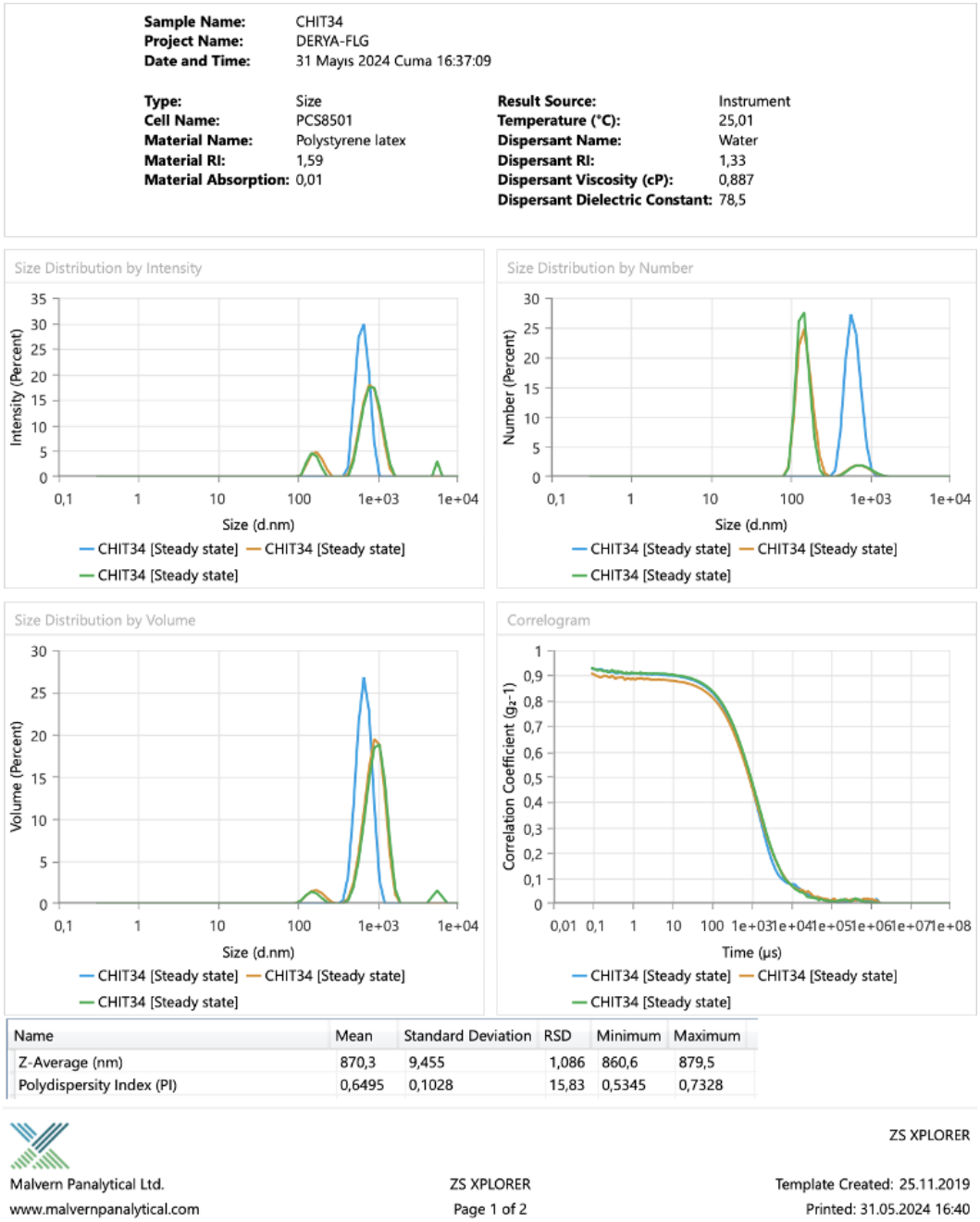

Figure B.34. DLS results of sample CHIT34, belongs to the data set of CHIT8

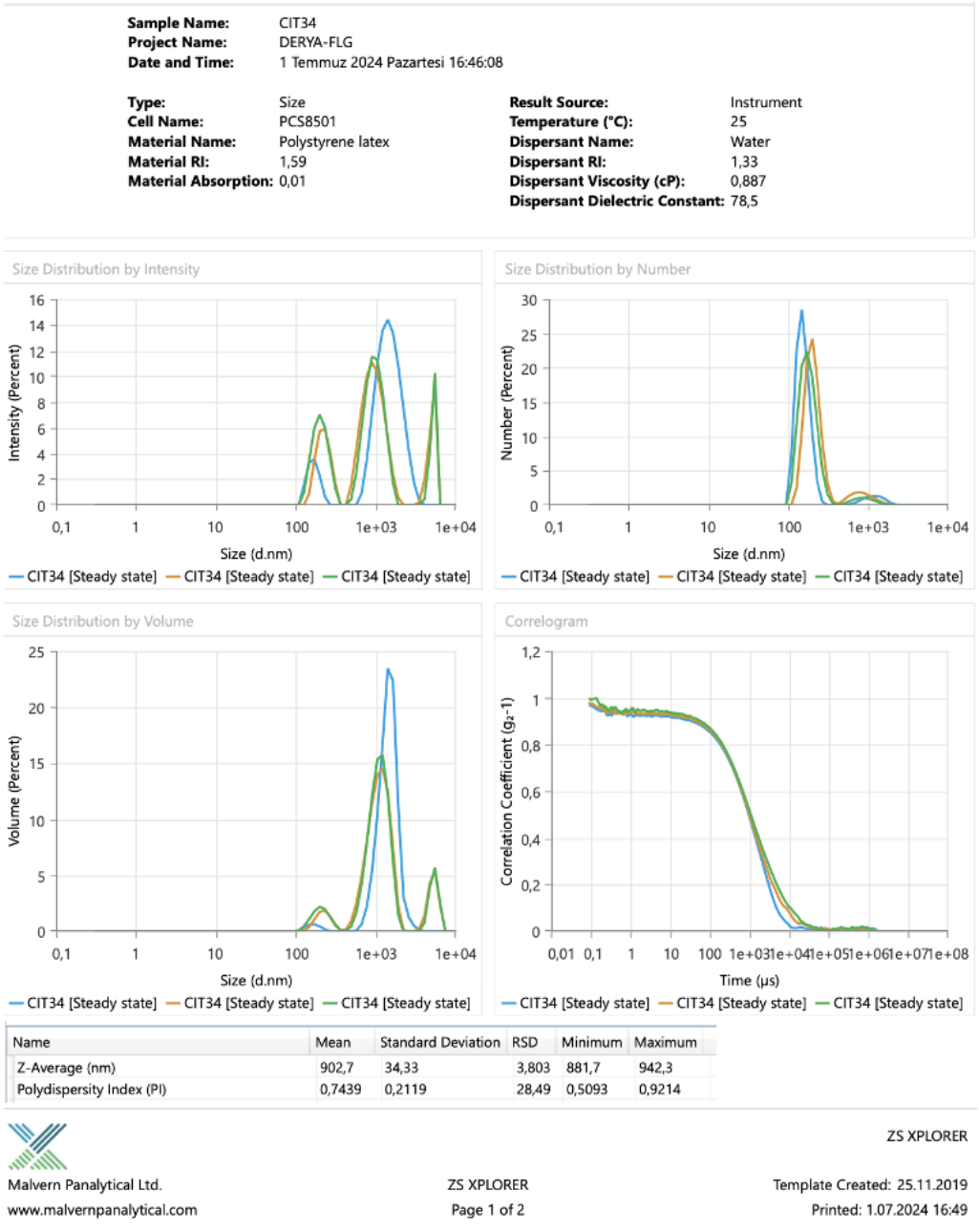

Figure B.35. 1-month DLS results of sample CHIT34, belongs to the data set of CHIT8

APPENDIX C: DLS RESULTS OF THE TEs IN CHAPTER 5

Size and PDI results of the vesicles obtained in chapter 5 can be found here.

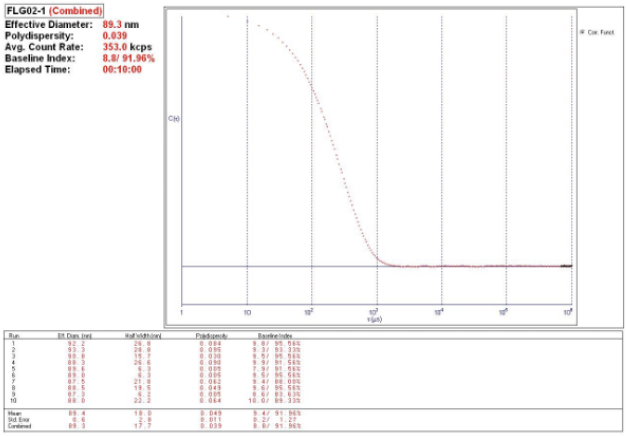

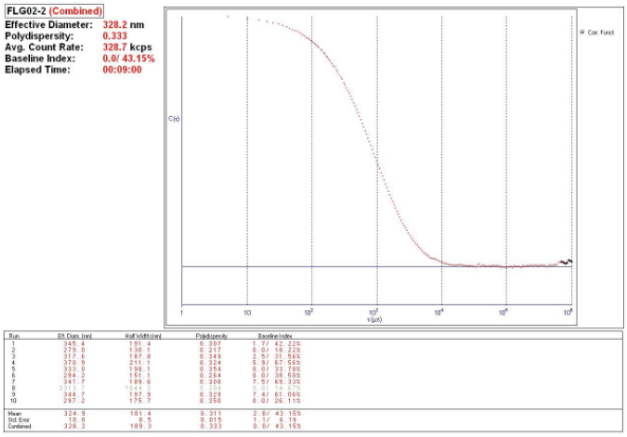

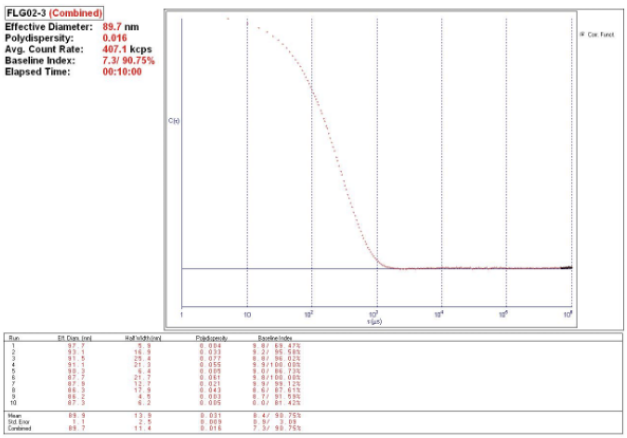

Figure C.1. DLS results belonging to the three trials of FLG samples

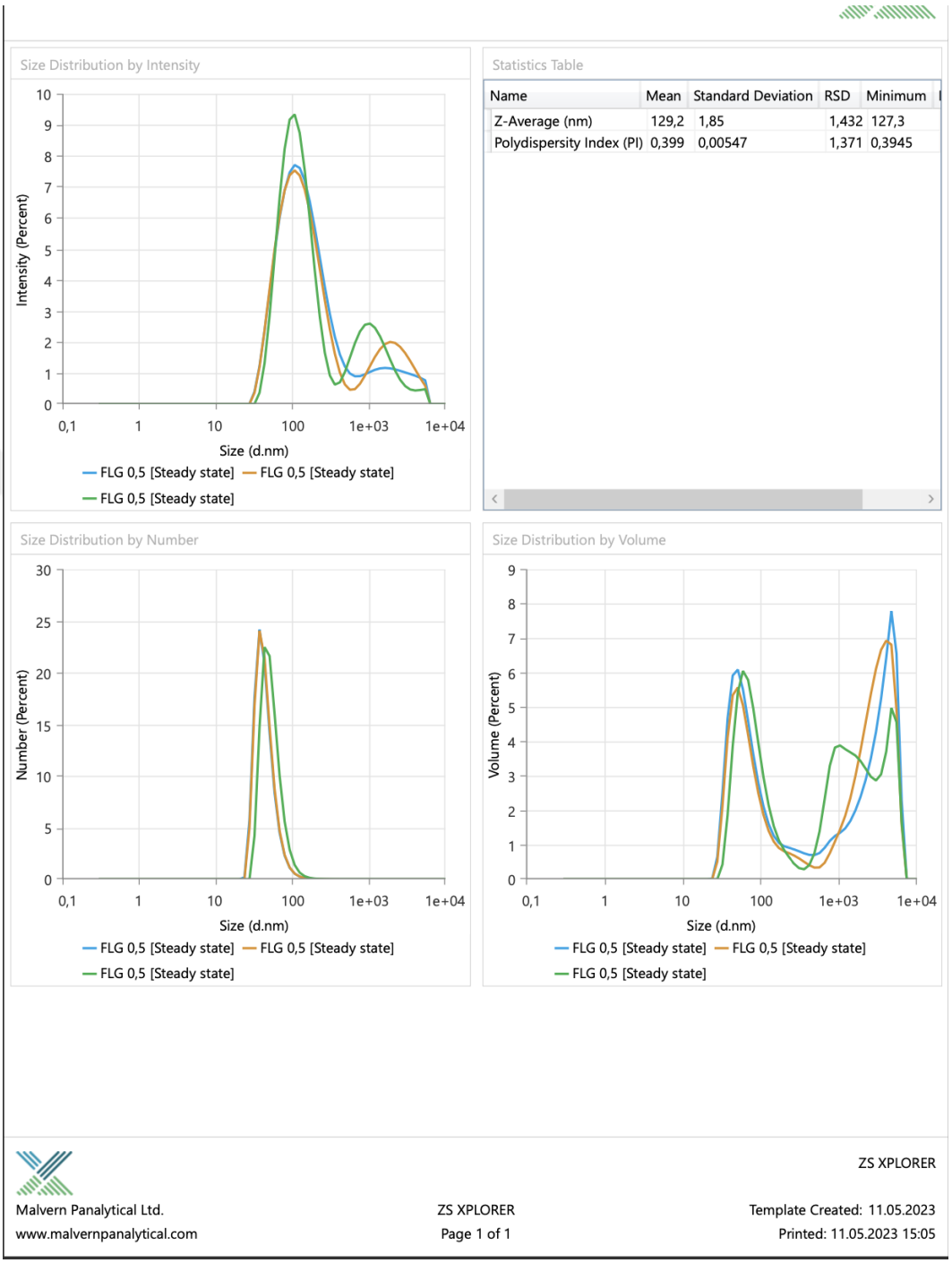

Figure C.2. 4-month DLS result of FLG1 belonging to the data set of FLG samples

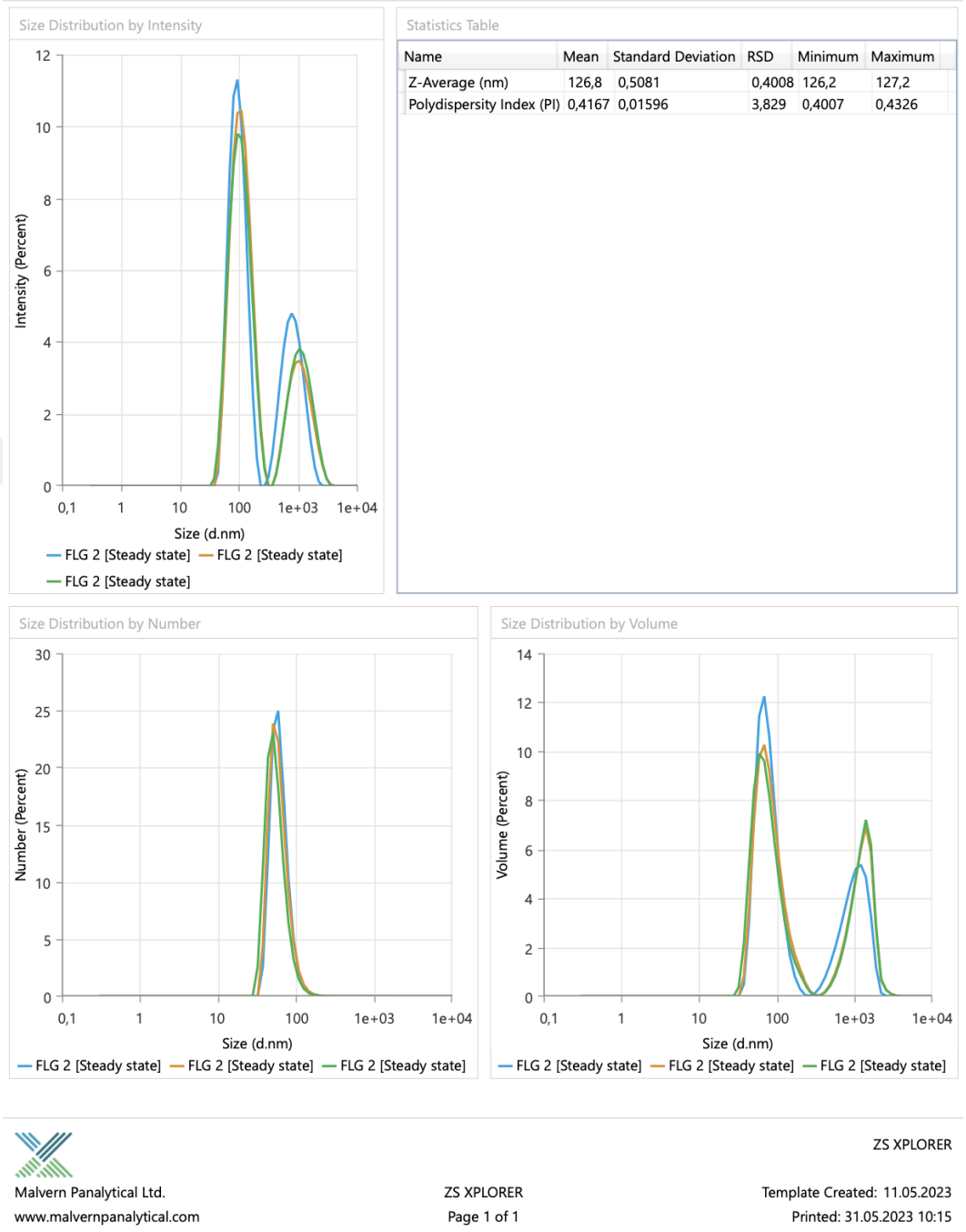

Figure C.3. 4-month DLS result of FLG2 belonging to the data set of FLG samples

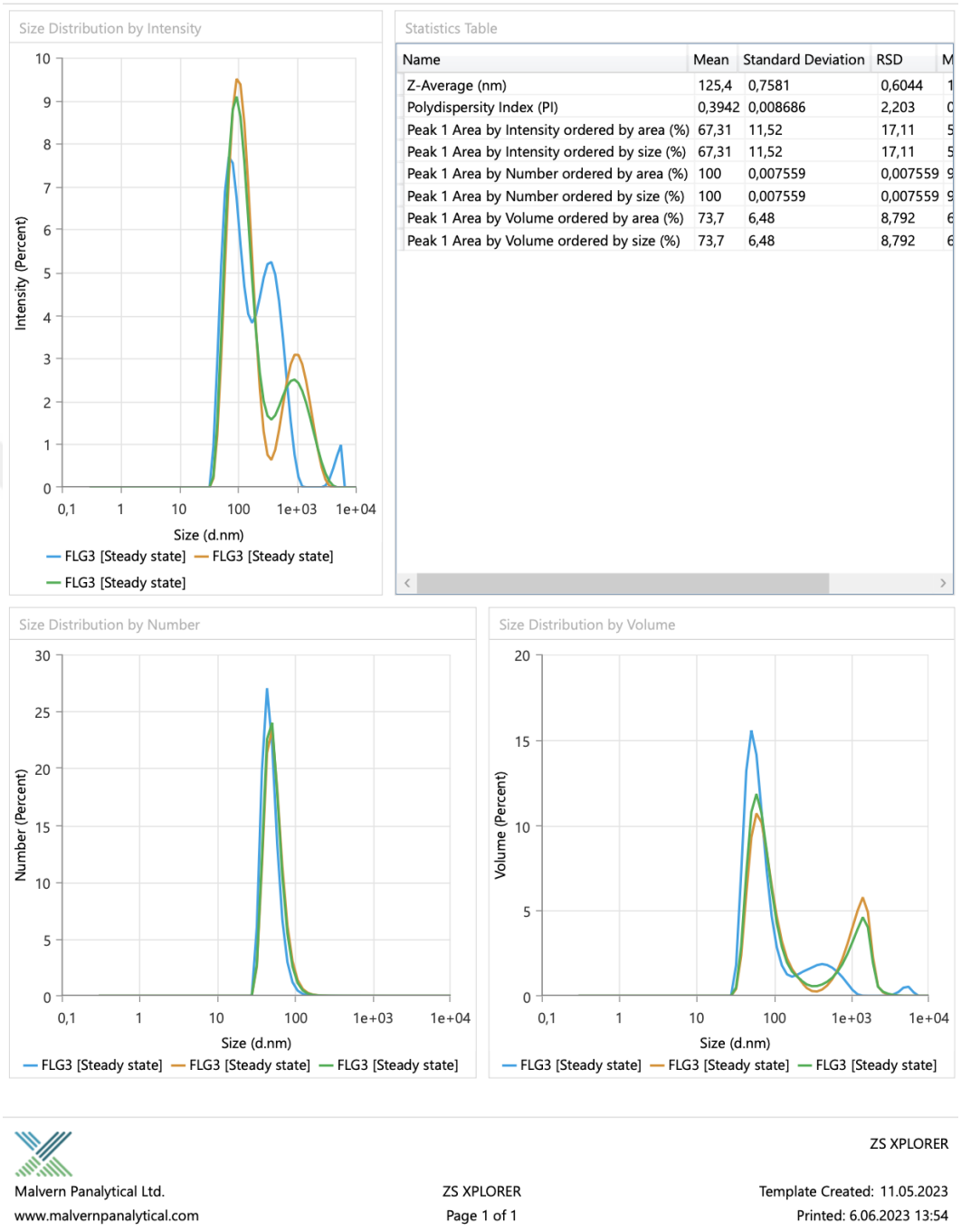

Figure C.4. 4-month DLS result of FLG3 belonging to the data set of FLG samples

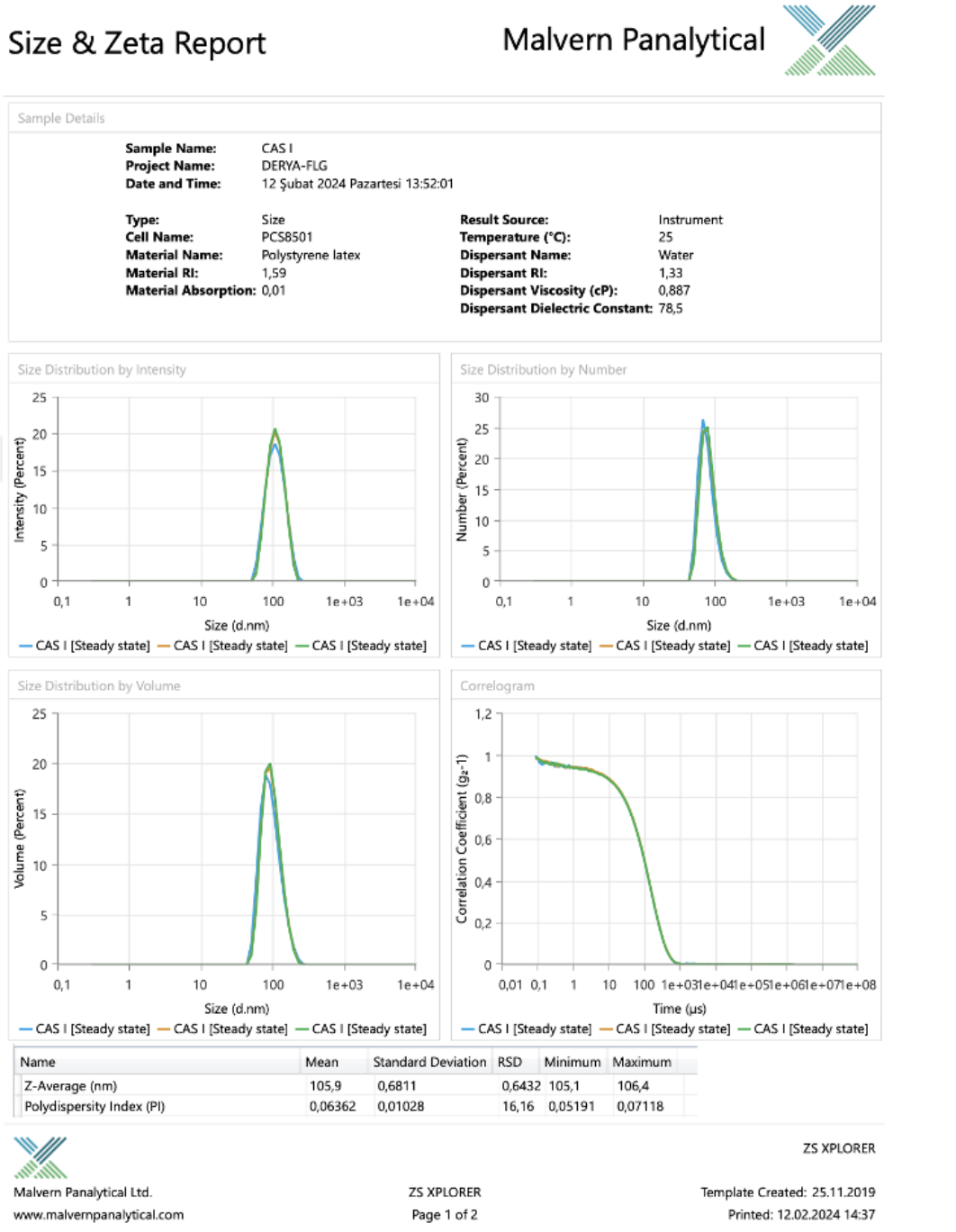

Figure C.5. DLS result of CAS1 belonging to the data set of CAS samples

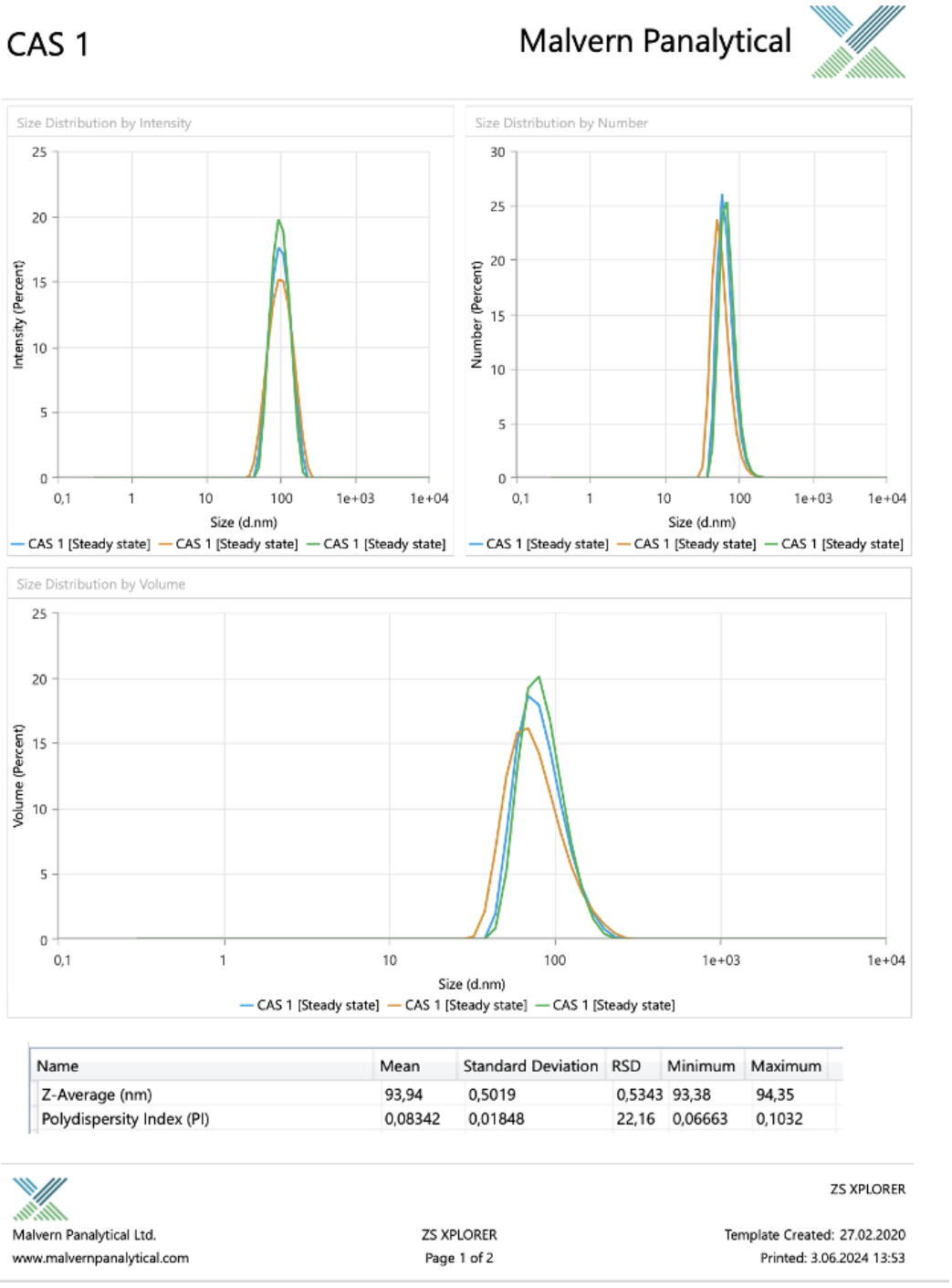

Figure C.6. 4-month DLS result of CAS1 belonging to the data set of CAS samples

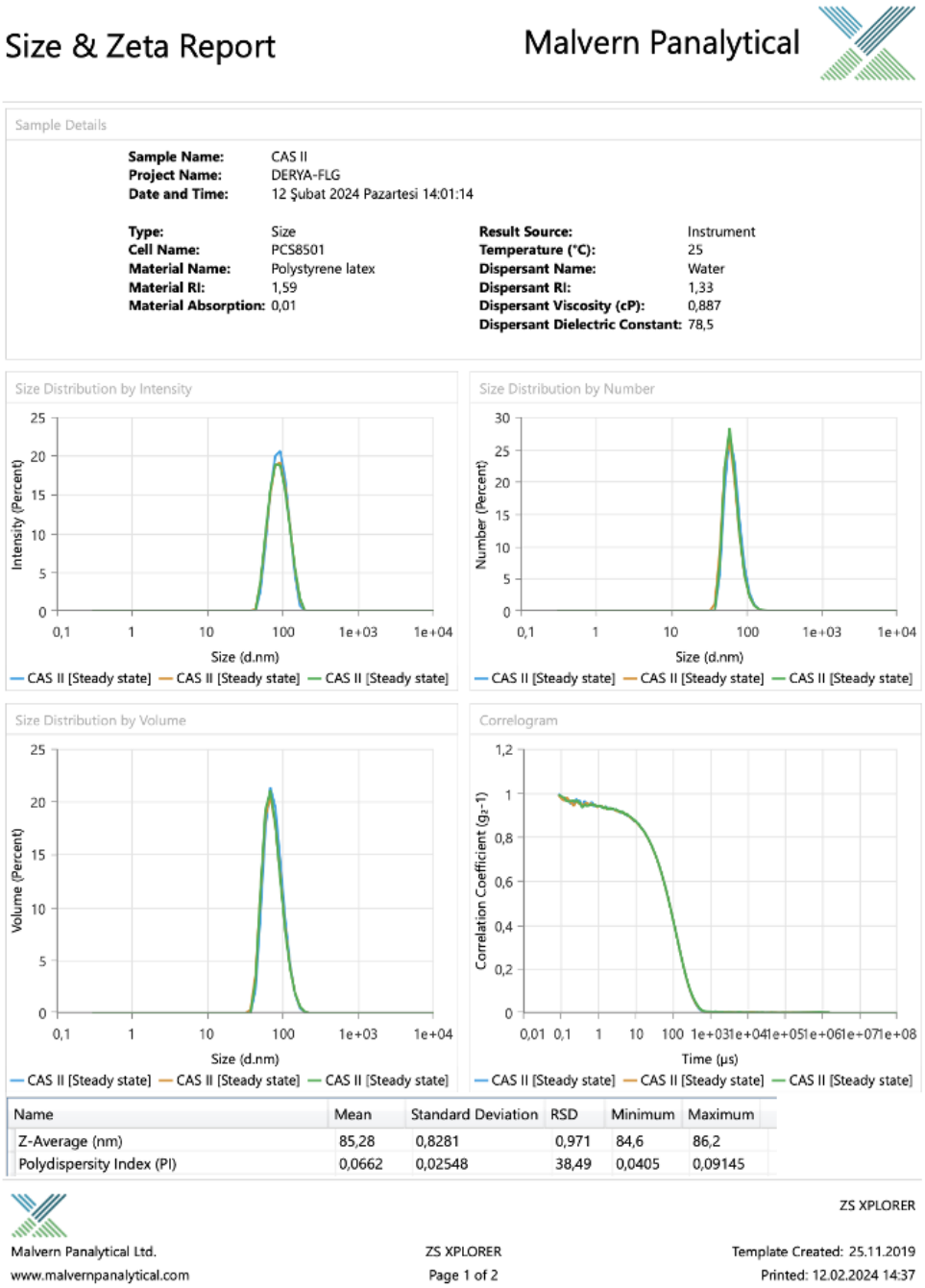

Figure C.7. DLS result of CAS2 belonging to the data set of CAS samples

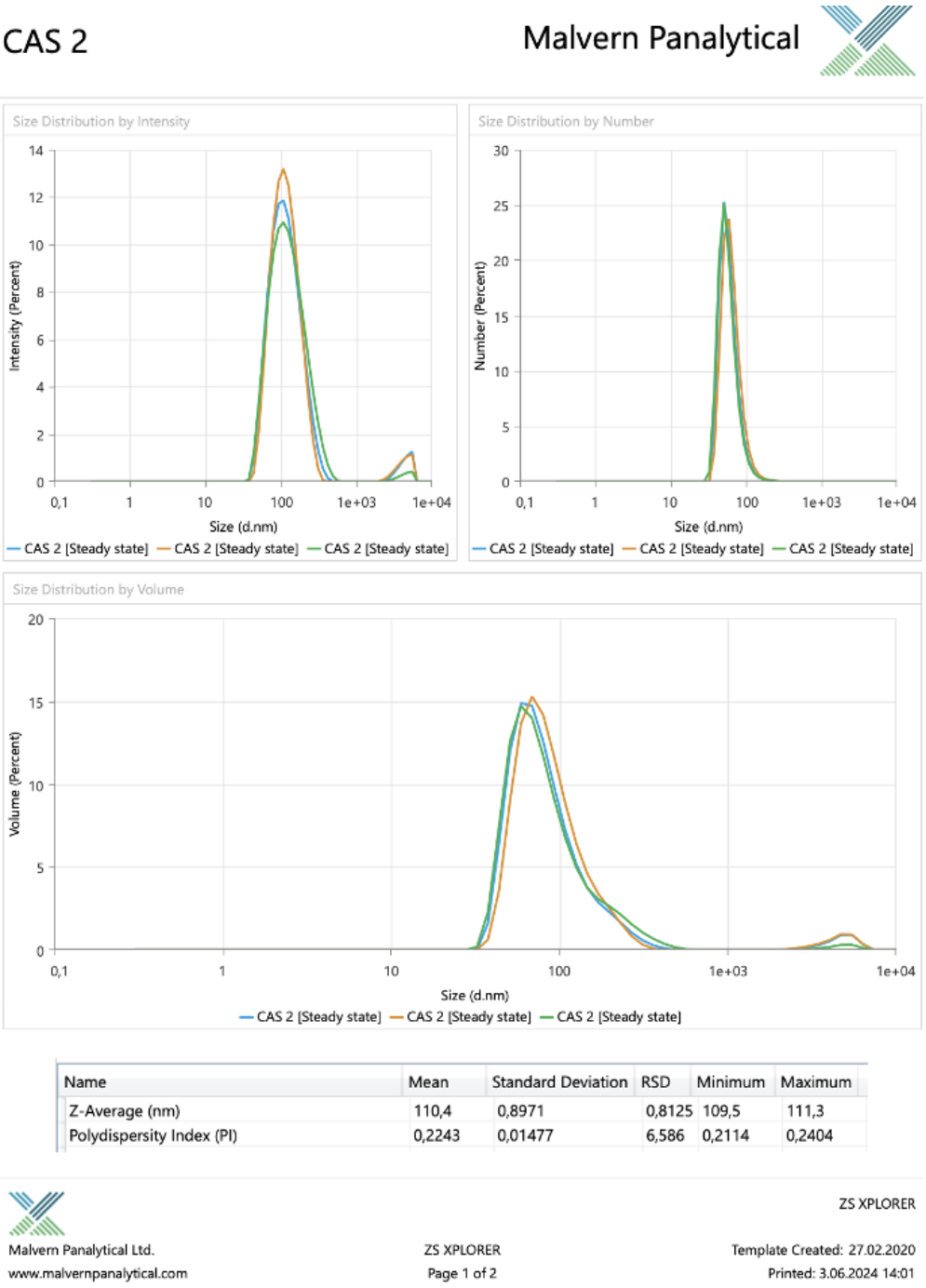

Figure C.8. 4-month DLS result of CAS2 belonging to the data set of CAS samples

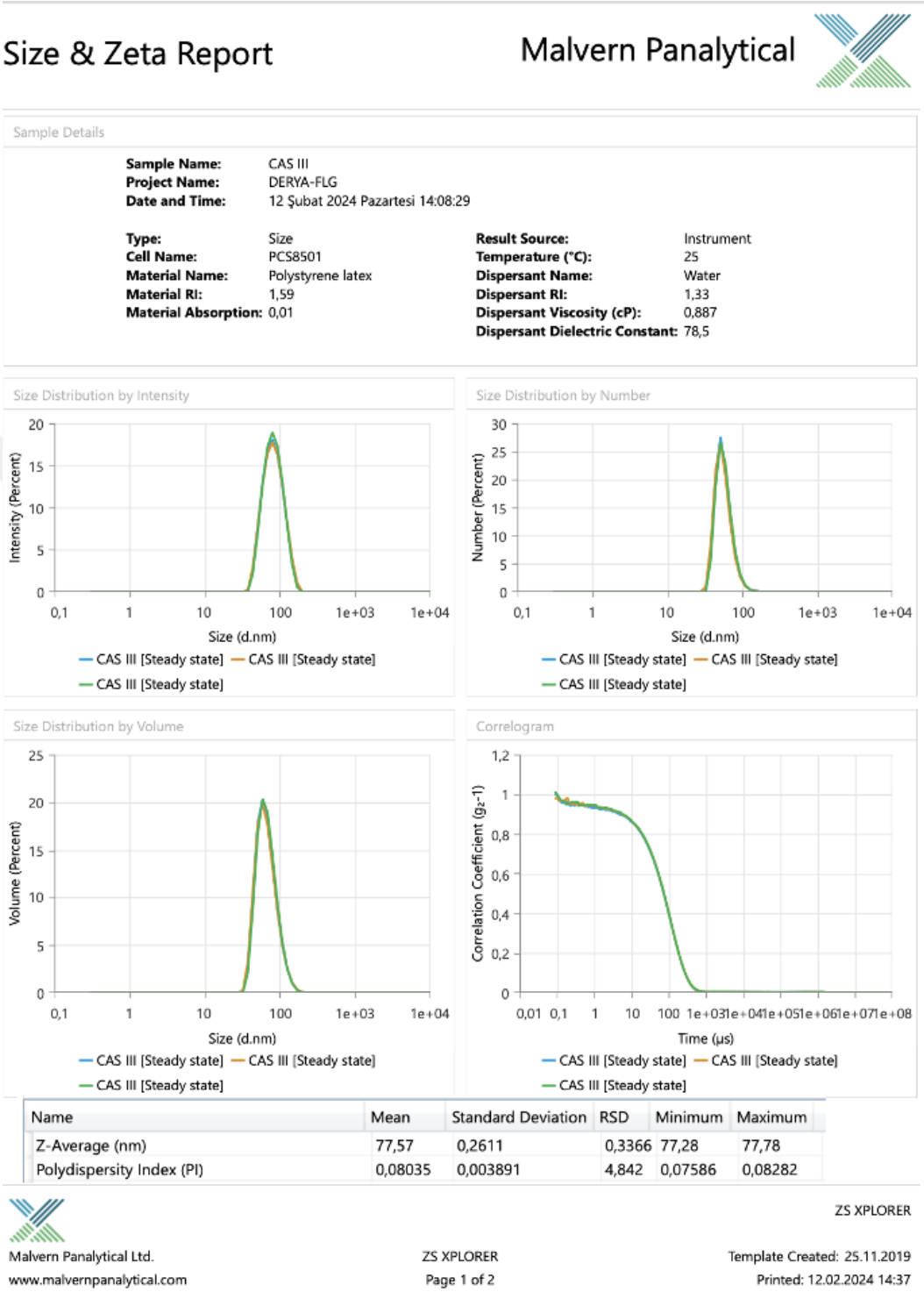

Figure C.9. DLS result of CAS3 belonging to the data set of CAS samples

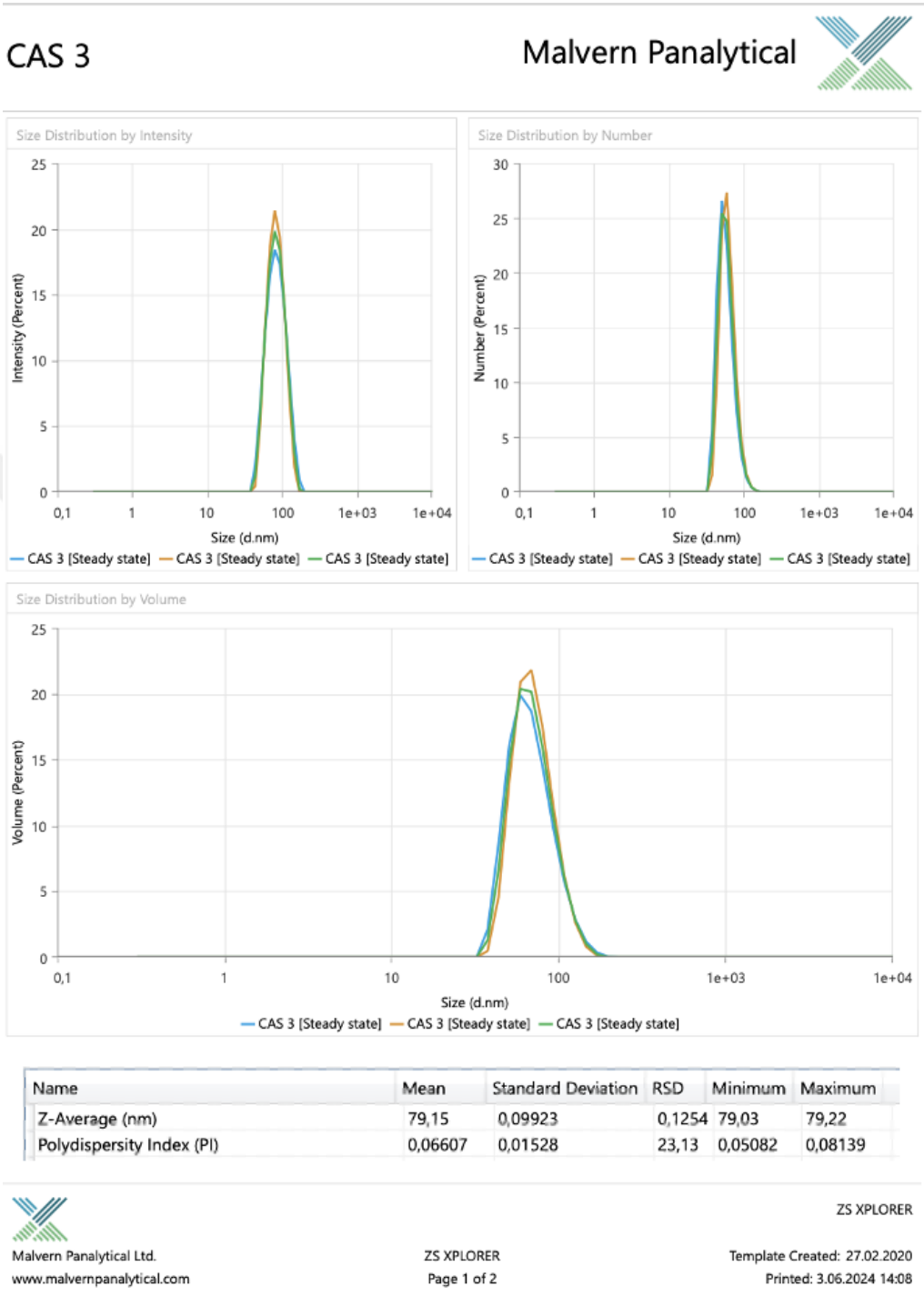

Name	Mean	Standard Deviation	RSD	Minimum	Maximum
Z-Average (nm)	79,15	0,09923	0,1254	79,03	79,22
Polydispersity Index (PI)	0,06607	0,01528	23,13	0,05082	0,08139

Figure C.10. 4-month DLS result of CAS3 belonging to the data set of CAS samples

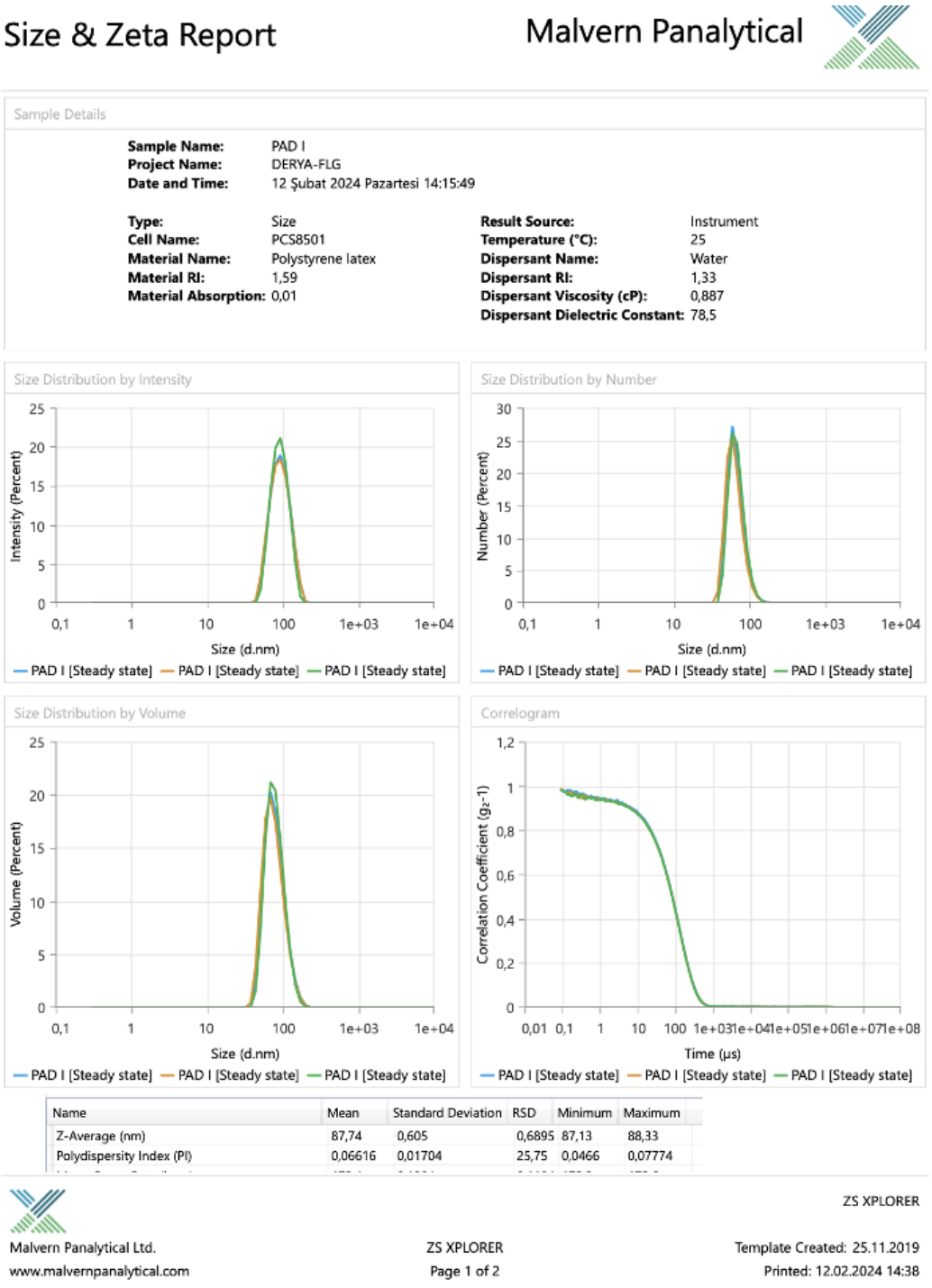

Figure C.11. DLS result of PAD1 belonging to the data set of PAD samples

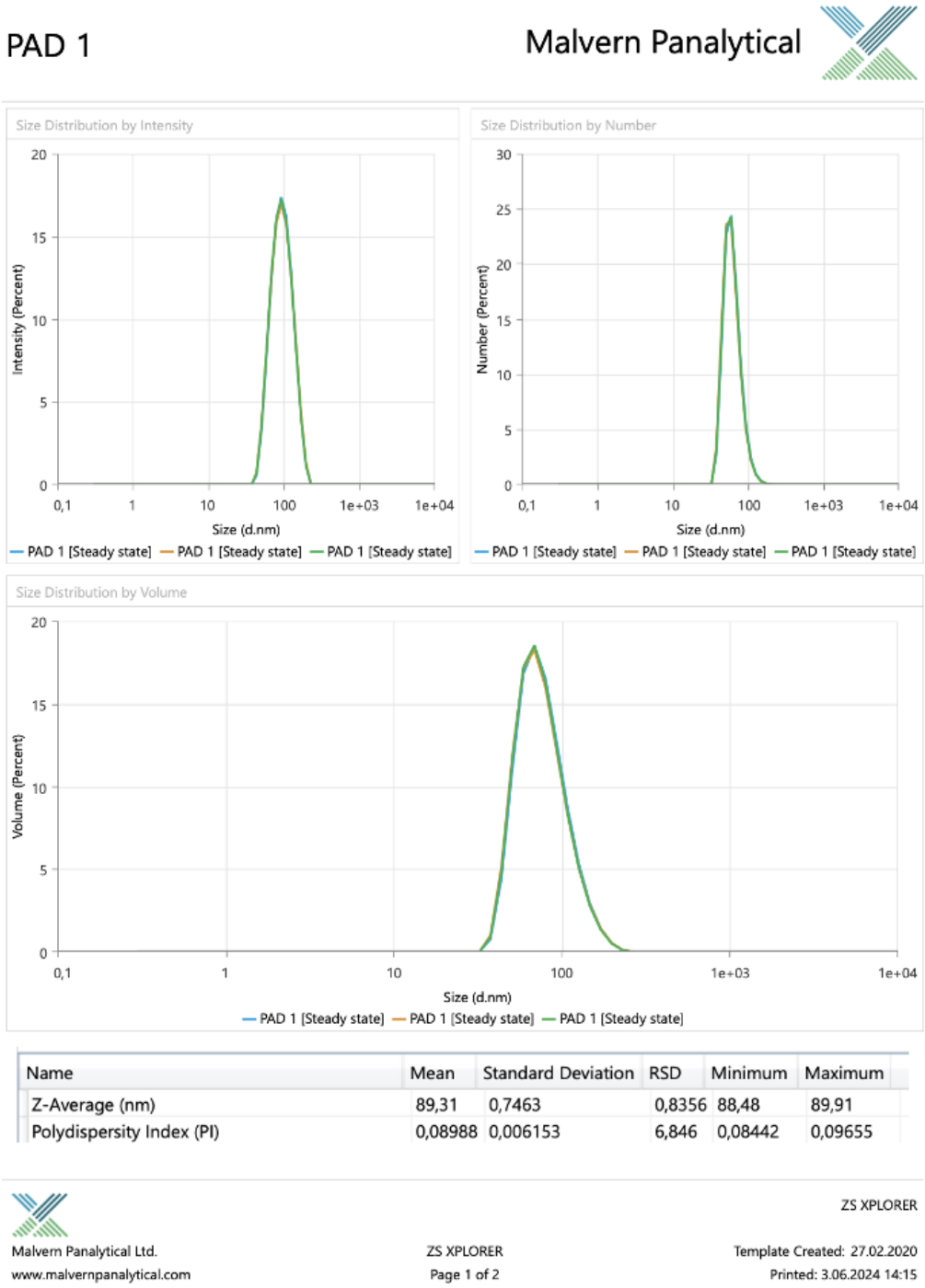

Figure C.12. 4-month DLS result of PAD1 belonging to the data set of PAD samples

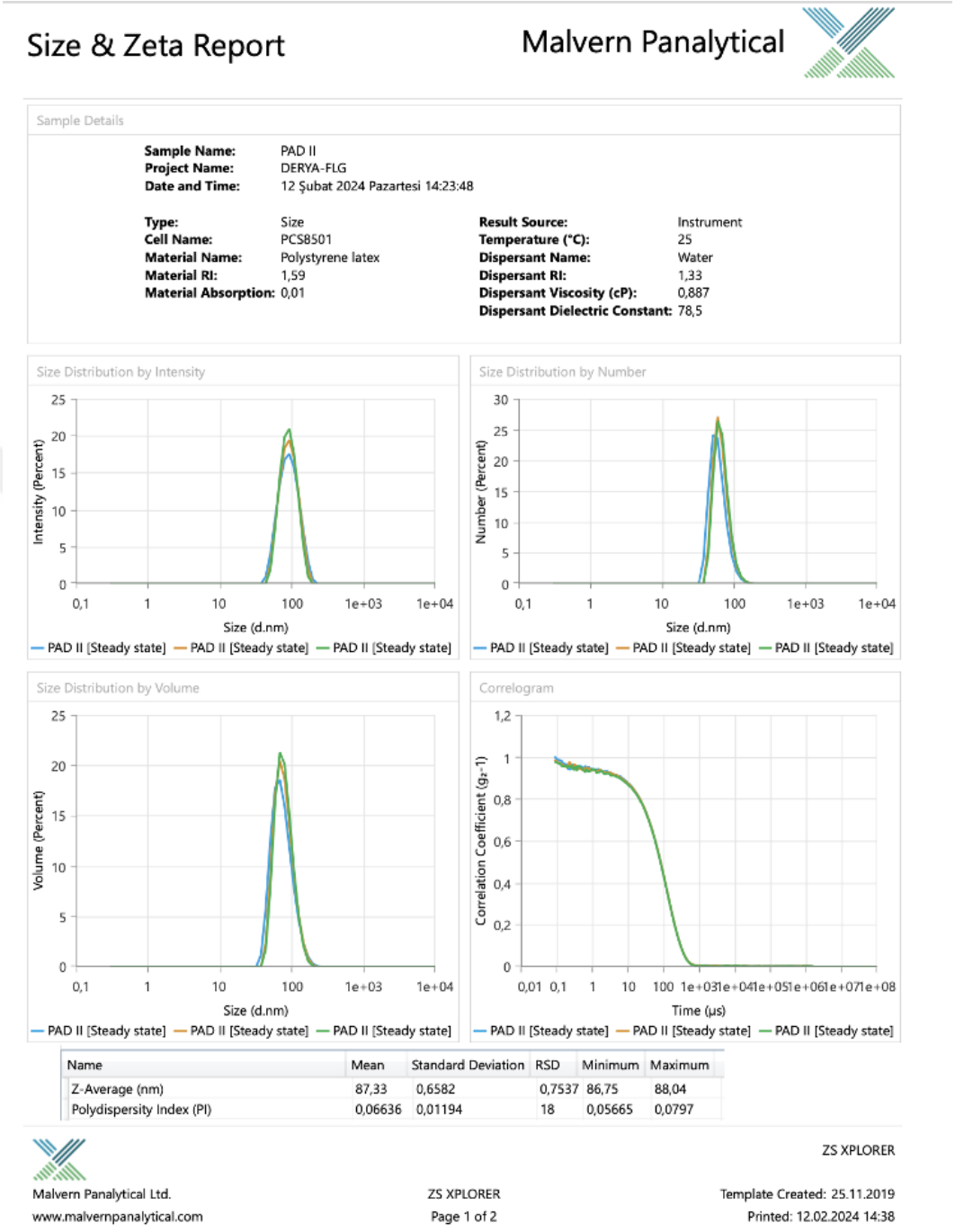

Figure C.13. DLS result of PAD2 belonging to the data set of PAD samples

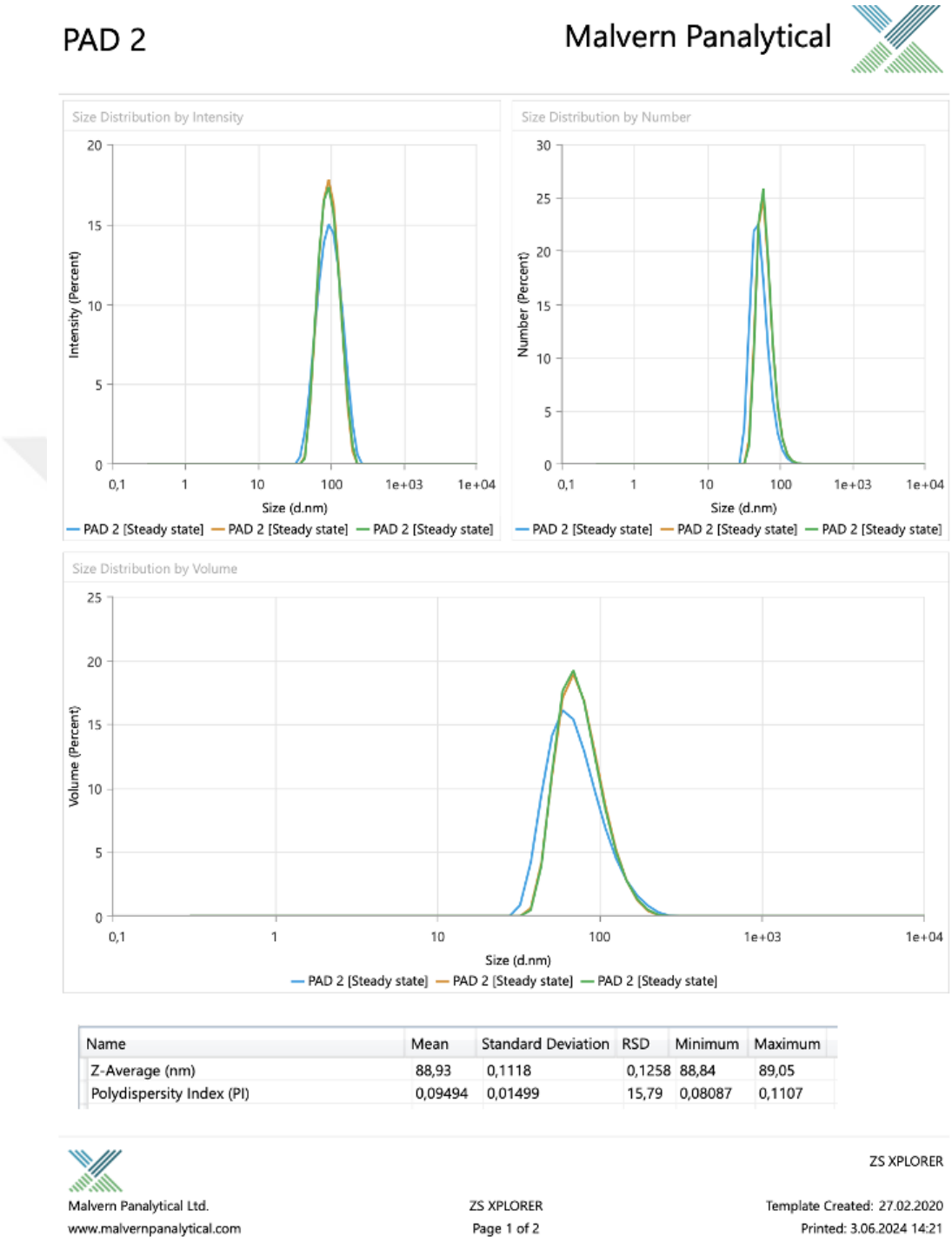

Figure C.14. 4-month DLS result of PAD2 belonging to the data set of PAD samples

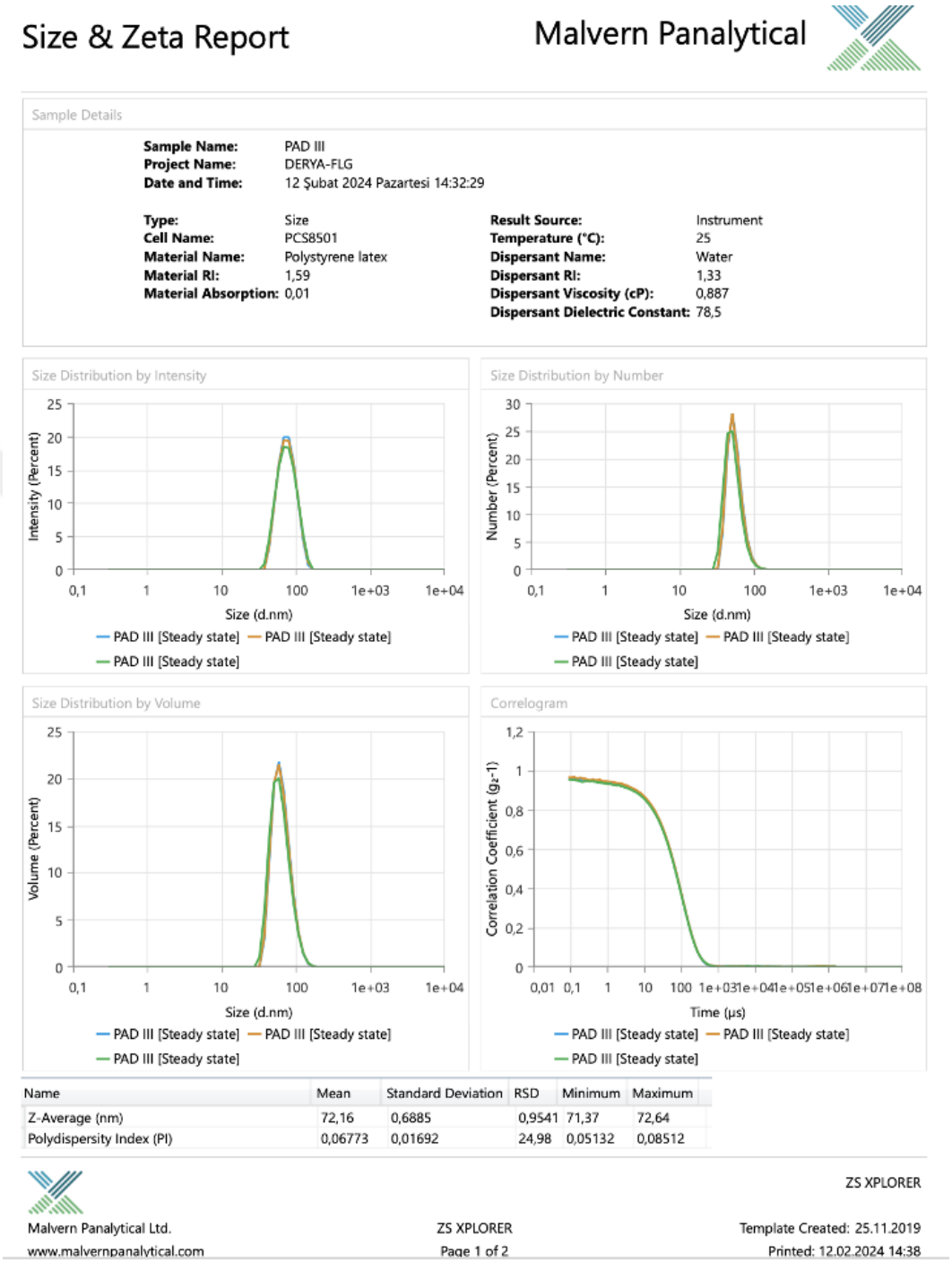

Figure C.15. DLS result of PAD3 belonging to the data set of PAD samples

PAD 3

Malvern Panalytical

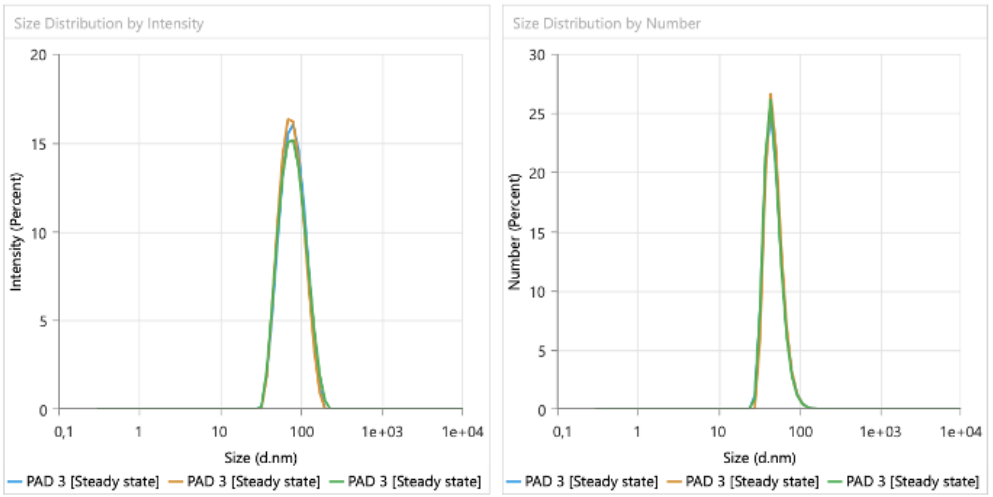

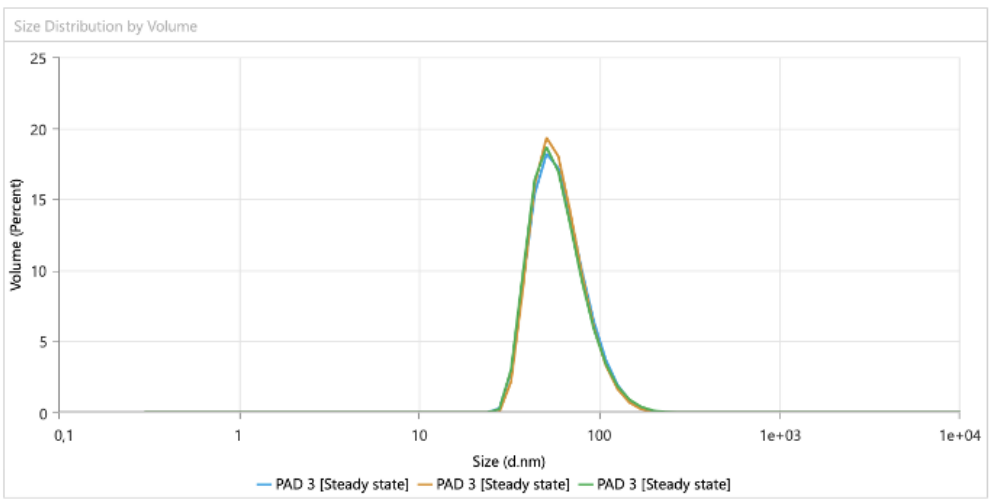

Name	Mean	Standard Deviation	RSD	Minimum	Maximum
Z-Average (nm)	73,38	0,1843	0,2512	73,21	73,58
Polydispersity Index (PI)	0,1127	0,01359	12,06	0,1001	0,1271

Figure C.16. 4-month DLS result of PAD3 belonging to the data set of PAD samples